Multi-isotope dietary reconstruction of modern and Beringian gray wolves

Eve Lindroos

Thesis submitted to the University of Ottawa in partial fulfillment of the requirements for the Master of Sciences degree in Earth Sciences

Department of Earth and Environmental Sciences

Faculty of Science

University of Ottawa

Abstract

Understanding how species adapt to environmental change is critical as many species are threatened by extinction under ongoing climate change. Beringia, the land mass that connected Yukon and Alaska with eastern Siberia throughout much of the Late Pleistocene (~115,000 to 11,700 years before present [BP]), experienced significant climatic warming during the terminal Pleistocene (~16,000−11,700 BP) and the increasing presence of humans in North America (~24,000−12,000 BP), both being coincident with a widespread North American megafaunal extinction event. However, species like the gray wolf (*Canis lupus*) survived, possibly due to dietary flexibility. I am revisiting this hypothesis by combining existing and novel palaeodietary proxies.

Stable isotopes in animal tissues reflect the consumers' diet, making them a powerful tool for dietary reconstructions of modern and extinct species. Carbon ($\delta^{13}C$) and nitrogen ($\delta^{15}N$) isotopes are commonly used in palaeodietary studies but are vulnerable to the degradation of organic molecules and to environmental baseline shifts. Calcium isotopes ($\delta^{44/42}Ca$), Sr/Ca, and Ba/Ca have been proposed as a complementary and potentially more robust dietary proxies.

I radiocarbon dated and analyzed $\delta^{13}C$, $\delta^{15}N$, $\delta^{44/42}Ca$, Sr/Ca, and Ba/Ca in the remains (bone and tooth enamel) of modern and Pleistocene wolves (*n*=15 and *n*=14, respectively) and their potential modern and Pleistocene prey species (*n*=20 and *n*=22*,* respectively). Using Bayesian stable isotope mixing models (BSIMMs), I reconstructed gray wolves’ prey preferences and dietary habits over the past 50,000 years.

As expected, BSIMMs relying on $\delta^{13}C$ and $\delta^{15}N$ data showed that Pleistocene wolves primarily consumed large ungulates, with pre-LGM and LGM wolves having a horse-specialized diet whereas modern wolves had a more generalist diet. When the $\delta^{44/42}Ca$ values were added as a third dimension, BSIMMs showed evidence of an even greater dietary shift with Pleistocene wolves consuming almost exclusively horses, whereas modern wolves showed a more diverse and small prey (i.e., snowshoe hare and arctic ground squirrel) dominated diet.

Calcium isotopes reinforce the hypothesis that Pleistocene wolves adapted to deglaciation and the extinction of Beringian horses during the terminal Pleistocene by shifting to a more generalist and flexible diet focusing on small prey and other large ungulates. This study provides

key information on the palaeoecology of Beringian mammals and underlines the importance of diet in biodiversity conservation, which can help inform effective management strategies for at-risk species in the face of current and future climate change. Besides the palaeoecological insights, my work also demonstrates a key methodological advance with the addition of calcium isotopes as a third, more robust palaeodietary dimension less influenced by environmental baselines and diagenesis. This offers an intriguing glimpse into the relatively unexplored potential of calcium isotopes to further investigate palaeodiets of animals and presents an exciting development in the integration of traditional (i.e., carbon and nitrogen) and non-traditional (i.e., calcium) isotope geochemistry into the field of palaeobiology.

Acknowledgments

Firstly, I would like to acknowledge that all specimens analyzed in this study were collected from the traditional unceded territories of the Vuntut Gwitchin and Tr'ondëk Hwëch'in Peoples. I also would like to acknowledge that the University of Ottawa is located on the traditional unceded territory of the Algonquin Anishnaabeg People.

I would like to start by thanking my supervisor Dr. Clément Bataille, as well as my mentors Dr. Auguste Hassler and PhD candidate Zoe Landry. Without their knowledge, expertise, guidance, and support this project and thesis would not have been possible. I am forever thankful for the many hours they spent mentoring and teaching me, including rigorous hours shadowing Dr. Auguste Hassler in the laboratory learning chromatography and the millions of questions I have asked him over the past two and half years; the numerous palaeontological and MixSIAR questions I have asked Zoe Landry, and all of her support during the writing of this thesis; and countless discussions, meetings, and thesis edits with Dr. Clément Bataille.

I would specifically like to thank Dr. Clément Bataille for his continued mentorship. You have provided me with countless educational and professional opportunities including my undergraduate honours thesis, our 2023 publication, and now this master's thesis, of which I am grateful. Your passion and scientific curiosity are only two of the reasons you are an amazing scientist, and I look forward to potential future collaborations. I am honoured to have been a student of yours over these past four years. Your knowledge, patience, and supportive nature are the foundation of why you are such an amazing supervisor. Thank you for a wonderful graduate school experience, in which you provided me with a project that tested me but also allowed me to learn and grow as a scientist.

I would also specifically like to thank Dr. Auguste Hassler, of which I cannot put my gratitude for our friendship and your mentorship into words, but I will try. Your patience, guidance, and the wealth of knowledge and skills you have shared with me have played a pivotal role in shaping my future career. Our many lunch, teatime, and laboratory conversations and laughs are some of my fondest memories of my time in graduate school. I look forward to future collaborations and for our continued friendship. It was an honour to be your shadow.

I thank Dr. Danille Fraser, Dr. Scott Rufolo, and Dr. Gregory Rand for providing guidance and access to the Palaeobiology and Quaternary Zoology Collections at the Canadian Museum of Nature. I thank the amazing staff at the AMS, geochemistry, and Jan Veizer labs at the University of Ottawa for your guidance and knowledge you have imparted to me while analyzing samples. I also thank Dr. Jonathan O'Neil for allowing us to use space in his clean laboratory. I thank Dr. Oliver Warr and Dr. Danielle Fraser for taking time out of their very busy schedules to sit on my master's defence committee.

To my family, I am so thankful and grateful for all your unwavering support, that again I find myself at a loss of words. Specifically, thank you to my parents— Kari Lindroos and

Pauline Jaworski, my sister—Katherine Lindroos, and my cousin (big sister) — Erika Petersen. All of you believed in me, at times I could not believe in myself and took care of me, at times when I could not take care of myself. You have and continue to demonstrate to me what is hard work and resilience, and I admire and love all of you so deeply.

Charlotte from *Sex and the City* once said, "*we could be each others' soulmates*", a statement on friendship that *I couldn't help but wonder* is true. I thank my friends, of which I am so lucky to have so many I cannot list you all, but know your friendships, endless laughs, and continued support hold a special place in my heart. Thank you to all my saive laboratory friends, specifically Shanie, Brent, Zoe, Megan, and Lea, your friendships are the most important thing I am taking away from graduate school. To the whole Percy gang, you welcomed me into your friend group around the same time I started this degree and took me in as one of your own. I am so happy to have all of you in my life, for which you bring so much joy and silliness. To my girls, Heather, Neri, Tegan, Shira, and of course Electra (my right-hand man and honorary sister), I do not know what I would do without your friendships, thank you for being a part of my life and for including me in yours.

Now enough of the sappy stuff and onto the science.

Table of Contents

List of Figures

List of Tables

Glossary

AER: Alkaline element ratios (Sr/Ca and Ba/Ca)
AMS: Accelerator mass spectrometer
BSIMM: Bayesian stable isotope mixing model
BP: Before present
HAp: Carbonated hydroxyapatite
HREE: Heavy Rare Earth Elements
ICP-MS: Inductively coupled plasma mass spectrometer
ICP-OES: Inductively coupled plasma optical emission spectrometer
ka: Thousand years
LGM: Last Glacial Maximum
LREE: Light Rare Earth Elements
MC-ICP-MS: Multicollector inductively coupled plasma mass spectrometer
NASC: North American Shale Composite
REE: Rare Earth Elements
P_{IDW}: Inverse distance weighting probability
PCA: Principal component analysis
TDF: Trophic discrimination factor
SIA: Stable isotope analysis
$\delta^{13}C$: Stable carbon isotope ratio
$\delta^{15}N$: Nitrogen stable isotope ratio
$\delta^{44/42}Ca$: Calcium stable isotope ratio
^{14}C: Radiocarbon
ppm: parts per million
ppb: parts per billion
‰: per mil

1 Introduction and background information

This thesis explores the integration of traditional and novel palaeodietary proxies with the aim to overcome the limitations of traditional palaeodietary proxies (i.e., organic degradation, increased susceptibility to diagenesis, influence from environmental baselines). Using traditional ($\delta^{13}C$ and $\delta^{15}N$) and novel ($\delta^{44/42}Ca$, Sr/Ca and Ba/Ca) palaeodietary proxies, I question the dietary preferences of Pleistocene and modern gray wolves (*Canis lupus* Linnaeus, 1758) to further decipher the mechanisms that may have facilitated their strong resilience to past environmental changes. The methodological advance from this thesis can be applied to a wide range of fossils and studies, such as Miocene trophic reconstructions, and future exploration into Pleistocene apex carnivore dietary habits, which can further inform conservation efforts of Canadian Arctic species and northern wildlife.

1.1 Background

1.1.1 The ecological role of apex predators

Carnivores play critical roles in ecosystem regulation and structure (Beschta & Ripple, 2009; Bruno & Cardinale, 2008; Estes et al., 2011; Ripple et al., 2014; Ritchie et al., 2012; Ritchie & Johnson, 2009). This is especially evident for large apex predators that hold the highest trophic levels in an ecosystem, some examples include but are not limited to, lions (*Panthera leo* Linnaeus, 1758), tigers (*Panthera tigris* Linnaeus, 1758), and polar bears (*Ursus maritimus* Phipps, 1774) (Ripple et al., 2014). Through a top-down trophic cascade, apex predators shape trophic dynamics (Beschta & Ripple, 2009; Bruno & Cardinale, 2008; Estes et al., 2011; Hairston et al., 1960; Paine, 1980; Ripple et al., 2014; Terborgh et al., 2001). Some of the ways in which apex predators shape trophic systems includes but is not limited to, regulating populations of intermediate trophic level species through competition with mesopredators (Ritchie & Johnson, 2009) and specific prey consumption (Estes et al., 2011; Griffin & Silliman, 2010) which in turn regulates plant-herbivore interactions and plant biomass (Schmitz, 2006, 2009; Schmitz et al., 2000). Collectively, these ecological interactions promote and sustain biodiversity (Beschta & Ripple, 2009; Bruno & Cardinale, 2008; Estes et al., 2011; Hairston et al., 1960; Paine, 1980; Ripple et al., 2014).

The most iconic example, though controversial, (Brice et al., 2022; Hobbs et al., 2024; Marshall et al., 2013) showcasing the important role of apex predators in shaping ecological communities has been the reintroduction of wolves in Yellowstone National Park (Beschta & Ripple, 2009; Ripple et al., 2025; Ripple & Beschta, 2012). Due to gray wolf eradication in the 1900s, common gray wolf prey, specifically elk (*Cervus canadensis* Erxleben,1777*)*, became overpopulated leading to overgrazing across the park, particularly of woody plants such as aspen (*Populus tremuloides* Michx), cottonwood and willow (*Salix* spp.) in riparian zones (Beschta, 2005; Halofsky & Ripple, 2008; Ripple & Beschta, 2012; Ripple & Larsen, 2000). However, once gray wolves were reintroduced in the 1990's, elk populations declined, and elk altered their behavior to avoid areas where they were most vulnerable to hunting such as in riparian zones allowing recovery of the vegetation (Beschta & Ripple, 2016; Beyer et al., 2007; Fortin et al., 2005). In these areas restoration in vegetation allowed tree growth, which stabilized river erosion and facilitated the return of beavers (*Castor canadensis* Kuhl, 1820*)* who engineered ponds and lakes, subsequently increasing aquatic animal biodiversity (Beschta & Ripple, 2016; D. W. Smith & Tyers, 2012). This example among others (e.g., sea otters [*Enhydra lutris* Linnaeus, 1758] in nearshore marine ecosystems [Estes & Duggins, 1995; Estes & Palmisano, 1974; Gorra et al., 2022]) showcase how apex predators not only regulate prey populations, but also have cascading effects on regulating the whole ecosystem (Dobson et al., 2006; Estes et al., 2011; Estes & Palmisano, 1974; Gorra et al., 2022; Ripple et al., 2014, 2025; Ritchie et al., 2012).

1.1.1.1 Communities with co-existing apex predators

While apex predators are at the top of the trophic pyramid, niche partitioning can enable multiple apex species to co-exist within the same ecosystem. This is typically achieved through differentiation in spatial, temporal, and/or dietary ecological niches—by targeting specific prey, occupying distinct habitats or territories, and exhibiting unique behaviors (Cong et al., 2024; Durant, 1998; Fedriani et al., 2000; Hayward & Kerley, 2008; Karanth & Sunquist, 2000; Lamichhane et al., 2025). For instance, in the African savanna, lions, leopards (*Panthera pardus* Linnaeus, 1758), and cheetahs (*Acinonyx jubatus* Schreber, 1775) coexist despite overlapping territories. Lions, as social hunters, tend to target medium-large ungulates (i.e., African buffalo

[*Syncerus caffer* Sparman, 1779], wildebeest [*Connochaetes* sp. Lichtenstein, 1812] and zebra [*Equus* sp. Linnaeus, 1758]) in open grasslands and are mostly active at night (Grant et al., 2005; Hayward & Kerley, 2005, 2008; Orsdol, 1984). Leopards hunt solitarily, often in covered areas during twilight hours, focusing on smaller ungulates (i.e., Impala [*Aepyceros melampus* Lichtenstein, 1812] and harnessed bushbuck [*Tragelaphus scriptus* Pallas, 1766]) and prey caching—hoisting their prey into trees to avoid scavengers and competition (Balme et al., 2007; Hayward et al., 2006; Hayward & Kerley, 2008). Cheetahs, on the other hand, rely on speed to hunt small-medium-sized prey (i.e., gazelle [*Eudorcas thomsonii* Günther, 1884 and *Nanger granti* Brooke, 1872] and blesbok [*Damaliscus pygargus phillipsi* Harper, 1939]) in open habitats during the day, reducing both spatial and temporal overlap with the other big felines (Durant, 1998; Hayward et al., 2006; Hayward & Kerley, 2008; Mutoro et al., 2022). These differences in hunting strategy, prey preference, habitat use, and activity patterns reduce direct competition and allow for stable coexistence (Durant, 1998; Hayward & Kerley, 2008). Evidence of niche partitioning are also found in the geological record. For example, in mid-Cretaceous ecosystems, dietary niche partitioning allowed large predators such as the spinosaurids, abelisaurids and crocodyliforms to coexist by targeting different prey and occupying distinct ecological roles (Hassler et al., 2018).

A high diversity of top predator species within the same ecosystem often creates a resilient and stable ecosystem due to more complex and balanced food web interactions (Estes et al., 2011; Estes & Duggins, 1995; Finke & Snyder, 2010; Liu et al., 2024; Mougi, 2022; Schmitz et al., 2000). However, specialization in diet, territory and behavior often associated with niche partitioning comes with a cost. Large-bodied mammals (>44 kg), commonly referred to as megafauna—including apex predators—face particularly high vulnerability in the face of anthropogenic climate change and habitat degradation (Fuller et al., 2016; Mccain & King, 2014). Megafauna typically are biomic specialists (Fernández & Vrba, 2005), have high energetic and metabolic demands (Carbone et al., 1999) with distinct diets (Pineda-Munoz et al., 2016), and exhibit slow reproductive rates which, in turn, contribute to delayed population recovery (Albaladejo-Robles et al., 2023). Collectively these factors limit megafauna's resilience to ecological disruption (Albaladejo-Robles et al., 2023; de Silva & Leimgruber, 2019), which can impact the resilience of an entire ecosystem (Cardillo et al., 2005; Fisher & Owens, 2004; Fuller et al., 2016; Mccain & King, 2014; Morueta-Holme et al., 2010; Quintero & Wiens, 2013).

Thus, top predators might become more vulnerable to environmental changes, habitat loss, and/or to changes in the population dynamic of their specified prey populations (Estes et al., 2011; Hatton et al., 2015; Ripple et al., 2015; Tyson et al., 2010). Despite ongoing global conservation efforts, megafaunal populations continue to decline at alarming rates (Ripple et al., 2016, 2017), threatening not only individual species but the ecological integrity of entire communities.

1.1.1.2 Ecological threats and implications for apex predators

Environmental change and anthropogenic impacts on top predators are a challenge for modern conservation efforts. Increased human disruption in natural ecosystems, including, but not limited to, anthropogenically driven climate change, deforestation, and agriculture expansion, poses significant threats to modern ecosystems (Díaz et al., 2019; Grimm et al., 2013; He & Silliman, 2019; King, 2004; Pecl et al., 2017; Pires et al., 2018; Thomas et al., 2004; Wassmann et al., 2011), often triggering large-scale landscape transformations that disrupts ecological structure and biodiversity (Bellard et al., 2012; Grimm et al., 2013; Newbold, 2018; Pecl et al., 2017; Pires et al., 2018; Schulte to Bühne et al., 2021; Weiskopf et al., 2020). Apex predators are particularly vulnerable to such environmental stressors because they are dependent on the stability of the entire food web (Hatton et al., 2015; Ripple et al., 2015; Tyson et al., 2010). Their decline or extinction can further accelerate the destabilisation of ecological communities through cascading trophic effects (e.g., aforementioned gray wolf eradication in Yellowstone) (Beschta & Ripple, 2009; Bestion et al., 2019; Bruno & Cardinale, 2008; Estes et al., 2010, 2011; Hairston et al., 1960; Paine, 1980; Ripple et al., 2014, 2015, 2024; Terborgh et al., 2001).

This dynamic is especially evident in the Canadian Arctic and sub-Arctic, where ecosystems—ranging from tundra to northern boreal forests—have experienced Arctic amplification, a doubling of the mean annual surface temperature increase relative to the global average during the 20th century (AMAP, 2021; Gilg et al., 2012; Bengtsson et al., 2004; Rowland et al., 2016; Screen & Simmonds, 2010; Serreze & Francis, 2006). Consequences include, among others, rapid glacial and permafrost melt with an increased input of moisture to soils and ecosystems (Barber et al., 2014; Lyon & Destouni, 2010), sea ice volume decline resulting in habitat loss (Screen & Simmonds, 2010; Simmonds, 2015), Arctic tundra shrubification (Danby et al., 2011; Hope et al., 2015), altered boreal forest composition (Massey et al., 2023), and advancing alpine treelines (Munier et al., 2014; Trant et al., 2020).

These landscape-level changes can severely impact top predators of the Arctic, in particular, climatically induced habitat shifts reshape predator-prey relationships and can trigger trophic collapses (Chambault et al., 2020; Derocher et al., 2013; Fuglei & Ims, 2008; Hamilton et al., 2017; Laws, 2017). For example, polar bears depend on sea ice to hunt seals and are thus greatly impacted by the loss in sea ice volume (Derocher et al., 2004, 2013; Hamilton et al., 2017; Stirling & Derocher, 2012). This has triggered alteration in polar bear habitat use patterns, which has led to range shifts resulting in territorial overlap with other top predators (i.e., grizzly bears [*Ursus arctos horribilis* Linnaeus, 1758] and gray wolves) leading to new interspecific competition, altered predator-prey dynamics, and ecological mismatches all of which have cascading trophic effects (Derocher et al., 1993, 2000; A. N. Laws, 2017; Rode et al., 2015).

In the Canadian Arctic and northern boreal forests, these megafaunal vulnerabilities are compounded by amplified warming, which further destabilizes ecosystems and places northern megafauna—and apex predators—at risk of population collapse (Hamilton et al., 2017; Laidre et al., 2020; E. Post et al., 2009). Human disturbance (e.g., anthropogenically driven habitat loss, increased human-wildlife conflict, and overharvesting [e.g., hunting, trapping]) further intensifies these threats, pushing many species toward decline or extinction (Ordiz et al., 2021) and thus can result in cascading trophic effects (Bestion et al., 2019; Ripple et al., 2024).

Understanding the trophic roles and dietary strategies of these at-risk species—particularly apex predators—within high-latitude, rapidly changing ecosystems is therefore essential. Insight into their ecological flexibility and niche constraints can help identify thresholds of vulnerability and inform adaptive conservation measures tailored to future climate scenarios (Ripple et al., 2016, 2017; Wiens et al., 2009). Given the keystone role that apex predators hold in ecosystems (Estes et al., 2011; Ripple et al., 2024), conservation strategies must account for their long-term responses to landscape transformation, trophic disruption, and climatic instability to preserve ecosystem resilience and biodiversity (Dobson et al., 2006).

1.1.2 The importance of the fossil record to investigate ecological baselines and inform modern conservation

Modern ecological monitoring is inherently constrained by its limited temporal scope, often covering only a few decades at most. This limits the use of modern studies for conservation efforts because the processes that shape ecosystems and ecological communities, such as climate change, species adaptation, and ecological turnover, unfold over long timescales, sometimes spanning centuries and millennia (Karl and Trenberth, 2003). The short timeframes of contemporary studies make it challenging to capture the full spectrum of these processes, particularly for carnivore species with complex prey interactions and dependence on the entire ecological community. A comprehensive understanding of species' responses to climate and environmental change requires the long-term perspective that the fossil record uniquely offers (Dietl et al., 2015; Fordham et al., 2020; Lanier et al., 2015). By examining the past, we can better anticipate future ecological shifts and species vulnerabilities.

The fossil record acts as a geohistorical archive, preserving species' foraging habits, mobility patterns, and habitat use, offering invaluable insights into past ecosystems and how their inhabitants responded to past climate events (Ben-David & Flaherty, 2012). Fossil bones and teeth, in particular, retain chemical signatures—such as isotopic compositions—that reflect a consumer’s diet and surrounding environment (Bearhop et al., 2004; Ben-David & Flaherty, 2012; Bryant et al., 1996; Clementz, 2012; Luz et al., 1984). The preserved isotopic compositions in fossilized bones and teeth provide a window into ancient ecological dynamics such as but not limited to species migratory patterns (e.g., Wooller et al., 2021), diets and foraging habits (e.g., Hardy & Rowland, 2024), trophic interactions (e.g., Martin et al., 2018), niche partitioning (Warsen et al., 2014), and species responses to environmental stressors (e.g., Fox-Dobbs et al., 2008). In turn, these records allow researchers to infer how modern species may react when facing analogous ecological pressures. For example, analysis of stable isotopes revealed that polar bears showed a significant dietary shift in modern times relative to individuals of the early Holocene (11.7 ka BP to1960s), undergoing a baseline dietary shift from primarily marine-based prey, such as seals, to more terrestrial sources, including birds and their eggs`, which occurred coevally with diminishing sea ice habitats (Routledge et al., 2023). The modification of polar bear diet further emphasizes the parallels between past and present ecological changes and illustrates how some species might be able to adapt to environmental changes, while other ultra-specialized taxa might be unable to adjust their diets to the extent needed for survival (e.g. Giant pandas [*Ailuropoda melanoleuca David, 1869]* face extinction due to inflexible dietary habits; Yang et al., 2024).

1.1.3 The potential of investigating the Beringian fossil record during the terminal Pleistocene for modern species conservation

1.1.3.1 Ecology of Beringia

Beringia, a vast multicontinental landmass that connected eastern Siberia (western Beringia) to Alaska and Yukon (eastern Beringia) via the Bering Land Bridge (BLB) during the Late Pleistocene (115 to 11.7 ka BP). Unlike most of North America, which was covered by continental ice sheets, eastern Beringia remained free from glaciation due to its dry climate associated with its high surrounding topography that acted as a rain barrier (Fritz et al., 2012; Froese et al., 2009; Schwartz-Narbonne et al., 2019; Zazula et al., 2006a,b; Zimov et al., 2012). This unique environment fostered a thriving steppe-tundra ecosystem— known as the mammoth steppe— with a flora dominated by permafrost and cold-adapted grasses and sedges (Froese et al., 2009; Zimov et al., 1995).

Beringia's arid and cold climate along with the open vast grasslands made it an ideal habitat for a diverse array of cold-adapted fauna composed of herbivorous megafauna species, with grazers such as woolly mammoth (*Mammuthus primigenius* Blumenbach, 1799), Beringian horse (*Equus* sp. and *Haringtonhippus* sp.), and bison (*Bison* sp. Smith, 1758), forming the backbone of this ecosystem and roaming across vast territories (Drucker, 2022; Harington, 2011; Schwartz-Narbonne et al., 2019; Zimov et al., 2012). This thriving herbivore biodiversity was matched by a unique range of predators, from mesopredators such as hyenas (*Chasmaporthetes* Hay, 1921), foxes (*Vulpes vulpes* Linneaus, 1758 and *Vulpes lagopus* Linnaeus, 1758), and wolverines (*Gulo gulo* Linnaeus, 1758), to large apex predators like the scimitar cat (*Homotherium latidens* Owen, 1846), cave lion (*Panthera leo spelaea* Boule & De Villlleneuve, 1927), gray wolf, and giant short-faced bear (*Arctodus simus* Cope, 1879) (Bocherens, 2015; Drucker, 2022; Harington, 2011; Schwartz-Narbonne et al., 2019), with these predators holding a key role in Pleistocene ecosystems (Ripple & Van Valkenburgh, 2010). The co-existence of these apex carnivores suggests a strong niche partitioning within the ecosystem

(Bocherens, 2015; Bocherens et al., 2011; Drucker, 2022), akin to the complex predator-prey dynamics observed in modern African savannas (Drucker, 2022). Each predator likely filled specific ecological niches, relying on specialized diets and hunting behaviors that were subjective to spatiotemporal variations between western and eastern Beringia (Bocherens, 2015; Shapiro & Cooper, 2003) as demonstrated in many studies (e.g., Boeskorov et al., 2012; Knapp et al., 2009).

While the multicontinental and wide-ranging landmass of Beringia caused regional variation between western and eastern species populations such as differences in species dietary preferences and interactions (i.e., predator-prey interactions) (Bocherens, 2015; Shapiro & Cooper, 2003; Szpak et al., 2010) this thesis focuses strictly on eastern Beringian populations (i.e., interior Alaska and Yukon). Studies have suggested that in eastern Beringia scimitar cats primarily preyed on large ungulates, specifically yak (*Bos mutus* Przewalski, 1883), caribou, and bison (Yeakel et al., 2013), while cave lions favored caribou (Bocherens, 2015; Yeakel et al., 2013), with giant short-faced bears fed mainly on caribou (*Rangifer tarandus* Linnaeus, 1758), muskox (*Ovibos moschatus* Zimmermann, 1780), and possibly carcases and plants (Bocherens, 2015; Fox-Dobbs et al., 2008; Matheus, 1995; Raghavan et al., 2014), and gray wolves had a diet dominated by horses (Landry et al., 2021). This specialization of diet and behavior in eastern Beringia's apex carnivores shaped the region's complex food webs and trophic interactions (Ripple & Van Valkenburgh, 2010).

1.1.3.2 Quaternary megafauna extinction event

The disappearance of many eastern Beringian species during the terminal Pleistocene (~16−11.7 ka BP), contributed to the Quaternary megafauna extinction event, where up to 72% of North American megafauna genera went extinct (~13–11 ka BP) (Barnosky, 2008; Fox-Dobbs et al., 2008; Koch & Barnosky, 2006; Mann et al., 2015).

There are two primary hypotheses to explain the large-scale disappearance of many eastern Beringian species. The first being that the Late Pleistocene, particularly the interval following the Last Glacial Maximum (LGM, 26-19 ka BP), marked a period of significant environmental upheaval in eastern Beringia (Rowland et al., 2016). Global temperatures rose, surrounding glaciers retreated, and permafrost began to melt. This led to the rapid transformation of the mammoth steppe biome into a boreal forest with increasing shrub and tree dominance

(Hardy & Rowland, 2024; Zimov et al., 1995). These landscape and vegetation changes may have led to the extinction of many megaherbivores which had cascading effects on carnivore species (Guthrie, 2001; Monteath et al., 2021; Zimov et al., 2012).The second hypothesis states that the expansion and increased activity of human populations in eastern Beringia resulted in the overhunting of many megafauna species and increased competition for carnivores (Lorenzen et al., 2011).

A hypothesis that combines both the climate change and overkilling hypotheses suggests that the specialized diets, high metabolic demands and energy constraints (Carbone et al., 1999) and slow reproductive rates and population recovery of megafauna limits their resilience to ecological changes caused by climate/landscape change and overkilling/competition from increased human activity (Albaladejo-Robles et al., 2023; Cardillo et al., 2005; de Silva & Leimgruber, 2019; Ordiz et al., 2021).

Overall, this widespread megafauna extinction had drastic effects on the Beringian ecosystem, including but not limited to altered species interactions (prey-predator dynamics) and changes in plant biomes (Monteath et al., 2021, 2022; Murchie et al., 2021; Piers et al., 2015, 2018; Doughty et al., 2016; Lyons et al., 2016; T´oth et al., 2019; Pineda-Munoz et al., 2021). Some species, such as caribou, muskox, Dall sheep (*Ovis dalli* Nelson, 1884), moose (*Alces alces* Linnaeus, 1758), and elk, persisted and still inhabit modern Alaska and Yukon. By the beginning of the Holocene, one of the few apex predators to survive extinction and persist into the modern day is the gray wolf.

Reconstructing the diets and trophic interactions of Pleistocene megafauna is central to understanding why certain species prevailed or went extinct during this period of environmental and ecological upheaval in the terminal Pleistocene. Through isotopic analysis of fossilized remains, we can investigate the diets of species during these long-term environmental and ecological changes (Clementz, 2012). For example, studies of the dietary habits of Beringian carnivores such as the gray wolf provide insights into their adaptive strategies during the Quaternary extinction event (Landry et al., 2021). Understanding how apex predators in Beringia responded to past ecological shifts can thus provide critical insights into the resilience of modern carnivores and inform conservation strategies aimed at preserving top predators in rapidly changing ecosystems (Dietl et al., 2015; Fordham et al., 2020).

1.1.3.3 The terminal Pleistocene extinction in eastern Beringia as an analog to modern global warming and human interference

The expansive fossil collection and quality of remains from eastern Beringia due to the cold climate and permafrost layer (Matsubayashi & Tayasu, 2019; Matthiesen et al., 2021) in Beringia and the Canadian Arctic makes this region ideal for palaeobiological studies (Fordham et al., 2020), of which can provide insights to past ecological dynamics. Trophic and dietary reconstructions of both extant and extinct northern species—spanning modern and Pleistocene ecosystems—using stable isotope proxies (e.g., Schwartz-Narbonne et al., 2019) and complementary techniques, offer critical insights into past ecological dynamics, of which is essential for informing contemporary conservation strategies, particularly for vulnerable megafauna and apex predators (Dietl et al., 2015; Fordham et al., 2020; Ripple & Van Valkenburgh, 2010). This is especially relevant in the Canadian Arctic and northern boreal forest biomes, which are undergoing climate-driven changes analogous to those during the terminal Pleistocene (i.e., increased temperatures, permafrost melt, shrubification, etc.,).

1.1.3.4 Wolves as an ideal study species for investigating carnivore response to climate and ecological changes

Gray wolves are an ideal species for investigating species' responses to environmental and ecological change in northern Canadian ecosystems. Their persistence from the terminal Pleistocene to the present-day allows for direct comparison between populations which experienced different climates, landscapes, and ecological conditions, thus allowing us to understand how this carnivorous species responded during climate and ecological changes over large timescales. There have been extensive ecological studies that have documented their current dietary habits (e.g., Dalerum et al., 2018; Evavold et al., 2024; Gable et al., 2018; Gauthier & Theberge, 1986; Hayes, 1995; Hayes et al., 2000, 2016; Hayes & Harestad, 2000; Merkle et al., 2017; Milakovic & Parker, 2011; Pilot et al., 2012). In Alaska and the Yukon, modern gray wolves are pack hunters and primarily prey on caribou, but their diet also includes smaller mammals such as beaver, snowshoe hare (*Lepus americanus* Erxleben, 1777), Arctic ground squirrel (*Urocitellus parryii* Richardson, 1825), and groundhog (*Marmota monax* Linnaeus,1758), depending on regional prey availability and seasonal variability (Dalerum et al., 2018; Gauthier & Theberge, 1986; Hayes, 1995, 2016; Hayes & Harestad, 2000; Merkle et al., 2017). By contrast, isotopic analyses from fossil material indicates that Pleistocene gray wolves in eastern Beringia had a more specialized diet heavily reliant on megafaunal herbivores (Bocherens, 2015; Fox-Dobbs et al., 2008; Landry et al., 2021). Landry et al. (2021) demonstrated that eastern Beringian Pleistocene wolves exhibited high $\delta^{13}C$ and $\delta^{15}N$ values consistent with a high trophic position and consumed mainly the flesh of large-bodied ungulates, particularly Beringian horses.

Genetic studies further support the uniqueness and evolutionary significance of Beringian gray wolves as shown in Loog et al. (2020). This study showed how contemporary gray wolf populations descended from the expansion of Beringian gray wolves following the LGM (Loog et al., 2020). Understanding why Beringian gray wolves survived, while other wolf lineages were replaced and other carnivore species went extinct, requires reconstruction of their dietary habits, habitat use, and interactions with changing prey communities. These insights are critical for understanding past ecosystem dynamics which can inform modern conservation efforts under ongoing climate change (Barnosky et al., 2017; Dietl et al., 2015; Fordham et al., 2020) .

1.1.4 Insights from traditional palaeodietary proxies ($\delta^{13}C$ and $\delta^{15}N$)

1.1.4.1 Review of carbon and nitrogen stable isotopes as dietary proxies

Stable isotope analysis (SIA) is a powerful and widely used tool to reconstruct diet and trophic interactions in both modern and ancient ecosystems (Clementz, 2012; DeNiro & Epstein, 1978, 1981; Fry, 2006). Carbon and nitrogen stable isotope compositions (i.e., $\delta^{13}C$ and $\delta^{15}N$, respectively) (Deniro & Epstein, 1978, 1981) provide biochemical signatures of an organism's diet and environment due to predictable isotopic fractionation during food digestion, assimilation, and ultimately during tissue and biologic mineral synthesis (Koch, 2008). These isotopic signals are preserved in tissues with slow turnover rates (i.e., bone), which allows them to reflect long-term dietary and environmental information (Clementz, 2012).

During collagen synthesis proteins that are enriched in the heavy stable carbon isotope (^{13}C) are preferred, influencing the bulk $\delta^{13}C$ value of the collagen and an approximate +5‰ offset between collagen and bulk diet (Ambrose & Norr, 1993; DeNiro & Epstein, 1978; Lee-Thorp et al., 1989; Tieszen & Fagre, 1993). In general, $\delta^{13}C$ values in collagen slightly increase with increasing trophic position, with an approximate $\delta^{13}C$ trophic discrimination factor (TDF) of

+1‰ (Bearhop et al., 2004; Bocherens, 2015; Bocherens & Drucker, 2003; Jim et al., 2006), with apex predators having the highest $\delta^{13}C$ values and primary producers having the lowest $\delta^{13}C$ values (Pilot et al., 2012). However, varying diets can result in some variation in the TDF among species and individuals complicating its use as an unambiguous dietary proxy (Bearhop et al., 2004; Caut et al., 2009).

Differences in photosynthetic pathways are a primary driver of $\delta^{13}C$ variation, as C_3 and C_4 plants differentiate the heavy and light carbon isotope to varying degrees (O'Leary, 1981, 1988). These effects cascade through the trophic chain and result in distinctions between C_3 vs C_4 plant feeding herbivores (Cerling & Harris, 1999; Codron et al., 2013; Jim et al., 2006; Tieszen, 19a). In carnivores, $\delta^{13}C$ variation is due to consumption of different prey species and the type of tissues consumed (i.e., muscle, fat, bone marrow, etc.,) (Ambrose & Norr, 1993; Lee-Thorp et al., 1989; Tieszen & Fagre, 1993, Tieszen, 1991). In the context of high-latitude systems like Beringia and the Yukon, where ecosystems are dominated by C_3 plants (Blinnikov et al., 2011; Tahmasebi et al., 2017; Wooller et al., 2007; Zazula, et al., 2006b), $\delta^{13}C$ variation among herbivores—and thus among carnivores—is not due to plant type (C_3 vs C_4). This can limit the distinction between species $\delta^{13}C$ values in these ecosystems (e.g., Landry et al., 2021), but some isotopic distinction may still be observed among plants (Kohn et al., 2010) and animal species (i.e., foregut and hindgut fermenters) (Cerling et al., 2021).

Nitrogen isotopes in bone collagen are reflective of the proteins from a consumer's diet, allowing for dietary and trophic reconstructions (Bocherens & Drucker, 2003). The light nitrogen isotope (^{14}N) is preferentially fractionated out of the body through waste products (i.e., urine) (Deniro & Epstein, 1981; Minagawa et al., 1984). The preferential fractionation of ^{14}N results in an increase in $\delta^{15}N$ between adjacent trophic levels, with a TDF of +3 to +5‰ (Bocherens & Drucker, 2003; Deniro & Epstein, 1981; Minagawa et al., 1984), thus apex predators have the highest $\delta^{15}N$ values compared to those of secondary consumers due to cumulative trophic enrichment, with primary producers (i.e., plants) having the lowest $\delta^{15}N$ values.

To more precisely infer the feeding strategies of modern and extinct carnivores, like Pleistocene gray wolves, dietary mixing models (i.e., Bayesian stable isotope mixing models [BSIMMs]) can be applied using $\delta^{13}C$ and $\delta^{15}N$ values of both predators and their potential prey (e.g., Cheung & Szpak, 2021; Fox-Dobbs et al., 2007; Landry et al., 2021). These models estimate the proportional contributions of different prey species to a predator's diet by integrating isotopic data and known trophic discrimination factors (TDFs). Bayesian mixing models, such as those implemented in MixSIAR or SIAR, allow for probabilistic reconstructions that incorporate uncertainty and variability in prey isotope values and TDFs (Stock, 2025). Landry et al. (2021) applied this approach to reconstruct the diet of Pleistocene wolves in eastern Beringia.. This study demonstrated that Pleistocene wolves have a high reliance on Pleistocene megafauna, particularly Beringian horses with approximately 54% contribution to their overall diet. By contrast, modern wolves have lower $\delta^{13}C$ and $\delta^{15}N$, and as shown in other studies, predominantly feed on caribou, moose and small mammals (i.e., beavers, snowshoe hare and arctic ground squirrel) (Dalerum et al., 2018; Gauthier & Theberge, 1986; Hayes, 1995; Hayes & Harestad, 2000; Merkle et al., 2017). Landry et al. (2021) contributed valuable insights into Beringian carnivore palaeoecology through $\delta^{13}C$ and $\delta^{15}N$ analysis, while also demonstrating the complexity of interpreting these isotopic systems due to various environmental and ecological influences.

1.1.4.2 Limitations of carbon and nitrogen stable isotopes as dietary proxies

While carbon and nitrogen isotopes have proven powerful tools for reconstructing modern and ancient diets and trophic positions, their interpretation can be confounded by environmental variables (Drucker et al., 2008; Heaton, 1999; Heaton et al., 1986), especially in dynamic ecosystems like Beringia (Drucker, 2022). This region experienced dramatic climatic shifts over time—from the cold, dry tundra-steppe conditions of the Pleistocene mammoth steppe (Alfimov & Berman, 2001; Brigham-Grette, 2001; Elias, 2000; Froese et al., 2009; Guthrie, 1982; Pushkar & Cherepanova, 2011) to the warmer, wetter, and more forested conditions of the Holocene and modern boreal environment (Aalto et al., 2022; Kemppinen et al., 2023). These environmental transitions directly influence isotopic baselines in plants and soils, which are then propagated up the food web, and can make it difficult to disentangle changes in diet from changes in the underlying isotopic landscape (Casey & Post, 2011).

Nitrogen isotopes are particularly sensitive to environmental conditions such as moisture and soil microbial activity (Craine, Brookshire, et al., 2015; Craine, Elmore, et al., 2015; Craine et al., 2009). During the Last Glacial Maximum (LGM ~26-19ka BP), significant climate and environmental shifts (i.e., colder temperatures, glacial advance, increased aridity) decreased moisture levels and profoundly influenced the nitrogen cycle, as suggested by increased $\delta^{15}N$ values in megafaunal remains from this time (Rabanus-Wallace et al., 2017). In arid and semi-arid environments where there is minimal precipitation and dry soil, inorganic nitrogen is not well retained, resulting in increased nitrogen cycling (Cleveland et al., 1999; Olson, 1958). This inhibits nitrogen fixation in plants and increases denitrification and volatilization processes, both of which fractionate ^{14}N out of the soil, reducing its abundance, resulting in increased $\delta^{15}N$ values in the soil and then plants (Ambrose, 1991; Amundson et al., 2003; Handley et al., 1999; Heaton, 1987; Hixon et al., 2018; Rabanus-Wallace et al., 2017; Stevens et al., 2004; Stevens et al., 2008). Since nitrogen isotopes cascade up the food chain from primary producers, the elevated $\delta^{15}N$ will be reflected in all trophic levels in that ecosystem (Ambrose, 1991; Schwartz-Narbonne et al., 2019; Stevens et al., 2008). During periods of warmer and less arid climates—such a modern Yukon and interstadial periods in eastern Beringia during the Pleistocene—increased moisture leads to enhanced nitrogen loss through leaching and denitrification, lowering the $\delta^{15}N$ of soil and plants, which is reflected through the trophic levels. These baseline shifts complicate trophic interpretations as variations in $\delta^{15}N$ values may reflect environmental change more than dietary behavior (Casey & Post, 2011), thus not allowing for direct comparison between varying ecosystems, regions and/or time periods without considering this baseline effect.

Carbon isotopes, though more stable across trophic levels (Bearhop et al., 2004; Bocherens, 2015; Bocherens & Drucker, 2003; Jim et al., 2006) are also environmentally dependent. Plant $\delta^{13}C$ values vary depending on canopy structure (Bonafini et al., 2013; Drucker et al., 2008; van der Merwe & Medina, 1991), water use efficiency (Dawson et al., 2002; Heaton, 1999; Tieszen, 1991), and primary productivity (O'Leary, 1981, 1988; Tieszen, 1991). In open and dry environments —such as the steppe tundra in eastern Beringia during the Late Pleistocene— plants are exposed to direct sunlight and limited water, leading to higher water-use efficiency and increased $\delta^{13}C$ values (Diefendorf et al., 2010; Kohn, 2010; Tieszen, 1991; Wooller et al., 2007). As the eastern Beringian landscape transitioned to boreal forest, increased moisture and canopy cover introduced the "canopy effect," whereby understory plants assimilated recycled CO_2 depleted in ^{13}C, lowering their $\delta^{13}C$ values (Bonafini et al., 2013; Drucker et al., 2008). Such variations are further complicated by altitude, temperature (Heaton, 1999; Kohn, 2010), and plant physiology (Diefendorf et al., 2010; Tieszen, 1991). Consequently,

$\delta^{15}N$ and $\delta^{13}C$ values in Beringian species like wolves may reflect not just prey composition, but also broader shifts in ecosystem structure and plant communities.

Beyond environmental effects, the material from which carbon and nitrogen isotopes are extracted (i.e., bone collagen), poses another major limitation for some (palaeo-)ecological studies. Collagen is a labile organic protein that degrades relatively rapidly post-mortem due to microbial activity, oxidation, and hydrolysis (Collins et al., 2002; Hedges, 2002). This degradation alters the original isotopic composition, particularly through the preferential loss of specific isotopes, leading to altered isotope compositions in older or poorly preserved specimens (Balzer et al., 1997). Diagenetic processes, including remineralization and contamination by exogenous carbon and nitrogen from soils and groundwater, further obscures the original dietary signal (Gillespie et al., 1984). As a result, collagen-based isotopic analyses are only reliable when the material passes strict preservation criteria (i.e., C:N ratios [ideally 2.9–3.6]) which reflects well preserved collagen (Ambrose, 1990; Deniro et al., 1985). Bone degradation and specimen preservation can vary dramatically depending on burial conditions, soil chemistry, and time since deposition (Matthiesen et al., 2021; Nielsen-Marsh & Hedges, 2000).

Given these limitations, relying solely on collagen-bound $\delta^{13}C$ and $\delta^{15}N$ values in Beringian wolves and other carnivores as dietary proxies can introduce significant uncertainty and ambiguity. Shifts in environmental baselines due to climate change and the potential conflation of dietary and ecological signals (Casey & Post, 2011), along with the varying preservation of specimens (Matthiesen et al., 2021), highlight the need for additional complementary dietary proxies. Robust, more diagenetically resistant materials—such as tooth enamel (Dodat et al., 2023)—offers promising avenues for dietary reconstruction, especially when paired with multi-isotope approaches or compound-specific techniques. Ultimately, a more nuanced understanding of trophic dynamics in Pleistocene ecosystems like Beringia requires expanding beyond traditional collagen isotopes to include proxies that can better withstand diagenesis and ecological complexity.

1.1.5 Calcium, strontium and barium in hydroxyapatite

Carbonated hydroxyapatite (HAp [$Ca_{10}(PO_4)_6(OH)_2$]), a calcium apatite mineral composing most of the bone and teeth inorganic component, is thermodynamically stable and relatively resistant to diagenesis (i.e. post-burial chemical alteration) (Lee-Thorp & Sponheimer, 2003; Sponheimer & Lee-Thorp, 2006; Tacail et al., 2020; Wang & Cerling, 1994). The resistant nature, stability, and preservation of HAp over geologic time makes it an ideal material in palaeobiological studies, specifically the ratios of Sr/Ca and Ba/Ca and isotopes in HAp have been proposed as indicators of diet and trophic level (Balter et al., 2002; Safont et al., 1998; Toots & Voorhies, 1965).

1.1.5.1 Strontium and barium ratios a dietary proxy

Interestingly, Ca, Ba, and Sr are incorporated into the body from diet and Sr and Ba can easily replace Ca in the HAp crystal structure due to the substitutive flexibility of HAp and the similarities between Sr, Ba, and Ca (i.e., ionic radii and charge) (Elliott, 2019; Posner & Betts, 1975). Among vertebrate animals, calcium is preferentially retained over strontium and barium in the body (and by extension in the HAp crystal structure) as it is an essential element for various bodily functions (i.e., muscle contraction, cellular signaling, and bone/teeth formation, etc.,). As a result, by means of different cellular and physiological processes, strontium and barium are preferentially excreted from the body via urine and stool (Burton & Wright, 1995; Harrison et al., 1967; Pors Nielsen, 2004; Sillen & Kavanagh, 1982). The depletion of strontium and barium relative to calcium results in low Sr/Ca and Ba/Ca ratios incorporated into bone/teeth relative to consumer diet (Burton & Wright, 1995; Sillen & Kavanagh, 1982). This effect cascades through trophic levels due to the biopurification of strontium and calcium incremented at every level of the food chain (Burton & Wright, 1995; Sillen & Kavanagh, 1982). Thus, apex predators will have the lowest Sr/Ca and Ba/Ca ratios compared to that of herbivores, with plants having the highest Sr/Ca and Ba/Ca ratios. The ingestion of bone in carnivores can contribute to increased proportions of calcium in their diet, which can further dilute strontium and barium and decrease Sr/Ca and Ba/Ca ratios and influence calcium isotopes (Schoeninger, 1979).

Despite the usefulness of Sr/Ca and Ba/Ca ratios as dietary and trophic level proxies, several factors complicate their interpretation. One major concern is diagenetic alteration, as post-mortem chemical alteration can modify the original elemental composition of HAp. While

HAp is more resistant to diagenesis than carbonates for example, it is still susceptible to elemental exchange with surrounding sediments and groundwater over time (Kohn, 2008; Trueman et al., 2008). Strontium and barium being only present in trace concentrations within HAp, even restricted amounts of exchange with the substrate can heavily affect resulting Sr/Ca and Ba/Ca ratios (Fabig & Herrmann, 2002). Additionally, environmental variables such as local soil geochemistry, plant mineral content, and differences in water sources can influence the baseline Sr/Ca and Ba/Ca values independently of trophic level, leading to potential overlap between dietary groups, and incomparability among distinct sites and time periods (Blum et al., 2000; Burton et al., 1999; Land et al., 2000; Peek & Clementz, 2012). As such, careful screening for diagenesis, as well as contextual environmental and ecological information, is essential to accurately interpret Sr/Ca and Ba/Ca signals in fossil tissues.

1.1.5.2 Stable calcium isotopes as a dietary proxy

One of the most promising tools currently available for dietary reconstruction in recent and deep geologic time are calcium isotopes. Most of calcium in the body is stored in HAp, and calcium is a major component of HAp with ~40 wt% Ca in bioapatite (Tacail et al., 2020). Through the small intestine, calcium is absorbed from the diet into the body through passive paracellular diffusion and active transcellular transport (Skulan & DePaolo, 1999; Tacail et al., 2020).

Calcium then circulates through the blood and is utilized in various physical processes including bone mineralization (Skulan & DePaolo, 1999; Tacail, 2017). Calcium excretion to primary urines and its partial reabsorption from primary urines back into the blood in the kidneys plays a critical role in the isotope fractionation and conditioning the calcium isotope composition of the body (Tacail, 2017; Tissot et al., 2024). During this process, light calcium isotopes (^{40}Ca and ^{42}Ca) will be preferentially reabsorbed from primary urines to the blood, resulting in urine being enriched in heavy calcium isotopes (^{44}Ca and ^{43}Ca), and the blood (and consequently the rest of the body) being comparatively depleted in heavy calcium isotopes (i.e. enriched in light calcium isotopes) (Tacail, 2017; Tissot et al., 2024). During the incorporation of calcium into hard tissues (i.e., bone and teeth) through biomineralization, further fractionation (of debated degree) can occur with light calcium isotopes being preferentially incorporated into HAp (Hassler et al., 2021a; Heuser et al., 2016; Skulan & DePaolo, 1999; Tacail, 2017; Toepfer et al., 2021). The result of the combined effect of all physiological fractionations on calcium isotopes, is that HAp in bones and teeth are depleted in heavy calcium isotopes relative to the source diet, with an offset of calcium isotope ratios between diet and HAp (generally expressed as $\delta^{44/42}$Ca and $\delta^{44/40}$Ca) remaining similar across mammalian species (Skulan & DePaolo, 1999; Tacail et al., 2020).

The predictable fractionation of calcium isotopes in HAp has two consequences; first, calcium isotope compositions from bones and teeth can be linked to diet composition, allowing for modern and palaeodietary identification (Assemat et al., 2024; Chu et al., 2006; Hassler et al., 2018; Skulan & DePaolo, 1999; Tacail et al., 2020). Second, the diet to HAp offset bioaccumulates through trophic levels, further fractionating at each level along the food chain and therefore informing about (palaeo-)ecosystem structures (Dodat et al., 2021; Hassler et al., 2018; Martin et al., 2015, 2017, 2018; Weber et al., 2025). Notably, apex predators will have the lowest $\delta^{44/42}$Ca (or $\delta^{44/40}$Ca) values compared to that of secondary consumers (herbivores), with primary producers having the highest $\delta^{44/42}$Ca (or $\delta^{44/40}$Ca) values (Martin et al., 2015, 2017, 2018). It is important to acknowledge that the literature contains a certain number of cases where linking calcium isotopes to diet or trophic level is complicated by specific physiological processes or behaviors (Hassler et al., 2021a,b; Martin et al., 2017, 2018). However, some of these factors (e.g. dairy consumption during nursing and lactation in mammals) can be accounted for to reveal accurate trophic information (Hassler et al., 2021a,b).

Calcium isotopes offer several advantages when used in combination with carbon and nitrogen isotopes for dietary reconstructions. Like carbon and nitrogen, calcium isotopes vary with diet and trophic level, but they can further the distinction between monogastric organisms (e.g., humans, carnivores, pigs, horses, woolly mammoths, hares, squirrels) and polygastric ruminants (e.g., deer, cattle, sheep, goats, moose) (e.g., Guiserix et al., 2024; Hu et al., 2022; Martin et al., 2018), of which has also been observed in carbon and nitrogen stable isotopes to a certain degree (Cerling et al., 2021; Sponheimer et al., 2003). Moreover, calcium in HAp in bones and teeth is significantly more resistant to diagenesis than collagen-bound carbon and nitrogen extracted from fossil tissues, enabling dietary inferences in fossil material that would otherwise be unsuitable for traditional stable isotope analysis (Dodat et al., 2023; Martin et al., 2017). While more resistant to diagenetic alteration, calcium isotopes —particularly in bone—

may still be susceptible to alteration such as adsorption or substitution processes during fossilization (Dodat et al., 2023). Thus, testing for diagenetic alteration of specimens is still recommended. Enamel is the preferred substrate for stable isotope dietary and trophic reconstructions, as calcium isotopes, in particular, are more resistant to diagenetic alteration than bone (Dodat et al., 2023).

Finally, calcium isotopes fractionate within plants during uptake and translocation from roots to leaves (Cobert et al., 2011; Holmden & Bélanger, 2010; Moynier & Fujii, 2017; Schmitt, 2016; Schmitt et al., 2012), which widens the baseline of calcium isotopic composition at the basis of the food chain. This can complexify conversions from calcium isotopic composition directly to trophic level, by generating overlap between primary and higher-level consumers, which in turn provides a great opportunity to study niche partitioning among individuals of the same trophic level (Martin et al., 2017), as demonstrated by studying the niche partitioning of apex predators in the African savanna (Martin et al., 2018). Consequently, calcium isotopes are likely complementary, more broadly applicable, and more robust than carbon and nitrogen isotopes making them an ideal proxy to be used in combination with carbon and nitrogen isotopes to test for gray wolf dietary shifts during the Pleistocene-Holocene transition.

Since HAp is not susceptible to organic degradation like collagen, calcium isotopes are applicable to deep-time studies (>2.6 Ma) in which carbon and nitrogen isotopes cannot be applied as dietary and trophic proxies (e.g., Martin et al., 2022). They are also useful for extant and recent geologic time fossil dietary and trophic reconstruction due to its robust nature, strong trophic partitioning, and additional species isotopic separation (e.g., Hassler et al., 2018; Martin et al., 2015). Since calcium isotopes can be applied to a wide range of geologic time periods and epochs, they are ideal for the comparison of extinct and extant species diets and trophic relationships (e.g., Martin et al., 2018), and provide an intriguing and as of yet unexplored means by which to compare the diets of modern and Pleistocene gray wolves.

1.2 Thesis objectives and hypotheses

1.2.1 Objectives

The overarching aim of this thesis is to evaluate the potential of novel palaeodietary proxies—specifically $\delta^{44/42}$Ca, Sr/Ca, and Ba/Ca—alongside traditional isotopic methods (δ^{13}C and δ^{15}N) in reconstructing the dietary habits of gray wolves over the past 50,000 years in eastern Beringia. By incorporating these novel proxies, we seek to provide a more robust and comprehensive understanding of trophic interactions and dietary shifts in wolves, particularly in relation to ecological and climate changes.

1.2.1.1 Objective 1: Methodological Development of New Dietary Proxies

The first objective of this study is methodological in nature and aims to test the incorporation of new dietary proxies in reconstructing the diet of gray wolves. Specifically, I will analyze $\delta^{44/42}$Ca, Sr/Ca, and Ba/Ca in tooth enamel in conjunction with δ^{13}C and δ^{15}N from bone collagen to assess the dietary habits of Pleistocene and modern wolves. This objective will be pursued through the following steps:

1. Selection of fossil wolves and potential prey: I first selected series of remains of wolves from Beringia and the Yukon territory and their prospective prey from the Pleistocene and Holocene periods to ensure representative samples from each time period.

2. Radiocarbon Dating: All selected fossil specimens were radiocarbon dated if not previously done so, ensuring accurate temporal control and facilitating classification into distinct age bins.

3. Isotopic Analysis: I conducted isotopic and elemental analyses, including δ^{13}C, δ^{15}N, and $\delta^{44/42}$Ca, Sr/Ca, and Ba/Ca, of bone collagen and tooth enamel of the selected fossils, respectively. During this step it is key to ensure that specimens are not compromised by diagenesis, through rigorous checks and the production of high-quality, reliable data.

By completing this first objective, I will demonstrate the feasibility of using multiple isotopic proxies in a single model species to assess diet, providing a more nuanced view of dietary shifts and trophic relationships in ancient and modern wolves using novel dietary proxies ($\delta^{44/42}$Ca, Sr/Ca and Ba/Ca).

1.2.1.2 Objective 2: Ecological Refinement and Isotopic Mixing Models

The second objective is more ecologically focused and is centred around refining the interpretation of wolf diets using the newly incorporated proxies in multi-isotope mixing models. This objective involves testing whether the addition of $\delta^{44/42}$Ca, Sr/Ca, and Ba/Ca provides new insights into the dietary shifts of wolves from the Pleistocene to the Holocene. Specifically, I will build increasingly complex multi-isotope mixing models (using δ^{13}C, δ^{15}N, $\delta^{44/42}$Ca, Sr/Ca, and Ba/Ca) to test whether the isotopic data can refine the understanding of wolves' dietary shifts. This will help us in terms of assessing if wolves were highly specialized carnivores during the Pleistocene, feeding primarily on horses, and whether they became more generalist in the Holocene, as shown by previous studies (e.g., Landry et al., 2021).

Through this objective, I seek to understand whether the introduction of novel dietary proxies can enhance the ability to reconstruct the dietary ecology of gray wolves and, more broadly, to assess the role of dietary flexibility in their survival during periods of significant ecological change.

1.2.2 Hypotheses

I hypothesized that the results of this study will align with those of previous research, indicating a dietary shift occurred in gray wolves from horses in the Pleistocene to a wider array of large ungulates and small prey in the Holocene (e.g., Bocherens, 2015; Dalerum et al., 2018; Fox-Dobbs et al., 2007; Hayes, 1995, 2016; Hayes & Harestad, 2000; Landry et al., 2021; Merkle et al., 2017). Additionally, I expect that the inclusion of $\delta^{44/42}$Ca, Sr/Ca, and Ba/Ca isotopes will add a new dimension to the understanding of this dietary shift, further supporting or challenging the idea that wolves exhibited dietary flexibility that contributed to their resilience throughout ecological and climatic transitions. Finally, I anticipate that the addition of these novel proxies will demonstrate their potential for broader application in palaeobiological studies, particularly in reconstructing trophic relationships and dietary habits across time.

2 Methodology

The flowchart in Figure 1 summarizes the sample processing and analytical steps (i.e., A: Sampling and enamel pre-treatment, B: Bone pre-treatment and collagen extraction, C: Carbon and nitrogen isotope analysis in collagen, D: Radiocarbon analysis in collagen, E: Elemental analysis in enamel, F: Calcium purification and calcium isotope analysis, and G: statistical analysis)

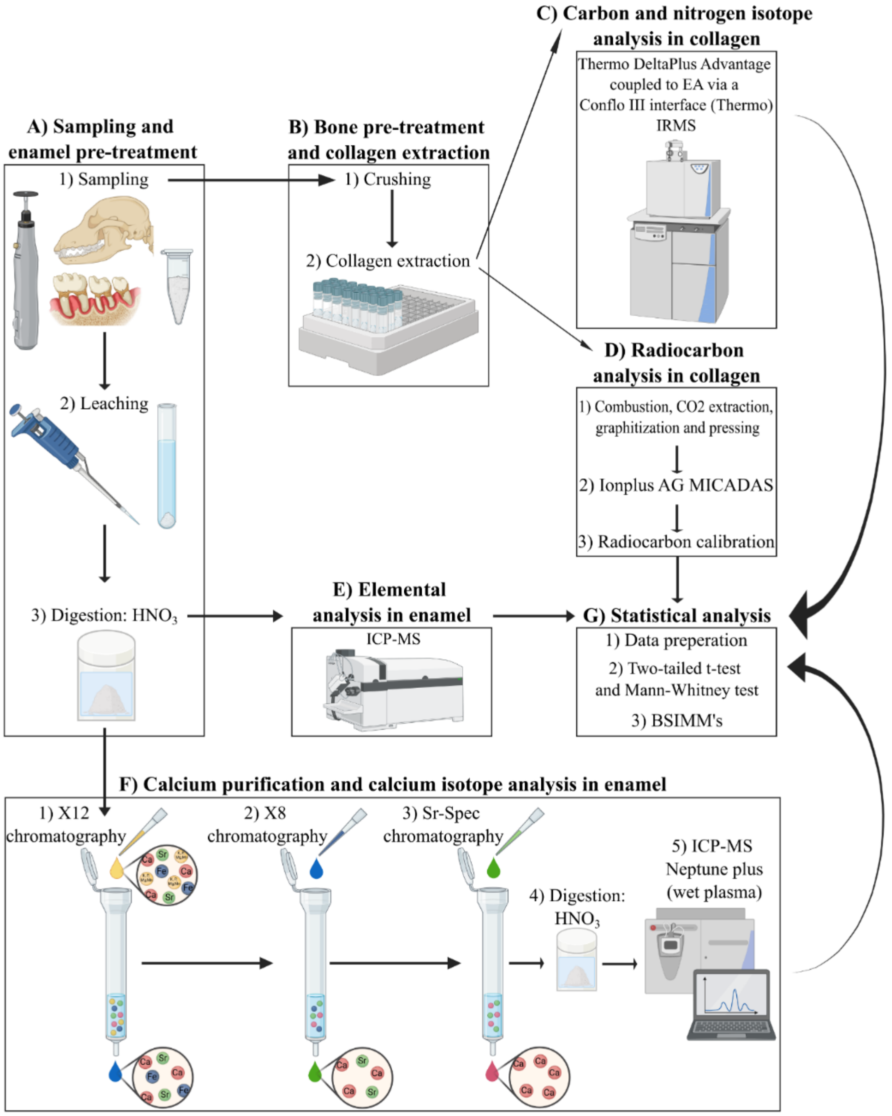

Figure 1. Flowchart summarizing the methodological framework used in this thesis. The workflow includes A) Sampling and enamel pre-treatment; B) Bone pre-treatment and collagen extraction; C) Carbon and nitrogen isotope analysis in collagen; D) Radiocarbon analysis in collagen; E) Elemental analysis in enamel; F) Calcium purification and calcium isotope analysis; and G) Statistical analysis.

2.1 Specimen selection

All the Beringian fossil (leached, *n*=41) and modern (not leached, *n*=30) specimens sampled in this study are from the Yukon territory and were obtained from the Canadian Museum of Nature (CMN) Palaeobiology and Quaternary Zoology collections, respectively, with a total of 71 specimens sampled in this study. The specimens that were not radiocarbon dated and/or analyzed for $\delta^{13}C$ and $\delta^{15}N$ in this study were obtained from Landry et al., 2021 (i.e., EL110, EL112, EL115, EL118, EL122, EL136, EL137, EL138, EL139, EL140, EL141, EL142, EL143, EL144, EL145, EL146, EL147, EL149, EL150, EL1551, EL152, EL153, EL159, EL160, EL161, EL162 EL163, EL220, EL223, EL224, and EL226). Horse specimens (i.e., EL229, EL230, EL231, EL232, and EL233) were radiocarbon dated and analyzed for $\delta^{13}C$ and $\delta^{15}N$ by Zoe Landry in 2024 as part of her PhD thesis (Landry et al. in prep). The remainder of specimens were radiocarbon dated and underwent stable carbon and nitrogen isotope ratio analyses in this study. All specimens analyzed in this study underwent stable calcium isotope ratio and elemental analyses.

The rationale for species selection was based on known modern and Pleistocene gray wolf prey preferences from previous studies (e.g., Bocherens, 2015; Dalerum et al., 2018; Fox-Dobbs et al., 2007; Hayes, 1995, 2016; Hayes & Harestad, 2000; Landry et al., 2021; Merkle et al., 2017). The species analyzed in this study are Arctic ground squirrel (*n*=3*)*, bison (*n*=5*)*, caribou (*n*=10*)*, Dall sheep (*n*=5*)*, horse (*n*=5*)*, moose (*n*=5*)*, muskox(*n*=1*)*, snowshoe hare (*n*=3*)*, woolly mammoth (*n*=5*)* and gray wolf (*n*=29). Specimens of these species were selected for sampling based on the following criteria:

1) Sample sites were localized within approximately 250 km of Dawson or Old Crow in the Yukon, to the best of my ability. I have four samples located within 350km of Whitehorse, Yukon. Local geology and environmental conditions are known to influence isotope compositions (see Chapter 1 for further details), so by minimizing the study region I attempted to minimize potential noise in the isotopic compositions that may be derived from locality (Figure 2). Unfortunately, site locations were located within distinct geochemical provinces of Yukon (MacFarlane, 2022) (Figure 2) leading to potentially different diagenetic history. To avoid any effect of differential diagenesis cause by specimen locality, all Pleistocene fossil samples underwent pre-treatment chemical leaching to remove any potential diagenetic overprinting.

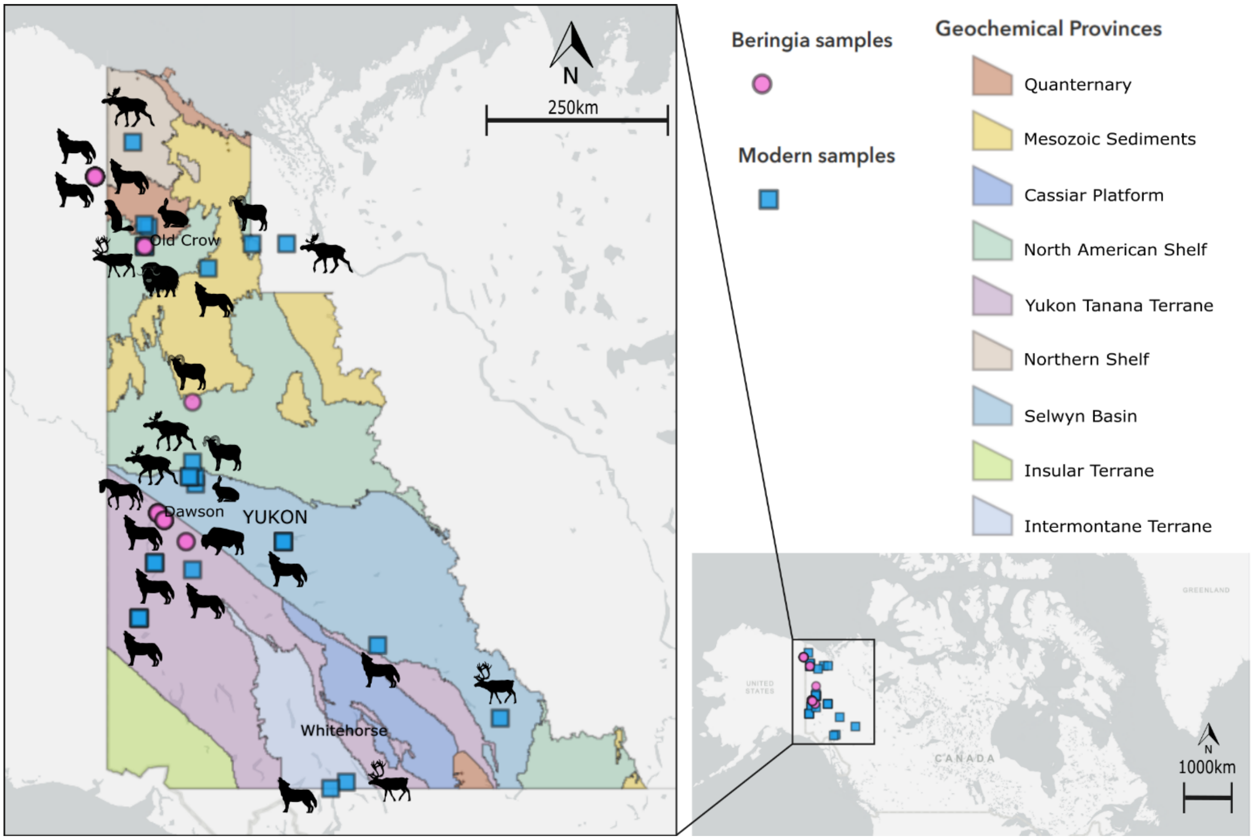

Figure 2. Geographic distribution of Beringian fossil (pink circles) and modern samples (blue squares) analyzed in this study, across present-day Yukon Territory, particularly constrained around the Dawson and Old Crow regions. The species type of each specimen is indicated by the animal silhouettes. The map includes geochemical provinces across Yukon (MacFarlane, 2022), illustrating that specimens originate from a diverse range of geological and geochemical settings.

2) A well-preserved tooth that erupted post-weaning. Due to the varying tooth mineralization and eruption sequences and varying nursing/weaning ages between mammal species, the targeted tooth for sampling for stable isotope and elemental concentration analyses varies between species and is summarized in Table 1. Sampling the tooth that erupted post-weaning creates consistency across the dataset containing various species and ensures that the stable isotope compositions reflect the adult diet by minimizing the effect of nursing/weaning (e.g., Martin et al., 2020; Tacail et al., 2017). For the small mammals (i.e., Arctic ground squirrel and snowshoe hare), the teeth were too small and the enamel too thin to accurately sample only enamel, so bone was preferentially sampled for these species for all analyses in this study.

Table 1. Tooth targeted for enamel sampling for each species.

Note: Arctic ground squirrel and snowshoe hare teeth were too small for enamel sampling, thus bone was sampled instead.

Species	Tooth targeted for enamel sampling
Gray wolf	P4 or M1
Arctic ground squirrel	N/A
Bison	M3
Caribou	M3
Dall Sheep	M3
Horse	P4
Moose	M3
Muskox	M3
Snowshoe hare	N/A
Woolly mammoth	M3 "M6"

3) A well-preserved (i.e., cortical bone) mandible or maxilla for collagen extractions for radiocarbon and/or stable carbon and nitrogen isotope ratio analyses. Dense bones such as cortical or mandibular bones are known to better preserve collagen than porous bones (Ásmundsdóttir et al., 2024; Matsubayashi & Tayasu, 2019; Suarez et al., 1996). Extraction of quality collagen is key to obtaining robust radiocarbon and isotope data.

2.2 Isotope and Elemental Analyses

2.2.1 Radiocarbon dating and carbon and nitrogen isotope analysis in collagen

2.2.1.1 Bone sampling

The mandible or maxilla of specimens that required stable carbon and nitrogen isotope ratio analyses and/or radiocarbon dating were sampled using a low-speed Dremel tool at the CMN. A surface area of the cortical bone was sanded using a Dremel tool with a sanding drum and band to remove any glue or polish. Following the sanding a 300-500 mg piece of cortical bone was sampled from the maxilla or mandible using a Dremel tool with a cleaned (using methanol and a Kim wipe®) diamond cutting wheel tip. For the woolly mammoth specimens, dentin was sampled instead of bone for stable carbon and nitrogen isotope analysis and/or radiocarbon dating, but the same preparation protocols used for bone samples were followed.

2.2.1.2 Collagen extraction

All the equipment (beakers, Pyrex break seals, PP transfer pipettes, tweezer/scoops, etc.,) for the following procedures (collagen extraction, analytical techniques and isotope measurements) were appropriately cleaned beforehand to avoid contamination.

The sampled bone piece was crushed into 1-2mm pieces and weighed into tubes to undergo collagen extraction at the Andre E. Lalonde Accelerator Mass Spectrometry (AMS) laboratory at the University of Ottawa, following procedures from Beaumont et al. (2010); Brock et al. (2010); Crann et al. (2017) Longin (1971). The first step of collagen extraction is 10 days of decalcification using 0.5M hydrochloric acid (HCl) maintaining a pH of 3.0 to remove the mineral (i.e. HAp) proportion of the bone to obtain the organic collagen matrix. The decalcification is followed by three rinses with 18.2 MΩ/cm grade Milli-Q water. Next, to remove humic acids, 0.1M sodium hydroxide (NaOH) is added for 30 minutes at room temperature and then rinsed three times with 18.2 MΩ/cm grade Milli-Q water. Then, 0.5M HCl is added at room temperature for 30 minutes to remove residual CO_2 that may be leftover from the NaOH wash and to decrease the pH of the sample prior to gelatinization, then rinsed three times with 18.2 MΩ/cm grade Milli-Q water.

Samples then undergo gelatinization (approx. 5mL) to breakdown and retain the collagen for 20 hours at 60°C and are then centrifuged. Filtration is then performed using cleaned Whatman® autovial syringeless filters. Beringian fossil samples underwent ultrafiltration whose procedure is outlined in Crann et al. (2017, 2019), and included three rounds of centrifuging with increasing rpm and respective rinses with 18.2 MΩ/cm grade Mili-Q water prior to filtering. Some samples underwent multiple rounds of gelatinization to maximize the amount of collagen collected. The collagen is then freeze-dried, and collagen subsets are weighed into tin capsules for further preparation for radiocarbon dating and/or for stable carbon and nitrogen isotope ratio analyses.

2.2.1.3 $F^{14}C$ analytical techniques and radiocarbon date calibration

Radiocarbon dated samples undergo combustion on a Thermo Flash 1112 elemental analyzer (EA) with extraction line to trap the CO_2 in clean Pyrex break seals (St-Jean et al., 2016). During this step preliminary C:N results indicate if samples are suitable for radiocarbon dating (i.e., $2.9<C:N<3.6$) (Ambrose, 1990; Deniro et al., 1985). If samples are deemed suitable for radiocarbon dating (i.e., $2.9<C:N<3.6$), the pure CO_2 samples now undergo graphitization in the presence of hydrogen and iron powder (Crann et al., 2017; St-Jean et al., 2016) before being pressed in aluminum targets and analyzed on the Ionplus AG MICADAS (Mini Carbon Dating System) at the Andre E. Lalonde AMS laboratory at the University of Ottawa, with data processing procedures from Wacker et al. (2010).

The fraction-modern ($F^{14}C$) are calculated based on the standardization of the $^{14}C/^{12}C$ ratio to that of primary international standard Oxford Isotope Standard 2 (Ox-II), following the protocol from Reimer et al. (2004). These $^{14}C/^{12}C$ ratio measurements are background corrected for natural, preparation and spectrometer fractionation from machine blank, $\delta^{13}C_{PDB} = -25‰$ measured on the Accelerator Mass spectrometer (AMS) at Andre E. Lalonde, Accelerator Mass Spectrometry (AMS) laboratory at the University of Ottawa.^{14}C ages are calculated following Stuiver et al. (1977) and reported as BP (BP = CE 1950) with error (SD) reported based on Poisson counting statistics, variation of repeated $^{14}C/^{12}C$ and $^{13}C/^{12}C$ ratios, and A.E Lalonde historical blank variability (Crann et al., 2019).

The ^{14}C ages are then calibrated using OxCal v4.4 (Bronk Ramsey, 2009) and reports an age range (BP) with associated probability (i.e., 95.4% for all calibrated dates in this study, Appendix A Figure 1). The median of this range is then calculated and used for statistical analyses.

2.2.1.4 Stable carbon and nitrogen isotope analytical techniques

The stable carbon and nitrogen isotope ratio measurements were performed at the Jan Veizer Stable Isotope Laboratory at the University of Ottawa on a Thermo DeltaPlus Advantage coupled to an elemental analyser (Vario EL Cube, Elementar) via a Conflo III interface (Thermo) isotope ratio mass spectrometry (IRMS). The $\delta^{15}N$ and $\delta^{13}C$ values are reported as parts per thousand (per mil [‰]) standardized to international standards AIR ($\delta^{15}N$) and V-PDB ($\delta^{13}C$), respectively.

$$\delta^{15/14}N_{Air} = \left[\frac{(15N/14N)_{Sample}}{(15N/14N)_{Air}} - 1\right] \times 1000$$

$$\delta^{13/12}C_{VPDB} = \left[\frac{(13C/12C)_{Sample}}{(13C/12C)_{VPDB}} - 1\right] \times 1000$$

The values were calibrated to three internal standards (C-51 Nicotiamide [δ^{15}N=0.07±0.2‰, δ^{13}C=-22.95±0.2‰,], C-52 mix of ammonium sulphate and sucrose [δ^{15}N=16.58±0.2‰,, δ^{13}C=-11.94±0.2‰,], and C-54 caffeine [δ^{15}N=-16.61±0.2‰, δ^{13}C=-34.46±0.2‰,]) which were calibrated to international standards (δ^{15}N: IAEA-N1 [+0.4±0.07‰; Kendall & Grim, 1990], IAEA-N2 [+20.3±0.12‰; Kendall & Grim, 1990], USGS-40 [-4.52±0.1‰; Qi et al., 2003], and USGS-41 [47.57±0.2‰; Qi et al., 2003] and δ^{13}C: IAEA-CH-6 [-10.4±0.003‰; Coplen et al., 2006], NBS-22 [-29.91±0.04‰; Coplen et al., 2006], USGS-40 [-26.24±0.042‰; Qi et al., 2003] and USGS-41 [37.76±0.049‰;Qi et al., 2003]). Values were corrected for linearity and drift.

Analytical precision (2SE) is reported based on L-glutamic acid internal standard C-55 reporting a δ^{15}N mean value of -4.0‰±0.134‰ (2SE, $n=5$) and δ^{13}C mean value of -28.5±0.09‰ (2SE, $n=4$) for the Beringian fossil sample run and a mean δ^{15}N of -4.0 ±0.078‰ (2SE, $n=12$) and δ^{13}C mean value of -28.6±0.064‰ (2SE, $n=12$) for the modern sample run, with expected values of δ^{15}N = -3.9±0.2‰, and δ^{13}C = -28.5±0.2‰. C-55 was not included in calibration as it was run as a blind standard. Cold fish water gelatine internal standard C-223 was analyzed as a quality check in the modern run and reported a mean δ^{15}N of 14.5±0.08‰ (SD, $n=8$), and δ^{13}C mean value of -16.5±0.09‰ (SD, $n=8$), with expected values of δ^{15}N = 14.71±0.2‰ and δ^{13}C = -16.33±0.2‰, and was not included in the calculation of the analytical precision and not included in calibration.

2.2.2 Calcium purification isotope analysis and elemental analysis

2.2.2.1 Enamel sampling

Enamel was preferentially sampled over bone or dentin for calcium stable isotope ratio and elemental analyses as bone and dentin have a greater porosity than enamel (up to 40% more porous) (Wang & Cerling, 1994). The porosity and smaller HAp crystal size (i.e. high surface/volume ratio) make dentin and bone more prone to sediment incorporation and diagenetic alteration than enamel, thus enamel is a preferable material for trace element concentration and/or isotopic compositions (e.g., Hassler et al., 2018; Jaouen et al., 2017; Joannes-Boyau et al., 2019; Martin et al., 2015, 2018).

The tooth targeted for sampling differed among species due to varying tooth mineralization and eruption sequences. Table 1 summarizes the target tooth that was sampled for each species. Enamel samples were consistently taken from the latest erupting teeth that typically occurs post-nursing and weaning: P4 or M1 in gray wolves (Geiger et al., 2016), P4 in horses (Hoppe et al., 2004), and M3 in caribou, bison, muskox, Dall sheep, and mammoths (sometimes referred to as M6 in mammoths) (Fuller, 1959; Laws, 1966; Metcalfe et al., 2010; Stimmelmayr et al., 2006; van den Berg et al., 2021). For small mammals (i.e., Arctic ground squirrel and snowshoe hare) bone was preferentially sampled instead of teeth, as their teeth were too small and the enamel too thin to properly sample.

The respective tooth being sampled was lightly sanded with a low-speed Dremel tool with a sanding drum and band to remove any glue/polish and to lightly clean the tooth surface, while ensuring enough enamel remained for sampling. Following the sanding the tooth surface was cleaned using methanol and Kim wipes® and briefly left to dry prior to sampling.

Using a clean 2mm pointed tip on a low-speed Dremel®, approximately 2mg of tooth enamel was collected from the middle of the tooth crown and was cleaned between each specimen using methanol and a Kim wipe®. As tooth enamel covers the dentin and mineralizes top-down (i.e., forming tooth cuspids in the crown first and mineralizing downward towards the tooth neck and root [Anemone et al., 1996]), the middle of the crown was preferentially sampled to avoid a juvenile dietary signal. The tooth neck and root were avoided when sampling due to thin enamel and increased presence of tooth cement. The sampling location for each species is shown in Figure 3, 4, and 5. Woolly mammoth specimens were specifically difficult to sample, due in part to their complex tooth morphology as shown in Figure 4, and as they typically are held together by lots of glue. By targeting the middle of the crown and sampling teeth that erupted post-weaning/nursing I minimized the influence of juvenile diet and nursing/weaning isotopic signals that may be preserved in younger growth layers, thus ensuring that my isotopic results reflect the bulk adult diet.

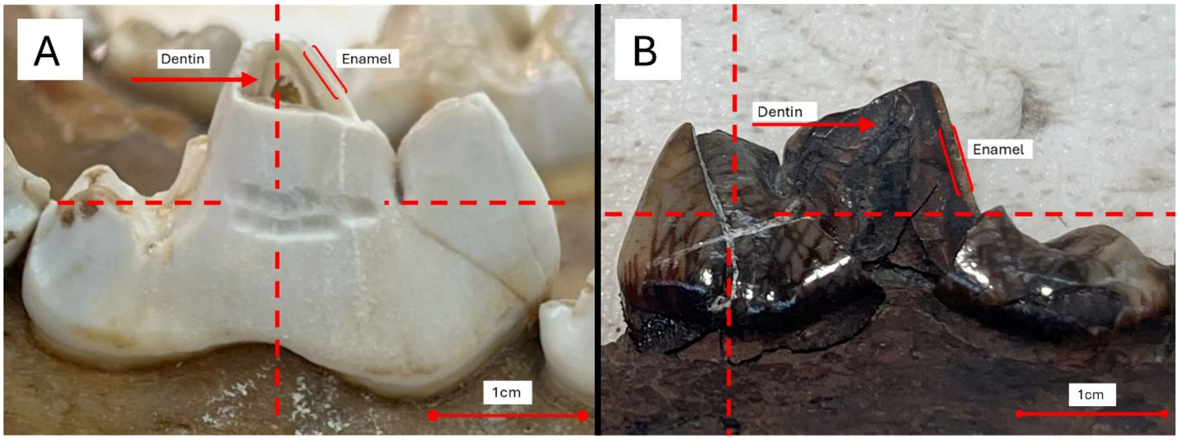

Figure 3. A) Modern wolf M1 specimen (CMNMA31759); and B) Beringian wolf fossil M1 specimen (CMNFV48454). Both A) and B) depict gray wolf molar morphology, highlighting the enamel and the dentin, and sampling locations.

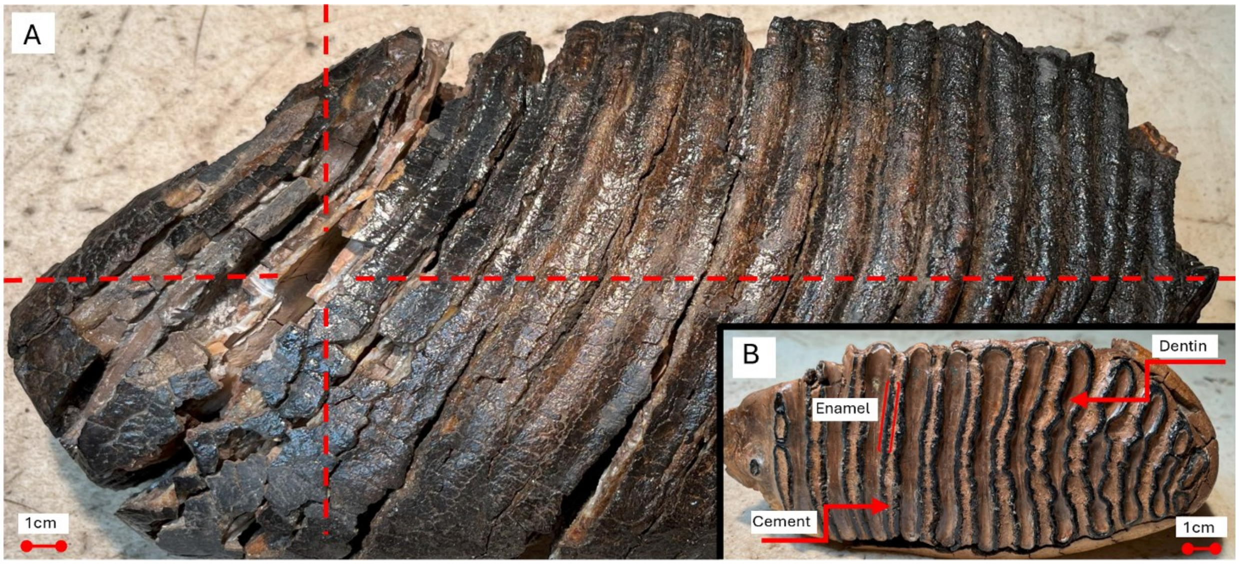

Figure 4. A) Woolly mammoth M3 "M6" (CMNFVC49389) depicting mammoth enamel sampling location; and B) Wolly mammoth M3 "M6" (CMNFV43088) displaying mammoth molar morphology, depicting the enamel from the dentin and cement.

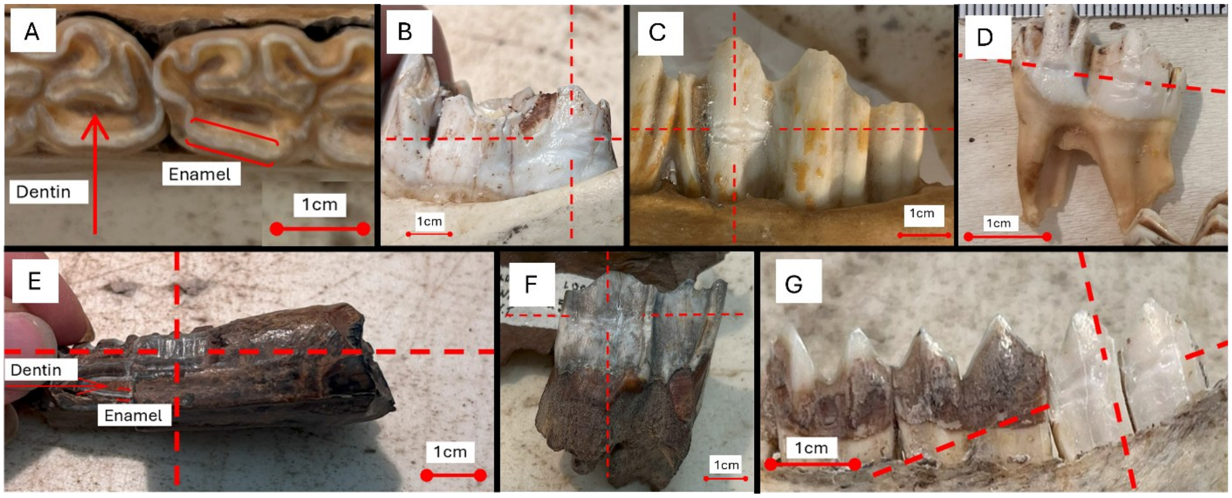

Figure 5. Enamel sampling locations for selected fossil and modern herbivore specimens analyzed in this study. A) Beringian bison molars (CMNFV34651) illustrating the distinction between enamel and dentin, with the enamel sampling region highlighted; B) Modern moose M3 (CMNMA 30623); C) Beringian bison M3 (CMNFV 34651); D) Modern caribou M3 (CMNMA 36094); E) Beringian horse P4 (CMNFV 20139); F) Beringian muskox M3 (CMNMA 22509); and G) Modern Dall sheep M3 (CMNMA30626). Sub-figures B-G show enamel sampling locations, where enamel was collected with a Dremel tool across a lateral shallow depth from the middle of the tooth crown.

Due to the differences in the composition, formation, and remodelling capacity of enamel, dentin, and tooth cementum (Hall, 2015), a key factor in this sampling is to ensure no dentin and/or tooth cementum are accidently sampled and mixed with the enamel. To avoid potentially sampling dentin and/or tooth cementum, the enamel powder was collected laterally over a shallow depth in the middle of the crown instead of a single point. Some specimens that had very thin enamel, specifically gray wolves, were scored with a clean scalpel blade and the enamel was manually removed from the dentin along these score lines. If any dentin remained on this piece of enamel, it was gently sanded away with a low-speed Dremel. Specimens with previously damaged enamel had pieces manually removed without the use of a Dremel. Samples were weighed (~2mg) and placed in 2mL acid clean centrifuge tubes.

2.2.2.2 Sample pre-treatment

The following procedures (i.e., sample pre-treatment, calcium purification and stable calcium isotope ratio measurement) were performed in clean laboratories at the University of Ottawa or National Research Council in Ottawa (NRC). All Teflon beakers, pipette tips, centrifuge tubes, columns, resin and acid containers used in this study were appropriately acid cleaned with a sequence of distilled acids for several days rinsed with 18.2 MΩ/cm grade Milli-Q water and dried prior to use. Only ultrapure (i.e., distilled American Chemical Society grade) HCl and/or HNO_3 were used in this study, and if need be, diluted using 18.2 MΩ/cm grade Milli-Q water.

2.2.2.2.1 Leaching, digestion and elemental analytical techniques

Beringian fossil samples underwent a leaching pre-treatment procedure outlined in Dodat et al. (2023) to revert diagenetic overprinting (Dodat et al., 2023; Koch et al., 1997; Nielsen-Marsh & Hedges, 2000; Sillen & LeGeros, 1991; Wathen et al., 2022). Leaching consisted of 0.5mL per sample mg of 0.1M acetic acid (ARISTAR® PLUS for trace metal analysis) in an ultrasonic bath for 30 minutes, followed by centrifuging and three 18.2 MΩ/cm grade Mili-Q rinses, with centrifuging between each. Due to the small mass of enamel samples (~2mg), there was no feasible method to weigh the remaining sample post-leaching which is common in the literature (e.g., Dodat et al., 2023), and thus elemental concentrations are calculated using a pre-leached mass. While leaching removed approximately 30% of material, there is no calcium isotopic fractionation and thus the $\delta^{44/42}$Ca values are unaffected by leaching (Dodat et al., 2023).

Modern (not leached) and Beringian fossil (leached) samples were then digested in clean Teflon beakers using 15M HNO_3 on a hotplate at 120°C for a minimum of 1 hour and then put to dry. Two aliquots of the digested samples were diluted in approximately 0.3M HNO_3, spiked with 2ppb indium in acid cleaned centrifuge tubes for major (Ca, P, etc.,) and trace (Sr, Ba, Rare Earth Element [REE]) element measurement on an Inductively coupled plasma mass spectrometer (ICP-MS) at the University of Ottawa. These values were corrected for machine drift using the spiked indium as an internal standard.

2.2.2.2.2 Calcium purification

The methods used for calcium purification in this study are based on the methods from Guiserix et al. (2022) and Tacail et al. (2014) with modifications for the Biorad PP columns (2mL bed and 10mL residual) and hand made PP transfer pipette columns (0.3ml volume, 2.5cm height x 0.39cm diameter beds) used in this study, outlined in Hassler et al. (in prep) and summarized in tables 2, 3, and 4. Prior to sample calcium purification, series of elution profiles for various international and internal standards including international bone standard SRM1486 and SRM1400, and international seawater standard IAPSO were performed to ensure >90%

calcium recovery to avoid fractionation during the purification processes. These elution profiles and procedural blanks are outlined in Hassler et al. (in prep). Figure 1F summarizes the calcium purification methods into a series of 3-steps, depicting the elution of each respective step.

The remaining post-digested sample aliquots were diluted in 10M HCl and then dried to prepare the samples for 6M HCl dilution for the first purification using cation exchange resin AG50WX12, 200-400 mesh in Biorad PP columns (2mL bed and 10mL residual) (Table 2). During this step the matrix elements (K, P, Mn, Mg, S, etc.,) are eluted and the Ca and Sr are recovered (Tacail et al., 2014; Hassler et al., in prep).

Following AG50WX12 purification, modern (not leached) samples were diluted in 15M HNO_3 and then dried to prepare the samples for 3M HNO_3 dilution. Next, the modern samples underwent Sr-specific (Sr-spec, Eichrom resin, 50-100µm particle size) purification to separate Sr from Ca in hand made PP transfer pipette columns (0.3ml volume, 2.5cm height x 0.39cm diameter beds), (Table 4) (Guiserix et al., 2022; Hassler et al., in prep; Tacail et al., 2014).

Based on the Fe concentrations of the Beringian fossil (leached) samples analyzed on an ICP-MS (Fe/Ca>0.0067), these samples underwent an AG1X8 resin, 100-200 mesh purification in Biorad PP columns (2mL bed and 10mL residual) to lower the concentration of Fe in these samples (Fe/Ca< 0.0067) to avoid potential matrix effect interferences on calcium isotope measurements (Hassler, 2021; Tacail et al., 2014). Modern samples have much lower Fe concentrations (Fe/Ca< 0.0067) than that of fossil samples due to minimal diagenetic overprinting and thus do not require further Fe elution (Table 3), (Tacail et al., 2014; Hassler et al., in prep).

After the AG1X8 purification the Beringian fossil (leached) samples were diluted in 15M HNO3 and then dried to prepare the samples for 3M HNO_3 dilution where they then underwent Sr-specific (Sr-spec, Eichrom resin, 50-100µm particle size) purification in hand made PP transfer pipette columns (0.3ml volume, 2.5cm height x 0.39cm diameter beds) to separate Sr from Ca (Table 4), (Guiserix et al., 2022; Hassler et al., in prep; Tacail et al., 2014).

Table 2. Steps for 1mL AG50WX12 resin, 200-400mesh for calcium purification with Biorad PP columns (2mL bed and 10mL residual), (Tacail et al., 2014; Hassler et al., in prep).

Step	Elution agent	Volume
Wash	6 M HCl*	10mL
	Milli-Q H2O	10mL
	6NHCl*	10mL
Conditioning	1M HCl	2mL
		2mL
Matrix elution	1M HCl	0.1mL sample loading
		0.9mL
		10mL
		10mL
		2mL
Collection (Ca, Sr)	6M HCl	1mL
		5mL
Wash	6M HCl*	10mL

Table 3. Steps for 2mL AG1X8 resin, 100-200mesh calcium purification with Biorad PP columns (2mL bed and 10mL residual) (Tacail et al., 2014; Hassler et al., in prep).

Step	Elution agent	Volume
Wash	Milli-Q H2O	10mL
	0.5M HNO_3*	10mL
	Milli-Q H2O	10mL
	6MHCl*	10mL
	Milli-Q H2O	10mL
Conditioning	6M HCl*	6mL
	6M HCl	2mL
Collection (Ca, Sr)	6M HCl	3.5mL sample loading
		0.5mL
		5mL

Fe and Zn elution	0.5M HNO_3*	5mL
		5mL
Wash	0.5M HNO_3*	10mL

Table 4. Steps for 0.3mL Sr-specific Eichrom resin, 50-100µm particle size for calcium purification with hand made PP transfer pipette columns (0.3ml volume, 2.5cm heightx0.39cm diameter beds) (Guiserix et al., 2022; Hassler et al., in prep; Tacail et al., 2014).

Step	Elution agent	Volume
Rinse columns with 7.5M HNO_3		
Load 0.3mL 50-100µm Sr-spec resin		
Wash	0.005M HNO_3*	3.5mL
		3.5mL
Conditioning	3M HNO_3	2mL
		2mL
Collection (Ca)	3M HNO_3	0.3mL sample loading
		0.7mL
		2.5mL
Sr elution	0.005M HNO_3*	2mL
		2mL
		3mL
Wash	0.005M HNO_3*	3.5mL

Once calcium purification is complete, samples were then digested in 15M HNO_3 on a hotplate at 120°C for a minimum of 1 hour to remove any organic particles that could have been introduced from the 0.3mL Sr-spec Eichrom resin. Samples were dried and then dissolved in 0.45M HNO_3 for calcium isotope ratio measurement.

2.2.2.3 Stable calcium isotope ratio analytical techniques

All $^{44/42}$Ca and $^{43/42}$Ca measurements were done on a Thermo Neptune Plus (MC-ICP-MS) at the NRC and Sr corrected following the procedure outlined in Tacail et al., 2014. $\delta^{44/42}$Ca values were calculated based on the standard-sample-standard bracketing method, standardized to the Alpha solution (Thermo Scientific Calcium, plasma standard solution, Specpure®, Ca 10,000µg/mL) and are reported as parts per thousand (per mil [‰]).

$$\delta^{44/42}Ca_{Alpha} = \left[\frac{(44Ca/42Ca)_{Sample}}{(44Ca/42Ca)_{Alpha}} - 1\right] \times 1000$$

SRM1486 and SRM1400 were used as secondary standards. We report a mean $\delta^{44/42}Ca_{Alpha}$ value of -1.004±0.080‰ (2SD, *n*=4) and mean $\delta^{43/42}Ca_{Alpha}$ of -0.508±0.040‰ (2SD, *n*=4) for SRM1486. SRM1400 analyzed in this study has a mean $\delta^{44/42}Ca_{Alpha}$ value of -1.127±0.206‰ (2SD, *n*=2) and mean $\delta^{43/42}Ca_{Alpha}$ of -0.555±0.454‰ (2SD, *n*=2). These values are consistent with published values (i.e., mean $\delta^{44/42}Ca_{ICP}$ value of -1.03±0.13‰ [2SD, *n*=120] for SRM1486 and -1.24±0.13‰ [2SD, *n*=26] for SRM1400; Tacail et al., 2015). Analytical precision is reported as 2SE of the mean for each sample and is found in Appendix C Table 2.

2.3 Data processing

2.3.1 Published source data and age subsets

After radiocarbon dating was performed, it was revealed that the selected specimens had a biased age distribution with most specimens older than 26ka BP and only a few specimens within the Last Glacial Maximum (LGM) and deglaciation periods 11-26 ka BP (i.e., two gray wolves, one bison, and two horses). To increase the representativeness of this sample-set for those important climate periods, $\delta^{13}C$ and $\delta^{15}N$ data from a range of prey species of complementary age was compiled from the literature to assess the wolves' diet during those periods. The compiled data was selected based on the following criteria:

1) I only included prey species that were analyzed in this study, across similar radiocarbon ages (~0-50 ka BP)
2) I only included radiocarbon dated samples with corresponding $\delta^{13}C$ and $\delta^{15}N$ values from cortical bone or dentin, ensuring comparability in preparation and analytical methods with my sample set.

3) I only selected specimens recovered from the same region as my sample set, restricting my search to latitude 60° to 66° and longitude -150° to -138° to further limit potential regional environmental effects on isotopic and elemental composition.

See Appendix D Table 4 for a list of the publications included in the compiled prey source database.

Prior to statistical analyses all samples (wolves and prey species) in this study and from the data compilation were classified into one of four age subsets (i.e., Modern, post-LGM, LGM and pre-LGM) based on their median calibrated radiocarbon age (BP). These age subsets represented different climate conditions defined using the δ^{18}O NGRIP Greenland ice core curve (Fuchs & Leuenberger, 1996; Sowers et al., 1989) and regional climate shifts over the late Pleistocene and Holocene.

A summary of the age subsets and associated climate in eastern Beringia are summarized in Table 5. The first age subset is ‘modern’, with samples ranging from 0 to11 ka BP corresponding to the Holocene and climate conditions similar to present-day with warm and wet climate and boreal forest ecosystem. The second age subset is ‘post-LGM’ and ranges from 11 to 19 ka BP and represents the deglaciating conditions between the LGM and Holocene, where climate gradually warms, and moisture and vegetation growth dominate the landscape (Rabanus-Wallace et al., 2017). The third age subset is ‘LGM’ and ranges from 19 to 26 ka BP and is characterized by the coldest and dryest conditions in Beringia with typical mammoth steppe ecosystems (i.e., cold, dry, grasslands; Rabanus-Wallace et al., 2017; Zazula et al., 2006b; Zimov et al., 2012). The last age subset is ‘pre-LGM’ with samples >26 ka BP representing the interstadial period occurring between Pleistocene glacial maximums, with glacial conditions but warmer and likely wetter than LGM conditions and dominance of tundra and mammoth steppe ecosystems (Rabanus-Wallace et al., 2017; Zazula et al., 2006b; Zimov et al., 2012).

Table 5. Age subset descriptions including associated age range and summaries of climate conditions and ecosystems in eastern Beringia over the last 50,000 years.

Age subset	Associated age range	Summary of climate	Summary of ecosystem
Modern	0-11,000 BP	Warm climate	Boreal forest, moist soils
Post-LGM	11,000-19,000 BP	Deglaciation, increasing temperatures, glacial and permafrost melt,	Transition from mammoth steppe to boreal forest, increasing soil moisture
LGM	19,000-26,000 BP	Coldest temperatures and arid climate	Mammoth-steppe, very low soil moisture
Pre-LGM	>26,000 BP	Cold temperatures and arid climate	Mammoth-steppe, low soil moisture

2.3.2 CO_2 atmospheric correction

All $\delta^{13}C$ values from this study and the published source dataset underwent atmospheric CO_2 correction. Due to increased anthropogenic fossil fuel activity since the industrial revolution in 1880, the atmospheric $\delta^{13}C$ baseline is higher than in the past and must be considered when comparing modern (younger than 1880) to fossil specimens (older than 1880) (Long et al., 2005). To directly compare all specimens from this study and the published source dataset, all $\delta^{13}C$ values, including modern specimens were corrected to the year 1967 (the youngest modern specimen from this study). The modern specimens were also corrected as their collection date ranges from 1935 to 1967. Over these 32 years, shifts in atmospheric $\delta^{13}C$ are observed (Long et al., 2005) so I corrected all $\delta^{13}C$ values to directly compare all specimens, no matter the deposition and collection date. I corrected $\delta^{13}C$ values based on the procedure and formula outlined in Long et al. (2005):

$$\delta^{13}\mathrm{C}_{Correction\ factor} = -5.5656 - \mathrm{e}^{(6.0932 \times 10^{-5})(1967-a)^2}$$

Where *a* refers to the year of collection for modern specimens or 1880 for fossil samples (specimens older than 1880).

This $\delta^{13}C$ correction factor is added to the measured $\delta^{13}C$ value. After this correction factor is applied, all specimens have baseline-corrected comparable $\delta^{13}C$ values. The baseline-corrected $\delta^{13}C$ values are used in all further statistical analyses.

2.3.3 Elemental concentrations, ratios and NASC normalization

2.3.3.1 Indicators of diagenetic alteration

Rare Earth Element (REE) patterns are indicative of the extent and type of diagenetic alteration a specimen experienced post-deposition (Reynard & Balter, 2014). REE concentrations were monitored in this study to support the quality of isotopic and elemental data. Due to post-depositional alteration, REE's become increasingly incorporated into the HAp crystal structure through two processes, additive or substitutive diagenesis (Reynard & Balter, 2014). The difference in ionic radius across the suite of REE, modulated by the diagenetic processes at play, allow certain REE to be more easily incorporated into the HAp crystal structure (e.g., Eu and Sm, both with ionic radii similar to Ca [~100pm]). The behaviour of the REE's, and resulting enrichment factors between them, will thus depend on their ionic radius and inform about the type and degree of diagenetic processes which affected the HAp crystals (Reynard & Balter, 2014).

For fossil samples that underwent leaching, the enamel concentrations (ppm) were calculated using the pre-leached mass. The REE concentrations (ppm) were normalized to the North American Shale Composite (NASC) (McLennan, 1989). The REE concentrations are normalized to NASC (or Post-Archean Average Shale [PASS]) so that REE can be compared between specimens from different depositional locations within this study and published studies. This normalization also assists in REE anomaly identification, which can be indicative of diagenetic alteration and therefore can be used to determine which samples should be removed as outliers.

Ca/P is used as an indicator of HAp preservation as any deviations from the natural HAp Ca/P range can indicate recrystallization, substitution, and/or secondary mineral precipitation (additive-like diagenesis) (Dodat et al., 2023; Sillen & LeGeros, 1991). Thus, Ca/P ratios are calculated in this study to inform about the type and extent of diagenetic overprinting. Additionally, Ca/P ratios also provide insight into the effectiveness of leaching pre-treatments, with some limitations (Fabig & Herrmann, 2002). Samples with a Ca/P ratio not within the natural HAp range (i.e., 1.6-2.7; Dodat et al., 2023; Shah, 2025) or that are clear outliers in this dataset suggest diagenetic alteration and thus should be removed. The Ca/P ratio is directly calculated from the drift corrected aliquot concentrations as these elements were both analyzed in the same aliquot and thus have the same dilution factors.

Comparison of REE patterns, Europium (Eu) concentrations, and Ca/P ratios among specimens and with other studies were used to indicate the level and type of diagenetic alteration and confirm that samples unaltered by post-depositional processes and can reliably use isotopic and elemental analysis are for dietary and trophic interpretations (Reynard & Balter, 2014).

2.3.3.2 Alkaline earth element ratios (Sr/Ca and Ba/Ca)

Alkaline Earth element ratios (AER) (i.e., Sr/Ca and Ba/Ca) are calculated as these ratios are commonly used in trophic reconstructions (Blum et al., 2000). Sr/Ca and Ba/Ca ratios are calculated from the enamel concentrations as two aliquots were taken for ICP-MS and were diluted based on major (i.e., Ca) and minor (i.e., Sr and Ba) element measurements. The aliquot concentrations cannot be directly compared as they have varying dilution factors. Thus, the enamel concentration (ppm) must be considered when calculating these ratios as it has been corrected for dilution factor.

2.3.4 Statistical analyses

All statistical analyses other than dietary mixing models were performed in Python (v.3.10.14; Python Software Foundation, 2024). For all statistical analyses and interpretations, the aforementioned outliers were removed (described in further detail in Chapter 3).

2.3.4.1 Two tailed t-test and Mann-Whitney test

Shapiro-Wilk tests were conducted to test if $\delta^{13}C$, $\delta^{15}N$, $\delta^{44/42}Ca_{Alpha}$, Sr/Ca and Ba/Ca are normally distributed to indicate the type of statistical analyses required for each variable. Based on the Shapiro-Wilk test and as observed in Appendix A Figure 2, $\delta^{13}C$ and $\delta^{15}N$ can be confidently assumed to be normally distributed (*Shapiro-Wilk test p=1.0*, Appendix A Figure 2). $\delta^{44/42}Ca_{Alpha}$, Sr/Ca and Ba/Ca are not normally distributed (Shapiro-Wilk W= 0.946*,* 0.948, and 0.900, respectively, and $p<0.05$, Appendix A Figure 2).

Paired two-tailed t-tests, assuming equal variance were performed to test if there was a statistically significant difference for $\delta^{13}C$, $\delta^{15}N$, $\delta^{44/42}Ca_{Alpha}$, Sr/Ca and Ba/Ca between the two independent groups: modern and pre-LGM gray wolves. As $\delta^{44/42}Ca_{Alpha}$, Sr/Ca and Ba/Ca are not normally distributed, as revealed by the Shapiro-Wilk test, I also performed a Mann-Whitney test in tandem with the t-tests. These tests were performed to determine if $\delta^{13}C$, $\delta^{15}N$, $\delta^{44/42}Ca_{Alpha}$, Sr/Ca and Ba/Ca differ for wolves from different time periods, which can yield insights regarding whether gray wolves have undergone dietary change from the Pleistocene to the present-day. As post-LGM and LGM gray wolf age subsets both only have one wolf specimen these age subsets can not be included in these statistical analyses.

2.3.4.2 Principal component analysis (PCA)

Principal component analysis (PCA) was performed to investigate if there are patterns of variation across the species in their respective age subsets explained by $\delta^{13}C$, $\delta^{15}N$, $\delta^{44/42}Ca_{Alpha}$, Sr/Ca, and Ba/Ca while reducing dimensionality in the data. This analysis visualizes the multivariate relationships that may exist between the variables regarding species and age subset.

Two PCA's were performed. The first considering $\delta^{13}C$, $\delta^{15}N$, and $\delta^{44/42}Ca_{Alpha}$ and the second considering $\delta^{13}C$, $\delta^{15}N$, $\delta^{44/42}Ca_{Alpha}$, Sr/Ca and Ba/Ca. Prior to the PCA, the data underwent z-score normalization. The PCA's were performed in Python using the scikit-learn decomposition module (v.1.2.2; Pedregosa et al., 2011) considering two principal components (PC1 and PC2). In addition to the PCA, ellipses with 95% confidence based on covariance matrices were plotted to show species clustering. The feature loading ($\delta^{13}C$, $\delta^{15}N$, $\delta^{44/42}Ca_{Alpha}$, Sr/Ca and Ba/Ca) were represented as vectors on the PCA to represent the contribution of each variable to the variation (PC1 and PC2).

2.3.5 Bayesian stable isotope mixing models (BSIMM)

To determine the primary prey species of gray wolves from different time periods (i.e., age subsets) Bayesian stable isotope mixing model (BSIMM) were run using MixSIAR (v.3.1.10; Stock, 2025) using the JAGS software (v.4.3.0; Plummer, 2003) in R (v.4.4.2; R Core Team, 2024) with 100,000 iterations. The MixSIAR package can analyze multi-isotope datasets and incorporates uncertainty in source isotope values and trophic discrimination factors (TDF) making it the ideal method to determine the primary prey of gray wolves from stable isotopes.

Variations of BSIMM's were run for each respective age subset (modern, post-LGM, LGM, and pre-LGM) and included time specific prey species. For all models the prey sources are considered by mean δ^{13}C, δ^{15}N, and $\delta^{44/42}$Ca$_{\text{Alpha}}$ and associated standard deviation. The wolves are input as a mixture with individual isotopic values loaded in the models as this incorporates intra-consumer variance (Stock, 2025). Two versions of BSIMMs were generated:

1) uninformed model, where the priors for all prey sources are weighted equally, thus all prey species are assumed as equally likely to contribute to wolf diet.

2) informed model, where priors are set to weigh the likelihood of a prey species' contribution to wolf diet based on the prey's mass in relation to the target prey mass of a wolf pack. Carnivores usually have a typical target prey mass that maximize the energy return (Carbone et al., 1999; Volmer et al., 2016). As wolves are known pack hunters, the target prey mass must be considered for a wolf pack and not an individual wolf (Volmer et al., 2016). To set the priors based on wolf pack target prey mass an inverse distance weighting probability (P_{IDW}) scaled to the number of prey species (n) in each respective model was calculated as followed:

$$P_{IDW\,i} = \frac{1}{(|average\ prey\ mass\ i - wolf\ pack\ target\ prey\ mass| + 1)}$$

$$Prior_i = P_{IDW\,i} \times \frac{n}{\sum_i^n P_{IDW\,i}}$$

The sum of priors should be equal to the number of prey species (n) analyzed in the model. Due to the multiple variations of models ran in this study, the priors calculated from the above formula are displayed with the BSIMM results in Appendix B Tables 1, 2, and 3, and are based off the wolf pack target prey mass of 251.6kg (Volmer et al., 2016). The masses of the prey species used to calculate the priors are as followed: Arctic ground squirrel —0.8kg (Yukon wildlife, 2024c), snowshoe hare —1.49kg (Yukon Wildlife, 2024b) , caribou —170kg (Yukon

Wildlife, 2025b), muskox—295kg (Yukon Wildlife, 2024a), moose —450kg (Yukon Wildlife, 2025c), bison —725kg (Yukon Wildlife, 2025a), horse — 285kg (Landry et al., 2022), Dall sheep —70kg (U.S. National Park Service, 2020), and woolly mammoth —5980kg (Larramendi, 2015).

Running the BSIMMs requires the input of trophic discrimination factors (TDF's) which account for the isotopic offset between an animal's tissues and its diet. The $\delta^{13}C$ and $\delta^{15}N$ TDF's are calculated from bone collagen and are wolf-specific from Fox-Dobbs et al. (2007). The TDF for $\delta^{44/42}Ca_{Alpha}$ is from Tacail et al. (2020) and calculated based on the regression of $\delta^{44/42}Ca$ bone vs $\delta^{44/42}Ca$ diet from seven vertebrae species. The TDF's and respective standard deviations used for wolves in this study are $\Delta^{13}C_{col} = +1.3‰ \pm 0.6‰$ (Fox-Dobbs et al., 2007), $\Delta^{15}N_{col} = +4.6‰ \pm 0.7‰$ (Fox-Dobbs et al., 2007), and $\Delta^{44}Ca_{bone} = -0.54‰ \pm 0.075‰$ (Tacail et al., 2020). No models were run including Sr/Ca and Ba/Ca as no TDF was identified in the literature for these variables.

To test the potential of calcium isotopes to refine the dietary inputs for gray wolves I ran three distinct BSIMM each with uniformed models and informed versions:

1) Traditional proxy BSIMMs including compiled prey source data

The first BSIMM was a typical carbon and nitrogen isotope dietary model in which I only used the $\delta^{13}C$ and $\delta^{15}N$ of gray wolves from this study to determine their diet (Appendix C Table 2). For the prey source data, I used the $\delta^{13}C$ and $\delta^{15}N$ data from the prey dataset compiled from the literature and the newly acquired prey $\delta^{13}C$ and $\delta^{15}N$ values (Appendix C Table 1, 2). This model was run for gray wolves in each age subset (i.e., modern [*n*=15], post-LGM [*n*=1], LGM [*n*=1], and pre-LGM [*n*=10]) with time-specific prey species belonging to those age bin.

2) Traditional proxy BSIMMs

The second BSIMM was also run using exclusively $\delta^{13}C$ and $\delta^{15}N$ of gray wolves (Appendix C Table 2). In this case, however, I limited the included prey species to only those for which data was collected in this study (Appendix C Table 2) to test whether potential geographic or methodological biases might have influenced the dietary results. Because I had only a limited number of prey species for the LGM and post-LGM subsets in this study, I only ran this BSIMM for gray wolves in the modern (*n*=15) and pre-LGM age subset (*n*=10) with time-specific prey species.

3) Traditional and novel proxy BSIMMs

The third BSIMM combines $\delta^{13}C$, $\delta^{15}N$, and $\delta^{44/42}Ca_{Alpha}$ of gray wolves from this study as well as prey $\delta^{13}C$, $\delta^{15}N$, and $\delta^{44/42}Ca_{Alpha}$ from this study (Appendix C Table 2). As for the previous BSIMM, due to the low representation of prey from the LGM and post-LGM age bins, this model was only run for modern (*n*=15) and pre-LGM gray wolves (*n*=10) with time-specific prey species.

The traditional proxy BSIMMs for modern and pre-LGM wolves were run to compare these models to the traditional and novel proxy BSIMMs to test if the model including calcium isotopes provides further insights into gray wolf dietary preferences. The traditional proxy BSIMM variations allow for comparison between modern and pre-LGM BSIMMs with prey values from only this study and prey sources including published values to ensure that my $\delta^{13}C$ and $\delta^{15}N$ values are comparable with that of published sources and have similar BSIMM outputs.

3 Results

The full dataset collected in this study including gray wolves and prey data is available in Appendix C Table 1,2, 3, which gathers site and specimen metadata, including CMN specimen ID, region, latitude and longitude, substrate, feeding type, gut physiology, radiocarbon data and metadata including radiocarbon ID, radiocarbon date (calibrated and uncalibrated), C:N ratio, age subset, stable isotope results including δ^{13}C (‰), δ^{15}N (‰), and $\delta^{44/42}Ca_{Alpha}$ (‰) and elemental results including Ca/P, Sr/Ca and Ba/Ca ratios, and rare earth element concentrations normalized to NASC. The prey isotope dataset compiled from the literature contains the same metadata except for calcium isotopes and elemental data and is available in Appendix C Table 4.

3.1 Data quality

3.1.1 Radiocarbon, δ^{13}C (‰) and δ^{15}N (‰)

All samples that underwent radiocarbon dating and/or δ^{13}C, and δ^{15}N, analysis in this study have a C:N ratio within 2.9–3.6 (Appendix A Figure 3) indicating minimal to no post depositional alteration and/or organic degradation (Ambrose, 1990; Deniro et al., 1985). As observed in Appendix A Figure 3, EL183 has a δ^{15}N value of -0.17‰, which is an outlier from the rest of the δ^{15}N values in this study and the prey source dataset, all of which have values of $\delta^{15}N > 0$. Thus, EL183 is deemed an outlier and has been removed from further statistical analyses. All radiocarbon dates calibrated on this study yielded robust calibration with >95.4% probability (Appendix A Figure 1).

3.1.2 $^{44/42}$Ca measurement

All samples and standards analyzed in this study fall on the $\delta^{43/42}Ca_{Alpha}$ vs $\delta^{44/42}Ca_{Alpha}$ line $y=(0.488\pm0.026)x + (-0.013\pm0.026)$, ($R^2=0.927$, $p\text{-value}<0.001$, Figure 6). This line is generally consistent with the predicted linear approximation of exponential mass dependent fractionation law ($y=0.507x$, Figure 6) (Tacail et al., 2015, 2020) and that from previously published studies (e.g., $y=(0.518\pm0.013)x + (0.003\pm0.021)$) (Tacail et al., 2015). In this study we report a mean $\delta^{44/42}Ca_{Alpha}$ of -1.004±0.080‰ (2SD, *n*=4) for SRM1486 and -1.127±0.206‰ (2SD, *n*=2) for SRM1400, both of which are consistent with published values (e.g., mean $\delta^{44/42}Ca_{ICP}$ value of -1.03±0.13‰ [2SD, *n*=120] for SRM1486 and -1.24±0.13‰ [2SD, *n*=26] for SRM1400 (Tacail et al., 2015).

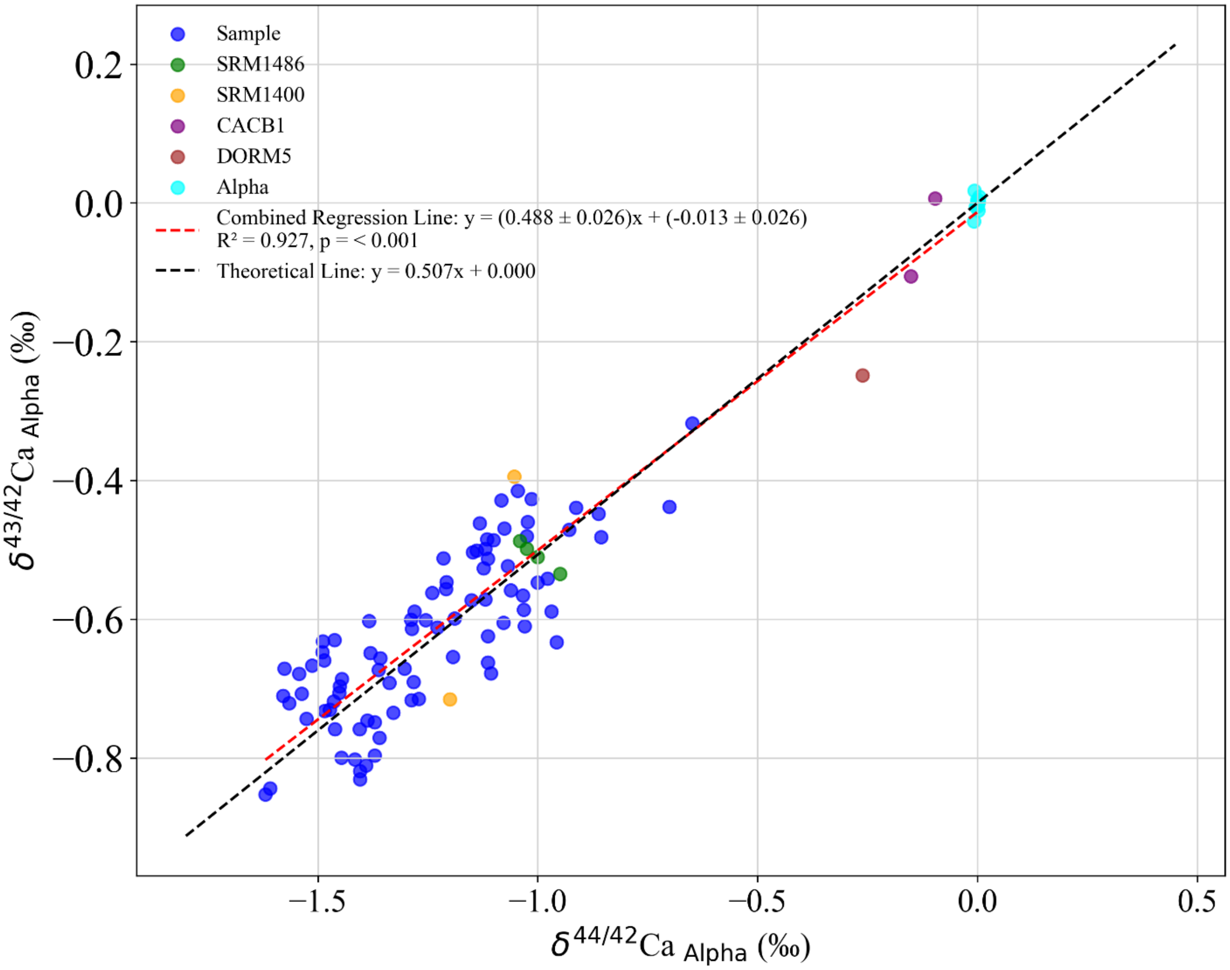

Figure 6. Plot of $\delta^{43/42}Ca_{alpha}$ (‰) versus $\delta^{44/42}Ca_{alpha}$ (‰) for all samples, bracketing standards, international reference materials, and internal standards analyzed in this study. The regression which depicts the mass-dependent fractionation line of these samples (red dashed line) is defined by the equation $y = (0.488 \pm 0.026)x + (-0.013 \pm 0.026)$, $R^2 = 0.927$, $p < 0.001$. The predicted linear mass fractionation law ($y = 0.507x$) is shown as the black dashed line for comparison. International standards SRM 1486 and SRM 1400 are shown in green and yellow, respectively.

3.1.3 Indicators of diagenetic alteration

All elemental concentrations (ppm) for Beringian leached fossil samples are calculated based on a pre-leached mass. This is common in the literature (e.g., Dodat et al., 2023) as for samples with small enamel masses (~2mg), there is no feasible method to weigh the remaining post-leached enamel.

3.1.3.1 Ca/P

Ca/P is used as an indicator of HAp preservation and secondary mineral precipitation (additive-like diagenesis) in fossil bone and enamel samples (Dodat et al., 2023; Sillen & LeGeros, 1991). All modern samples that did not undergo leaching plot within the expected Ca/P range of modern HAp (i.e., 1.6-1.9; Dodat et al., 2023; Shah, 2025), (Figure 7). For post-leached Beringian fossil samples, I expect and observe a lower Ca/P to that of the non-leached modern samples. The decrease in Ca/P of post-leached Beringian samples shows that leaching removed a portion of the authigenic Ca but also remove potential diagenetic Ca, as expected (Dodat et al., 2023; Sillen & LeGeros, 1991). I observed a few outliers on the Ca/P plot (Figure 7), EL208 and EL234 with Ca/P values of 1.2 and 1.1, lower than the expected Ca/P even for diagenetically altered samples, possibly indicating remaining presence of secondary carbonate phosphates, and EL156 and EL220 with Ca/P values of 2.3 and 2.0, respectively, which is higher than modern samples suggesting that some diagenetic Ca may have remained in those samples (Dodat et al., 2023; Sillen & LeGeros, 1991). These outliers were removed from further statistical analyses as their Ca/P value could indicate diagenetic alteration.

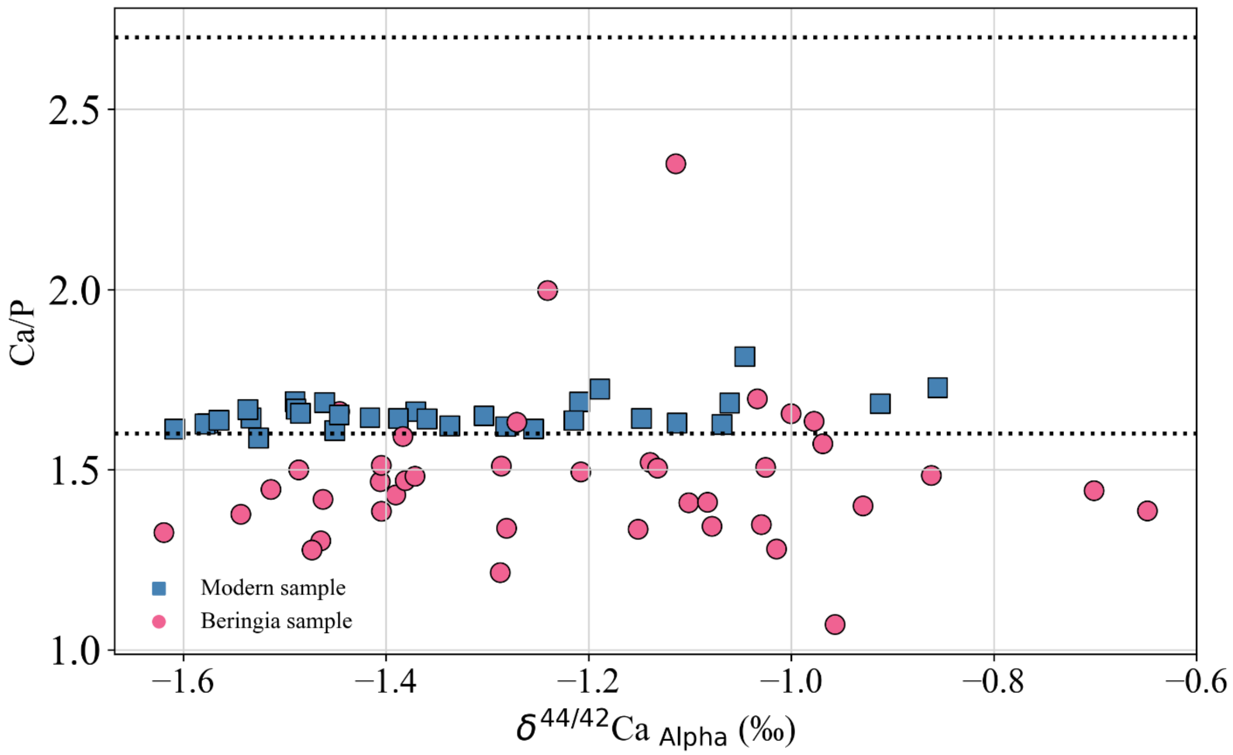

Figure 7. Plot of $\delta^{44/42}$Ca$_{alpha}$ (‰) versus Ca/P ratios for modern (blue squares) and Beringian fossil (pink circles) samples. The expected natural range of Ca/P in enamel bioapatite (1.6–2.7) is depicted by the dashed black lines. Ca/P was used to assess potential diagenetic alteration and pre-treatment leaching efficiency.

3.1.3.2 Rare Earth Elements

Normalized Rare Earth Element (REE) elemental concentrations are used to test the extent and type of diagenetic alteration because certain REEs preferentially incorporate in biogenic matrices (see Chapter 2 for more details) (Dodat et al., 2023; Reynard & Balter, 2014). All Beringian fossil sample REE profiles from the two main regions (i.e., Dawson and Old Crow Yukon, Figure 8A and 8B, respectively) in this study plot within the same normalized concentration range (i.e., 10^0-10^{-4}, Figure 8A, 8B). All REE profiles are relatively flat with no enrichment in light-REE (LREE) and/or heavy-REE (HREE), or Ce anomalies. These findings show that diagenetic alteration does not appear in one region more than another and thus samples from the two regions can be directly compared. This also shows minimal diagenetic alteration. (Reynard & Balter, 2014). EL234 was furthermore indicated to be an outlier by its relatively greater REE concentrations compared to all other samples in this study, which indicates diagenetic input (Dodat et al., 2023; Reynard & Balter, 2014).

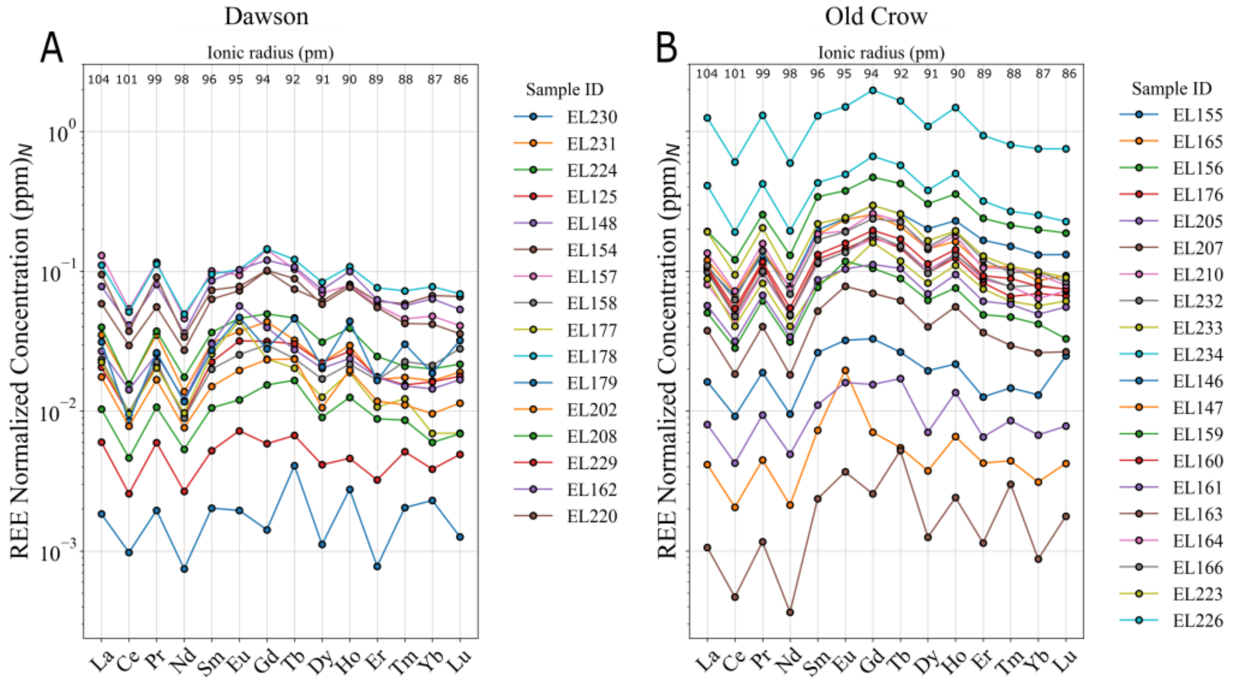

Figure 8. NASC normalized rare earth element (REE) profiles of Beringian fossil bioapatite enamel samples that underwent pre-treatment leaching. A) Specimens from Dawson, Yukon; and B) specimens from Old Crow, Yukon. Patterns are used to evaluate diagenetic alteration and assess preservation quality of fossil samples from the two study regions.

Sm and Eu are REE with a medium ionic radius that are used as indicators of HAp diagenetic alteration as they have similar ionic radii as Ca (~100pm), making them more prone to be incorporated into the HAp crystal lattice during post-depositional alteration processes (Dodat et al., 2023; Reynard & Balter, 2014). The lack of enrichment of these elements, in all but two samples, along with the relatively flat shape of the REE profiles indicate minimal post-depositional diagenetic alteration (Dodat et al., 2023; Reynard & Balter, 2014). In addition, there are no trends observed between $\delta^{44/42}\mathrm{Ca}_{\mathrm{Alpha}}$ and Eu (ppm) in this dataset as observed in Figure 9, shown by the weak linear regression between these variables ($R^2=0.02$ *and* $p>0.05$, Figure 9). Two outliers are observed in the Eu concentrations. EL201 and EL234 have much greater Eu concentrations to that of the other modern and Beringian samples, respectively, with values of 0.8 and 1.9ppm, respectively. Thus, EL201 and furthermore EL234, are potentially diagenetically altered (Dodat et al., 2023; Reynard & Balter, 2014) and are considered outliers.

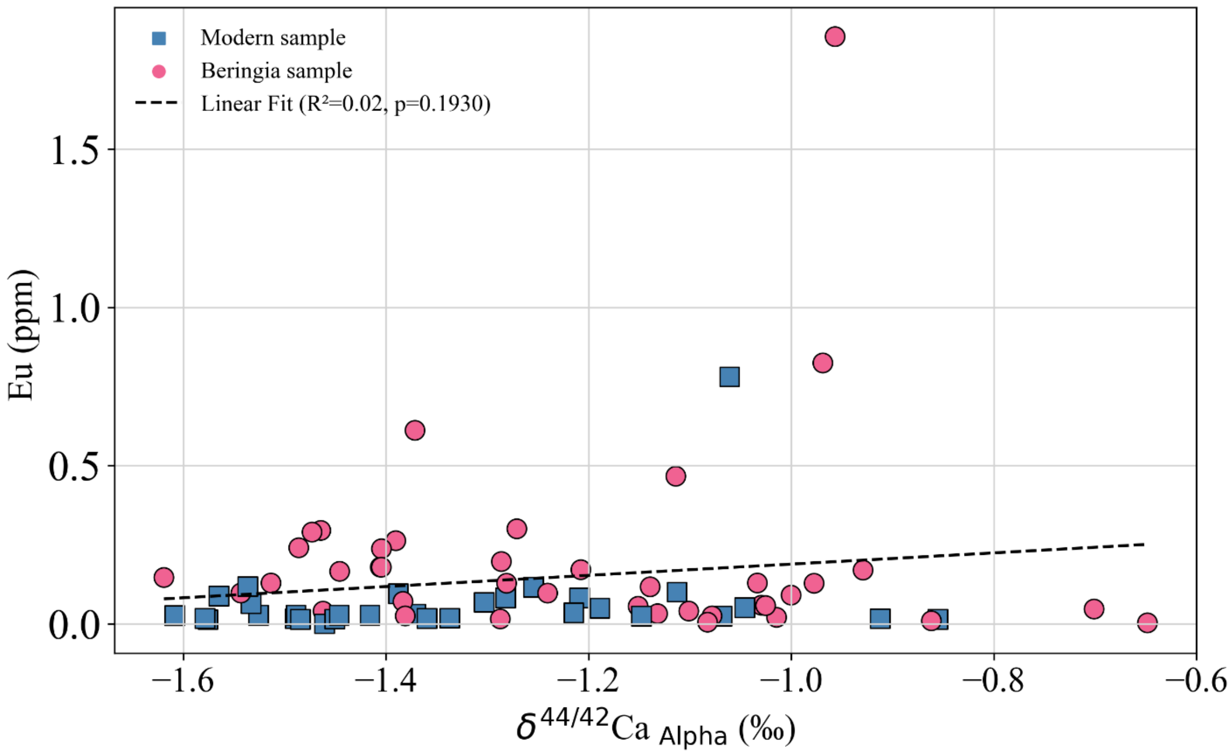

Figure 9. Plot of $\delta^{44/42}Ca_{alpha}$ (‰) versus europium (Eu, ppm) concentrations in modern (blue squares) and Beringian fossil (pink circles) enamel samples that underwent pre-treatment leaching. Eu concentrations (ppm) were used to assess potential diagenetic alteration. The dashed black line represents the weak linear regression between these variables (*R^2=0.02 and p>0.05*).

La/Yb and La/Sm ratios normalized to NASC (or PAAS) can also be used as indicators of diagenetic processes in fossil HAp. La is a LREE, whereas Yb is a HREE. A ratio of light-heavy (La/Yb) and light-middle (La/Sm), are indicative of the type and extent of diagenetic alteration (Reynard & Balter, 2014). As seen in Figure 10, on a $(La/Yb)_N$ (NASC) vs $(La/Sm)_N$ (NASC) plot, all Beringian fossil samples cluster around (1,1). Dawson samples have slightly higher mean values of $(La/Sm)_N$ (NASC) (1.1±0.1 [SD, *n=16*]) and $(La/Yb)_N$ (NASC) (1.7±0.7 [SD, *n=16*]), compared to that of Old Crow (i.e., $(La/Sm)_N$ (NASC): 0.7±0.2 [SD, *n=24]*), and $(La/Yb)_N$ (NASC):1.3±0.3 [SD, *n=24*]). Despite the slight difference between Dawson and Old Crow $(La/Sm)_N$ (NASC) and $(La/Yb)_N$ (NASC) values, the majority of Beringian samples plot within the contemporary quaternary $(La/Yb)_N$ (NASC) and $(La/Sm)_N$ (NASC) range from published studies that have minimal digenetic input (Figure 10, modified from Reynard & Balter (2014). The few samples that do not plot within this range fall within a $(La/Yb)_N$ (NASC) and/or

$(La/Sm)_N$ NASC) range that is indicative of early diagenesis or protracted diagenesis (inorganic absorption) (Figure 10) (Reynard & Balter, 2014).

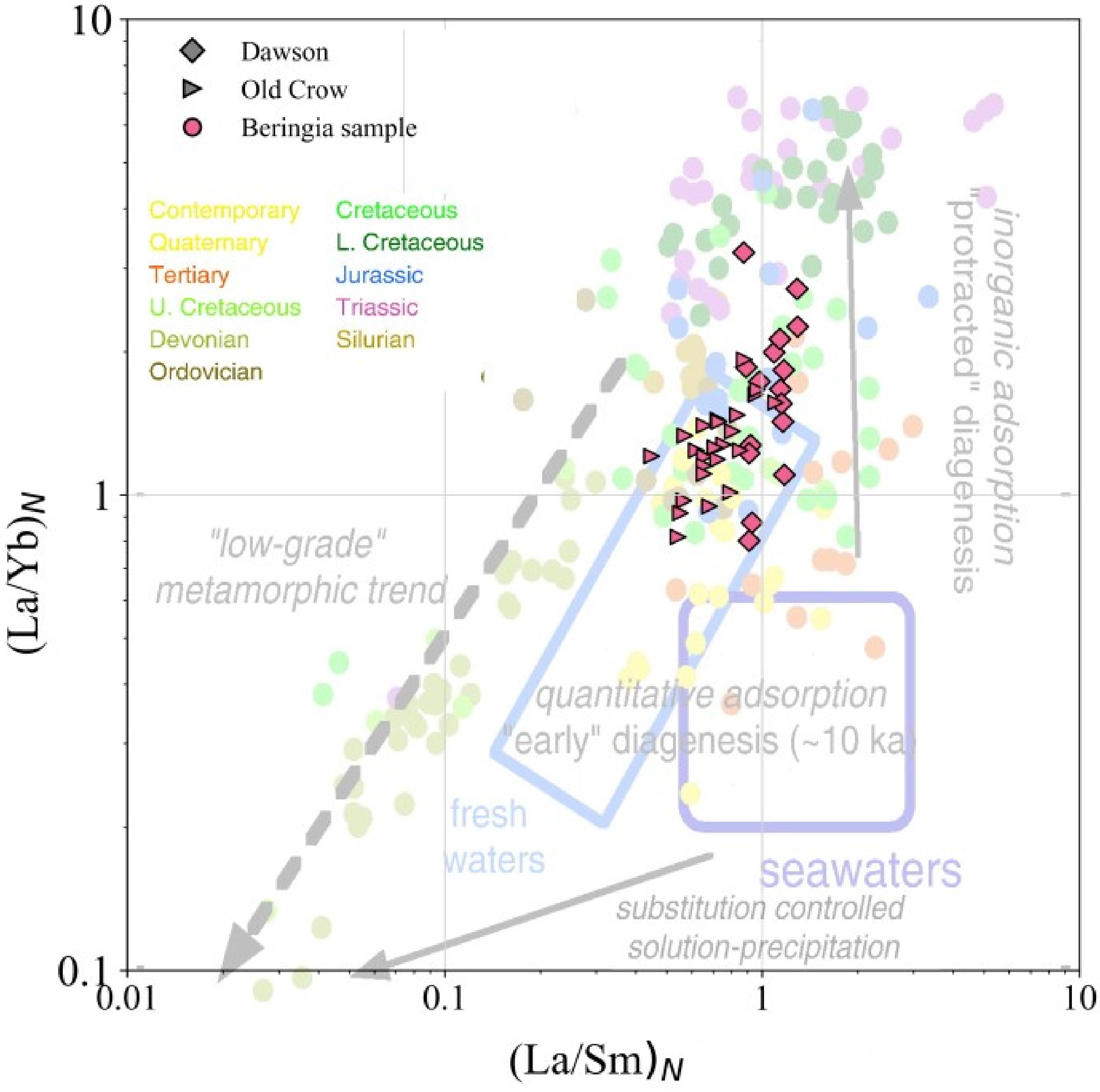

Figure 10. Plot of La/Yb versus La/Sm ratios in Beringian fossil enamel samples that underwent pre-treatment leaching, depicted by sample locality; Dawson (diamonds) and Old Crow, Yukon (triangle), used to assess the type and extent of potential diagenetic alteration. The samples from this study (pink squares or triangles) are plotted with a modified figure from (Reynard & Balter (2014) depicting La/Yb and La/Sm of fossil apatite with colour scale showing age of samples. The modified figure depicts the shift and fractionation associated with digenetic process (adsorption and substitution trends, as well as metamorphic trends.

As the Beringian samples are Late Pleistocene fossils, some early diagenesis and inorganic absorption is expected. Despite this, when the Ca/P, REE profiles, Eu (ppm), and $(La/Yb)_N$ (NASC) vs $(La/Sm)_N$ (NASC) analyses are considered in tandem and considering that calcium isotopes in enamel are largely immune to digenetic alteration (Dodat et al., 2023), I conclude that there is minimal post-depositional diagenetic alteration of the Beringian fossil samples making them ideal for $\delta^{44/42}Ca_{Alpha}$ and elemental analyses. Thus, they can reliably be used for dietary interpretation. The samples that are outliers for one or more of these analyses have been removed from further analyses and trend interpretation (i.e., Bison sample EL156, snowshoe hare sample EL183, moose sample EL201, woolly mammoth sample EL208, gray wolf sample EL220, and Arctic ground squirrel sample EL234).

3.2 Radiocarbon dating and Age subsets

Of the 24 samples radiocarbon dated in this study 14 were dated as a non-finite age and are henceforth represented as >50,000 BP. Upon radiocarbon dating some specimens that were initially categorized as a modern(non-leached) or Beringian (leached) samples were reassigned to a different age category for the remainder of the analyses. These samples include caribou samples EL127, EL130 and EL133 and snowshoe hare EL228, all of which were classified in the museum as fossil samples but yielded radiocarbon dates of 6490 ± 25, 690 ± 20, 1040 ± 20 and 4940 ±25, BP, respectively. These samples were reassigned to the modern subset for the remainder of the analyses but also underwent leaching because of their older ages.

All samples were assigned into one of four age subsets (i.e., Modern; 0-11Ka BP, post-LGM; 11-19 ka BP, LGM; 19-26 ka BP, and pre-LGM; >26 ka BP) based on their median calibrated radiocarbon age (BP) (Appendix D Table 2 and 4). For this study the modern subset consists of arctic ground squirrel (n=2), caribou (n=8), Dall sheep (n=2), gray wolves (n=15), moose (n=4), and snowshoe hare (n=2). A bison (n=1) and gray wolf (n=1) make up the post-LGM age subset. The LGM subset contains a gray wolf (n=1) and horses (n=2). The pre-LGM subset contains bison (n=3), caribou (n=2), Dall sheep (n=3), gray wolves (n=11), horses (n=3), muskox (n=1), and woolly mammoths (n=4).

Upon radiocarbon dating it was revealed that the LGM and post-LGM age subsets only contain 1 wolf specimen and thus cannot be included in the two-tailed t-tests for stable isotopes and elemental ratios between gray wolf age subsets. These age subsets also lack herbivore specimens, thus the only BSIMM ran for these age subsets was for $\delta^{13}C$ and $\delta^{15}N$ and included prey source material.

3.3 Stable Isotopes

The stable isotope compositions and trends vary based on species, age subset and isotope system (i.e., $\delta^{13}C$, $\delta^{15}N$ and $\delta^{44/42}Ca_{Alpha}$) as observed in Figure 11 and 12. The $\delta^{13}C$ and $\delta^{15}N$ values of prey species obtained in this study plot within the range of those from the dataset compiled from published literature that is constrained to Alaska and Yukon as seen in Figure 11A,B.

To test if there are statistically significant differences in gray wolf stable isotopes and elemental ratios over time, I performed a paired two-tailed t-test between the modern and pre-LGM gray wolf $\delta^{13}C$, $\delta^{15}N$, $\delta^{44/42}Ca_{Alpha}$, Sr/Ca and Ba/Ca, respectively. Additionally, Mann-Whitney tests between modern and pre-LGM gray wolf as $\delta^{44/42}Ca_{Alpha}$, Sr/Ca, and Ba/Ca values as these variables are not normally distributed (see Chapter 2 for further details).Table 6, Two-tailed t-test (*T-statistic and p-value*) and Mann Whitney (*Mann-Whitney U and p-value*) results testing the difference between $\delta^{13}C$ (‰), $\delta^{15}N$ (‰), $\delta^{44/42}Ca_{Alpha}$ (‰), Sr/Ca, and Ba/Ca of modern (n=15) and pre-LGM gray wolves (n=10 for $\delta^{13}C$ and $\delta^{15}N$ and n=11 *for* $\delta^{44/42}Ca_{Alpha}$, Sr/Ca, and Ba/Ca). * *T-test and Mann-Whitney U results with a significant difference between the compared gray wolf subsets (p-value < 0.05).*

Variable	**Paired two-tailed t-test**		**Mann-Whitney U test**	
	t	***p-value***	***U***	***p-value***
$\delta^{13}C$	1.68	0.106	NA	NA
$\delta^{15}N$	4.259	0.001*	NA	NA
$\delta^{44/42}Ca_{Alpha}$	1.474	0.159	58.0	0.213
Sr/Ca	2.692	0.016*	34.0	0.013*
Ba/Ca	6.791	0.4×10^{-4} *	0.0	2.1×10^{-5} *

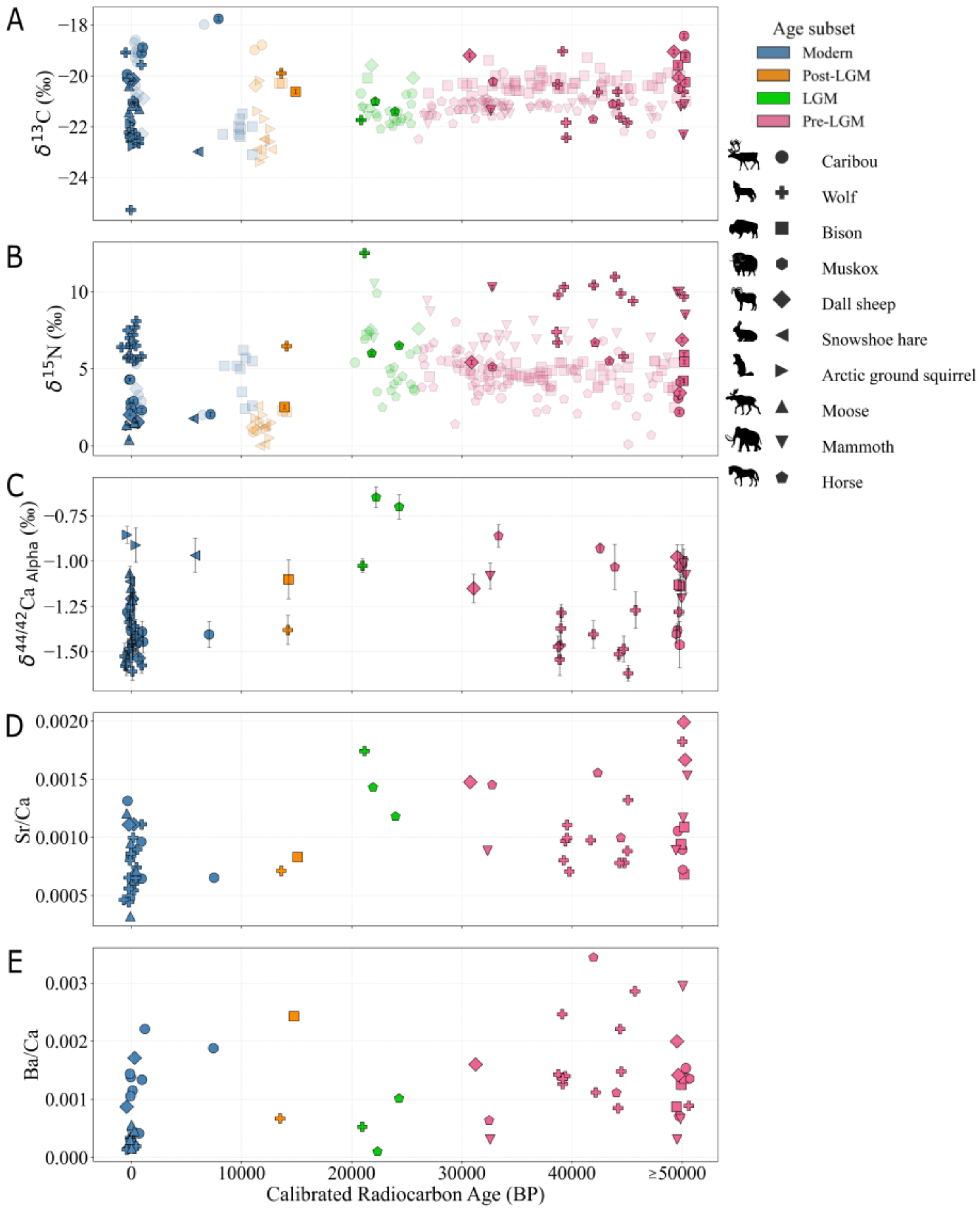

Figure 11. Median calibrated radiocarbon age (years BP) plotted against isotopic values and alkaline earth elemental ratios (AER) for fossil and modern specimens. Age subset is depicted by colour (modern [blue], post-LGM [orange], LGM [green], and pre-LGM [pink]) and species by shape. A) δ^{13}C (‰) and B) δ^{15}N (‰) values from collagen analyzed in this study with error bars representing ±2 standard error (SE) analytical uncertainty, along with values from the compiled prey database shown transparently in the background for comparison*; C) $\delta^{44/42}Ca_{alpha}$ (‰) values from tooth enamel with error bars representing ±2SE analytical uncertainty.; D) Sr/Ca and E) Ba/Ca values from tooth enamel. **Note: References for compiled prey database in Appendix C Table 4*.

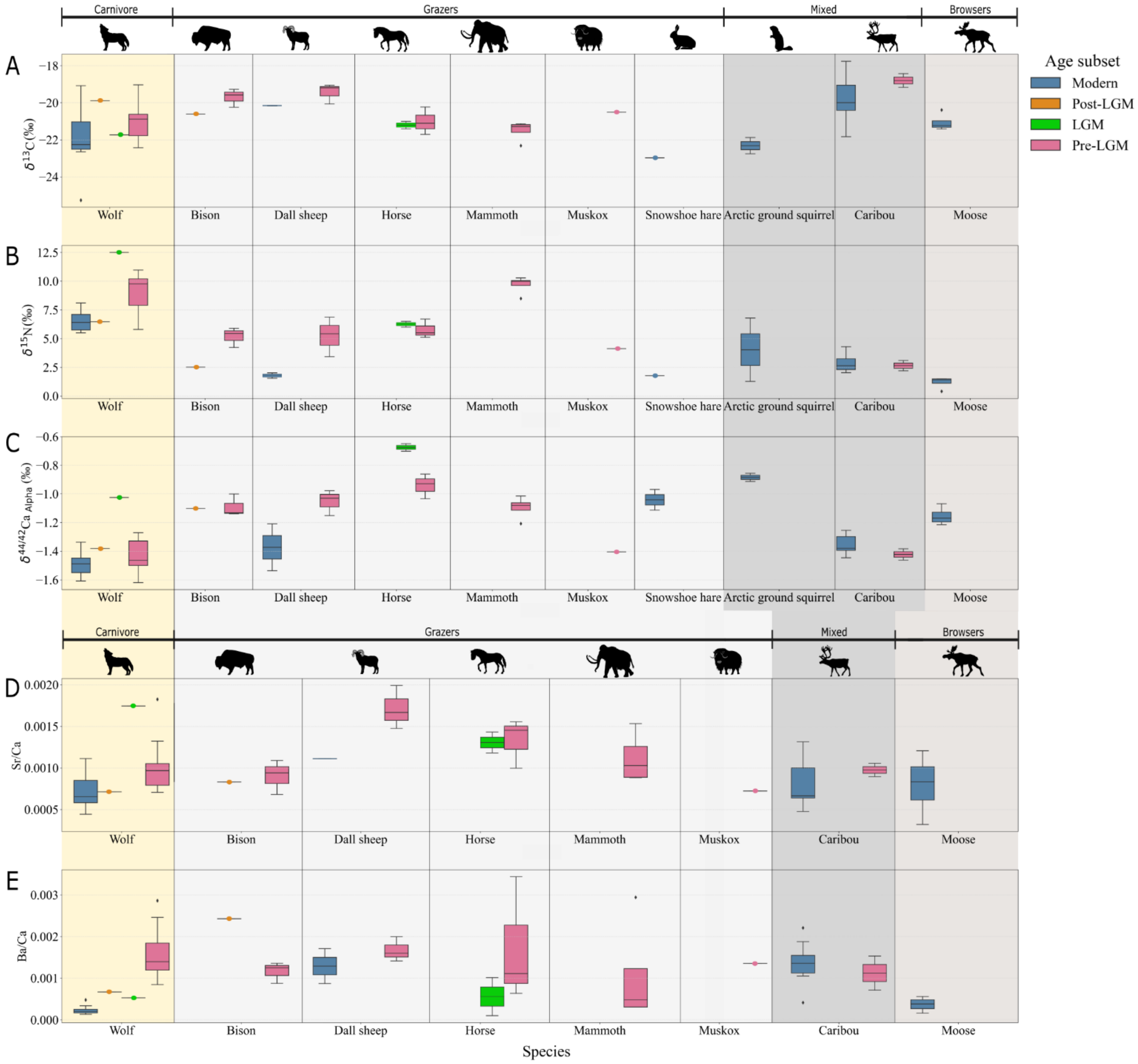

Figure 12. Box-and-whisker plots showing isotopic values and alkaline earth elemental ratios (AER) for fossil and modern specimens organized by age subset, depicted by colour (modern [blue], post-LGM [orange], LGM [green], and pre-LGM [pink]). A) $\delta^{13}C$ (‰); B) $\delta^{15}N$ (‰); C) $\delta^{44/42}Ca_{alpha}$ (‰); D) Sr/Ca*; and E) Ba/Ca*. The horizontal black line within each box indicates the median; boxes represent the interquartile range (IQR), and whiskers denote the range of non-outlier values. Outliers are plotted as black diamonds. Species with *n* = 1 in respective age subsets are shown as a black line with a single data point. **Note: Arctic ground squirrel and snowshoe hare are excluded from the Sr/Ca and Ba/Ca plots due to highly IQRs likely resulting from the sampling of bone rather than enamel.*

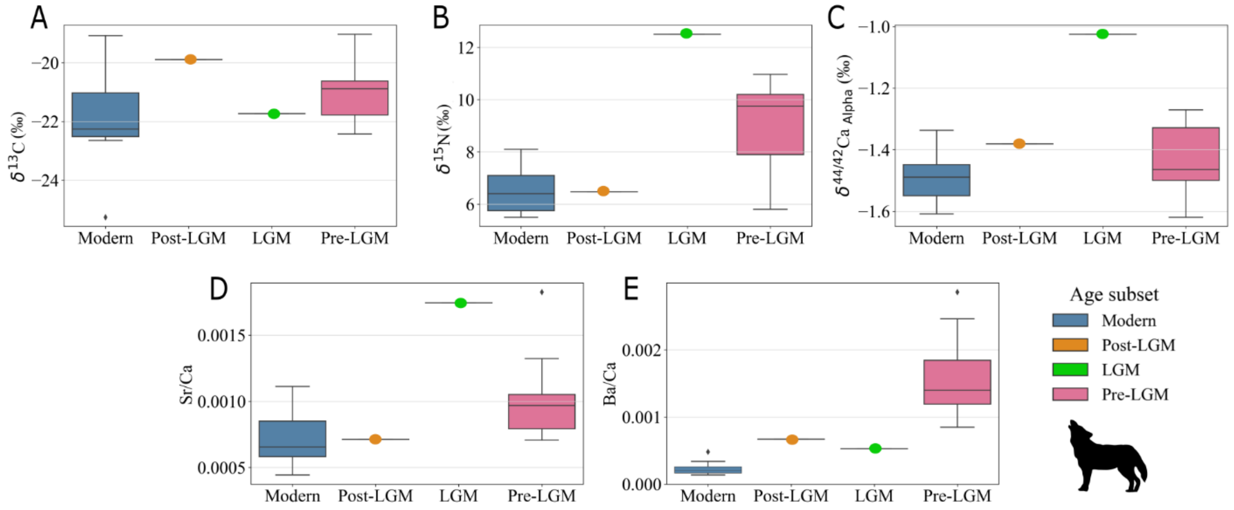

Figure 13. Box-and-whisker plots showing isotopic values and alkaline earth elemental ratios (AER) for fossil and modern gray wolves organized by age subset, depicted by colour (modern [blue], post-LGM [orange], LGM [green], and pre-LGM [pink]). A) $\delta^{13}C$ (‰); B) $\delta^{15}N$ (‰); C) $\delta^{44/42}Ca_{alpha}$ (‰); D) Sr/Ca; and E) Ba/Ca. The horizontal black line within each box indicates the median; boxes represent the interquartile range (IQR), and whiskers denote the range of non-outlier values. Outliers are plotted as black diamonds. Species with $n = 1$ in respective age subsets are shown as a black line with a single data point.

3.3.1 Carbon ($\delta^{13}C$ ‰)

$\delta^{13}C$ values show minimal difference among species as seen in Figure 11A, and 12A, with minimal clustering and extensive overlap of species $\delta^{13}C$ values in each respective age subset. Minimal differences in $\delta^{13}C$ values are observed for each species over time (Figure 11A, 12A). There are minimal differences between gray wolf $\delta^{13}C$ values over time as seen in the scatter plot (Figure 11A) and boxplots, where all gray wolf $\delta^{13}C$ values fall within the same range on the box and whisker plots (Figure 12A, 13A). Of all the species analyzed, modern and pre-LGM gray wolves, and modern caribou have the largest range in $\delta^{13}C$ values (Figure 12A, 13A).

Modern gray wolves have a mean $\delta^{13}C$ of -21.8±1.5‰ (SD, n=15), the post-LGM wolf has a $\delta^{13}C$ value of -19.9‰, the LGM wolf has a $\delta^{13}C$ value of -21.7‰, and pre-LGM gray wolves have a mean $\delta^{13}C$ of -21.0‰±0.98‰ (SD, n=10) (Figure 13A). There is no significant difference between $\delta^{13}C$ of modern and pre-LGM gray wolves as shown by a two-tailed t-test (t=1.68 and p>0.05, Table 6), indicating no change to gray wolf $\delta^{13}C$ over the last 50,000 years.

3.3.2 Nitrogen (δ^{15}N ‰)

As observed in Figure 11B and 12B δ^{15}N varies between species with distinct clustering of species across all four age subsets (Figure 11B). Gray wolves have the highest δ^{15}N compared to the herbivore species across all four age subsets, except for woolly mammoths which have high δ^{15}N values, which can be expected for woolly mammoths (Schwartz-Narbonne et al., 2015) and is comparable to data from published sources as seen in Figure 11B.

As observed in Figure 11B and 12B δ^{15}N values vary over time for all prey species. This is also observed for the gray wolves, which based on a two-tailed t-test, show a significant difference between modern and pre-LGM gray wolf δ^{15}N values ($t=4.259$ *and* $p<0.05$, Table 6). Modern wolves have a mean δ^{15}N of 6.5±0.8‰ (SD, $n=15$), the post-LGM gray wolf has a δ^{15}N value of 6.4‰, and pre-LGM wolves have a mean δ^{15}N of 9.0±1.8‰ (SD, $n=10$) (Figure 13B). The LGM wolf has the most enriched δ^{15}N with a value of 12.5‰ (Figure 9B). Overall, δ^{15}N values change over time for gray wolves based on the t-test and appear to peak during the LGM.

3.3.3 Calcium ($\delta^{44/42}\mathrm{Ca}_{\mathrm{Alpha}}$ ‰)

$\delta^{44/42}\mathrm{Ca}_{\mathrm{Alpha}}$ values vary between species, with gray wolves exhibiting the lowest $\delta^{44/42}\mathrm{Ca}_{\mathrm{Alpha}}$ values compared to the herbivore prey species in each respective age subset (Figure 11C, 12C). LGM and pre-LGM horses have the highest $\delta^{44/42}\mathrm{Ca}_{\mathrm{Alpha}}$ with mean values of -0.675± 0.037‰ (SD, $n=2$) and -1.053± 0.089‰ (SD, $n=3$), respectively, with other monogastric prey species (i.e., Arctic ground squirrel, snowshoe hare, woolly mammoth) also having elevated $\delta^{44/42}\mathrm{Ca}_{\mathrm{Alpha}}$ values compared to ruminants (i.e., polygastric [Dall sheep, muskox, caribou, bison, moose])(Figure 11C, 12C).

As observed in Figure 11C, 12C and 13C, the LGM gray wolf has the highest $\delta^{44/42}\mathrm{Ca}_{\mathrm{Alpha}}$ value compared to the other gray wolf age subsets with a value of -1.0‰. The post-LGM gray wolf has a $\delta^{44/42}\mathrm{Ca}_{\mathrm{Alpha}}$ value of -1.3‰ and has higher $\delta^{44/42}\mathrm{Ca}_{\mathrm{Alpha}}$ values compared to that of the modern and pre-LGM gray wolves [i.e., modern $\delta^{44/42}\mathrm{Ca}_{\mathrm{Alpha}}$ mean of -1.5±0.1‰ (SD, $n=15$) and pre-LGM with a mean $\delta^{44/42}\mathrm{Ca}_{\mathrm{Alpha}}$ of -1.4±0.1‰ (SD, $n=11$)]. The modern and pre-LGM wolves do not have a significantly different mean $\delta^{44/42}\mathrm{Ca}_{\mathrm{Alpha}}$ as shown by a two-tailed t-test ($t=1.474$ and $p>0.05$, Table 6), and a Mann-Whitney test ($U=58.0$ *and* $p>0.05$, Table 6).

While there is no significant difference between modern and pre-LGM gray wolf $\delta^{44/42}Ca_{Alpha}$ values, the LGM gray wolf has higher $\delta^{44/42}Ca_{Alpha}$ values than the other age subsets, specifically when compared to the modern gray wolves. These results are preliminarily but indicate a difference in gray wolf $\delta^{44/42}Ca_{Alpha}$ over time, with values peaking during the LGM. Unfortunately, the LGM and post-LGM gray wolves cannot be included in the t-test or Mann-Whitney U analyses due to a lack of specimens in these age subsets (n=1).

3.4 Alkaline earth elemental ratios (Sr/Ca and Ba/Ca)

Sr/Ca and Ba/Ca values have some species clustering, but greater intraspecies variation and overlap compared to $\delta^{13}C$, $\delta^{15}N$ and $\delta^{44/42}Ca_{Alpha}$ values (Figure 11D, 11E and 12D, 12E). Sr/Ca values do not vary over time for all species, but there are differences in Sr/Ca values between age subsets of gray wolves and Dall sheep, with LGM gray wolf having the highest Sr/Ca compared to other gray wolves (Figure 12D, 13D). Ba/Ca values vary between age subsets for the following species: gray wolves, bison and horse (Figure 12E, 13E).

Gray wolves have the lowest median Sr/Ca and Ba/Ca values compared to the herbivore prey species (Figure 12D,12 E). Modern gray wolves have a mean Sr/Ca of $7.190 \times 10^{-4} \pm 1.960 \times 10^{-4}$ and mean Ba/Ca of $2.280 \times 10^{-4} \pm 9.180 \times 10^{-5}$(SD, n=15). The post-LGM gray wolf has a Sr/Ca value of 7.129×10^{-4} and Ba/Ca value of 6.700×10^{-4}, whereas the LGM gray wolf has a value of 1.744×10^{-3} and 5.290×10^{-4}, respectively. Pre-LGM gray wolves have a mean Sr/Ca of $1.013 \times 10^{-3} \pm 3.209 \times 10^{-4}$ and mean Ba/Ca of $1.574 \times 10^{-3} \pm 6.525 \times 10^{-4}$ (SD, n=11), (Figure 13D, 13E). Based on the two-tailed t-test and Mann-Whitney U test, modern and pre-LGM wolves Sr/Ca and Ba/Ca have a significant difference (t=2.692 and 6.791, respectively, and U= 34 and <0.1, respectively, all with p's<0.05, Table 6), indicating that there was a change in gray wolf Sr/Ca and Ba/Ca compositions over the last 50,00 years.

3.5 Principal component analyses

The PCA plot in Figure 14A shows the clustering of species and respective age subset based on $\delta^{13}C$, $\delta^{15}N$ and $\delta^{44/42}Ca_{Alpha}$. Principal Component 1 (PC1) accounts for 41.18% variance and Principal Component 2 (PC2) explains 33.04% variance. Cumulatively PC1 and PC2 capture

74.22% of the total variation in this study's dataset. The dominant variable in PC1 is $\delta^{15}N$ pointing to the right and for PC2 is $\delta^{44/42}Ca_{Alpha}$ pointing in the upper left quadrant. $\delta^{13}C$ plots diagonally along PC1 and PC2, pointing in the lower left quadrant (Figure 14A).

Trophic position and gut physiology appear to influence the distribution and clustering of species in the PCA plot. Gray wolves of all age subsets cluster on the right side of the plot, which is associated with higher $\delta^{15}N$ values and lower and $\delta^{44/42}Ca_{Alpha}$ values (Figure 14A). Herbivores have lower $\delta^{15}N$ and higher $\delta^{44/42}Ca_{Alpha}$ values than the gray wolves and cluster on the left side of the plot. The monogastric prey species (i.e., horse and woolly mammoth) have higher $\delta^{44/42}Ca_{Alpha}$ values and cluster towards the top of the plot (Figure 14A).

A PCA considering five variables ($\delta^{13}C$, $\delta^{15}N$, $\delta^{44/42}Ca_{Alpha}$, Sr/Ca, and Ba/Ca) explains 62.65% of the variation in this dataset with the first two axes alone, with PC1 accounting for 36.04% variation and PC2 with 26.61% variation (Figure 14B). Compared to the PCA with only three variables ($\delta^{13}C$, $\delta^{15}N$ and $\delta^{44/42}Ca_{Alpha}$), the PCA considering five variables appears to explain 11.57% less variation in the dataset, possibly indicating that adding Sr/Ca and Ba/Ca introduces noise into the dataset, which is not unexpected when adding more variables to a PCA (Figure 14A, B). $\delta^{15}N$ and $\delta^{13}C$ plot along PC2, and $\delta^{44/42}Ca_{Alpha}$, Sr/Ca, and Ba/Ca plot along PC1.

Similar trends are observed in the five variable PCA as the three variable PCA but there appears to be more overlap of the species clusters. Gray wolves of all age subsets are associated with higher $\delta^{15}N$ and lower $\delta^{44/42}Ca_{Alpha}$ values. Woolly mammoths overlap with gray wolves in this PCA as they also have high $\delta^{15}N$ values compared to the other herbivore species (Figure 14B). As in the previous PCA, monogastric species are associated with high $\delta^{44/42}Ca_{Alpha}$ and higher Sr/Ca values.

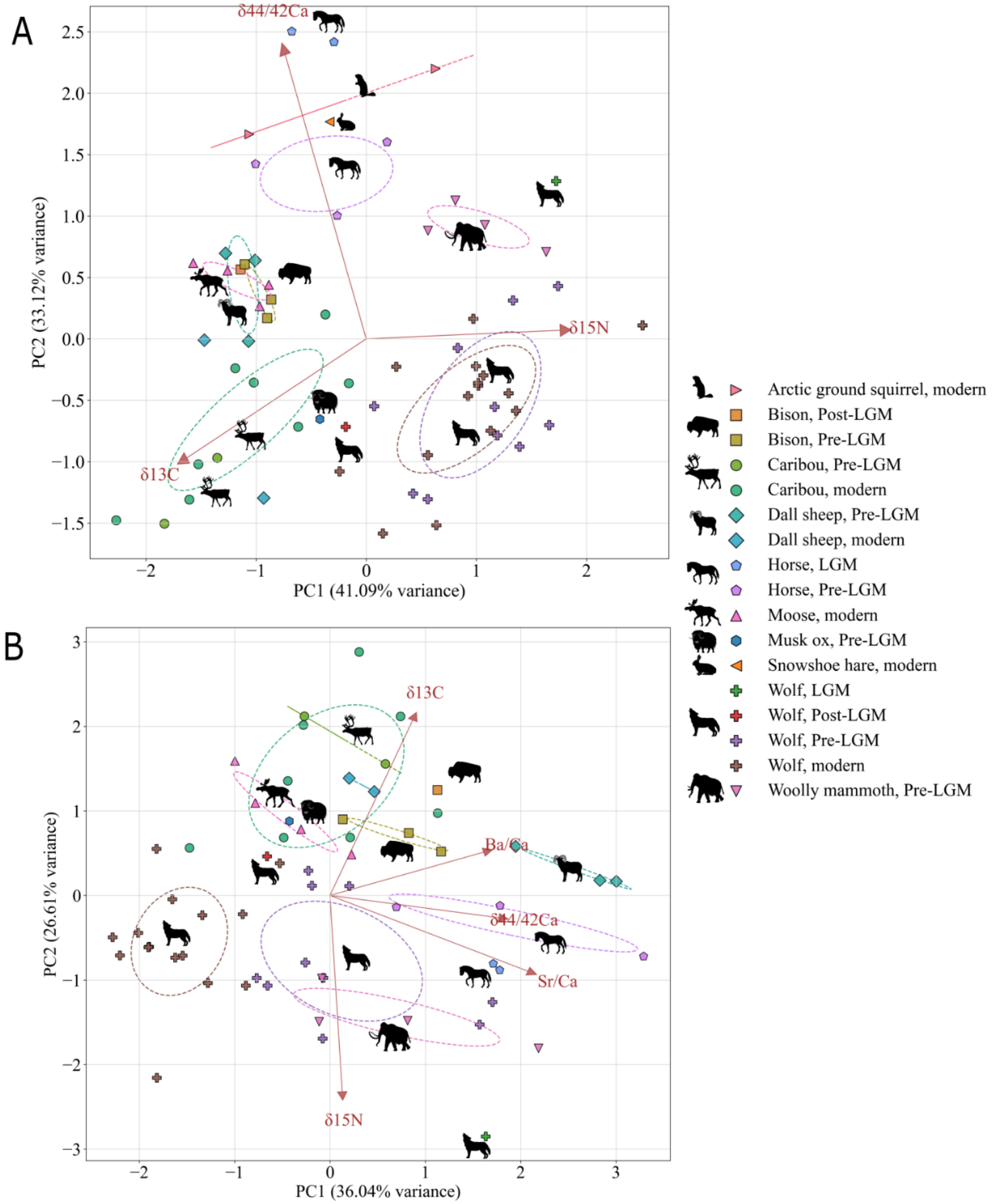

Figure 14. Principal Component Analysis (PCA) of isotopic and elemental data categorized by species and age subset (modern, Post-LGM, LGM, and Pre-LGM). A) PCA incorporating δ^{13}C (‰), δ^{15}N (‰), and $\delta^{44/42}$Ca$_{alpha}$ (‰) values, with Principal Component 1 (PC1) explaining 41.18% of the variance and Principal Component 2 (PC2) explaining 33.04%; and B) PCA incorporating: δ^{13}C (‰), δ^{15}N (‰), $\delta^{44/42}$Ca$_{alpha}$ (‰), Sr/Ca, and Ba/Ca*, with PC1 explaining 36.04% of the variance and PC2 explaining 26.61%. **Note: The PCA including Sr/Ca and Ba/Ca do not include Arctic ground squirrel and snowshoe hare due to high degrees of intraspecies variations likely resulting from the sampling of bone rather than enamel and flexible diet of small mammals.*

3.6 Gray wolf dietary mixing models

Bayesian stable isotope mixing models (BSIMMs) were used to assess the prey consumed by gray wolves through changing environmental conditions of glacial and interglacial periods. Appendix B Table 1, 2, 3 compile outputs from all BSIMM variations and versions.

All BSIMM variations reveal similar results for the modern gray wolves, revealing that modern gray wolves consume primarily snowshoe hare (Traditional proxy BSIMMs including compiled prey source data: 56.9±19.4%; Figure 15A), (Traditional proxy BSIMMs: 62.2±19.2%; Figure 16A), and (Traditional and novel proxy BSIMMs: 58.2±26.9%; Figure 17A) with a more minor contribution from large prey such as caribou (Traditional proxy BSIMMs including compiled prey source data: 10.5±6.5%; Figure 15A), (Traditional proxy BSIMMs: 12.1±8.2%; Figure 16A), and (Traditional and novel proxy BSIMMs: 6.7±4.1%; Figure 17A).

Conversely, all pre-LGM BSIMM reveal that the primary prey source of gray wolves during the pre-LGM was horse [(Traditional proxy BSIMMs including compiled prey source data: 44.8±10.7%; Figure D), (Traditional proxy BSIMM*s*: 69.4±13.4%; Figure 16B), and (Traditional and novel proxy BSIMM: 83.5±8.1%; Figure 17B). The BSIMM's for pre-LGM gray wolves with $\delta^{44/42}$Ca show a significant improvement in precision with a small standard deviation of 8.1%, the lowest standard deviation observed for primary prey species in all BSIMM variations.

Additionally, traditional proxy BSIMMs including compiled prey source data were run for the post-LGM and LGM age subsets revealed post-LGM gray wolves primary prey species was caribou (28.3±13.1%), and large contribution of snowshoe hare (22.7±16.7%), arctic ground squirrel (20.7±16%), and Dall sheep (18.6±15.4) (Figure 15B), whereas the primary prey source of LGM gray wolves were horses (77.8±20.1%; Figure 15C).

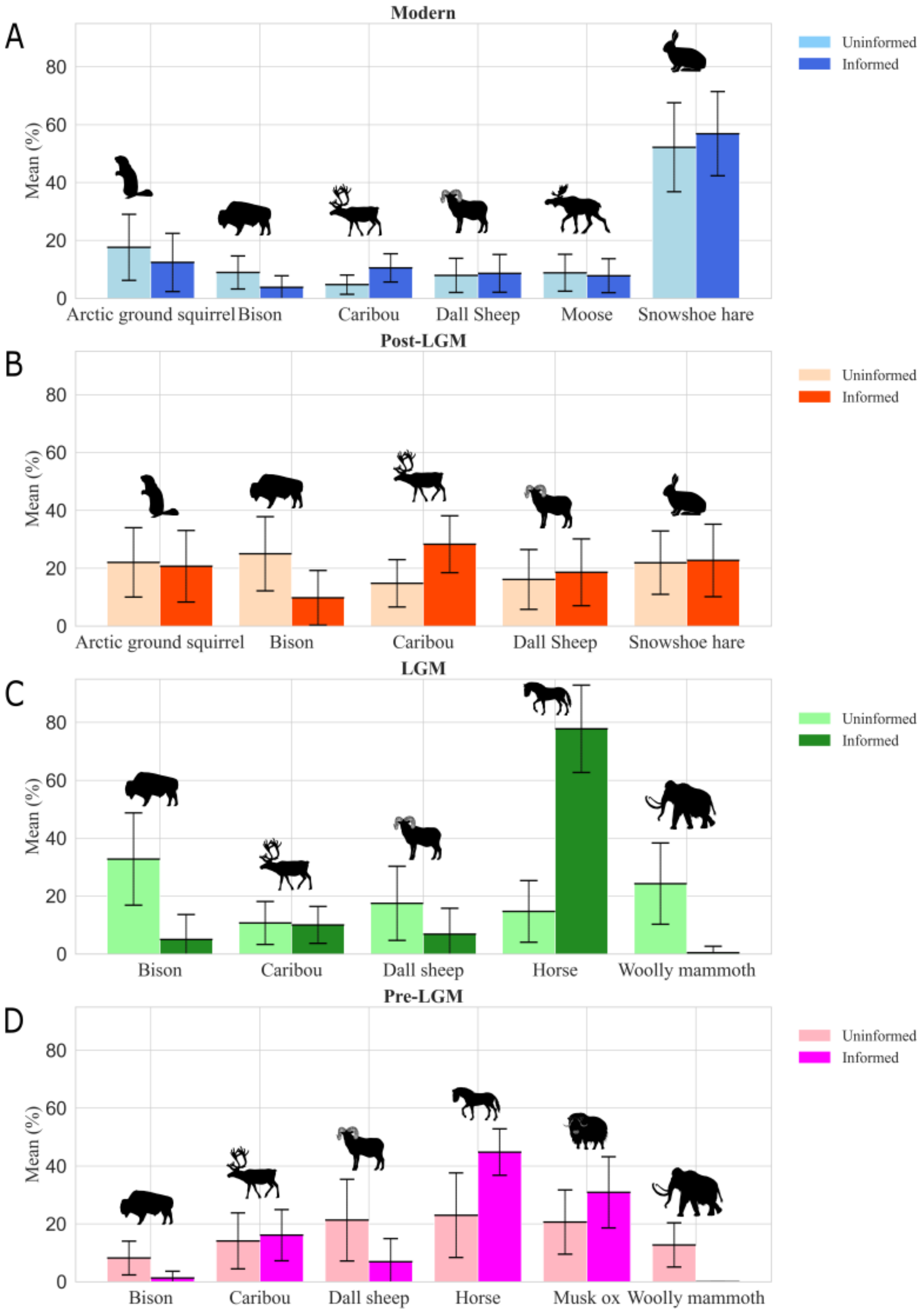

Figure 15. Plot of percent contributions (±standard deviation) of prey species sources to the diets of A) Modern gray wolves [<11 ka BP]; B) Post-LGM gray wolf [11-19 ka BP]; C) LGM gray wolf [19-26 ka BP]; and D) Pre-LGM gray wolves [>26ka BP], from traditional proxy ($\delta^{13}C$ [‰] and $\delta^{15}N$ [‰]) BSIMMs that include values from compiled published prey source dataset. Generated by uninformed and informed mixing models.

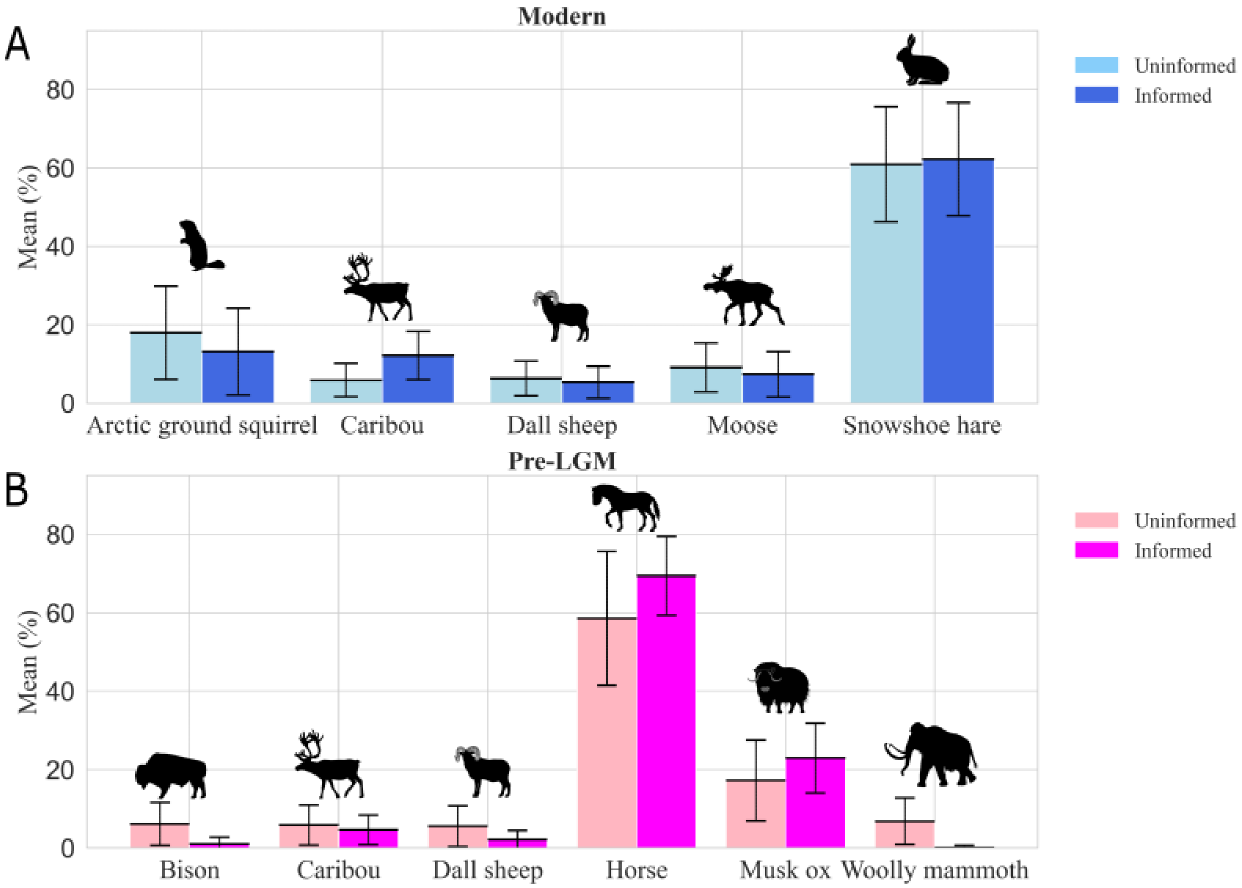

Figure 16. Plot of percent contributions (±standard deviation) of prey species sources to the diets of A) Modern gray wolves [<11 ka BP]; and B) Pre-LGM gray wolves [>26ka BP], from traditional proxy ($\delta^{13}C$ [‰] and $\delta^{15}N$ [‰]) BSIMMs. Generated by uninformed and informed mixing models.

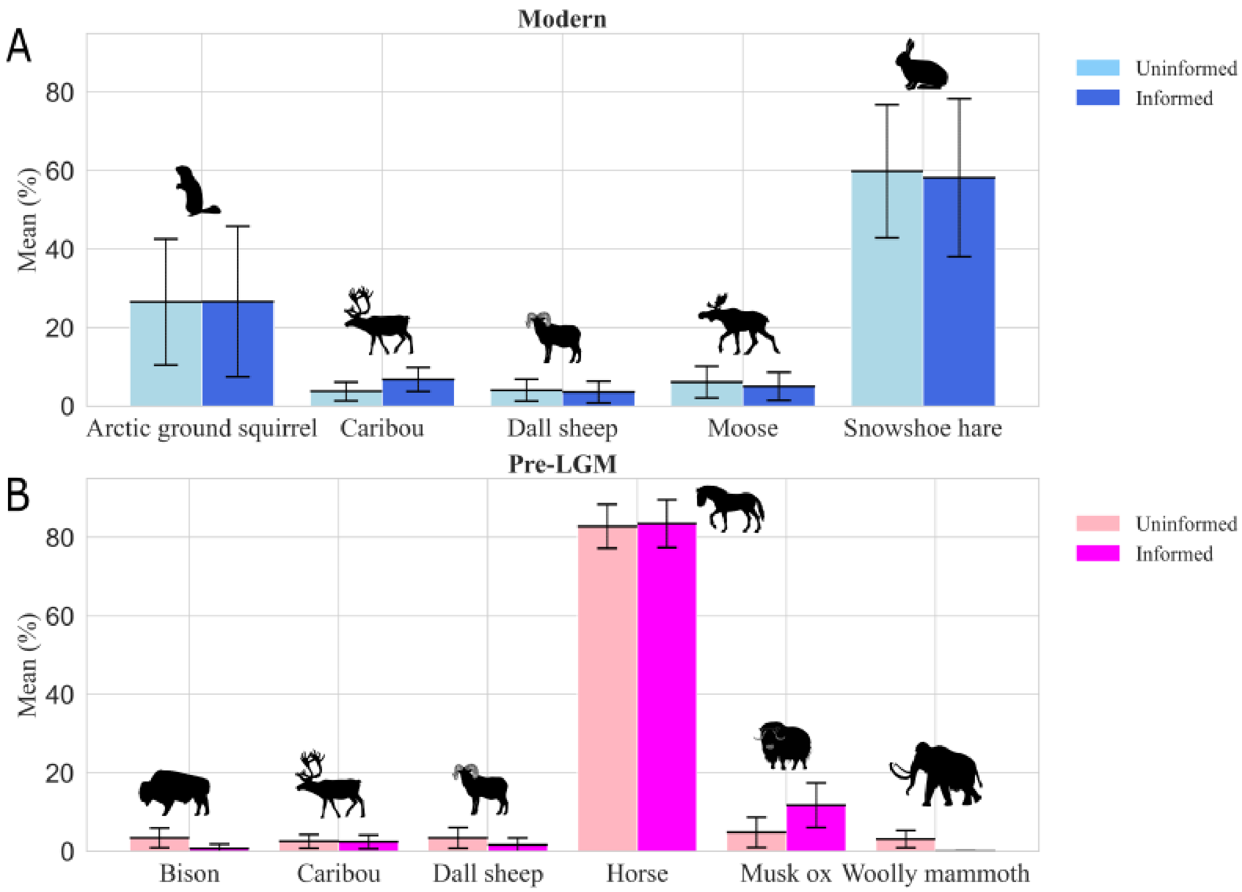

Figure 17. Plot of percent contributions (±standard deviation) of prey species sources to the diets of A) Modern gray wolves [<11 ka BP]; and B) Pre-LGM gray wolves [>26ka BP], from traditional and novel proxies ($\delta^{13}C$ [‰], $\delta^{15}N$ [‰], and $\delta^{44/42}Ca_{alpha}$ [‰]) BSIMMs. Generated by uninformed and informed mixing models.

4 Discussion

The effects of anthropogenic climate change will reach far beyond our lifetimes, limiting our ability to use present-day data to effectively predict how species will respond to future shifts in climatic and environmental conditions. By studying the fossil record, we can interpret how the feeding habits of top predators evolved in response to rapid climatic and environmental changes, which provides direct insights into the long-term dynamics of trophic relationships in palaeoecological communities. Reconstructing past trophic dynamics and ecological shifts are critical to predict the long-term response of ecosystems to modern global changes, specifically in response to anthropogenic climate change (Barnosky et al., 2017; Dietl et al., 2015; Fordham et al., 2020). Eastern Beringian gray wolves provide an excellent case study opportunity to assess the dietary evolution of a top predator species from the Late Pleistocene to the present-day, and allows us to examine how feeding behavior and dietary flexibility may have contributed to this species survival amid large-scale climatic, environmental, and ecological changes, a hypothesis that had been explored in a previous study (e.g., Landry et al., 2021).

Changes in stable isotope compositions in consumers tissues reflect ecological differences, including but not limited to landscape, climate, habitat-use, and dietary changes (Ben-David & Flaherty, 2012). Thus, the stable isotopes compositions (i.e., $\delta^{13}C$, $\delta^{15}N$, and $\delta^{44/42}Ca$) in gray wolf tissues can provide insights into their feeding ecology over time (Bocherens & Drucker, 2003) but may also reflect environmental changes (Heaton et al., 1986; Hixon et al., 2018). Previous studies have investigated the diets of modern and Pleistocene gray wolves in eastern Beringia using traditional stable isotope dietary proxies (i.e., $\delta^{13}C$ and $\delta^{15}N$) (e.g., Landry et al., 2021). Landry et al. (2021) found that gray wolves might have survived to modern times by shifting their diet from predominantly horses to a more generalist diet including other large ungulates and smaller prey. However, as nitrogen and carbon isotopes are strongly influenced by environmental and climate baseline conditions, shifts in $\delta^{13}C$ and $\delta^{15}N$ values might represent a mixture of dietary and environmental changes (Ben-David & Flaherty, 2012). The limitations of these traditional stable isotope proxies (see details in Chapter 1) can result in ambiguous dietary reconstructions unless proper spatiotemporal constraints are considered. Thus, further investigation using independent dietary proxies, such as $\delta^{44/42}Ca$, is required to further refine dietary studies.

In this study, I analyzed a broad combination of dietary proxies including δ^{13}C, δ^{15}N, $\delta^{44/42}$Ca, Sr/Ca, and Ba/Ca of Pleistocene and modern wolves from eastern Beringia and the Yukon territory, as well as associated prey to test and refine gray wolf feeding habits over the changing environmental conditions of the last 50,000 years. Using Bayesian stable isotope mixing models I reconstruct the dietary contribution of each prey to gray wolf diet across four age categories (i.e., modern [0 to 11 ka BP], post-LGM [11 to 19 ka BP], LGM [19 to 26 ka BP] and pre-LGM [>26 ka BP]), with each age subset having distinct climate and landscape conditions as described in Chapter 2.

4.1 Data quality

A critical prerequisite for this study was to ensure that all isotopic data used in my dietary reconstructions accurately reflect biogenic signals and are not compromised by diagenetic alteration. For this reason, I applied stringent protocols and screening criteria for both bone collagen and enamel derived isotopic data.

Carbon (δ^{13}C) and nitrogen (δ^{15}N) isotopes were analyzed in bone collagen (see Chapter 2). Collagen, being an organic matrix, is highly susceptible to diagenetic degradation (e.g., van Klinken, 1999), which can lead to contamination by exogenous materials and isotopic shifts (Balzer et al., 1997). To mitigate this risk, we employed an ultrafiltration protocol for collagen extractions which maximizes the recovery of collagen while minimizing possible contamination by low-molecular-weight compounds such as degraded proteins and other contaminants (i.e., salts and microorganisms) (Talamo et al., 2021).

Only samples that met rigorous preservation criteria were retained for analysis. Specifically, we applied a narrow range of acceptable atomic C:N ratios (2.9-3.6), a widely used proxy for collagen integrity (Deniro et al., 1985; Ambrose, 1990). All collagen samples included in this study fell within the accepted C:N range (Appendix A Figure 3) indicating excellent collagen preservation and/or the reflecting the efficiency of ultrafiltration collagen extraction methods. This high degree of preservation is consistent for subfossil material recovered from cold, high-latitude environments, where collagen degradation is generally slower (Matsubayashi & Tayasu, 2019; Matthiesen et al., 2021). Radiocarbon dating confirmed the expected chronological placement of the samples, and both $\delta^{13}C$ and $\delta^{15}N$ data demonstrated excellent analytical precision and reproducibility (see Chapter 2).

In contrast to collagen and bone, tooth enamel is an inorganic matrix and is generally more resistant to diagenetic alteration (Dodat et al., 2023; Reynard & Balter, 2014). However, during fossilization some diagenetic alteration can still occur through processes such as chemical exchange or recrystallization, which may introduce or replace biogenic calcium with exogenous material (Hoppe et al., 2004; Trueman et al., 2008). To assess the extent and type of diagenetic alteration in enamel, I employed a multi-proxy screening approach using established geochemical indicators including, rare earth element (REE) profiles, europium (Eu) concentrations, and La/Yb and Sm/Yb ratios (Dodat et al., 2023; Reynard & Balter, 2014). The high La/Yb and Sm/Yb ratios are indicative of early diagenesis and adsorption (Reynard & Balter, 2014). Overall, these ratios suggest minimal diagenetic overprinting, as samples from this study have similar La/Yb and Sm/Yb values to that of Quaternary samples with limited diagenetic input (Figure 10). The potential diagenetic input as indicated by La/Yb and Sm/Yb ratios, will negligibly alter calcium isotope compositions in enamel as shown by Dodat et al. (2023), confirming the reliability of the isotopic compositions.

The relatively flat REE profiles (Figure 8) and low Eu concentrations (Figure 9) both indicate minimal diagenetic uptake (Dodat et al., 2023; Reynard & Balter, 2014; Tütken et al., 2008). The similar ranges and patterns between REE profiles between the two main regions (i.e., Dawson and Old Crow [Figure 8]) shows that despite different geochemical provinces (Figure 2), fossil samples underwent minimal types and extents of diagenetic alteration. Thus, I can compare fossil samples form the various sites across the Yukon. Ca/P molar ratios were also evaluated to detect possible mineral replacement or post-secondary deposition (Dodat et al., 2023; Sillen & LeGeros, 1991; Trueman & Tuross, 2002) where all but four samples showed consistent and expected Ca/P values (Figure 7).

All but six enamel sample outliers (i.e., EL156, EL183, EL201, EL208, EL220, and EL234) passed these diagenetic screening criteria and were deemed well-preserved (see Chapter 3 for details). The six outliers showed mild deviations from the diagenetic screenings and were excluded from statistical analyses and trend interpretation, despite having isotopic values within typical dietary ranges. Together, these stringent diagenetic assessments confirm that the $\delta^{13}C$,

δ^{15}N, AER, and $\delta^{44/42}$Ca values reported in this study represent biologically meaningful signals. The combined use of reliable organic and inorganic geochemical proxies ensures the robustness of my dietary reconstructions and enhances confidence in interpreting trophic dynamics across space and time.

4.2 Gray wolf diet; Insights from isotope and elemental dietary proxies

4.2.1 Traditional dietary proxies (δ^{13}C and δ^{15}N)

Carbon and nitrogen isotopes are commonly used as dietary indicators to reconstruct diet and trophic relationships (Bocherens & Drucker, 2003). Across all age subsets, gray wolves exhibit δ^{13}C values that are broadly similar to those of their potential prey (Figure 11A, 12A), suggesting limited carbon isotopic distinction between trophic levels. Additionally, only the modern small mammals have a lower mean δ^{13}C values compared to modern gray wolves whereas for Pleistocene gray wolves, horses and mammoths are the only prey that have lower mean δ^{13}C values (Figure 11A, 12A).

The lack of δ^{13}C value distinction between gray wolves and their prey observed in this study is likely the result of the small δ^{13}C trophic discrimination factor (TDF). With only a +1 ‰ enrichment in δ^{13}C between adjacent trophic levels, it is unlikely that when used in isolation carbon isotopes would provide a diagnostic tool to assess prey consumption (Fry et al., 1991; Perkins et al., 2014; Post, 2002). This is particularly true when considering the range of other factors that can overprint the δ^{13}C discrimination associated with trophic level, such as environmental conditions (Heaton, 1999; Kohn, 2010), habitat (Bonafini et al., 2013; Drucker et al., 2008), and plant types (Diefendorf et al., 2010; Tieszen, 1991). All these factors create a high intraspecies δ^{13}C range, as observed in the results in this study, (Figure 11A, 12A), which makes it difficult to observe the TDF effect.

Additionally, I observe minimal difference in gray wolf δ^{13}C values over time (Figure 13A). This is likely a consequence of the similar δ^{13}C values among prey, which likely reflects the shared C_3 plant-based diets between herbivore species in this study area (Blinnikov et al., 2011; Tahmasebi et al., 2017; Wooller et al., 2007 Zazula et al., 2006a) (Figure 11A, 12A) and does not imply dietary continuity between modern and Pleistocene gray wolves. Even if gray wolves had significantly shifted their diet, this shift would be difficult to quantify with carbon isotopes due to the overarching similarity of prey $\delta^{13}C$ values. These collective findings further support that $\delta^{13}C$ cannot independently be used as a dietary proxy (Fry et al., 1991; Perkins et al., 2014; Post, 2002), particularly in environments where $\delta^{13}C$ does not distinguish among prey species, coupled with the existence of only one dominant plant photosynthetic pathway (i.e, C_3 vs C_4 plants)—such as in Yukon and eastern Beringia—as this can lead to an ambiguous trophic reconstruction and mislead carnivore diet reconstruction (Casey & Post, 2011).

Nitrogen stable isotopes are commonly used in combination with $\delta^{13}C$ for trophic and diet reconstructions because of the distinct trophic enrichment in the heavy nitrogen isotope with increasing trophic position (Bocherens & Drucker, 2003; Deniro & Epstein, 1981; Minagawa et al., 1984). As expected, gray wolves have the highest $\delta^{15}N$ values compared to herbivores in each age subset (Figure 11B, 12B). However, gray wolf $\delta^{15}N$ values vary significantly over the last 50,00 years with higher values prior to and during the LGM, and lower values after the LGM (Figure 13B). This could indicate a dietary shift between modern and Pleistocene gray wolves as interpreted by Landry et al. (2021). However, since $\delta^{15}N$ values are known to vary with habitat and environmental conditions (Craine,et al., 2015a,b; Craine et al., 2009), observed changes in $\delta^{15}N$ values may not solely indicate dietary shifts, but could also reflect environmental changes within the region, which has been shown in previous studies (e.g., Fox-Dobbs et al., 2008; Schwartz-Narbonne et al., 2019; Stevens et al., 2008; Tahmasebi et al., 2018).

Interestingly, prey $\delta^{15}N$ values show similar trends as wolves with lower values during the Holocene and post-LGM subsets compared to the LGM and pre-LGM subsets (Figure 11B, 12B). While shifts in dominant vegetation and plant types have occurred in this region over the last 50,000 years (Rowland et al., 2016; Zimov et al., 1995), it is unlikely that all herbivore species completely shifted their diet during these periods. Rather it is more likely that the observed variation in prey $\delta^{15}N$ values could be attributed to changes in baseline environmental conditions, particularly moisture availability in soils, that are known to affect $\delta^{15}N$ values (Craine et al., 2015a,b; Craine et al., 2009). Prior to and during the LGM, global temperatures were colder, and eastern Beringia was more arid with minimal soil moisture, resulting in higher $\delta^{15}N$ values in plants that was likely propagated throughout the food chain (Ambrose, 1991; Amundson et al., 2003; Handley et al., 1999; Heaton, 1987; Hixon et al., 2018; Rabanus-Wallace et al., 2017; Stevens et al., 2004; Stevens et al., 2008). As global temperatures increased, glacial retreat and permafrost thaw led to an influx of moisture in eastern Beringia soils and ecosystems (Rabanus-Wallace et al., 2017; Rowland et al., 2016). This resulted in lower $\delta^{15}N$ in plants and herbivores because increased moisture influences nitrogen cycling in soils (Cleveland et al., 1999; Rabanus-Wallace et al., 2017). This Late Glacial Nitrogen Excursion (LGNE) is characterized by a significant drop in herbivore $\delta^{15}N$ values across Europe, Siberia, and the Americas, coinciding with the Last Glacial-Interglacial transition (Rabanus-Wallace et al., 2017; Reade et al., 2023; Tahmasebi et al., 2018). Thus, the difference and trends observed in gray wolf $\delta^{15}N$ values over time might be, at least partially, reflective of changing environmental baselines. Teasing out the portion of $\delta^{15}N$ variations linked to environmental changes from that associated with dietary modifications requires additional proxies.

The resolution of $\delta^{13}C$ and $\delta^{15}N$ alone as dietary proxies in regions like eastern Beringia and the Yukon is limited due to shifts in isotopic baselines due to changing environmental conditions and where vegetation is dominated by a single photosynthetic pathway (C_3), both of which further complicate dietary interpretation. In conclusion, the $\delta^{13}C$ and $\delta^{15}N$ data collected in this thesis are not sufficient to support large-scale dietary shifts in gray wolve diet across the last 50,000 years. Such interpretations require consideration of spatial and temporal constraints and nonetheless, additional dietary proxies are necessary to support more robust conclusions.

4.2.2 Novel dietary proxies ($\delta^{44/42}Ca$, Sr/Ca, and Ba/Ca)

The limitations of $\delta^{13}C$ and $\delta^{15}N$, as previously described, can result in ambiguous diet and trophic reconstructions (Balzer et al., 1997; Casey & Post, 2011). Therefore, it is critical to use additional independent proxies to validate previous findings that suggest that wolves completely shifted their diet between the late Pleistocene to now (e.g., Landry et al., 2021). Novel dietary proxies such as $\delta^{44/42}Ca$, Sr/Ca, and Ba/Ca have the potential to achieve a more nuanced understanding of feeding ecology and trophic relationships in extinct prey species, by adding independent dimensions in the isotope dietary space (Balter et al., 2002; Martin et al., 2017; Reynard & Balter, 2014; Safont et al., 1998; Tacail et al., 2020; Toots & Voorhies, 1965).

Compared to traditional isotopic proxies, trophic reconstructions based on alkaline Earth element ratios (AER) such as Sr/Ca and Ba/Ca ratios, are used less frequently due to perceived sensitivity to baseline shifts and diagenetic alteration (e.g., Blum et al., 2000; Peek & Clementz, 2012; Price et al., 2002; Terrill et al., 2022).

Due to trophic depletion, I would expect AER in gray wolves to be lower than that of herbivores (Burton & Wright, 1995; Sillen & Kavanagh, 1982). However, my results do not consistently reflect a predicted trophic depletion, as the gray wolf AER values in this study are not consistently lower than herbivores in each respective age subset (Figure 11D, E and 12D, E). This is likely because the relative abundances of Sr and Ba to Ca are more sensitive to local baselines and will change with local geology and environmental conditions (Balter, 2004). This baseline effect can create high degrees of intraspecies variation particularly when pooling samples from different sites as done in this study. This can result in inconsistent biological fractionation of Sr and Ba relative to Ca, specifically in carnivores as the most significant and consistent biological fractionation of Sr and Ba usually occurs in lower trophic levels (Balter, 2004; Blum et al., 2000; Price et al., 2002).

I observe changes in gray wolf Sr/Ca and Ba/Ca ratios over time (Figure 13D, E), but due to the variation and inconsistency it is difficult to distinguish if this reflects a dietary shift, local geology, post-depositional diagenetic alteration, or a combination of these factors. Based on my findings I suggest rather to use Sr/Ca and Ba/Ca at singular sites and horizons, as they can be heavily influenced by local geology and diagenetic alteration. The limited and variable biologic fractionation, findings shown in this thesis as well as in previous studies, highlight that Sr/Ca and Ba/Ca should not be independently applied in dietary and trophic reconstructions (e.g., Fabig & Herrmann, 2002; Hassler et al., 2018; Martin et al., 2015; Nitzsche et al., 2022; Peek & Clementz 2012).

In addition to AER, I tested the potential of $\delta^{44/42}$Ca as an independent dietary proxy. Gray wolves generally displayed the lowest $\delta^{44/42}$Ca values compared to herbivores in each respective age subset (Figure 11C, 12C). This was expected because calcium isotopes are known to fractionate along the trophic chain with decreasing $\delta^{44/42}$Ca values with increasing trophic level (Dodat et al., 2021; Hassler et al., 2018; Martin et al., 2015, 2017, 2018; Weber et al., 2025). Interestingly, it is observed that there are potential $\delta^{44/42}$Ca differences between monogastric and polygastric organisms in each age subset, where monogastric species (i.e., horse, snowshoe hare, Arctic ground squirrel, and mammoth) have higher $\delta^{44/42}$Ca values than polygastric species (i.e., caribou, moose, Dall sheep, muskox, and bison) (Figure 12C,14A, B), consistent with findings from previous studies (e.g., Guiserix et al., 2024; Hu et al., 2022; Martin et al., 2018). This difference in $\delta^{44/42}$Ca values between monogastric and polygastric organisms may also be driven by differences in diet (grazing and browsing feeding habits) as suggested by data from ecosystems and plants (e.g., Guiserix et al., 2024; Martin et al., 2018). The $\delta^{44/42}$Ca values further the isotopic distinction between species, which is ideal in diet and trophic reconstructions. The possibility to distinguish a carnivorous diet dominated by specific herbivorous prey adds an important dimension to the multi-isotope dietary framework.

Gray wolf $\delta^{44/42}$Ca values show some variation over time, being the highest during the LGM, and lowest in Holocene wolves (Figure 13C). Unlike δ^{15}N values, I do not observe a significant baseline shift in $\delta^{44/42}$Ca values, as indicated by the $\delta^{44/42}$Ca similarity between Holocene and post-LGM herbivores compared to LGM and pre-LGM herbivores (Figure 11C, 12C). This suggests that unlike nitrogen, calcium stable isotopes experienced minimal to no baseline shift despite climatic, landscape, and environmental changes occurring in eastern Beringia during this time. Thus, the observed change in gray wolf $\delta^{44/42}$Ca values over time is likely not reflective of environmental changes, but of a dietary shift. These findings demonstrate that incorporating $\delta^{44/42}$Ca as a dietary proxy provides a method to evaluate whether shifts in gray wolf isotopic compositions over the past 50,000 years reflect dietary changes, with minimal influence from environmental baseline variability and will strongly complement δ^{13}C and δ^{15}N dietary interpretations. This highlights the robustness of calcium isotopes and supports the reliability of δ^{44}Ca as a dietary proxy, particularly in environmentally dynamic systems where other dietary proxies might be more challenging to interpret.

4.3 Dietary Mixing Models reveal shift in Gray Wolf Feeding Ecology

Understanding the ecology of gray wolves over time offers a unique window into predator-prey dynamics and broader ecosystem transformations. Using Bayesian stable isotope mixing models (BSIMMs), I used the new isotopic data generated in this study to reconstruct precise dietary profiles of gray wolves across four time periods from the Pleistocene to the present-day. Through this exercise, I find further support for and refine the major ecological transition of this species with a shift from a highly specialized diet to a more generalist and opportunistic diet.

I employed three variations of BSIMMs based on a combination of $\delta^{13}C$, $\delta^{15}N$, and $\delta^{44/42}Ca$ isotopic data (see Chapter 2 for details). Each model was run with two prior settings; uninformative priors— which assumed equal likelihood of all prey sources (the MixSIAR default settings) — and informative priors—which incorporate ecological knowledge of wolf predatory behavior, particularly prey size preferences (see Chapter 2 for more details and Appendix B Tables 1, 2, 3 for list of priors). While uninformative priors offer a neutral baseline, the informative models provide more ecologically realistic reconstructions, particularly for species with known hunting strategies like wolves.

4.3.1 Pleistocene Wolves: Horse Specialists in an Abundant Ecosystem

Consistent across all informed BSIMMs, Pleistocene gray wolves (before 19 ka BP) from eastern Beringia exhibited a highly specialized diet, dominated by Beringian horses (Figure 15C, 15D, 16B, 17B). These findings corroborate earlier work (e.g., Landry et al., 2021), but calcium isotopes further highlight the degree of specialization than previously recognized from carbon and nitrogen isotopes alone with up to 84% of the diet coming from horses (Figure 17B). Pleistocene wolves appear to have had an extremely specialized diet, taking advantage of the high abundance of horses across the mammoth steppe (Guthrie, 2003; Harington, 2011). Despite limited specimen availability during the Last Glacial Maximum (26–19 ka BP), even the informed traditional proxy BSIMM that included published prey source data primarily suggests that gray wolves remained highly specialized on Beringian horses during the LGM (Figure 15C). As this model only contains one wolf specimen, I recommend that future studies include more samples and run additional BSIMMs with traditional and novel dietary proxies for a more in-depth view on gray wolf diet during the LGM.

Intriguingly, recent ancient DNA analyses suggest that Beringia was the home to now-extinct lineages of gray wolves called the Beringian wolf that likely exhibited slightly distinct hunting habits focused on megafauna as evidenced by their robust jaws, large, broad carnassial teeth, and wide, short snouts – all modifications for higher bite force and better carcass processing stronger jaws (Loog et al., 2020; Leonard et al., 2007). These results imply that during the Pleistocene, gray wolves likely occupied a distinct ecological niche with minimal dietary overlap with other apex predators, enabled by the high biomass of large herbivores and potential ecological niche partitioning (Bocherens, 2015; Drucker, 2022; Schwartz-Narbonne et al., 2019). The presence of this morphologically and genetically distinct lineage, the so-called Beringian wolf, raises compelling questions about the drivers of such extreme dietary specialization. Further morphometric, isotopic, and genomic analyses of Pleistocene specimens are needed to determine whether this specialization reflects an inherited, genetically encoded trait of a now-extinct hypercarnivorous lineage, or a flexible, behavioral modification by gray wolves in response to the unique ecological conditions of the mammoth steppe.

4.3.2 Post-LGM Transition: From Specialization to Generalism

Between 19 and 11 ka BP, major climatic and vegetational shifts—particularly the onset of warming temperatures, increased moisture, and the northward expansion of shrub tundra and boreal forests—transformed eastern Beringian ecosystems (Zimov et al., 1995). The collapse of the mammoth steppe biome, characterized by its nutrient-rich grasslands and herbaceous cover, led to significant habitat loss for grazing megafauna (Guthrie, 2001; Zazula et al., 2006b). Around 13.5 ka BP, the proliferation of woody shrubs further reduced the viability of open grasslands, compounding pressures on grazing specialists (e.g., woolly mammoth, Beringian horse, etc.,) many of which experienced steep population declines or went extinct shortly thereafter (Monteath et al., 2021, 2022; Murchie et al., 2021). Horses in particular showed signs of a rapid demographic collapse, as revealed by palaeogenomic reconstructions indicating a severe population bottleneck across much of Beringia (Guthrie, 2003; Running Horse Collins et al., 2025).

As this faunal turnover progressed, new herbivore communities began to emerge in the changing tundra-taiga landscape, with species such as caribou and moose, expanding their ranges and ecological roles (Meiri et al., 2020; Taylor et al., 2021). In response, gray wolves underwent a marked dietary shift, as shown by traditional proxy BSIMMs which reveal a significant broadening in gray wolf diets between 19 and 11 ka BP, with increasing reliance on a wider suite of large ungulates—particularly caribou and Dall sheep—as well as a surprising and consistent intake of small mammals such as Arctic ground squirrels and snowshoe hares (Figure 15B). These small mammals contributed as much to the diets of the wolves analyzed in this study as ungulates, underscoring a strategic shift in foraging behavior. Similar to the LGM BSSIM, the post-LGM model only contains one wolf specimen, so further research is recommended to understand this dietary shift in greater detail between 19 to 11 ka BP.

This transition from a specialist to generalist supports a profound example of ecological and behavioral flexibility in gray wolves instead of a complete change of lineages with distinct hunting habits. Unlike other Beringian predators such as the scimitar cat, the short-faced bear, which were heavily dependent on megaherbivore prey and appear to have been unable to adapt to the disappearance of those ecological niches (Ripple & Van Valkenburgh, 2010; Van Valkenburgh, 2009), gray wolves demonstrated the capacity to diversify their diet from an almost exclusively horse-based diet in the Pleistocene to a more diversified diet during deglaciation. This flexibility likely contributed to their survival into the Holocene and beyond as well as the success of the Beringian lineage of gray wolves across the globe (Loog et al., 2020). Such dietary flexibility—possibly rooted in both behavioral alteration and social foraging dynamics—enabled wolves to reorient their ecological role and persist through a time that proved more challenging for their co-existing apex predators.

4.3.3 Modern Wolves in Southern Yukon: Opportunistic Generalists

Modern informed BSIMMs reveal a highly opportunistic foraging strategy among modern gray wolves in southern and central Yukon. In some cases, up to 84% of their dietary intake is composed of small mammals, with snowshoe hares comprising the majority, followed by Arctic ground squirrels (Figure 15A, 16A, 17A). Whereas large ungulates (caribou and moose) contribute only minimally to the diet (Figure 15A, 16A, 17A), in contrary to other studies which show that moose and caribou are the preferred prey of modern gray wolves (e.g., Gauthier & Theberge, 1986; Hayes et al., 2016).

All but one of the modern gray wolves analysed in this study inhabit southern and central Yukon, around the Whitehorse and Dawson areas (Figure 2). In southern and central Yukon, the boreal (woodland) caribou populations occur at relatively low population densities compared to regions that are inhabited by northern mountain (migratory) caribou (i.e., Porcupine and Fortymile herds that inhabit northern Yukon and Alaska) (Yukon Wildlife, 2025b ;Porcupine Caribou Technical Committee, 2022; Fortymile Harvest Management Committee, 2020; Kelsey Russell et al., 2024; Wildlife Management Advisory Council (North Slope), 2021; Yukon Department of Environment et al., 2024). The Fortymile caribou herd inhabits parts of central Yukon, but the majority of their range is located within Alaska (Fortymile Harvest Management Committee, 2020; Yukon Department of Environment et al., 2024). Moose are relatively abundant across all regions in the Yukon, but when comparing their population densities (Bergeron et al., 2024; Hodges, 1999; Milligan et al., 2023), they are still less available than snowshoe hare and Arctic ground squirrel populations which are both ubiquitous and seasonally abundant across the boreal forest and subarctic landscapes of the Yukon (Hodges, 1999; Milligan et al., 2023).

Gray wolves are known to exploit a wide range of prey types and undergo switches in feeding habits depending on the local abundance, seasonality and vulnerability of prey species, from a diet primarily comprised of large ungulates (caribou and moose) to one that includes a greater diversity of prey species (i.e., not restricted to ungulates) which incorporates small mammals (Arctic ground squirrel, snowshoe hare, muskrat [Ondatra zibethicus Linnaeus 1766], and beaver; Gable et al., 2018; Merkle et al., 2017; Dalerum et al., 2018), and even foraging on berries (Evavold et al., 2024) and eating salmon (Adams et al., 2010). Thus, I hypothesize that the increased representation of small mammals in gray wolf diet in southern and central Yukon, as revealed by the modern BSIMMs, is likely due to the greater abundance of these species compared to caribou and moose in this region.

These findings further underscore the role of environmental context in shaping gray wolf trophic behavior, highlighting how modern wolves remain ecologically flexible predators capable of switching between prey guilds based on availability, seasonality, and energetic payoff (Adams et al., 2010; Evavold et al., 2024; Gable et al., 2018; Merkle et al., 2017; Dalerum et al., 2018). Such flexibility may be one of the key traits that has allowed gray wolves to persist across millennia of environmental perturbations and into diverse Holocene and Anthropocene environments—unlike more specialized carnivores whose survival may have been tightly linked to the fate of their megafaunal prey (Ripple & Van Valkenburgh, 2010; Van Valkenburgh, 2009).

4.3.4 Ecological Interpretation and Broader Implications

Collectively, these findings reveal a profound ecological transformation in gray wolf feeding behavior over the last 50,000 years:

- Pleistocene wolves functioned as dietary specialists, relying heavily on Beringian horses in the mammoth steppe ecosystem.
- Post-LGM wolves transitioned toward generalist foraging strategies, adapting to the disappearance of key megafaunal prey and the restructuring of northern ecosystems during the terminal Pleistocene.
- Modern wolves, particularly in southern Yukon, exemplify continued dietary flexibility, subsisting primarily on locally abundant small mammals such as snowshoe hares and Arctic ground squirrels.

This remarkable niche flexibility appears to be a critical factor in the long-term persistence of gray wolves, enabling them to survive dramatic ecological upheavals, including the extinction of their primary prey, habitat turnover, and shifting community structures. In contrast to more specialized carnivores like the short-faced bear or the scimitar cat, whose extinction has been partly attributed to limited dietary flexibility (DeSantis et al., 2021; Donohue et al., 2013), gray wolves demonstrate how the ability for dietary modification can serve as a buffer against extinction pressures.

The application of Bayesian Stable Isotope Mixing Models (BSIMM), especially those incorporating calcium isotopes ($\delta^{44/42}$Ca), offers a novel and more nuanced lens into long-term trophic dynamics. These multi-isotope approaches not only improve dietary resolution as shown in this thesis but also allow us to track shifts in predator-prey interactions with unprecedented specificity. As such, they represent a powerful tool for reconstructing ecological resilience and the adaptive strategies of apex predators across recent and deep geologic time.

4.4 Advantages of Incorporating Calcium Isotopes in Dietary Mixing Models

The limitations of $\delta^{13}C$ and $\delta^{15}N$ as dietary proxies—stemming from the degradation and alteration of collagen (see Chapter 1 for further details), combined with the low trophic discrimination of carbon isotopes, minimal $\delta^{13}C$ distinction between species, and the sensitivity of $\delta^{15}N$ to environmental baseline shifts which are observed in this study, can lead to ambiguous BSIMM outputs that have large uncertainties, limitations that have been documented in previous studies such as that of (Landry et al., 2021).

In this thesis, BSIMMs were run using traditional ($\delta^{13}C$ and $\delta^{15}N$) and novel ($\delta^{44}Ca$) dietary proxies, and the outputs were compared to models using only traditional proxies ($\delta^{13}C$ and $\delta^{15}N$). However, due to a limited number of prey specimens in the LGM and post-LGM subsets—which were only identified following radiocarbon dating—BSIMMs incorporating $\delta^{44}Ca$ were only conducted for the modern and pre-LGM gray wolf age subsets. By comparing the outputs of the BSIMMs run with traditional dietary proxies ($\delta^{13}C$ and $\delta^{15}N$) to the outputs of BSIMMs combining traditional and novel dietary proxies ($\delta^{13}C$, $\delta^{15}N$, and $\delta^{44/42}Ca$) I test the feasibility of using multiple isotopic proxies (i.e., $\delta^{13}C$, $\delta^{15}N$, and $\delta^{44/42}Ca$) to improve the outputs of BSIMMs in a single model species (i.e., the gray wolf).

The addition of $\delta^{44/42}Ca$ adds a third dimension that increases the distinctiveness of the prey sources, likely due to the ability of $\delta^{44/42}Ca$ to distinguish monogastric and polygastric species. As expected, I observe that not only do calcium isotopes highlight general trophic organisation, but also to a smaller scale the diet preferences and gut physiology (i.e., monogastric and polygastric organisms) within herbivores and carnivores (Figure 14, 18). The degree of isotopic distinctiveness between species achieved in this study cannot be obtained with only carbon and nitrogen isotopes as observed in Figure 18, highlighting the benefit of incorporating $\delta^{44/42}Ca$ alongside $\delta^{13}C$ and $\delta^{15}N$ in dietary mixing models.

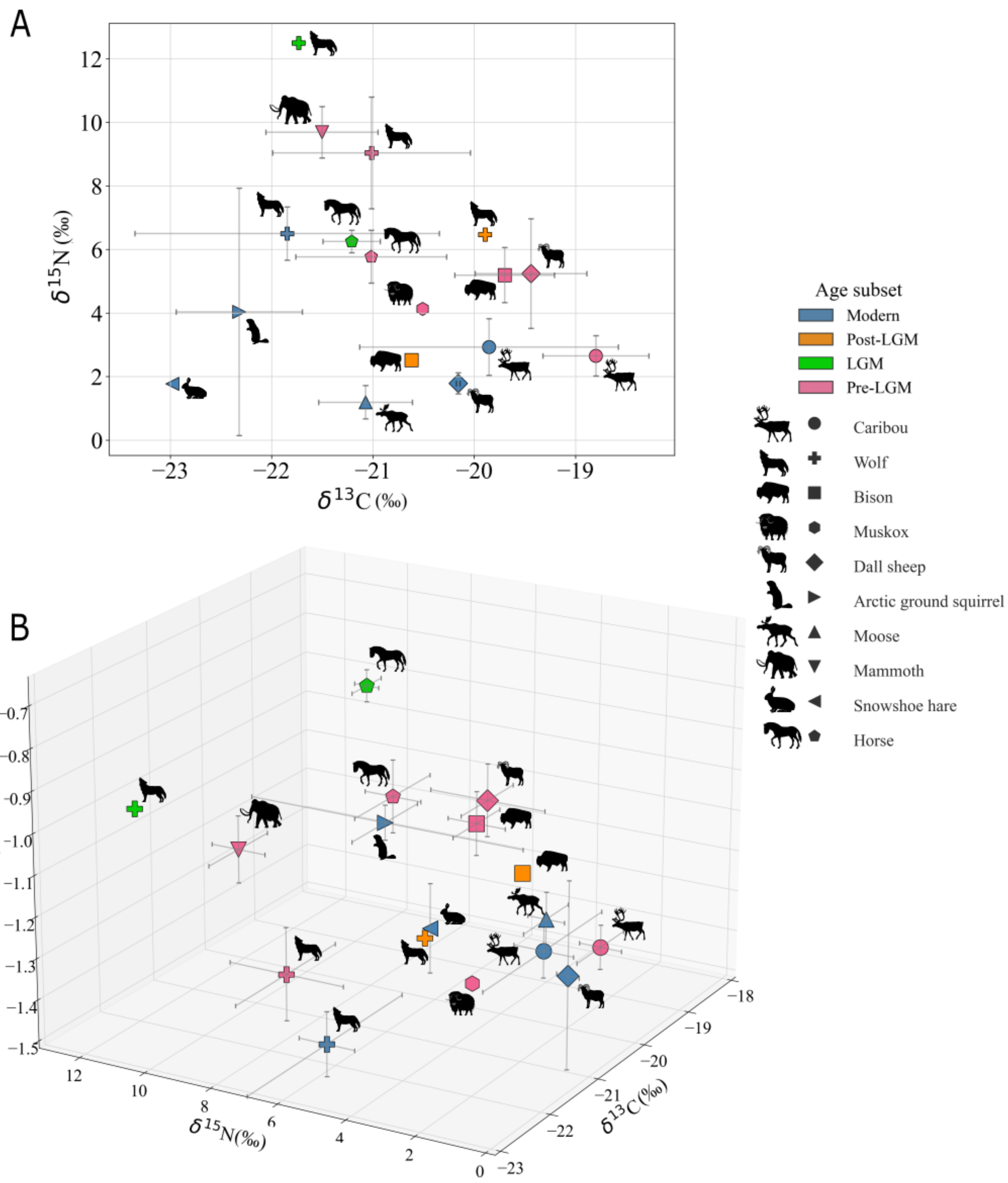

Figure 18. A) Two-dimension isospace plot of mean $\delta^{13}C$ (‰) and $\delta^{15}N$ (‰) values (±standard deviation) of gray wolves and their potential prey species, depicted by age subset (modern [blue], post-LGM [orange], LGM [green], and pre-LGM [pink]); and B) Three-dimension isospace plot of mean $\delta^{13}C$ (‰), $\delta^{15}N$ (‰), and $\delta^{44/42}Ca_{alpha}$ (‰) values (±standard deviation) of gray wolves and their potential prey species, depicted by age subset (modern [blue], post-LGM [orange], LGM [green], and pre-LGM [pink]).

BSIMMs ability to distinguish the isotopic sources of a consumer are strongly influenced by the degree of distinctiveness between source isotopic compositions (Lerner et al., 2018). I found that the additional dimension provided by calcium isotopes furthers the isotopic separation of species (Figure 18), which results in more precise dietary interpretations and BSIMM outputs as indicated by the reduced standard deviations in prey contribution estimates (Appendix B Tables 1, 2, 3), strongly observed in the pre-LGM BSIMM. The informative pre-LGM BSIMM ran only using traditional dietary proxies show that horses contribute 58.2±26.9% to overall gray wolf diet (Figure 16B and Appendix B Table 2). The addition of $\delta^{44/42}$Ca to the pre-LGM BSIMM not only showed that Pleistocene wolves hyperspecialized in horse, revealing that horse makes up to 83.5±8.1% of their diet Figure 17B and Appendix B Table 3), it also drastically reduces the standard deviation by 18.8%, showing that the inclusion of $\delta^{44/42}$Ca improved the precision of my dietary mixing models. The other prey contributions in the pre-LGM model also had reduced standard deviations compared to the BSIMM ran with traditional dietary proxies (Figure 16A, 17A and Appendix B Table 1, 2).

Overall, the precision of the modern gray wolf BSIMMs also improved, as the standard deviation of prey contribution decreased for all prey sources except snowshoe hare and Arctic ground squirrel which remained relatively constant between BSIMM variations (Figure 16A, 17A and Appendix B Table 2, 3). I believe that the consistently high standard deviation of the small mammals in the modern BSIMMs are attributed to their high degree of isotopic variation (SD) as observed in Figure 18. Prey source isotopic variation can greatly influence the precision of BSIMMs (Phillips et al., 2014). High degrees of intraspecies isotopic variation can result in increased overlap between prey sources, which can increase the uncertainty of BSIMM outputs (i.e., prey contribution) (Phillips et al., 2014). Small mammals such as snowshoe hare and Arctic ground squirrels, typically have broad ecological niches and flexible diets, consuming a range of plant, fungal, and even animal matter depending on region, ecological niche, and season (Batzli & Sobaski, 1980; Elliott et al., 2022; Hobbie et al., 2017; Wolff, 1978). The large variation in small mammals' diet likely resulted in high degrees of intraspecies isotopic variation as observed in this study (Figure 18) which subsequently drove the high degrees of uncertainty in the small mammals in the BSIMMs, despite the addition of $\delta^{44/42}$Ca. In addition, the small mammal's calcium isotope compositions are from bone, which is more susceptible to digenetic alteration then enamel (e.g., Dodat et al., 2023), this may have also increased the isotopic variation of these species. Even so, the modern BSIMM that included calcium isotopes further refines the understanding of contemporary gray wolf feeding habits. This model revealed that small mammals make up to approximately 84% of gray wolf diet, whereas the $\delta^{13}C$ and $\delta^{15}N$ BSIMMs showed they contribute only up to 75% (Figure 16A, 17A and Appendix B Tables 2, 3).

4.5 Limitations of this study

Despite considerable effort to constrain this study spatiotemporally and to analyze the isotope composition of most of the potential gray wolf prey across different time periods, the interpretation of this work has several limitations regarding these factors that should be taken into account.

Some prey species but particularly Arctic ground squirrel, snowshoe hare, and muskox were represented by very few specimens. In general, this type of dietary study requires a large dataset to account for intraspecies dietary and isotope variance. In this study some species in respective age subsets only had one specimen, in these cases the standard deviations (SD) used in the Bayesian Stable Isotope Mixing Models (BSIMMs) could not be calculated. For example, muskox was represented by only one specimen, and its variability was approximated using SD values from other species within the same age subset. Additionally, sample sizes (n) had to be manually adjusted to meet MixSIAR's minimum requirement (n=2), further contributing to potential overestimation of isotopic variability and increased uncertainty in dietary estimates.

The prey dataset did not include all species that likely contribute to the gray wolf diet. Notably, the American beaver is a known dietary component of modern wolves in the Yukon were not included in this study (Gable et al., 2018). As aquatic herbivores, beavers have distinct isotopic composition (particularly for $\delta^{13}C$ values; Severud et al., 2013) , and their absence may have led to inaccuracies or inflated uncertainty in the modern BSIMM outputs. Future studies should incorporate beaver isotopic data, either through new sampling or published values, to test their contribution more robustly.

All BSIMMs assumed constant trophic discrimination factors across prey species, despite known differences in diet, physiology, and metabolism. This assumption likely limited the precision and ecological accuracy of the modeled wolf diets (Veselý et al., 2024) because the TDFs between species may vary based on tissues synthesis and physiology (Stephens et al., 2023). Future models should incorporate species-specific or experimentally derived TDFs wherever possible.

When calculating priors for informed BSIMMs, contemporary average body masses were applied across all age subsets. However, prey body sizes likely varied significantly over the past 50,000 years in response to climate and environmental changes (Smith et al., 2018). As a result, using modern body mass values for Pleistocene scenarios may have biased the outputs. Future studies should account for temporal variability in animal size to refine biomass-based priors.

The dataset lacks sufficient representation of prey and wolf specimens from the Last Glacial Maximum (LGM) and post-LGM periods, preventing the inclusion of $\delta^{44/42}$Ca data in BSIMMS for these time slices. As a result, BSIMMs for these periods relied heavily on literature-derived prey data, and any conclusions regarding these timeframes remain preliminary. More targeted sampling from these periods is necessary for robust interpretation.

Although efforts were made to limit geographic spread, specimens were collected from multiple sites across the Yukon (Figure 2). This spatial variability may have introduced isotopic noise related to local geology or environmental differences, as well as potential regional dietary adaptations among wolf populations. Future research should aim for even tighter spatial and temporal control to minimize confounding factors particularly in dietary models.

5 Conclusions

5.1 Summary of main findings

The pre-Last Glacial Maximum (LGM) and modern Bayesian stable isotope mixing model (BSIMM) variations highlights how the addition of a third and independent dietary proxy, such as calcium isotopes, can provide critical insights that complement $\delta^{13}C$ and $\delta^{15}N$ dietary proxies (Figure 16, 17). The addition of calcium isotopes increased species isotopic distinctiveness (Figure 18) which allowed for increased precision of the BSIMMs. Based on those collective findings I recommend $\delta^{44/42}Ca$ be applied in combination with $\delta^{13}C$ and $\delta^{15}N$ in dietary mixing models to improve precision and decrease ambiguity in isotopic interpretation potentially caused by $\delta^{13}C$ and $\delta^{15}N$, particularly for studies with limited $\delta^{13}C$ distinctiveness and largescale climate and landscape changes that may drive changes in $\delta^{15}N$. These findings not only refine the understanding of gray wolf feeding ecology but also present and further the development of a new and exiting methodological advance that can be widely applicable for future palaeobiological studies.

These findings not only highlight the benefit of introducing calcium isotopes as a third dimension in diet and trophic reconstructions, but they provide critical insights on the palaeoecology of Beringia. The BSIMM analyses using $\delta^{13}C$, $\delta^{15}N$, and $\delta^{44/42}Ca$ provide compelling evidence that Pleistocene gray wolves (>19 ka BP) in eastern Beringia maintained a highly specialized diet, primarily focused on Beringian horses (Figure 15C,D, 16B, 17B)—findings that are consistent with those of previous research (e.g., Landry et al., 2021). The addition of calcium isotopes from this study further shows the degree to which Pleistocene gray wolf diet was specialized on horse, findings that were not made possible by only applying traditional stable isotopes dietary proxies.

The post-LGM (11 to 19 ka BP) BSIMM using $\delta^{13}C$ and $\delta^{15}N$ revealed that once gray wolves lost their primary prey species following the extinction of horses in North America (~13ka BP; (Guthrie, 2003; Running Horse Collins et al., 2025) they transitioned to a more generalist and opportunistic feeding strategy, incorporating a broader range of prey including both large ungulates (caribou and Dall sheep) and small mammals (Arctic ground squirrel and snowshoe hare) (Figure 15B).

The opportunistic nature of gray wolf diet persists in modern populations as shown by the modern (<11 ka BP) BSIMM outputs that show gray wolves from southern Yukon primarily consumed snowshoe hare and Arctic ground squirrels (Figure 15A, 16A, 17A)—likely reflecting the high local abundance of these small mammals and the comparatively low availability of caribou and moose in the region (Bergeron et al., 2024; Hodges, 1999; Milligan et al., 2023; Yukon Wildlife, 2025e). This suggests and confirms that contemporary gray wolf diet is heavily influenced by regional prey abundance (Dalerum et al., 2018; Gable et al., 2018; Merkle et al., 2017).

Collectively, these results reveal that over the past 50,000 years, gray wolves have undergone a significant shift in feeding habits—from a more specialized and rigid diet to one that is flexible and opportunistic. My findings not only support the hypothesis that gray wolves underwent a dietary shift that was likely driven by the extinction of horses in North America (Guthrie, 2003; Running Horse Collins et al., 2025) that coincided with large-scale ecological and landscape changes across the region (Drucker, 2022; Rowland et al., 2016; Schwartz-Narbonne et al., 2019; Yeakel et al., 2013), but they further demonstrate the extent to which gray wolf diet was horse specialized and further illustrate the influence of regional prey abundance in modern gray wolf diet. The capacity of gray wolves to adapt their diet and foraging strategies may have been a key factor in their persistence through the terminal Pleistocene, a period marked by the widespread extinction of megafauna (Barnosky, 2008; Koch & Barnosky, 2006; Mann et al., 2015; Ripple & Van Valkenburgh, 2010).

5.2 Future studies and recommendations

The findings from this thesis highlight the robustness of calcium isotopes and supports their reliability as a dietary proxy, particularly in environmentally dynamic systems where other dietary proxies might be more limited and potentially introduce ambiguity. I show that incorporating calcium isotopes as a dietary proxy provides a powerful method for recreating the diet of a carnivore species. These findings illustrate a promising novel methodology that can be reliably applied to a wide range of species, ecosystems, and epoch due to the robust and resistant nature of calcium isotopes in bioapatite (i.e., tooth enamel) (Dodat et al., 2023). This can provide critical insights into long-term predator-prey and trophic interactions, not only in extant ecosystems but in palaeo-communities.

Specifically, this methodological advancement can be applied to other species in eastern Beringia. I recommend that future studies use this approach to enhance the understanding of trophic relationships and potential niche partitioning among coexisting apex predators in eastern Beringia during the terminal Pleistocene (e.g., scimitar cat, cave lion, giant short-faced bear, etc.,). Applying the methods outlined in this thesis could not only advance the palaeoecological reconstruction of Beringia but also shed light on why certain species persisted while others went extinct during the terminal Pleistocene. These insights may also inform the conservation of modern carnivore species by giving insights to how extant species and modern ecosystem might respond when facing similar ecological pressures, such as anthropogenically driven climate change. This would be particularly useful for extant Arctic and northern species which are at high risk due to Arctic amplified warming which is resulting in largescale landscape, habitat and ecological changes (Hamilton et al., 2017; Laidre et al., 2020; Post et al., 2009).

Furthermore, I recommend that calcium isotopes in HAp can be used for dietary and trophic reconstruction in systems where traditional proxies (carbon and nitrogen isotopes) may introduce ambiguity in dietary interpretations due to the influence of shifting environmental baselines (Casey & Post, 2011), the organic degradation of collagen (Balzer et al., 1997; Collins et al., 2002; Hedges, 2002), and the increased susceptibility of bone to diagenetic alteration (Dodat et al., 2023; Gillespie et al., 1984). The applicability of calcium isotopes across recent and deep geologic time can provide critical insights to the trophic interactions of past ecosystems, some of which have not been studied in detail due to a lack of reliable methodology.

Overall, multi-isotope approaches not only improve the resolution of dietary and trophic reconstructions but also allow us to track shifts in feeding ecology, predator-prey interactions and species response across long time scales with unprecedented specificity. As such, they represent a powerful method for exploring ecological resilience and the adaptive feeding strategies of species across recent and deep time.

References

Aalto, J., Tyystjärvi, V., Niittynen, P., Kemppinen, J., Rissanen, T., Gregow, H., & Luoto, M. (2022). Microclimate temperature variations from boreal forests to the tundra. *Agricultural and Forest Meteorology*, *323*, 109037. https://doi.org/10.1016/J.AGRFORMET.2022.109037

Adams, L. G., Farley, S. D., Stricker, C. A., Demma, D. J., Roffler, G. H., Miller, D. C., & Rye, R. O. (2010). Are inland wolf–ungulate systems influenced by marine subsidies of Pacific salmon? *Ecological Applications*, *20*(1), 251–262. https://doi.org/10.1890/08-1437.1

Albaladejo-Robles, G., Böhm, M., & Newbold, T. (2023). Species life-history strategies affect population responses to temperature and land-cover changes. *Global Change Biology*, *29*(1), 97–109. https://doi.org/10.1111/GCB.16454

Alfimov, A. V., & Berman, D. I. (2001). Beringian climate during the Late Pleistocene and Holocene. *Quaternary Science Reviews*, *20*(1–3), 127–134. https://doi.org/10.1016/S0277-3791(00)00128-1

AMAP. (2021). *AMAP Arctic Climate Change Update 2021: Key Trends and Impacts. Arctic Monitoring and Assessment Programme* .

Ambrose, S. H. (1990). Preparation and characterization of bone and tooth collagen for isotopic analysis. *Journal of Archaeological Science*, *17*(4), 431–451. https://doi.org/10.1016/0305-4403(90)90007-R

Ambrose, S. H. (1991). Effects of diet, climate and physiology on nitrogen isotope abundances in terrestrial foodwebs. *Journal of Archaeological Science*, *18*(3), 293–317. https://doi.org/10.1016/0305-4403(91)90067-Y

Ambrose, S. H., & Norr, L. (1993). Experimental Evidence for the Relationship of the Carbon Isotope Ratios of Whole Diet and Dietary Protein to Those of Bone Collagen and Carbonate. *Prehistoric Human Bone*, 1–37. https://doi.org/10.1007/978-3-662-02894-0_1

Amundson, R., Austin, A. T., Schuur, E. A. G., Yoo, K., Matzek, V., Kendall, C., Uebersax, A., Brenner, D., & Baisden, W. T. (2003). Global patterns of the isotopic composition of soil and plant nitrogen. *Global Biogeochemical Cycles*, *17*(1), 1031. https://doi.org/10.1029/2002GB001903

Anemone, R. L., Mooney, M. P., & Siegel, M. I. (1996). Longitudinal Study of Dental Development in Chimpanzees of Known Chronological Age: Implications for Understanding the Age at Death of Plio-Pleistocene Hominids. *AMERICAN JOURNAL OF PHYSICAL ANTHROPOLOGY*, *99*, 119–133. https://doi.org/10.1002/(SICI)1096-8644(199601)99:1

Ásmundsdóttir, R. D., Hansen, J., Fagernäs, Z., Troché, G., Olsen, J. V., Saña Seguí, M., & Welker, F. (2024). Early Holocene preservation differences between cortical and trabecular bone proteomes.

Journal of Archaeological Science: Reports, *57*, 104643. https://doi.org/10.1016/J.JASREP.2024.104643

Assemat, A., Adnet, S., Bayez, K., Hassler, A., Arnaud-Godet, F., Mollen, F. H., Girard, C., & Martin, J. E. (2024). Exploring diet shifts and ecology in modern sharks using calcium isotopes and trace metal records of their teeth. *Journal of Fish Biology*, *105*(5). https://doi.org/10.1111/JFB.15211

Balme, G., Hunter, L., & Slotow, R. (2007). Feeding habitat selection by hunting leopards Panthera pardus in a woodland savanna: prey catchability versus abundance. *Animal Behaviour*, *74*(3), 589–598. https://doi.org/10.1016/J.ANBEHAV.2006.12.014

Balter, V. (2004). Allometric constraints on Sr/Ca and Ba/Ca partitioning in terrestrial mammalian trophic chains. *Oecologia*, *139*(1), 83–88. https://doi.org/10.1007/S00442-003-1476-0

Balter, V., Bocherens, H., Person, A., Labourdette, N., Renard, M., & Vandermeersch, B. (2002). Ecological and physiological variability of Sr/Ca and Ba/Ca in mammals of West European mid-Würmian food webs. *Palaeogeography, Palaeoclimatology, Palaeoecology*, *186*(1–2), 127–143. https://doi.org/10.1016/S0031-0182(02)00448-0

Balzer, A., Gleixner, G., Grupe, G., Schmidt, H. L., Schramm, S., & Turban-Just, S. (1997). In vitro decomposition of bone collagen by soil bacteria: The implications for stable isotope analysis in archaeometry. *Archaeometry*, *39*(2), 415–429. https://doi.org/10.1111/J.1475-4754.1997.TB00817.X

Barber, D. G., Ehn, J. K., Pućko, M., Rysgaard, S., Deming, J. W., Bowman, J. S., Papakyriakou, T., Galley, R. J., & Søgaard, D. H. (2014). Frost flowers on young Arctic sea ice: The climatic, chemical, and microbial significance of an emerging ice type. *Journal of Geophysical Research: Atmospheres*, *119*(20), 11,593-11,612. https://doi.org/10.1002/2014JD021736

Barnosky, A. D. (2008). Megafauna biomass tradeoff as a driver of Quaternary and future extinctions. *Proceedings of the National Academy of Sciences*, *105*(supplement_1), 11543–11548. https://doi.org/10.1073/PNAS.0801918105

Barnosky, A. D., Hadly, E. A., Gonzalez, P., Head, J., Polly, P. D., Lawing, A. M., Eronen, J. T., Ackerly, D. D., Alex, K., Biber, E., Blois, J., Brashares, J., Ceballos, G., Davis, E., Dietl, G. P., Dirzo, R., Doremus, H., Fortelius, M., Greene, H. W., … Zhang, Z. (2017). Merging paleobiology with conservation biology to guide the future of terrestrial ecosystems. *Science*, *355*(6325). https://doi.org/10.1126/SCIENCE.AAH4787/ASSET/ACFCA20B-AE8C-43D1-94F7-B2E48726F1E5/ASSETS/GRAPHIC/355_AAH4787_F6.JPEG

Batzli, G. O., & Sobaski, S. T. (1980). Distribution, Abundance, and Foraging Patterns of Ground Squirrels near Atkasook, Alaska. *Arctic and Alpine Research*, *12*(4), 501–510. https://doi.org/10.1080/00040851.1980.12004209

Bearhop, S., Adams, C. E., Waldron, S., Fuller, R. A., & Macleod, H. (2004). Determining trophic niche width: A novel approach using stable isotope analysis. *Journal of Animal Ecology*, *73*(5), 1007–1012. https://doi.org/10.1111/j.0021-8790.2004.00861.x

Beaumont, W., Beverly, R., Southon, J., & Taylor, R. E. (2010). Bone preparation at the KCCAMS laboratory. *Nuclear Instruments and Methods in Physics Research Section B: Beam Interactions with Materials and Atoms*, *268*(7–8), 906–909. https://doi.org/10.1016/J.NIMB.2009.10.061

Bellard, C., Bertelsmeier, C., Leadley, P., Thuiller, W., & Courchamp, F. (2012). Impacts of climate change on the future of biodiversity. *Ecology Letters*, *15*(4), 365–377. https://doi.org/10.1111/J.1461-0248.2011.01736.X

Ben-David, M., & Flaherty, E. A. (2012). Stable isotopes in mammalian research: A beginner's guide. *Journal of Mammalogy*, *93*(2), 312–328. https://doi.org/10.1644/11-MAMM-S-166.1/2/JMAMMAL-93-2-312-FIG8.JPEG

Bengtsson, L., Semenov, V. A., & Johannessen, O. M. (2004). The Early Twentieth-Century Warming in the Arctic—A Possible Mechanism. *Journal of Climate*, *17*(20), 4045–4057. https://doi.org/10.1175/1520-0442(2004)017<4045:TETWIT>2.0.CO;2

Bergeron, B. A. , A., Morgan, T., Czetwertynski, S., & Ross, T. (2024). *Moose Survey: Faro Moose Management Unit, Early-winter 2020.*

Beschta, R. L. (2005). REDUCED COTTONWOOD RECRUITMENT FOLLOWING EXTIRPATION OF WOLVES IN YELLOWSTONE'S NORTHERN RANGE. *Ecology*, *86*(2), 391–403. https://doi.org/10.1890/04-0964

Beschta, R. L., & Ripple, W. J. (2009). Large predators and trophic cascades in terrestrial ecosystems of the western United States. *Biological Conservation*, *142*(11), 2401–2414. https://doi.org/10.1016/J.BIOCON.2009.06.015

Beschta, R. L., & Ripple, W. J. (2016). Riparian vegetation recovery in Yellowstone: The first two decades after wolf reintroduction. *Biological Conservation*, *198*, 93–103. https://doi.org/10.1016/J.BIOCON.2016.03.031

Bestion, E., Soriano-Redondo, A., Cucherousset, J., Jacob, S., White, J., Zinger, L., Fourtune, L., Di Gesu, L., Teyssier, A., & Cote, J. (2019). Altered trophic interactions in warming climates: consequences for predator diet breadth and fitness. *Proceedings. Biological Sciences*, *286*(1914). https://doi.org/10.1098/RSPB.2019.2227

Beyer, H. L., Merrill, E. H., Varley, N., & Boyce, M. S. (2007). WILLOW ON YELLOWSTONE'S NORTHERN RANGE: EVIDENCE FOR A TROPHIC CASCADE? *Ecological Applications*, *17*(6), 1563–1571. https://doi.org/10.1890/06-1254.1

Blinnikov, M. S., Gaglioti, B. V., Walker, D. A., Wooller, M. J., & Zazula, G. D. (2011). Pleistocene graminoid-dominated ecosystems in the Arctic. *Quaternary Science Reviews*, *30*(21–22), 2906–2929. https://doi.org/10.1016/J.QUASCIREV.2011.07.002

Blum, J. D., Taliaferro, E. H., Weisse, M. T., & Holmes, R. T. (2000). Changes in Sr/Ca, Ba/Ca and 87Sr/86Sr ratios between trophic levels in two forest ecosystems in the northeastern U.S.A. *Biogeochemistry*, *49*(1), 87–101. https://doi.org/10.1023/A:1006390707989

Bocherens, H. (2015). Isotopic tracking of large carnivore palaeoecology in the mammoth steppe. *Quaternary Science Reviews*, *117*, 42–71. https://doi.org/10.1016/J.QUASCIREV.2015.03.018

Bocherens, H., & Drucker, D. (2003). Trophic level isotopic enrichment of carbon and nitrogen in bone collagen: case studies from recent and ancient terrestrial ecosystems. *International Journal of Osteoarchaeology*, *13*(1–2), 46–53. https://doi.org/10.1002/OA.662

Bocherens, H., Drucker, D. G., Bonjean, D., Bridault, A., Conard, N. J., Cupillard, C., Germonpré, M., Höneisen, M., Münzel, S. C., Napierala, H., Patou-Mathis, M., Stephan, E., Uerpmann, H. P., & Ziegler, R. (2011). Isotopic evidence for dietary ecology of cave lion (Panthera spelaea) in North-Western Europe: Prey choice, competition and implications for extinction. *Quaternary International*, *245*(2), 249–261. https://doi.org/10.1016/J.QUAINT.2011.02.023

Boeskorov, G. G., Grigoriev, S. E., & Baryshnikov, G. F. (2012). New evidence for the existence of pleistocene cave bears in Arctic Siberia. *Doklady Biological Sciences : Proceedings of the Academy of Sciences of the USSR, Biological Sciences Sections*, *445*(1), 239–243. https://doi.org/10.1134/S0012496612040060

Bonafini, M., Pellegrini, M., Ditchfield, P., & Pollard, A. M. (2013). Investigation of the 'canopy effect' in the isotope ecology of temperate woodlands. *Journal of Archaeological Science*, *40*(11), 3926–3935. https://doi.org/10.1016/J.JAS.2013.03.028

Brice, E. M., Larsen, E. J., & MacNulty, D. R. (2022). Sampling bias exaggerates a textbook example of a trophic cascade. *Ecology Letters*, *25*(1), 177–188. https://doi.org/10.1111/ELE.13915

Brigham-Grette, J. (2001). New perspectives on Beringian Quaternary paleogeography, stratigraphy, and glacial history. *Quaternary Science Reviews*, *20*(1–3), 15–24. https://doi.org/10.1016/S0277-3791(00)00134-7

Brock, F., Higham, T., Ditchfield, P., & Ramsey, C. B. (2010). Current Pretreatment Methods for AMS Radiocarbon Dating at the Oxford Radiocarbon Accelerator Unit (Orau). *Radiocarbon*, *52*(1), 103–112. https://doi.org/10.1017/S0033822200045069

Bronk Ramsey, C. (2009). Bayesian analysis of radiocarbon dates. *Radiocarbon*, *51*(1), 337–360.

Bruno, J. F., & Cardinale, B. J. (2008). Cascading effects of predator richness. *Frontiers in Ecology and the Environment*, *6*(10), 539–546. https://doi.org/10.1890/070136

Bryant, J. D., Froelich, P. N., Showers, W. J., & Genna, B. J. (1996). A tale of two quarries: Biologic and taphonomic signatures in the oxygen isotope composition of tooth enamel phosphate from modern and miocene equids. *Palaios*, *11*(4), 397–408. https://doi.org/10.2307/3515249

Burton, J. H., Price, T. D., & Middleton, W. D. (1999). Correlation of Bone Ba/Ca and Sr/Ca due to Biological Purification of Calcium. *Journal of Archaeological Science*, *26*(6), 609–616. https://doi.org/10.1006/JASC.1998.0378

Burton, J. H., & Wright, L. E. (1995). Nonlinearity in the relationship between bone Sr/Ca and diet: paleodietary implications. *American Journal of Physical Anthropology*, *96*(3), 273–282. https://doi.org/10.1002/AJPA.1330960305

Carbone, C., Mace, G. M., Roberts, S. C., & Macdonald, D. W. (1999). Energetic constraints on the diet of terrestrial carnivores. *Nature 1999 402:6759*, *402*(6759), 286–288. https://doi.org/10.1038/46266

Cardillo, M., Mace, G. M., Jones, K. E., Bielby, J., Bininda-Emonds, O. R. P., Sechrest, W., Orme, C. D. L., & Purvis, A. (2005). Evolution: Multiple causes of high extinction risk in large mammal species. *Science*, *309*(5738), 1239–1241. https://doi.org/10.1126/SCIENCE.1116030/SUPPL_FILE/CARDILLO.SOM.PDF

Casey, M. M., & Post, D. M. (2011). The problem of isotopic baseline: Reconstructing the diet and trophic position of fossil animals. *Earth-Science Reviews*, *106*(1–2), 131–148. https://doi.org/10.1016/J.EARSCIREV.2011.02.001

Caut, S., Angulo, E., & Courchamp, F. (2009). Variation in discrimination factors (Δ15N and Δ13C): the effect of diet isotopic values and applications for diet reconstruction. *Journal of Applied Ecology*, *46*(2), 443–453. https://doi.org/10.1111/J.1365-2664.2009.01620.X

Cerling, T. E., & Harris, J. M. (1999). Carbon isotope fractionation between diet and bioapatite in ungulate mammals and implications for ecological and paleoecological studies. *Oecologia*, *120*(3), 347–363. https://doi.org/10.1007/S004420050868/METRICS

Cerling, T. E., Bernasconi, S. M., Hofstetter, L. S., Jaggi, M., Wyss, F., Rudolf von Rohr, C., & Clauss, M. (2021). CH_4/CO_2 ratios and carbon isotope enrichment between diet and breath in herbivorous mammals. *Frontiers in Ecology and Evolution*, 9, 638568. https://doi.org/10.3389/fevo.2021.638568Chambault, P., Tervo, O. M., Garde, E., Hansen, R. G., Blackwell, S. B., Williams, T. M., Dietz, R., Albertsen, C. M., Laidre, K. L., Nielsen, N. H., Richard, P., Sinding, M. H. S., Schmidt, H. C., & Heide-Jørgensen, M. P. (2020). The impact of rising sea temperatures on an Arctic top predator, the narwhal. *Scientific Reports 2020 10:1*, *10*(1), 1–10. https://doi.org/10.1038/s41598-020-75658-6

Cheung, C., & Szpak, P. (2021). Interpreting Past Human Diets Using Stable Isotope Mixing Models—Best Practices for Data Acquisition. *Journal of Archaeological Method and Theory 2021 29:1*, *29*(1), 138–161. https://doi.org/10.1007/S10816-021-09514-W

Chu, N. C., Henderson, G. M., Belshaw, N. S., & Hedges, R. E. M. (2006). Establishing the potential of Ca isotopes as proxy for consumption of dairy products. *Applied Geochemistry*, *21*(10), 1656–1667. https://doi.org/10.1016/J.APGEOCHEM.2006.07.003

Clementz, M. T. (2012). New insight from old bones: Stable isotope analysis of fossil mammals. *Journal of Mammalogy*, *93*(2), 368–380. https://doi.org/10.1644/11-MAMM-S-179.1/2/JMAMMAL-93-2-368-FIG5.JPEG

Cleveland, C. C., Townsend, A. R., Schimel, D. S., Fisher, H., Howarth, R. W., Hedin, L. O., Perakis, S. S., Latty, E. F., Fischer, J. C. Von, Elseroad, A., & Wasson, M. F. (1999). Global patterns of terrestrial biological nitrogen (N2) fixation in natural ecosystems. *Global Biogeochemical Cycles*, *13*(2), 623–645. https://doi.org/10.1029/1999GB900014

Cobert, F., Schmitt, A. D., Bourgeade, P., Labolle, F., Badot, P. M., Chabaux, F., & Stille, P. (2011). Experimental identification of Ca isotopic fractionations in higher plants. *Geochimica et Cosmochimica Acta*, *75*(19), 5467–5482. https://doi.org/10.1016/J.GCA.2011.06.032

Codron, J., Lee-Thorp, J. A., Sponheimer, M., & Codron, D. (2013). Plant stable isotope composition across habitat gradients in a semi-arid savanna: implications for environmental reconstruction. *Journal of Quaternary Science*, *28*(3), 301–310. https://doi.org/10.1002/JQS.2614

Collins, M. J., Nielsen-Marsh, C. M., Hiller, J., Smith, C. I., Roberts, J. P., Prigodich, R. V., Wess, T. J., Csapò, J., Millard, A. R., & Turner-Walker, G. (2002). The survival of organic matter in bone: a review. *Archaeometry*, *44*(3), 383–394. https://doi.org/10.1111/1475-4754.T01-1-00071

Cong, W., Li, J., Hacker, C., Li, Y., Zhang, Y., Jin, L., Zhang, Y., Li, D., Xue, Y., & Zhang, Y. (2024). Different coexistence patterns between apex carnivores and mesocarnivores based on temporal, spatial, and dietary niche partitioning analysis in Qilian Mountain National Park, China. *ELife*, *13*. https://doi.org/10.7554/ELIFE.90559

Coplen, T. B., Brand, W. A., Gehre, M., Gröning, M., Meijer, H. A. J., Toman, B., & Verkouteren, R. M. (2006). New guidelines for delta13C measurements. *Analytical Chemistry*, *78*(7), 2439–2441. https://doi.org/10.1021/AC052027C

Craine, J. M., Brookshire, E. N. J., Cramer, M. D., Hasselquist, N. J., Koba, K., Marin-Spiotta, E., Wang, L., Craine, J. M., Ventures, J., Cramer, M. D., Hasselquist, N. J., Koba, K., Marin-Spiotta, E., & Wang, L. (2015a). Ecological interpretations of nitrogen isotope ratios of terrestrial plants and soils. *Plant and Soil 2015 396:1*, *396*(1), 1–26. https://doi.org/10.1007/S11104-015-2542-1

Craine, J. M., Elmore, A. J., Aidar, M. P. M., Bustamante, M., Dawson, T. E., Hobbie, E. A., Kahmen, A., MacK, M. C., McLauchlan, K. K., Michelsen, A., Nardoto, G. B., Pardo, L. H., Peñuelas, J., Reich, P. B., Schuur, E. A. G., Stock, W. D., Templer, P. H., Virginia, R. A., Welker, J. M., & Wright, I. J. (2009). Global patterns of foliar nitrogen isotopes and their relationships with climate, mycorrhizal fungi, foliar nutrient concentrations, and nitrogen availability. *New Phytologist*, *183*(4), 980–992. https://doi.org/10.1111/J.1469-8137.2009.02917.X

Craine, J. M., Elmore, A. J., Wang, L., Augusto, L., Baisden, W. T., Brookshire, E. N. J., Cramer, M. D., Hasselquist, N. J., Hobbie, E. A., Kahmen, A., Koba, K., Kranabetter, J. M., Mack, M. C., Marin-Spiotta, E., Mayor, J. R., McLauchlan, K. K., Michelsen, A., Nardoto, G. B., Oliveira, R. S., … Zeller, B. (2015b). Convergence of soil nitrogen isotopes across global climate gradients. *Scientific Reports 2015 5:1*, *5*(1), 1–8. https://doi.org/10.1038/SREP08280

Crann, C. A., Doucet, A. M., Richards, M. P., & Talamo, S. (2019). The old bone project: Quality assurance on radiocarbon dating bone in the 30,000–50,000 age range at the A.E. Lalonde AMS Laboratory (Ottawa, Canada). *Nuclear Instruments and Methods in Physics Research Section B: Beam Interactions with Materials and Atoms*, *456*, 247–251. https://doi.org/10.1016/J.NIMB.2019.03.032

Crann, C. A., Murseli, S., St-Jean, G., Zhao, X., Clark, I. D., & Kieser, W. E. (2017). First Status Report on Radiocarbon Sample Preparation Techniques at the A.E. Lalonde AMS Laboratory (Ottawa, Canada). *Radiocarbon*, *59*(3), 695–704. https://doi.org/10.1017/RDC.2016.55

Dalerum, F., Freire, S., Angerbjörn, A., Lecomte, N., Lindgren, Meijer, T., Pečnerová, P., & Dalén, L. (2018). Exploring the diet of arctic wolves (Canis lupus arctos) at their northern range limit. *Canadian Journal of Zoology*, *96*(3), 277–281. https://doi.org/10.1139/CJZ-2017-0054

Danby, R. K., Koh, S., Hik, D. S., & Price, L. W. (2011). Four decades of plant community change in the Alpine tundra of southwest Yukon, Canada. *Ambio*, *40*(6), 660–671. https://doi.org/10.1007/S13280-011-0172-2

Dawson, T. E., Mambelli, S., Plamboeck, A. H., Templer, P. H., & Tu, K. P. (2002). Stable isotopes in plant ecology. *Annual Review of Ecology and Systematics*, *33*(Volume 33, 2002), 507–559. https://doi.org/10.1146/ANNUREV.ECOLSYS.33.020602.095451/CITE/REFWORKS

de Silva, S., & Leimgruber, P. (2019). Demographic tipping points as early indicators of vulnerability for slow-breeding megafaunal populations. *Frontiers in Ecology and Evolution*, *7*(May), 431809. https://doi.org/10.3389/FEVO.2019.00171/BIBTEX

DeNiro, M. J., & Epstein, S. (1978). Influence of diet on the distribution of carbon isotopes in animals. *GeCoA*, *42*(5), 495–506. https://doi.org/10.1016/0016-7037(78)90199-0

Deniro, M. J., & Epstein, S. (1981). Influence of diet on the distribution of nitrogen isotopes in animals. *GeCoA*, *45*(3), 341–351. https://doi.org/10.1016/0016-7037(81)90244-1

Deniro, M. J., Schoeninger, M. J., & Hastorf, C. A. (1985). Effect of heating on the stable carbon and nitrogen isotope ratios of bone collagen. *Journal of Archaeological Science*, *12*(1), 1–7. https://doi.org/10.1016/0305-4403(85)90011-1

Derocher, A. E., Aars, J., Amstrup, S. C., Cutting, A., Lunn, N. J., Molnár, P. K., Obbard, M. E., Stirling, I., Thiemann, G. W., Vongraven, D., Wiig, Ø., & York, G. (2013). Rapid ecosystem change and polar bear conservation. *Conservation Letters*, *6*(5), 368–375. https://doi.org/10.1111/CONL.12009

Derocher, A. E., Andriashek, D., & Stirling, I. (1993). Terrestrial foraging by polar bears during the ice-free period in western Hudson Bay. *Arctic*, *46*(3), 251–254. https://doi.org/10.14430/ARCTIC1350

Derocher, A. E., Lunn, N. J., & Stirling, I. (2004). Polar Bears in a Warming Climate. *Integrative and Comparative Biology*, *44*(2), 163–176. https://doi.org/10.1093/ICB/44.2.163

Derocher, A. E., Wiig, Ø., & Bangjord, G. (2000). Predation of Svalbard reindeer by polar bears. *Polar Biology*, *23*(10), 675–678. https://doi.org/10.1007/S003000000138/METRICS

DeSantis, L. R. G., Feranec, R. S., Antón, M., & Lundelius, E. L. (2021). Dietary ecology of the scimitar-toothed cat Homotherium serum. *Current Biology*, *31*(12), 2674-2681.e3. https://doi.org/10.1016/J.CUB.2021.03.061

Díaz, S., Settele, J., Brondízio, E. S., Ngo, H. T., Agard, J., Arneth, A., Balvanera, P., Brauman, K. A., Butchart, S. H. M., Chan, K. M. A., Lucas, A. G., Ichii, K., Liu, J., Subramanian, S. M., Midgley, G. F., Miloslavich, P., Molnár, Z., Obura, D., Pfaff, A., … Zayas, C. N. (2019). Pervasive human-driven decline of life on Earth points to the need for transformative change. *Science*, *366*(6471). https://doi.org/10.1126/SCIENCE.AAX3100/SUPPL_FILE/AAX3100-DIAZ-SM.PDF

Diefendorf, A. F., Mueller, K. E., Wing, S. L., Koch, P. L., & Freeman, K. H. (2010). Global patterns in leaf 13C discrimination and implications for studies of past and future climate. *Proceedings of the National Academy of Sciences of the United States of America*, *107*(13), 5738–5743. https://doi.org/10.1073/PNAS.0910513107/ASSET/85401A40-B9BC-4C7D-81F4-028329DB8C59/ASSETS/GRAPHIC/PNAS.0910513107EQ59.GIF

Dietl, G. P., Kidwell, S. M., Brenner, M., Burney, D. A., Flessa, K. W., Jackson, S. T., & Koch, P. L. (2015). Conservation paleobiology: Leveraging knowledge of the past to inform conservation and restoration. *Annual Review of Earth and Planetary Sciences*, *43*(Volume 43, 2015), 79–103. https://doi.org/10.1146/ANNUREV-EARTH-040610-133349/CITE/REFWORKS

Dobson, A., Lodge, D., Alder, J., Cumming, G. S., Keymer, J., Mcglade, J., Mooney, H., Rusak, J. A., Sala, O., Wolters, V., Wall, D., Winfree, R., & Xenopoulos, M. A. (2006). HABITAT LOSS, TROPHIC COLLAPSE, AND THE DECLINE OF ECOSYSTEM SERVICES. *Ecology*, *87*(8), 1915–1924. https://doi.org/10.1890/0012-9658(2006)87

Dodat, P. J., Tacail, T., Albalat, E., Gómez-Olivencia, A., Couture-Veschambre, C., Holliday, T., Madelaine, S., Martin, J. E., Rmoutilova, R., Maureille, B., & Balter, V. (2021). Isotopic calcium biogeochemistry of MIS 5 fossil vertebrate bones: Application to the study of the dietary reconstruction of Regourdou 1 Neandertal fossil. *Journal of Human Evolution*, 151, 102925. https://doi.org/10.1016/j.jhevol.2020.102925

Dodat, P. J., Martin, J. E., Olive, S., Hassler, A., Albalat, E., Boisserie, J. R., Merceron, G., Souron, A., Maureille, B., & Balter, V. (2023). Limits of calcium isotopes diagenesis in fossil bone and enamel. *Geochimica et Cosmochimica Acta*, *351*, 45–50. https://doi.org/10.1016/J.GCA.2023.04.012

Donohue, S. L., DeSantis, L. R. G., Schubert, B. W., & Ungar, P. S. (2013). Was the Giant Short-Faced Bear a Hyper-Scavenger? A New Approach to the Dietary Study of Ursids Using Dental Microwear Textures. *PLoS ONE*, *8*(10), e77531. https://doi.org/10.1371/JOURNAL.PONE.0077531

Drucker, D. G. (2022). The Isotopic Ecology of the Mammoth Steppe. *Annual Review of Earth and Planetary Sciences*, *50*(Volume 50, 2022), 395–418. https://doi.org/10.1146/ANNUREV-EARTH-100821-081832/1

Drucker, D. G., Bridault, A., Hobson, K. A., Szuma, E., & Bocherens, H. (2008). Can carbon-13 in large herbivores reflect the canopy effect in temperate and boreal ecosystems? Evidence from modern and ancient ungulates. *Palaeogeography, Palaeoclimatology, Palaeoecology*, *266*(1–2), 69–82. https://doi.org/10.1016/J.PALAEO.2008.03.020

Durant, S. M. (1998). Competition refuges and coexistence: an example from Serengeti carnivores. *Journal of Animal Ecology*, *67*(3), 370–386. https://doi.org/10.1046/J.1365-2656.1998.00202.X

Elias, S. A. (2000). Late Pleistocene Climates of Beringia, Based on Analysis of Fossil Beetles. *Quaternary Research*, *53*(2), 229–235. https://doi.org/10.1006/QRES.1999.2093

Elliott, J. C. (2019). Calcium phosphate biominerals. *Phosphates: Geochemical, Geobiological and Materials Importance*, *48*, 427–454. https://doi.org/10.2138/RMG.2002.48.11

Elliott, T. F., Truong, C., Jackson, S. M., Zuniga, C. L., Trappe, J. M., & Vernes, K. (2022). Mammalian mycophagy: A global review of ecosystem interactions between mammals and fungi. *Fungal Systematics and Evolution*, *9*(1), 99. https://doi.org/10.3114/FUSE.2022.09.07

Estes, J. A., & Duggins, D. O. (1995). Sea Otters and Kelp Forests in Alaska: Generality and Variation in a Community Ecological Paradigm. *Ecological Monographs*, *65*(1), 75–100. https://doi.org/10.2307/2937159

Estes, J. A., & Palmisano, J. F. (1974). Sea Otters: Their Role in Structuring Nearshore Communities. *Science*, *185*(4156), 1058–1060. https://doi.org/10.1126/SCIENCE.185.4156.1058

Estes, J. A., Terborgh, J., Brashares, J. S., Power, M. E., Berger, J., Bond, W. J., Carpenter, S. R., Essington, T. E., Holt, R. D., Jackson, J. B. C., Marquis, R. J., Oksanen, L., Oksanen, T., Paine, R. T., Pikitch, E. K., Ripple, W. J., Sandin, S. A., Scheffer, M., Schoener, T. W., … Wardle, D. A. (2011). Trophic downgrading of planet earth. *Science*, *333*(6040), 301–306. https://doi.org/10.1126/SCIENCE.1205106/SUPPL_FILE/ESTES.SOM.PDF

Estes, J. A., Tinker, M. T., & Bodkin, J. L. (2010). Using Ecological Function to Develop Recovery Criteria for Depleted Species: Sea Otters and Kelp Forests in the Aleutian ArchipelagoUtilización de la Función Ecológica para Desarrollar Criterios de Recuperación para Especies Disminuidas: Nutrias Marinas y Bosques de Algas en el Archipiélago Aleutiano. *Conservation Biology*, *24*(3), 852–860. https://doi.org/10.1111/J.1523-1739.2009.01428.X

Evavold, I. C., Gable, T. D., Homkes, A. T., & Bump, J. K. (2024). Wolves foraging on berries is likely a widespread behavior in southern boreal ecosystems. *Ecosphere*, *15*(10), e70035. https://doi.org/10.1002/ECS2.70035

Fabig, A., & Herrmann, B. (2002). Trace elements in buried human bones: intra-population variability of Sr/Ca and Ba/Ca ratios--diet or diagenesis? *Die Naturwissenschaften*, *89*(3), 115–119. https://doi.org/10.1007/S00114-001-0294-7

Fedriani, J. M., Fuller, T. K., Sauvajot, R. M., & York, E. C. (2000). Competition and intraguild predation among three sympatric carnivores. *Oecologia*, *125*(2), 258–270. https://doi.org/10.1007/S004420000448/METRICS

Fernández, M. H., & Vrba, E. S. (2005). Body size, biomic specialization and range size of African large mammals. *Journal of Biogeography*, *32*(7), 1243–1256. https://doi.org/10.1111/J.1365-2699.2005.01270.X

Finke, D. L., & Snyder, W. E. (2010). Conserving the benefits of predator biodiversity. *Biological Conservation*, *143*(10), 2260–2269. https://doi.org/10.1016/J.BIOCON.2010.03.022

Fisher, D. O., & Owens, I. P. F. (2004). The comparative method in conservation biology. *Trends in Ecology & Evolution*, *19*(7), 391–398. https://doi.org/10.1016/J.TREE.2004.05.004

Fordham, D. A., Jackson, S. T., Brown, S. C., Huntley, B., Brook, B. W., Dahl-Jensen, D., Thomas Gilbert, M. P., Otto-Bliesner, B. L., Svensson, A., Theodoridis, S., Wilmshurst, J. M., Buettel, J. C., Canteri, E., McDowell, M., Orlando, L., Pilowsky, J., Rahbek, C., & Nogues-Bravo, D. (2020). Using paleo-archives to safeguard biodiversity under climate change. *Science*, *369*(6507). https://doi.org/10.1126/SCIENCE.ABC5654/SUPPL_FILE/ABC5654-FORDHAM-SM.PDF

Fortin, D., Beyer, H. L., Boyce, M. S., Smith, D. W., Duchesne, T., & Mao, J. S. (2005). WOLVES INFLUENCE ELK MOVEMENTS: BEHAVIOR SHAPES A TROPHIC CASCADE IN YELLOWSTONE NATIONAL PARK. *Ecology*, *86*(5), 1320–1330. https://doi.org/10.1890/04-0953

Fortymile Harvest Management Committee. (2020). *Fortymile Caribou Herd Harvest Management Plan*.

Fox-Dobbs, K., Bump, J. K., Peterson, R. O., Fox, D. L., & Koch, P. L. (2007). Carnivore-specific stable isotope variables and variation in the foraging ecology of modern and ancient wolf populations: Case studies from Isle Royale, Minnesota, and La Brea. *Canadian Journal of Zoology*, *85*(4), 458–471. https://doi.org/10.1139/Z07-018/SUPPL_FILE/Z07-018SUPPL.XLS

Fox-Dobbs, K., Leonard, J. A., & Koch, P. L. (2008). Pleistocene megafauna from eastern Beringia: Paleoecological and paleoenvironmental interpretations of stable carbon and nitrogen isotope and radiocarbon records. *Palaeogeography, Palaeoclimatology, Palaeoecology*, *261*(1–2), 30–46. https://doi.org/10.1016/J.PALAEO.2007.12.011

Fritz, M., Herzschuh, U., Wetterich, S., Lantuit, H., De Pascale, G. P., Pollard, W. H., & Schirrmeister, L. (2012). Late glacial and Holocene sedimentation, vegetation, and climate history from easternmost Beringia (northern Yukon Territory, Canada). *Quaternary Research*, *78*(3), 549–560. https://doi.org/10.1016/J.YQRES.2012.07.007

Froese, D. G., Zazula, G. D., Westgate, J. A., Preece, S. J., Sanborn, P. T., Reyes, A. V., & Pearce, N. J. G. (2009). The Klondike goldfields and Pleistocene environments of Beringia. *GSA Today*, *19*(8), 4–10. https://doi.org/10.1130/GSATG54A.1

Fry, B. (2006). Stable Isotope Ecology. *Stable Isotope Ecology*. https://doi.org/10.1007/0-387-33745-8

Fry, B., Jannasch, H. W., Molyneaux, S. J., Wirsen, C. O., Muramoto, J. A., & King, S. (1991). Stable isotope studies of the carbon, nitrogen and sulfur cycles in the Black Sea and the Cariaco Trench. *Deep Sea Research Part A. Oceanographic Research Papers*, *38*(Suppl. 2A), S1003–S1019. https://doi.org/10.1016/S0198-0149(10)80021-4

Fuchs, A., & Leuenberger, M. C. (1996). δ18O of atmospheric oxygen measured on the GRIP Ice Core Document Stratigraphic disturbances in the lowest 10% of the core. *Geophysical Research Letters*, *23*(9), 1049–1052. https://doi.org/10.1029/96GL00588

Fuglei, E., & Ims, R. A. (2008). Global warming and effects on the arctic fox. *Science Progress*, *91*(2), 175–191. https://doi.org/10.3184/003685008X327468

Fuller W. A., (1959). *The horns and teeth as indicators of age in bison*. *23*(3). http://fgs.athabascau.ca/

Fuller, A., Mitchell, D., Maloney, S. K., & Hetem, R. S. (2016). Towards a mechanistic understanding of the responses of large terrestrial mammals to heat and aridity associated with climate change. *Climate Change Responses 2016 3:1*, *3*(1), 1–19. https://doi.org/10.1186/S40665-016-0024-1

Gable, T. D., Windels, S. K., Bruggink, J. G., & Barber-Meyer, S. M. (2018). Weekly Summer Diet of Gray Wolves (Canis lupus) in Northeastern Minnesota. *Https://Doi-Org.Proxy.Bib.Uottawa.ca/10.1674/0003-0031-179.1.15*, *179*(1), 15–27. https://doi.org/10.1674/0003-0031-179.1.15

Gauthier, D. A., & Theberge, J. B. (1986). Wolf predation in the Burwash caribou herd, southwest Yukon. *Rangifer*, *6*(2), 137–144. https://doi.org/10.7557/2.6.2.638

Geiger, M., Gendron, K., Willmitzer, F., & Sánchez-Villagra, M. R. (2016). Unaltered sequence of dental, skeletal, and sexual maturity in domestic dogs compared to the wolf. *Zoological Letters 2016 2:1*, *2*(1), 1–8. https://doi.org/10.1186/S40851-016-0055-2

Gilg, O., Kovacs, K. M., Aars, J., Fort, J., Gauthier, G., Grémillet, D., Ims, R. A., Meltofte, H., Moreau, J., Post, E., Schmidt, N. M., Yannic, G., & Bollache, L. (2012). Climate change and the ecology and evolution of Arctic vertebrates. *Annals of the New York Academy of Sciences*, *1249*(1), 166–190. https://doi.org/10.1111/J.1749-6632.2011.06412.X

Gillespie, R., Hedges, R. E. M., & Wand, J. O. (1984). Radiocarbon dating of bone by accelerator mass spectrometry. *Journal of Archaeological Science*, *11*(2), 165–170. https://doi.org/10.1016/0305-4403(84)90051-7

Gorra, T. R., Garcia, S. C. R., Langhans, M. R., Hoshijima, U., Estes, J. A., Raimondi, P. T., Tinker, M. T., Kenner, M. C., & Kroeker, K. J. (2022). Southeast Alaskan kelp forests: inferences of process from large-scale patterns of variation in space and time. *Proceedings. Biological Sciences*, *289*(1967). https://doi.org/10.1098/RSPB.2021.1697

Grant, J., Hopcraft, C., Sinclair, A. R. E., & Packer, C. (2005). Planning for success: Serengeti lions seek prey accessibility rather than abundance. *Journal of Animal Ecology*, *74*(3), 559–566. https://doi.org/10.1111/J.1365-2656.2005.00955.X

Griffin, J. N., & Silliman, B. R. (2010). Predator diversity stabilizes and strengthens trophic control of a keystone grazer. *Biology Letters*, *7*(1), 79. https://doi.org/10.1098/RSBL.2010.0626

Grimm, N. B., Chapin, F. S., Bierwagen, B., Gonzalez, P., Groffman, P. M., Luo, Y., Melton, F., Nadelhoffer, K., Pairis, A., Raymond, P. A., Schimel, J., & Williamson, C. E. (2013). The impacts of climate change on ecosystem structure and function. *Frontiers in Ecology and the Environment*, *11*(9), 474–482. https://doi.org/10.1890/120282

Guiserix, D., Albalat, E., Ueckermann, H., Davechand, P., Iaccheri, L. M., Bybee, G., Badenhorst, S., & Balter, V. (2022). Simultaneous analysis of stable and radiogenic strontium isotopes in reference materials, plants and modern tooth enamel. *Chemical Geology*, *606*, 121000. https://doi.org/10.1016/J.CHEMGEO.2022.121000

Guiserix, D., Dodat, P. J., Jaouen, K., Albalat, E., Mendes Cardoso, J., Maureille, B., & Balter, V. (2024). Stable isotope composition and concentration systematics of Ca and trace elements (Zn, Sr) in single aliquots of fossil bone and enamel. *Geochimica et Cosmochimica Acta*, *367*, 123–132. https://doi.org/10.1016/J.GCA.2023.12.021

Guthrie, R. D. (2001). Origin and causes of the mammoth steppe: a story of cloud cover, woolly mammal tooth pits, buckles, and inside-out Beringia. *Quaternary Science Reviews*, *20*(1–3), 549–574. https://doi.org/10.1016/S0277-3791(00)00099-8

Guthrie, R. D. (2003). Rapid body size decline in Alaskan Pleistocene horses before extinction. *Nature 2003 426:6963*, *426*(6963), 169–171. https://doi.org/10.1038/nature02098

Hairston, N. G., Smith, F. E., & Slobodkin, L. B. (1960). Community Structure, Population Control, and Competition. *The American Naturalist*, *94*(879), 421–425. https://doi.org/10.1086/282146

Hall, B. K. (2015). Vertebrate Skeletal Tissues. In *Bones and Cartilage* (Second, pp. 3–16).

Halofsky, J., & Ripple, W. (2008). Linkages between wolf presence and aspen recruitment in the Gallatin elk winter range of southwestern Montana, USA. *Forestry: An International Journal of Forest Research*, *81*(2), 195–207. https://doi.org/10.1093/FORESTRY/CPM044

Hamilton, C. D., Kovacs, K. M., Ims, R. A., Aars, J., & Lydersen, C. (2017). An Arctic predator-prey system in flux: climate change impacts on coastal space use by polar bears and ringed seals. *The Journal of Animal Ecology*, *86*(5), 1054–1064. https://doi.org/10.1111/1365-2656.12685

Handley, L. L., Austin, A. T., Robinson, D., Scrimgeour, C. M., Raven, J. A., Heaton, T. H. E., Schmidt, S., & Stewart, G. R. (1999). The 15N natural abundance (δ15N) of ecosystem samples reflects measures of water availability. *Functional Plant Biology*, *26*(2), 185–199. https://doi.org/10.1071/PP98146

Hardy, F. C., & Rowland, S. M. (2024). Stable isotopic analysis of fossil Bison tooth enamel indicates flexible dietary ecology across Pleistocene North America. *Quaternary Science Reviews*, *334*, 108741. https://doi.org/10.1016/J.QUASCIREV.2024.108741

Harington, C. R. (2011). Pleistocene vertebrates of the Yukon Territory. *Quaternary Science Reviews*, *30*(17–18), 2341–2354. https://doi.org/10.1016/J.QUASCIREV.2011.05.020

Harrison, G. E., Carr, T. E. F., & Sutton, A. (1967). Distribution of radioactive calcium, strontium, barium and radium following intravenous injection into a healthy man. *International Journal of Radiation Biology and Related Studies in Physics, Chemistry, and Medicine*, *13*(3), 235–247. https://doi.org/10.1080/09553006814550161

Hassler, A. (2021). *Stratégies de reproduction mammaliennes et isotopie du calcium : témoins actuels et perspectives fossiles* [Doctoral dissertation, Université de Lyon]. https://doi.org/10.34894/VQ1DJA

Hassler, A., Martin, J. E., Amiot, R., Tacail, T., Godet, F. A., Allain, R., & Balter, V. (2018). Calcium isotopes offer clues on resource partitioning among Cretaceous predatory dinosaurs. *Proceedings. Biological Sciences*, *285*(1876). https://doi.org/10.1098/RSPB.2018.0197

Hassler, A., Martin, J. E., Ferchaud, S., Grivault, D., Le Goff, S., Albalat, E., Hernandez, J. A., Tacail, T., & Balter, V. (2021a). Lactation and gestation controls on calcium isotopic compositions in a mammalian model. *Metallomics : Integrated Biometal Science*, *13*(6). https://doi.org/10.1093/MTOMCS/MFAB019

Hassler, A., Martin, J. E., Merceron, G., Garel, M., & Balter, V. (2021b). Calcium isotopic variability of cervid bioapatite and implications for mammalian physiology and diet. *Palaeogeography, Palaeoclimatology, Palaeoecology*, *573*, 110418. https://doi.org/10.1016/J.PALAEO.2021.110418

Hassler, A., Lindroos, E.E., Yang, L., Terzi, C., Blake, J., Dosseto, A., Dux, F., Mester, Z., Briton, K., Bataille, C. (in prep). Exploring the benefits of 10*13*Ω amplifiers for measuring stable calcium isotope ratios: a pilot study of lactation record in adult reindeer (*Rangifer tarandus*).

Hatton, I. A., McCann, K. S., Fryxell, J. M., Davies, T. J., Smerlak, M., Sinclair, A. R. E., & Loreau, M. (2015). The predator-prey power law: Biomass scaling across terrestrial and aquatic biomes. *Science*, *349*(6252). https://doi.org/10.1126/SCIENCE.AAC6284/SUPPL_FILE/HATTON.SM.PDF

Hayes, R. D. (1995). Numerical and functional responses of wolves, and regulation of moose in the Yukon (Master's thesis, Simon Fraser University). https://summit.sfu.ca/item/6764

Hayes, R.D., Baer, A.M., Clarkson, P. (2016). Ecology and Management of Wolves in the Porcupine Caribou Range, Canada: 1987 to 1993. Prepared for Environment Yukon. Yukon Fish and Wildlife Branch Report TRC-16-01, Whitehorse, Yukon, Canada.

Hayes, R. D., Baer, A. M., Wotschikowsky, U., & Harestad, A. S. (2000). Kill rate by wolves on moose in the Yukon. *Canadian Journal of Zoology*, *78*(1), 49–59. https://doi.org/10.1139/CJZ-78-1-49

Hayes, R. D., & Harestad, A. S. (2000). Demography of a recovering wolf population in the Yukon. *Article in Canadian Journal of Zoology*. https://doi.org/10.1139/cjz-78-1-36

Hayward, M. W., Hofmeyr, M., O'Brien, J., & Kerley, G. I. H. (2006). Prey preferences of the cheetah (Acinonyx jubatus) (Felidae: Carnivora): morphological limitations or the need to capture rapidly consumable prey before kleptoparasites arrive? *Journal of Zoology*, *270*(4), 615–627. https://doi.org/10.1111/J.1469-7998.2006.00184.X

Hayward, M. W., & Kerley, G. I. H. (2005). Prey preferences of the lion (Panthera leo). *Journal of Zoology*, *267*(3), 309–322. https://doi.org/10.1017/S0952836905007508

Hayward, M. W., & Kerley, G. I. H. (2008). Prey preferences and dietary overlap amongst Africa's large predators. *Https://Doi.Org/10.3957/0379-4369-38.2.93*, *38*(2), 93–108. https://doi.org/10.3957/0379-4369-38.2.93

He, Q., & Silliman, B. R. (2019). Climate Change, Human Impacts, and Coastal Ecosystems in the Anthropocene. *Current Biology*, *29*(19), R1021–R1035. https://doi.org/10.1016/J.CUB.2019.08.042

Heaton, T. H. E. (1987). 15N14N ratios of nitrate and ammonium in rain at Pretoria, South Africa. *Atmospheric Environment (1967)*, *21*(4), 843–852. https://doi.org/10.1016/0004-6981(87)90080-1

Heaton, T. H. E. (1999). Spatial, Species, and Temporal Variations in the13C/12C Ratios of C3Plants: Implications for Palaeodiet Studies. *Journal of Archaeological Science*, *26*(6), 637–649. https://doi.org/10.1006/JASC.1998.0381

Heaton, T. H. E., Vogel, J. C., Von La Chevallerie, G., & Collett, G. (1986). Climatic influence on the isotopic composition of bone nitrogen. *Nature 1986 322:6082*, *322*(6082), 822–823. https://doi.org/10.1038/322822A0

Hedges, R. E. M. (2002). Bone diagenesis: An overview of processes. *Archaeometry*, *44*(3), 319–328. https://doi.org/10.1111/1475-4754.00064

Heuser, A., Eisenhauer, A., Scholz-Ahrens, K. E., & Schrezenmeir, J. (2016). Biological fractionation of stable Ca isotopes in Göttingen minipigs as a physiological model for Ca homeostasis in humans. *Isotopes in Environmental and Health Studies*, *52*(6), 633–648. https://doi.org/10.1080/10256016.2016.1151017

Hixon, S. W., Elliott Smith, E. A., Crowley, B. E., Perry, G. H., Randrianasy, J., Ranaivoarisoa, J. F., Kennett, D. J., & Newsome, S. D. (2018). Nitrogen isotope (δ15N) patterns for amino acids in lemur bones are inconsistent with aridity driving megafaunal extinction in south-western Madagascar. *Journal of Quaternary Science*, *33*(8), 958–968. https://doi.org/10.1002/JQS.3073

Hobbie, E. A., Shamhart, J., Sheriff, M., Ouimette, A. P., Trappe, M., Schuur, E. A. G., Hobbie, J. E., Boonstra, R., & Barnes, B. M. (2017). Stable Isotopes and Radiocarbon Assess Variable Importance of Plants and Fungi in Diets of Arctic Ground Squirrels. *Arctic, Antarctic, and Alpine Research*, *49*(3), 487–500. https://doi.org/10.1657/AAAR0016-062;WGROUP:STRING:PUBLICATION

Hobbs, N. T., Johnston, D. B., Marshall, K. N., Wolf, E. C., & Cooper, D. J. (2024). Does restoring apex predators to food webs restore ecosystems? Large carnivores in Yellowstone as a model system. *Ecological Monographs*, *94*(2), e1598. https://doi.org/10.1002/ECM.1598

Hodges, K. E. (1999). *Ecology of Snowshoe Hares in Southern Boreal and Montane Forests*.

Holmden, C., & Bélanger, N. (2010). Ca isotope cycling in a forested ecosystem. *Geochimica et Cosmochimica Acta*, *74*(3), 995–1015. https://doi.org/10.1016/J.GCA.2009.10.020

Hope, A. G., Waltari, E., Malaney, J. L., Payer, D. C., Cook, J. A., & Talbot, S. L. (2015). Arctic biodiversity: increasing richness accompanies shrinking refugia for a cold-associated tundra fauna. *Ecosphere*, *6*(9), 1–67. https://doi.org/10.1890/ES15-00104.1

Hoppe, K. A., Stover, S. M., Pascoe, J. R., & Amundson, R. (2004). Tooth enamel biomineralization in extant horses: implications for isotopic microsampling. *Palaeogeography, Palaeoclimatology, Palaeoecology*, *206*(3–4), 355–365. https://doi.org/10.1016/J.PALAEO.2004.01.012

Jaouen, K., Herrscher, E., & Balter, V. (2017). Copper and zinc isotope ratios in human bone and enamel. *American Journal of Physical Anthropology*, *162*(3), 491–500. https://doi.org/10.1002/AJPA.23132

Jim, S., Jones, V., Ambrose, S. H., & Evershed, R. P. (2006). Quantifying dietary macronutrient sources of carbon for bone collagen biosynthesis using natural abundance stable carbon isotope analysis. *British Journal of Nutrition*, *95*(6), 1055–1062. https://doi.org/10.1079/BJN20051685

Joannes-Boyau, R., Adams, J. W., Austin, C., Arora, M., Moffat, I., Herries, A. I. R., Tonge, M. P., Benazzi, S., Evans, A. R., Kullmer, O., Wroe, S., Dosseto, A., & Fiorenza, L. (2019). Elemental signatures of Australopithecus africanus teeth reveal seasonal dietary stress. *Nature*, *572*(7767), 112–115. https://doi.org/10.1038/S41586-019-1370-5

Karanth, K. U., & Sunquist, M. E. (2000). Behavioural correlates of predation by tiger (Panthera tigris), leopard (Panthera pardus) and dhole (Cuon alpinus) in Nagarahole, India. *Journal of Zoology*, *250*(2), 255–265. https://doi.org/10.1111/J.1469-7998.2000.TB01076.X

Kelsey Russell, A. L., Beckmann, K., Potié, J., & Russell, K. (2024). *Caribou population and distribution studies in the Tay River region Caribou population and distribution studies in the Tay River region Government of Yukon Fish and Wildlife Branch SR-24-11*. www.yukon.ca

Kemppinen, J., Niittynen, P., Rissanen, T., Tyystjärvi, V., Aalto, J., & Luoto, M. (2023). Soil Moisture Variations From Boreal Forests to the Tundra. *Water Resources Research*, *59*(6), e2022WR032719. https://doi.org/10.1029/2022WR032719

Kendall, C., & Grim, E. (1990). Combustion tube method for measurement of nitrogen isotope ratios using calcium oxide for total rmoval of carbon dioxide and water. *Analytical Chemistry*, *62*(5), 526–529. https://doi.org/10.1021/AC00204A019

King, D. A. (2004). Environment. Climate change science: adapt, mitigate, or ignore? *Science (New York, N.Y.)*, *303*(5655), 176–177. https://doi.org/10.1126/SCIENCE.1094329

Knapp, M., Rohland, N., Weinstock, J., Baryshnikov, G., Sher, A., Nagel, D., Rabeder, G., Pinhasi, R., Schmidt, H. A., & Hofreiter, M. (2009). First DNA sequences from Asian cave bear fossils reveal deep divergences and complex phylogeographic patterns. *Molecular Ecology*, *18*(6), 1225–1238. https://doi.org/10.1111/J.1365-294X.2009.04088.X

Koch, P. L. (2008). Isotopic Study of the Biology of Modern and Fossil Vertebrates. *Stable Isotopes in Ecology and Environmental Science: Second Edition*, 99–154. https://doi.org/10.1002/9780470691854.CH5

Koch, P. L., & Barnosky, A. D. (2006). Late quaternary extinctions: State of the debate. *Annual Review of Ecology, Evolution, and Systematics*, *37*(Volume 37, 2006), 215–250. https://doi.org/10.1146/ANNUREV.ECOLSYS.34.011802.132415/1

Koch, P. L., Tuross, N., & Fogel, M. L. (1997). The Effects of Sample Treatment and Diagenesis on the Isotopic Integrity of Carbonate in Biogenic Hydroxylapatite. *Journal of Archaeological Science*, *24*(5), 417–429. https://doi.org/10.1006/JASC.1996.0126

Kohn, M. J. (2008). Models of diffusion-limited uptake of trace elements in fossils and rates of fossilization. *Geochimica et Cosmochimica Acta*, *72*(15), 3758–3770. https://doi.org/10.1016/J.GCA.2008.05.045

Kohn, M. J. (2010). Carbon isotope compositions of terrestrial C3 plants as indicators of (palaeo)ecology and (palaeo)climate. *Proceedings of the National Academy of Sciences of the United States of America*, *107*(46), 19691–19695. https://doi.org/10.1073/PNAS.1004933107/ASSET/4727F7F9-ED31-481D-A11E-E6B5201EF84F/ASSETS/GRAPHIC/PNAS.1004933107EQ27.GIF

Laidre, K. L., Atkinson, S., Regehr, E. V., Stern, H. L., Born, E. W., Wiig, Ø., Lunn, N. J., & Dyck, M. (2020). Interrelated ecological impacts of climate change on an apex predator. *Ecological Applications*, *30*(4). https://doi.org/10.1002/EAP.2071/FULL

Lamichhane, S., Shrestha, B., Tharu, B. P. C., Koirala, R. K., Bhattarai, B. P., Poudel, P., Adhikari, B., & Khanal, G. (2025). Narrow Dietary Niche With High Overlap Between Snow Leopards and Himalayan Wolves Indicates Potential for Resource Competition in Shey Phoksundo National Park, Nepal. *Ecology and Evolution*, *15*(1), e70873. https://doi.org/10.1002/ECE3.70873

Land, M., Ingri, J., Andersson, P. S., & Öhlander, B. (2000). Ba/Sr, Ca/Sr and 87Sr/86Sr ratios in soil water and groundwater: Implications for relative contributions to stream water discharge. *Applied Geochemistry*, *15*(3), 311–325. https://doi.org/10.1016/S0883-2927(99)00054-2

Landry, Z., Kim, S., Trayler, R. B., Gilbert, M., Zazula, G., Southon, J., & Fraser, D. (2021). Dietary reconstruction and evidence of prey shifting in Pleistocene and recent gray wolves (Canis lupus) from Yukon Territory. *Palaeogeography, Palaeoclimatology, Palaeoecology*, *571*. https://doi.org/10.1016/j.palaeo.2021.110368

Landry, Z., Roloson, M. J., & Fraser, D. (2022). Investigating the reliability of metapodials as taxonomic Indicators for Beringian horses. *Journal of Mammalian Evolution*, *29*(4), 863–875. https://doi.org/10.1007/S10914-022-09626-4/TABLES/3

Lanier, H. C., Gunderson, A. M., Weksler, M., Fedorov, V. B., & Olson, L. E. (2015). Comparative Phylogeography Highlights the Double-Edged Sword of Climate Change Faced by Arctic- and Alpine-Adapted Mammals. *PLOS ONE*, *10*(3), e0118396. https://doi.org/10.1371/JOURNAL.PONE.0118396

Larramendi, A. (2015). Shoulder Height, Body Mass, and Shape of Proboscideans. *Https://Doi-Org.Proxy.Bib.Uottawa.ca/10.4202/App.00136.2014*, *61*(3), 537–574. https://doi.org/10.4202/APP.00136.2014

Laws, A. N. (2017). Climate change effects on predator–prey interactions. *Current Opinion in Insect Science*, *23*, 28–34. https://doi.org/10.1016/J.COIS.2017.06.010

Laws, R. M. (1966). AGE CRITERIA FOR THE AFRICAN ELEPHANT. *African Journal of Ecology*, *4*(1), 1–37. https://doi.org/10.1111/J.1365-2028.1966.TB00878.X

Lee-Thorp, J. A., Sealy, J. C., & van der Merwe, N. J. (1989). Stable carbon isotope ratio differences between bone collagen and bone apatite, and their relationship to diet. *Journal of Archaeological Science*, *16*(6), 585–599. https://doi.org/10.1016/0305-4403(89)90024-1

Lee-Thorp, J., & Sponheimer, M. (2003). Three case studies used to reassess the reliability of fossil bone and enamel isotope signals for paleodietary studies. *Journal of Anthropological Archaeology*, *22*(3), 208–216. https://doi.org/10.1016/S0278-4165(03)00035-7

Leonard, J. A., Vilà, C., Fox-Dobbs, K., Koch, P. L., Wayne, R. K., & Van Valkenburgh, B. (2007). Megafaunal Extinctions and the Disappearance of a Specialized Wolf Ecomorph. *Current Biology*, *17*(13), 1146–1150. https://doi.org/10.1016/J.CUB.2007.05.072

Lerner, J. E., Ono, K., Hernandez, K. M., Runstadler, J. A., Puryear, W. B., & Polito, M. J. (2018). Evaluating the use of stable isotope analysis to infer the feeding ecology of a growing US gray seal (Halichoerus grypus) population. *PLOS ONE*, *13*(2), e0192241. https://doi.org/10.1371/JOURNAL.PONE.0192241

Liu, Y., Hu, J., & Gore, J. (2024). Ecosystem stability relies on diversity difference between trophic levels. *Proceedings of the National Academy of Sciences*, *121*(50), e2416740121. https://doi.org/10.1073/PNAS.2416740121

Long, E. S., Sweitzer, R. A., Diefenbach, D. R., & Ben-David, M. (2005). Controlling for anthropogenically induced atmospheric variation in stable carbon isotope studies. *Oecologia*, *146*(1), 148–156. https://doi.org/10.1007/S00442-005-0181-6/FIGURES/4

Longin, R. (1971). New Method of Collagen Extraction for Radiocarbon Dating. *Nature 1971 230:5291*, *230*(5291), 241–242. https://doi.org/10.1038/230241A0

Loog, L., Thalmann, O., Sinding, M. H. S., Schuenemann, V. J., Perri, A., Germonpré, M., Bocherens, H., Witt, K. E., Samaniego Castruita, J. A., Velasco, M. S., Lundstrøm, I. K. C., Wales, N., Sonet, G., Frantz, L., Schroeder, H., Budd, J., Jimenez, E. L., Fedorov, S., Gasparyan, B., … Manica, A. (2020). Ancient DNA suggests modern wolves trace their origin to a Late Pleistocene expansion from Beringia. *Molecular Ecology*, *29*(9), 1596–1610. https://doi.org/10.1111/MEC.15329

Lorenzen, E. D., Nogués-Bravo, D., Orlando, L., Weinstock, J., Binladen, J., Marske, K. A., Ugan, A., Borregaard, M. K., Gilbert, M. T. P., Nielsen, R., Ho, S. Y. W., Goebel, T., Graf, K. E., Byers, D., Stenderup, J. T., Rasmussen, M., Campos, P. F., Leonard, J. A., Koepfli, K. P., … Willerslev, E. (2011). Species-specific responses of Late Quaternary megafauna to climate and humans. *Nature 2011 479:7373*, *479*(7373), 359–364. https://doi.org/10.1038/NATURE10574

Luz, B., Kolodny, Y., & Horowitz, M. (1984). Fractionation of oxygen isotopes between mammalian bone-phosphate and environmental drinking water. *Geochimica et Cosmochimica Acta*, *48*(8), 1689–1693. https://doi.org/10.1016/0016-7037(84)90338-7

Lyon, S. W., & Destouni, G. (2010). Changes in Catchment-Scale Recession Flow Properties in Response to Permafrost Thawing in the Yukon River Basin. *International Journal of Climatology*, *30*(14), 2138–2145. https://doi.org/10.1002/JOC.1993

MacFarlane, K. E. (2022). Yukon Exploration and Geology Overview 2022. *Yukon Geological Survey, 70 p.*

Yukon Exploration and Geology Overview (2022). MacFarlane K.E. (ed.), 2023. Yukon Geological Survey, 70 p.

Mann, D. H., Groves, P., Reanier, R. E., VGaglioti, B., LKunz, M., & BethShapiro, B. (2015). Life and extinction of megafauna in the ice-age Arctic. *Proceedings of the National Academy of Sciences of the United States of America*, *112*(46), 14301–14306. https://doi.org/10.1073/PNAS.1516573112/SUPPL_FILE/PNAS.1516573112.SAPP.PDF

Marshall, K. N., Thompson Hobbs, N., & Cooper, D. J. (2013). Stream hydrology limits recovery of riparian ecosystems after wolf reintroduction. *Proceedings of the Royal Society B: Biological Sciences*, *280*(1756). https://doi.org/10.1098/RSPB.2012.2977

Martin, J. E., Hassler, A., Montagnac, G., Therrien, F., & Balter, V. (2022). The stability of dinosaur communities before the Cretaceous–Paleogene (K–Pg) boundary: A perspective from southern Alberta using calcium isotopes as a dietary proxy. *Bulletin of the Geological Society of America*, *134*(9–10). https://doi.org/10.1130/B36222.1

Martin, J. E., Tacail, T., Adnet, S., Girard, C., & Balter, V. (2015). Calcium isotopes reveal the trophic position of extant and fossil elasmobranchs. *Chemical Geology*, *415*, 118–125. https://doi.org/10.1016/j.chemgeo.2015.09.011

Martin, J. E., Tacail, T., & Balter, V. (2017). Non-traditional isotope perspectives in vertebrate palaeobiology. *Palaeontology*, *60*(4), 485–502. https://doi.org/10.1111/PALA.12300

Martin, J. E., Tacail, T., Braga, J., Cerling, T. E., & Balter, V. (2020). Calcium isotopic ecology of Turkana Basin hominins. *Nature Communications 2020 11:1*, *11*(1), 1–7. https://doi.org/10.1038/S41467-020-17427-7

Martin, J. E., Tacail, T., Cerling, T. E., & Balter, V. (2018). Calcium isotopes in enamel of modern and Plio-Pleistocene East African mammals. *Earth and Planetary Science Letters*, *503*, 227–235. https://doi.org/10.1016/J.EPSL.2018.09.026

Massey, R., Rogers, B. M., Berner, L. T., Cooperdock, S., Mack, M. C., Walker, X. J., & Goetz, S. J. (2023). Forest composition change and biophysical climate feedbacks across boreal North America. *Nature Climate Change*, *13*(12), 1368. https://doi.org/10.1038/S41558-023-01851-W

Matheus, P. E. (1995). Diet and Co-ecology of Pleistocene Short-Faced Bears and Brown Bears in Eastern Beringia. *Quaternary Research*, *44*(3), 447–453. https://doi.org/10.1006/QRES.1995.1090

Matsubayashi, J., & Tayasu, I. (2019). Collagen turnover and isotopic records in cortical bone. *Journal of Archaeological Science*, *106*, 37–44. https://doi.org/10.1016/J.JAS.2019.03.010

Matthiesen, H., Høier Eriksen, A. M., Hollesen, J., & Collins, M. (2021). Bone degradation at five Arctic archaeological sites: Quantifying the importance of burial environment and bone characteristics. *Journal of Archaeological Science*, *125*, 105296. https://doi.org/10.1016/J.JAS.2020.105296

Mccain, C. M., & King, S. R. B. (2014). Body size and activity times mediate mammalian responses to climate change. *Global Change Biology*, *20*(6), 1760–1769. https://doi.org/10.1111/GCB.12499

McLennan, S. M. (1989). Rare Earth Elements in Sedimentary Rocks: Influence of Provenance and Sedimentary Processes. In *ochemistry And Mineralogy of Rare Earth Elements, Reviews in Mineralogy* (Vol. 21, pp. 169–200).

Meiri, M., Lister, A., Kosintsev, P., Zazula, G., & Barnes, I. (2020). Population dynamics and range shifts of moose (Alces alces) during the Late Quaternary. *Journal of Biogeography*, *47*(10), 2223–2234. https://doi.org/10.1111/JBI.13935

Merkle, J. A., Polfus, J. L., Derbridge, J. J., & Heinemeyer, K. S. (2017). Dietary niche partitioning among black bears, grizzly bears, and wolves in a multiprey ecosystem. *Canadian Journal of Zoology*, *95*(9), 663–671. https://doi.org/10.1139/CJZ-2016-0258/SUPPL_FILE/CJZ-2016-0258SUPPLA.DOCX

Metcalfe, J. Z., Longstaffe, F. J., & Zazula, G. D. (2010). Nursing, weaning, and tooth development in woolly mammoths from Old Crow, Yukon, Canada: Implications for Pleistocene extinctions. *Palaeogeography, Palaeoclimatology, Palaeoecology*, *298*(3–4), 257–270. https://doi.org/10.1016/J.PALAEO.2010.09.032

Milakovic, B., & Parker, K. L. (2011). Using stable isotopes to define diets of wolves in northern British Columbia, Canada. *Journal of Mammalogy*, *92*(2), 295–304. https://doi.org/10.1644/10-MAMM-A-038.1

Milligan, H. E., Kukka, P. M., Willier, C. N., Brown-Dussault, É., Kuba, K., Taylor, S. D., & Jung, T. S. (2023). *Results of a 2021 Survey of Arctic Ground Squirrels (Urocitellus parryii) in Southwestern Yukon*.

Minagawa, M., Wada, E., Minagawa, M., & Wada, E. (1984). Stepwise enrichment of ^{15}N along food chains: Further evidence and the relation between δ^{15}N and animal age. *GeCoA*, *48*(5), 1135–1140. https://doi.org/10.1016/0016-7037(84)90204-7

Monteath, A. J., Gaglioti, B. V., Edwards, M. E., & Froese, D. (2021). Late Pleistocene shrub expansion preceded megafauna turnover and extinctions in eastern Beringia. *Proceedings of the National Academy of Sciences of the United States of America*, *118*(52), e2107977118. https://doi.org/10.1073/PNAS.2107977118/SUPPL_FILE/PNAS.2107977118.SAPP01.PDF

Monteath, A. J., Kuzmina, S., Mahony, M., Calmels, F., Porter, T., Mathewes, R., Sanborn, P., Zazula, G., Shapiro, B., Murchie, T. J., Poinar, H. N., Sadoway, T., Hall, E., Hewitson, S., & Froese, D. (2022). *Relict permafrost preserves megafauna, insects, pollen, soils and pore-ice isotopes of the mammoth steppe and its collapse in central Yukon*. https://doi.org/10.1016/j.quascirev.2022.107878

Morueta-Holme, N., Flöjgaard, C., & Svenning, J. C. (2010). Climate Change Risks and Conservation Implications for a Threatened Small-Range Mammal Species. *PLOS ONE*, *5*(4), e10360. https://doi.org/10.1371/JOURNAL.PONE.0010360

Mougi, A. (2022). Predator interference and complexity–stability in food webs. *Scientific Reports 2022 12:1*, *12*(1), 1–8. https://doi.org/10.1038/s41598-022-06524-w

Moynier, F., & Fujii, T. (2017). Calcium isotope fractionation between aqueous compounds relevant to low-temperature geochemistry, biology and medicine. *Scientific Reports 2017 7:1*, *7*(1), 1–7. https://doi.org/10.1038/SREP44255

Munier, A., Hermanutz, L., Jacobs, J. D., & Lewis, K. (2014). Erratum to The interacting effects of temperature, ground disturbance, and herbivory on seedling establishment: Implications for treeline advance with climate warming (Plant Ecol, (2010), 210, (19-30), 10.1007/s11258-010-9724-y). *Plant Ecology*, *215*(4), 479. https://doi.org/10.1007/S11258-014-0300-8/METRICS

Murchie, T. J., Monteath, A. J., Mahony, M. E., Long, G. S., Cocker, S., Sadoway, T., Karpinski, E., Zazula, G., MacPhee, R. D. E., Froese, D., & Poinar, H. N. (2021). Collapse of the mammoth-steppe in central Yukon as revealed by ancient environmental DNA. *Nature Communications*, *12*(1), 7120. https://doi.org/10.1038/S41467-021-27439-6

Mutoro, N. M., Chira, R., Gichuki, N., Kariuki, E., Eberle, J., Habel, J. C., & Wykstra, M. (2022). Dietary preference of cheetahs (Acinonyx jubatus) in south-eastern Kenya. *Ecology and Evolution*, *12*(3), e8556. https://doi.org/10.1002/ECE3.8556

Newbold, T. (2018). Future effects of climate and land-use change on terrestrial vertebrate community diversity under different scenarios. *Proceedings of the Royal Society B*, *285*(1881). https://doi.org/10.1098/RSPB.2018.0792

Nielsen-Marsh, C. M., & Hedges, R. E. M. (2000). Patterns of Diagenesis in Bone I: The Effects of Site Environments. *Journal of Archaeological Science*, *27*(12), 1139–1150. https://doi.org/10.1006/JASC.1999.0537

Nitzsche, K. N., Wakaki, S., Yamashita, K., Shin, K. C., Kato, Y., Kamauchi, H., & Tayasu, I. (2022). Calcium and strontium stable isotopes reveal similar behaviors of essential Ca and nonessential Sr in stream food webs. *Ecosphere*, *13*(2), e3921. https://doi.org/10.1002/ECS2.3921

O'Leary, M. H. (1981). Carbon isotope fractionation in plants. *Phytochemistry*, *20*(4), 553–567. https://doi.org/10.1016/0031-9422(81)85134-5

O'Leary, M. H. (1988). Carbon Isotopes in Photosynthesis. *BioScience*, *38*(5), 328–336. https://doi.org/10.2307/1310735

Olson, J. S. (1958). Rates of Succession and Soil Changes on Southern Lake Michigan Sand Dunes. *Https://Doi.Org/10.1086/335973*, *119*(3), 125–170. https://doi.org/10.1086/335973

Ordiz, A., Aronsson, M., Persson, J., Støen, O. G., Swenson, J. E., & Kindberg, J. (2021). Effects of Human Disturbance on Terrestrial Apex Predators. *Diversity 2021, Vol. 13, Page 68*, *13*(2), 68. https://doi.org/10.3390/D13020068

Orsdol, K. G. V. (1984). Foraging behaviour and hunting success of lions in Queen Elizabeth National Park, Uganda. *African Journal of Ecology*, *22*(2), 79–99. https://doi.org/10.1111/J.1365-2028.1984.TB00682.X

Paine, R. T. (1980). Food Webs: Linkage, Interaction Strength and Community Infrastructure. *The Journal of Animal Ecology*, *49*(3), 666. https://doi.org/10.2307/4220

Pecl, G. T., Araújo, M. B., Bell, J. D., Blanchard, J., Bonebrake, T. C., Chen, I. C., Clark, T. D., Colwell, R. K., Danielsen, F., Evengård, B., Falconi, L., Ferrier, S., Frusher, S., Garcia, R. A., Griffis, R. B., Hobday, A. J., Janion-Scheepers, C., Jarzyna, M. A., Jennings, S., … Williams, S. E. (2017). Biodiversity redistribution under climate change: Impacts on ecosystems and human well-being. *Science*, *355*(6332). https://doi.org/10.1126/SCIENCE.AAI9214/SUPPL_FILE/PECL.SM.PDF

Pedregosa F., Michel, V., Grisel O., Blondel, M., Prettenhofer, P., Weiss, R., Vanderplas, J., Cournapeau, D., Pedregosa, F., Varoquaux, G., Gramfort, A., Thirion, B., Grisel, O., Dubourg, V., Passos, A., Brucher, M., Perrot M., Duchesnay E., (2011). Scikit-learn: Machine Learning in Python. *Journal of Machine Learning Research*, *12*(85), 2825–2830. http://jmlr.org/papers/v12/pedregosa11a.html

Peek, S., & Clementz, M. T. (2012). Sr/Ca and Ba/Ca variations in environmental and biological sources: A survey of marine and terrestrial systems. *Geochimica et Cosmochimica Acta*, *95*, 36–52. https://doi.org/10.1016/J.GCA.2012.07.026

Perkins, M. J., McDonald, R. A., Van Veen, F. J. F., Kelly, S. D., Rees, G., & Bearhop, S. (2014). Application of Nitrogen and Carbon Stable Isotopes (δ15N and δ13C) to Quantify Food Chain Length and Trophic Structure. *PLOS ONE*, *9*(3), e93281. https://doi.org/10.1371/JOURNAL.PONE.0093281

Phillips, D. L., Inger, R., Bearhop, S., Jackson, A. L., Moore, J. W., Parnell, A. C., Semmens, B. X., & Ward, E. J. (2014). Best practices for use of stable isotope mixing models in food-web studies. *Canadian Journal of Zoology*, *92*(10), 823–835. https://doi.org/10.1139/CJZ-2014-0127/ASSET/IMAGES/LARGE/CJZ-2014-0127F5.JPEG

Pilot, M., Jedrzejewski, W., Sidorovich, V. E., Meier-Augenstein, W., & Hoelzel, A. R. (2012). Dietary differentiation and the evolution of population genetic structure in a highly mobile carnivore. *PLoS ONE*, *7*(6). https://doi.org/10.1371/JOURNAL.PONE.0039341

Pineda-Munoz, S., Evans, A. R., & Alroy, J. (2016). The relationship between diet and body mass in terrestrial mammals. *Paleobiology*, *42*(4), 659–669. https://doi.org/10.1017/PAB.2016.6

Pires, A. P. F., Srivastava, D. S., Marino, N. A. C., MacDonald, A. A. M., Figueiredo-Barros, M. P., & Farjalla, V. F. (2018). Interactive effects of climate change and biodiversity loss on ecosystem functioning. *Ecology*, *99*(5), 1203–1213. https://doi.org/10.1002/ECY.2202

Plummer, M. (2003). *JAGS: A program for analysis of Bayesian graphical models using Gibbs sampling* (4.3.0).

Porcupine Caribou Technical Committee. (2022). *The Porcupine Caribou Herd Annual Summary Report*.

Pors Nielsen, S. (2004). The biological role of strontium. *Bone*, *35*(3), 583–588. https://doi.org/10.1016/j.bone.2004.04.026

Posner, A. S., & Betts, F. (1975). Synthetic Amorphous Calcium Phosphate and Its Relation to Bone Mineral Structure. *Accounts of Chemical Research*, *8*(8), 273–281. https://doi.org/10.1021/AR50092A003/ASSET/AR50092A003.FP.PNG_V03

Post, D. M. (2002). USING STABLE ISOTOPES TO ESTIMATE TROPHIC POSITION: MODELS, METHODS, AND ASSUMPTIONS. *Ecology*, *83*(3), 703–718. https://doi.org/10.1890/0012-9658(2002)083

Post, E., Forchhammer, M. C., Bret-Harte, M. S., Callaghan, T. V., Christensen, T. R., Elberling, B., Fox, A. D., Gilg, O., Hik, D. S., Høye, T. T., Ims, R. A., Jeppesen, E., Klein, D. R., Madsen, J., McGuire, A. D., Rysgaard, S., Schindler, D. E., Stirling, I., Tamstorf, M. P., … Aastrup, P. (2009). Ecological dynamics across the arctic associated with recent climate change. *Science*, *325*(5946), 1355–1358. https://doi.org/10.1126/SCIENCE.1173113

Price, T. D., Burton, J. H., & Bentley, R. A. (2002). THE CHARACTERIZATION OF BIOLOGICALLY AVAILABLE STRONTIUM ISOTOPE RATIOS FOR THE STUDY OF PREHISTORIC MIGRATION*. *Archaeometry*, *44*, 117–135.

Pushkar, V. S., & Cherepanova, M. V. (2011). Beringia: Impact on paleoclimates of northeast Asia and North Pacific during Last Pleistocene glaciation. *Quaternary International*, *237*(1–2), 32–38. https://doi.org/10.1016/J.QUAINT.2011.01.010

Python Software Foundation. (2024). *Python* (3.10.14).

Qi, H., Coplen, T. B., Geilmann, H., Brand, W. A., & Böhlke, J. K. (2003). Two new organic reference materials for delta13C and delta15N measurements and a new value for the delta13C of NBS 22 oil. *Rapid Communications in Mass Spectrometry : RCM*, *17*(22), 2483–2487. https://doi.org/10.1002/RCM.1219

Quintero, I., & Wiens, J. J. (2013). Rates of projected climate change dramatically exceed past rates of climatic niche evolution among vertebrate species. *Ecology Letters*, *16*(8), 1095–1103. https://doi.org/10.1111/ELE.12144

R Core Team. (2024). *R: A language and environment for statistical computing* (4.4.2).

Rabanus-Wallace, M. T., Wooller, M. J., Zazula, G. D., Shute, E., Jahren, A. H., Kosintsev, P., Burns, J. A., Breen, J., Llamas, B., & Cooper, A. (2017). Megafaunal isotopes reveal role of increased moisture on rangeland during late Pleistocene extinctions. *Nature Ecology & Evolution 2017 1:5*, *1*(5), 1–5. https://doi.org/10.1038/S41559-017-0125

Raghavan, M., Espregueira Themudo, G., Smith, C. I., Zazula, G., & Campos, P. F. (2014). Muskox (Ovibos moschatus) of the mammoth steppe: tracing palaeodietary and palaeoenvironmental changes over the last 50,000 years using carbon and nitrogen isotopic analysis. *Quaternary Science Reviews*, *102*, 192–201. https://doi.org/10.1016/J.QUASCIREV.2014.08.001

Reade, H., Tripp, J. A., Frémondeau, D., Sayle, K. L., Higham, T. F. G., Street, M., & Stevens, R. E. (2023). Nitrogen palaeo-isoscapes: Changing spatial gradients of faunal δ15N in late Pleistocene and early Holocene Europe. *PLOS ONE*, *18*(2), e0268607. https://doi.org/10.1371/JOURNAL.PONE.0268607

Reynard, B., & Balter, V. (2014). Trace elements and their isotopes in bones and teeth: Diet, environments, diagenesis, and dating of archeological and paleontological samples. *Palaeogeography, Palaeoclimatology, Palaeoecology*, *416*, 4–16. https://doi.org/10.1016/J.PALAEO.2014.07.038

Ripple, W. J., & Beschta, R. L. (2012). *Trophic cascades in Yellowstone: The first 15 years after wolf reintroduction*. https://doi.org/10.1016/j.biocon.2011.11.005

Ripple, W. J., Beschta, R. L., Wolf, C., Painter, L. E., & Wirsing, A. J. (2025). The strength of the Yellowstone trophic cascade after wolf reintroduction. *Global Ecology and Conservation*, *58*, e03428. https://doi.org/10.1016/J.GECCO.2025.E03428

Ripple, W. J., Chapron, G., López-Bao, J. V., Durant, S. M., Macdonald, D. W., Lindsey, P. A., Bennett, E. L., Beschta, R. L., Bruskotter, J. T., Campos-Arceiz, A., Corlett, R. T., Darimont, C. T., Dickman, A. J., Dirzo, R., Dublin, H. T., Estes, J. A., Everatt, K. T., Galetti, M., Goswami, V. R., … Zhang, L. (2016). Saving the World's Terrestrial Megafauna. *BioScience*, *66*(10), 807–812. https://doi.org/10.1093/BIOSCI/BIW092

Ripple, W. J., Chapron, G., López-Bao, J. V., Durant, S. M., MacDonald, D. W., Lindsey, P. A., Bennett, E. L., Beschta, R. L., Bruskotter, J. T., Campos-Arceiz, A., Corlett, R. T., Darimont, C. T., Dickman, A. J., Dirzo, R., Dublin, H. T., Estes, J. A., Everatt, K. T., Galetti, M., Goswami, V. R., … Zhang, L. (2017). Conserving the World's Megafauna and Biodiversity: The Fierce Urgency of Now. *BioScience*, *67*(3), 197–200. https://doi.org/10.1093/BIOSCI/BIW168

Ripple, W. J., Estes, J. A., Beschta, R. L., Wilmers, C. C., Ritchie, E. G., Hebblewhite, M., Berger, J., Elmhagen, B., Letnic, M., Nelson, M. P., Schmitz, O. J., Smith, D. W., Wallach, A. D., & Wirsing, A. J. (2014). Status and ecological effects of the world's largest carnivores. *Science*, *343*(6167). https://doi.org/10.1126/SCIENCE.1241484/SUPPL_FILE/RIPPLE.SM.PDF

Ripple, W. J., & Larsen, E. J. (2000). Historic aspen recruitment, elk, and wolves in northern Yellowstone National Park, USA. *Biological Conservation*, *95*(3), 361–370. https://doi.org/10.1016/S0006-3207(00)00014-8

Ripple, W. J., Newsome, T. M., Wolf, C., Dirzo, R., Everatt, K. T., Galetti, M., Hayward, M. W., Kerley, G. I. H., Levi, T., Lindsey, P. A., Macdonald, D. W., Malhi, Y., Painter, L. E., Sandom, C. J., Terborgh, J., & Van Valkenburgh, B. (2015). Collapse of the world's largest herbivores. *Science Advances*, *1*(4). https://doi.org/10.1126/SCIADV.1400103/SUPPL_FILE/1400103_SM.PDF

Ripple, W. J., & Van Valkenburgh, B. (2010). Linking Top-down Forces to the Pleistocene Megafaunal Extinctions. *BioScience*, *60*(7), 516–526. https://doi.org/10.1525/BIO.2010.60.7.7

Ripple, W. J., Whalen, D. N., Wolf, C., Cao, Y., Schulte, J., Swann, S., Woodrich, S. T., Newsome, T., Cairncross, R., & Wirsing, A. J. (2024). Trophic cascades and climate change. *Food Webs*, *41*, e00362. https://doi.org/10.1016/J.FOOWEB.2024.E00362

Ritchie, E. G., Elmhagen, B., Glen, A. S., Letnic, M., Ludwig, G., & McDonald, R. A. (2012). Ecosystem restoration with teeth: what role for predators? *Trends in Ecology & Evolution*, *27*(5), 265–271. https://doi.org/10.1016/J.TREE.2012.01.001

Ritchie, E. G., & Johnson, C. N. (2009). Predator interactions, mesopredator release and biodiversity conservation. *Ecology Letters*, *12*(9), 982–998. https://doi.org/10.1111/J.1461-0248.2009.01347.X

Rode, K. D., Robbins, C. T., Nelson, L., & Amstrup, S. C. (2015). Can polar bears use terrestrial foods to offset lost ice-based hunting opportunities? *Frontiers in Ecology and the Environment*, *13*(3), 138–145. https://doi.org/10.1890/140202

Routledge, J., Sonne, C., Letcher, R. J., Dietz, R., & Szpak, P. (2023). Unprecedented shift in Canadian High Arctic polar bear food web unsettles four millennia of stability. *Anthropocene*, *43*, 100397. https://doi.org/10.1016/J.ANCENE.2023.100397

Rowland, E. L., Fresco, N., Reid, D., & Cooke, H. A. (2016). Examining climate-biome ("cliome") shifts for Yukon and its protected areas. *Global Ecology and Conservation*, *8*, 1–17. https://doi.org/10.1016/J.GECCO.2016.07.006

Running Horse Collin, Y. (Tašunke Iyanke Wiŋ), Bataille, C. P., Hershauer, S., Hunska Tašunke Icu, M. (Chief Joe American Horse), Left Heron, H. (Akil Nujipi), Justin, W., Stelkia, J. (qwyxnmitkw), C'wyelx (Pierre, T.), Stelkia, J. A., Asikłuk Topkok, S., Leonard, B. (Ginondidoy), Soop, B. (Naatoonistaahs), Gonzalez, M. (Hinapan, N.), Afraid of Bear-Cook, A. L. (Luta Wiŋ), Afraid of Bear, A. (Wakiŋyala Wiŋ), Omniya, T. (Robert Milo Yellow Hair), Dull Knife, B. (Mah'piya Keyaké Wiŋ), Yellow Bull, W. W. (Mažasu), Means, B., Tecumseh Collin, C. (Wanka'tuya Kiya), Koskey, M., Kapp, J. D., Landry, Z., Fraser, D., Southon, J., Lindroos, E. E., Hassler, A., Chauvey, L., Tressières, G., Tonasso-Calvière, L., Schiavinato, S., Seguin-Orlando, A., Perdereau, A., Oliveira, P. H., Aury, J., Wincker, P., Kirillova, I. V., Vasiliev, S. K., Kusliy, M. A., Graphdotsky, A. S., Tishkin, A., Barnes, I., Druckenmiller, P., Jass, C. N., MacPhee, R. D. E., Barrón-Ortiz, C. I., Groves, P., Mann, D., Froese, D. G., Wooller, M., Miller, J. H., Crowley, B., Zazula, G., Hall, E., Hewitson, S., Shapiro, B., Orlando, L. (2025). Sustainability insights from Late Pleistocene climate change and horse migration patterns. *Science* 388, 748-755(2025). DOI:10.1126/science.adr2355.

Safont, S., Malgosa, A., Subiraà, M. E., & Gibert, J. (1998). Can Trace Elements in Fossils Provide Information about Palaeodiet? *International Journal of Osteoarchaeology Int. J. Osteoarchaeol*, *8*, 23–37. https://doi.org/10.1002/(SICI)1099-1212(199801/02)8:1

Schmitt, A. D. (2016). Earth-surface ca isotopic fractionations. *Advances in Isotope Geochemistry*, 145–172. https://doi.org/10.1007/978-3-540-68953-9_5

Schmitt, A. D., Vigier, N., Lemarchand, D., Millot, R., Stille, P., & Chabaux, F. (2012). Processes controlling the stable isotope compositions of Li, B, Mg and Ca in plants, soils and waters: A review. *Comptes Rendus Geoscience*, *344*(11–12), 704–722. https://doi.org/10.1016/J.CRTE.2012.10.002

Schmitz, O. J. (2006). PREDATORS HAVE LARGE EFFECTS ON ECOSYSTEM PROPERTIES BY CHANGING PLANT DIVERSITY, NOT PLANT BIOMASS. *REPORTS Ecology*, *87*(6), 1432–1437. https://doi.org/10.1890/0012-9658(2006)87

Schmitz, O. J. (2009). Effects of predator functional diversity on grassland ecosystem function. *Ecology*, *90*(9), 2339–2345. https://doi.org/10.1890/08-1919.1

Schmitz, O. J., Hambäck, P. A., & Beckerman, A. P. (2000). Trophic cascades in terrestrial systems: A review of the effects of carnivore removals on plants. *American Naturalist*, *155*(2), 141–153. https://doi.org/10.1086/303311/ASSET/IMAGES/LARGE/FG2.JPEG

Schoeninger, M. J. (1979). Diet and status at Chalcatzingo: Some empirical and technical aspects of strontium analysis. *American Journal of Physical Anthropology*, *51*(3), 295–309. https://doi.org/10.1002/AJPA.1330510302

Schulte to Bühne, H., Tobias, J. A., Durant, S. M., & Pettorelli, N. (2021). Improving Predictions of Climate Change–Land Use Change Interactions. *Trends in Ecology & Evolution*, *36*(1), 29–38. https://doi.org/10.1016/J.TREE.2020.08.019

Schwartz-Narbonne, R., Longstaffe, F., Metcalfe, J. *et al.* Solving the woolly mammoth conundrum: amino acid ^{15}N-enrichment suggests a distinct forage or habitat. *Sci Rep* **5**, 9791 (2015). https://doi.org/10.1038/srep09791

Schwartz-Narbonne, R., Longstaffe, F. J., Kardynal, K. J., Druckenmiller, P., Hobson, K. A., Jass, C. N., Metcalfe, J. Z., & Zazula, G. (2019). Reframing the mammoth steppe: Insights from analysis of isotopic niches. *Quaternary Science Reviews*, *215*, 1–21. https://doi.org/10.1016/J.QUASCIREV.2019.04.025

Screen, J. A., & Simmonds, I. (2010). The central role of diminishing sea ice in recent Arctic temperature amplification. *Nature 2010 464:7293*, *464*(7293), 1334–1337. https://doi.org/10.1038/nature09051

Serreze, M. C., & Francis, J. A. (2006). The arctic amplification debate. *Climatic Change*, *76*(3–4), 241–264. https://doi.org/10.1007/S10584-005-9017-Y/METRICS

Severud, W. J., Belant, J. L., Windels, S. K., & Bruggink, J. G. (2013). Seasonal variation in assimilated diets of American beavers. *American Midland Naturalist*, *169*(1), 30–42. https://doi.org/10.1674/0003-0031-169.1.30

Shah, F. A. (2025). Revisiting the physical and chemical nature of the mineral component of bone. *Acta Biomaterialia*, *196*, 1–16. https://doi.org/10.1016/J.ACTBIO.2025.01.055

Shapiro, B., & Cooper, A. (2003). *Beringia as an Ice Age genetic museum*. https://doi.org/10.1016/S0033-5894(03)00009-7

Sillen, A., & Kavanagh M. (1982). Strontium and paleodietary research: A review. *American Journal of Physical Anthropology*. https://www.academia.edu/70738693/Strontium_and_paleodietary_research_A_review

Sillen, A., & LeGeros, R. (1991). Solubility profiles of synthetic apatites and of modern and fossil bones. *Journal of Archaeological Science*, *18*(3), 385–397. https://doi.org/10.1016/0305-4403(91)90073-X

Simmonds, I. (2015). Comparing and contrasting the behaviour of Arctic and Antarctic sea ice over the 35 year period 1979-2013. *Annals of Glaciology*, *56*(69), 18–28. https://doi.org/10.3189/2015AOG69A909

Skulan, J., & DePaolo, D. J. (1999). Calcium isotope fractionation between soft and mineralized tissues as a monitor of calcium use in vertebrates. *Proceedings of the National Academy of Sciences*, *96*(24), 13709–13713. https://doi.org/10.1073/PNAS.96.24.13709

Smith, D. W., & Tyers, D. B. (2012). The History and Current Status and Distribution of Beavers in Yellowstone National Park. *Https://Doi.Org/10.3955/046.086.0404*, *86*(4), 276–288. https://doi.org/10.3955/046.086.0404

Smith, F. A., Smith, R. E. E., Lyons, S. K., & Payne, J. L. (2018). Body size downgrading of mammals over the late Quaternary. *Science (New York, N.Y.)*, *360*(6386), 310–313. https://doi.org/10.1126/SCIENCE.AAO5987

Sowers, T., Bender, M., & Raynaud, D. (1989). Elemental and isotopic composition of occluded O2 and N2 in polar ice. *Journal of Geophysical Research: Atmospheres*, *94*(D4), 5137–5150. https://doi.org/10.1029/JD094ID04P05137

Sponheimer, M., Robinson, T., Ayliffe, L., Roeder, B., Hammer, J., Passey, B., West, A., Cerling, T., Dearing, D., & Ehleringer, J. (2003). Nitrogen isotopes in mammalian herbivores: Hair δ^{15}N values from a controlled feeding study. *International Journal of Osteoarchaeology*, 13(1–2), 80–87. https://doi.org/10.1002/oa.655

Sponheimer, M., & Lee-Thorp, J. A. (2006). Enamel diagenesis at South African Australopith sites: Implications for paleoecological reconstruction with trace elements. *Geochimica et Cosmochimica Acta*, *70*(7), 1644–1654. https://doi.org/10.1016/J.GCA.2005.12.022

Stephens, R. B., Shipley, O. N., & Moll, R. J. (2023). Meta-analysis and critical review of trophic discrimination factors (Δ13C and Δ15N): Importance of tissue, trophic level and diet source. *Functional Ecology*, *37*(9), 2535–2548. https://doi.org/10.1111/1365-2435.14403

Stevens, C. J., Dise, N. B., Mountford, J. O., & Gowing, D. J. (2004). Impact of nitrogen deposition on the species richness of grasslands. *Science (New York, N.Y.)*, *303*(5665), 1876–1879. https://doi.org/10.1126/SCIENCE.1094678

Stevens, R. E., Jacobi, R., Street, M., Germonpré, M., Conard, N. J., Münzel, S. C., & Hedges, R. E. M. (2008). Nitrogen isotope analyses of reindeer (Rangifer tarandus), 45,000 BP to 9,000 BP: Palaeoenvironmental reconstructions. *Palaeogeography, Palaeoclimatology, Palaeoecology*, *262*(1–2), 32–45. https://doi.org/10.1016/J.PALAEO.2008.01.019

Stimmelmayr, R., Maier, J. A. K., Persons, K., & Battig, J. (2006). INCISOR TOOTH BREAKAGE, ENAMEL DEFECTS, AND PERIODONTITIS IN A DECLINING ALASKAN MOOSE POPULATION. *ALCES*, *42*, 65–74. http://www.

Stirling, I., & Derocher, A. E. (2012). Effects of climate warming on polar bears: a review of the evidence. *Global Change Biology*, *18*(9), 2694–2706. https://doi.org/10.1111/J.1365-2486.2012.02753.X

St-Jean, G., William, Kieser, E., Crann, C. A., & Murseli, S. (2016). *SEMI-AUTOMATED EQUIPMENT FOR CO 2 PURIFICATION AND GRAPHITIZATION AT THE A.E. LALONDE AMS LABORATORY (OTTAWA, CANADA)*. https://doi.org/10.1017/RDC.2016.57

Stock, B. (2025). *Title Bayesian Mixing Models in R*. https://github.com/brianstock/MixSIAR/issues

Stuiver, M., Polach, H. A., Stuiver, M., & Polach, H. A. (1977). Discussion Reporting of 14C Data. *Radcb*, *19*(3), 355–363. https://doi.org/10.1017/S0033822200003672

Suarez, K. N., Romanello, M., Bettica, P., & Moro, L. (1996). Collagen type I of rat cortical and trabecular bone differs in the extent of posttranslational modifications. *Calcified Tissue International*, *58*(1), 65–69. https://doi.org/10.1007/BF02509548

Szpak, P., Gröcke, D. R., Debruyne, R., MacPhee, R. D. E., Guthrie, R. D., Froese, D., Zazula, G. D., Patterson, W. P., & Poinar, H. N. (2010). Regional differences in bone collagen δ13C and δ15N of Pleistocene mammoths: Implications for paleoecology of the mammoth steppe. *Palaeogeography, Palaeoclimatology, Palaeoecology*, *286*(1–2), 88–96. https://doi.org/10.1016/J.PALAEO.2009.12.009

Tacail, T. (2017). *Physiologie isotopique du Calcium chez les mammifères* [Doctoral dissertation]. Université de Lyon.

Tacail, T., Albalat, E., Télouk, P., & Balter, V. (2014). A simplified protocol for measurement of Ca isotopes in biological samples. *Journal of Analytical Atomic Spectrometry*, *29*(3), 529–535. https://doi.org/10.1039/C3JA50337B

Tacail, T., Le Houedec, S., & Skulan, J. L. (2020). New frontiers in calcium stable isotope geochemistry: Perspectives in present and past vertebrate biology. *Chemical Geology*, *537*. https://doi.org/10.1016/J.CHEMGEO.2020.119471

Tacail, T., Télouk, P., & Balter, V. (2015). Precise analysis of calcium stable isotope variations in biological apatites using laser ablation MC-ICPMS. *Journal of Analytical Atomic Spectrometry*, *31*(1), 152–162. https://doi.org/10.1039/C5JA00239G

Tacail, T., Thivichon-Prince, B., Martin, J. E., Charles, C., Viriot, L., & Balter, V. (2017). Assessing human Weaning practices with calcium isotopes in tooth enamel. *Proceedings of the National Academy of Sciences of the United States of America*, *114*(24), 6268–6273. https://doi.org/10.1073/PNAS.1704412114/SUPPL_FILE/PNAS.1704412114.SFIG04.PDF

Tahmasebi, F., Longstaffe, F. J., & Zazula, G. (2018). Nitrogen isotopes suggest a change in nitrogen dynamics between the Late Pleistocene and modern time in Yukon, Canada. *PLoS ONE*, *13*(2), e0192713. https://doi.org/10.1371/JOURNAL.PONE.0192713

Tahmasebi, F., Longstaffe, F. J., Zazula, G., & Bennett, B. (2017). Nitrogen and carbon isotopic dynamics of subarctic soils and plants in southern Yukon Territory and its implications for paleoecological and paleodietary studies. *PLOS ONE*, *12*(8), e0183016. https://doi.org/10.1371/JOURNAL.PONE.0183016

Talamo, S., Fewlass, H., Maria, R., & Jaouen, K. (2021). "Here we go again": the inspection of collagen extraction protocols for 14C dating and palaeodietary analysis. *STAR: Science & Technology of Archaeological Research*, *7*(1), 62–77. https://doi.org/10.1080/20548923.2021.1944479

Taylor, R. S., Manseau, M., Klütsch, C. F. C., Polfus, J. L., Steedman, A., Hervieux, D., Kelly, A., Larter, N. C., Gamberg, M., Schwantje, H., & Wilson, P. J. (2021). Population dynamics of caribou shaped by glacial cycles before the last glacial maximum. *Molecular Ecology*, *30*(23), 6121. https://doi.org/10.1111/MEC.16166

Terborgh, J., Lopez, L., Nuñez, P. V., Rao, M., Shahabuddin, G., Orihuela, G., Riveros, M., Ascanio, R., Adler, G. H., Lambert, T. D., & Balbas, L. (2001). Ecological Meltdown in Predator-Free Forest Fragments. *Science*, *294*(5548), 1923–1926. https://doi.org/10.1126/SCIENCE.1064397

Terrill, D. F., Jarochowska, E., Henderson, C. M., Shirley, B., & Bremer, O. (2022). Sr/Ca and Ba/Ca ratios support trophic partitioning within a Silurian conodont community from Gotland, Sweden. *Paleobiology*, *48*(4), 601–621. https://doi.org/10.1017/PAB.2022.9

Thomas, C. D., Cameron, A., Green, R. E., Bakkenes, M., Beaumont, L. J., Collingham, Y. C., Erasmus, B. F. N., Ferreira De Siqueira, M., Grainger, A., Hannah, L., Hughes, L., Huntley, B., Van Jaarsveld, A. S., Midgley, G. F., Miles, L., Ortega-Huerta, M. A., Peterson, A. T., Phillips, O. L., & Williams, S. E. (2004). Extinction risk from climate change. *Nature 2003 427:6970*, *427*(6970), 145–148. https://doi.org/10.1038/nature02121

Tieszen, L. L. (1991). Natural variations in the carbon isotope values of plants: Implications for archaeology, ecology, and paleoecology. *Journal of Archaeological Science*, *18*(3), 227–248. https://doi.org/10.1016/0305-4403(91)90063-U

Tieszen, L. L., & Fagre, T. (1993). Effect of Diet Quality and Composition on the Isotopic Composition of Respiratory CO2, Bone Collagen, Bioapatite, and Soft Tissues. *Prehistoric Human Bone*, 121–155. https://doi.org/10.1007/978-3-662-02894-0_5

Tissot, F. L. H., Cleveland, D., Grigoryan, R., Kipp, M. A., Shafiee, R. T., Miaou, E., Chunduri, R., Melton, H., Tacail, T., & Razionale, D. (2024). Magnitude and timescales of Ca isotope variability in human urine: implications for bone mass balance monitoring. *Metallomics : Integrated Biometal Science*, *16*(11). https://doi.org/10.1093/MTOMCS/MFAE050

Toepfer, E. T., Rott, J., Bartosova, M., Kolevica, A., Machuca-Gayet, I., Heuser, A., Rabe, M., Shroff, R., Bacchetta, J., Zarogiannis, S. G., Eisenhauer, A., & Schmitt, C. P. (2021). Calcium isotope fractionation by osteoblasts and osteoclasts, across endothelial and epithelial cell barriers, and with binding to proteins. *American Journal of Physiology. Regulatory, Integrative and Comparative Physiology*, *321*(1), R29–R40. https://doi.org/10.1152/AJPREGU.00334.2020

Toots, H., & Voorhies, M. R. (1965). Strontium in Fossil Bones and the Reconstruction of Food Chains. *Science*, *149*(3686), 854–855. https://doi.org/10.1126/SCIENCE.149.3686.854

Trant, A., Higgs, E., & Starzomski, B. M. (2020). A century of high elevation ecosystem change in the Canadian Rocky Mountains. *Scientific Reports 2020 10:1*, *10*(1), 1–10. https://doi.org/10.1038/s41598-020-66277-2

Trueman, C. N., Privat, K., & Field, J. (2008). Why do crystallinity values fail to predict the extent of diagenetic alteration of bone mineral? *Palaeogeography, Palaeoclimatology, Palaeoecology*, *266*(3–4), 160–167. https://doi.org/10.1016/J.PALAEO.2008.03.038

Trueman, C. N., & Tuross, N. (2002). Trace Elements in Recent and Fossil Bone Apatite. *Reviews in Mineralogy and Geochemistry*, *48*(1), 489–521. https://doi.org/10.2138/RMG.2002.48.13

Tütken, T., Vennemann, T. W., & Pfretzschner, H. U. (2008). Early diagenesis of bone and tooth apatite in fluvial and marine settings: Constraints from combined oxygen isotope, nitrogen and REE analysis. *Palaeogeography, Palaeoclimatology, Palaeoecology*, *266*(3–4), 254–268. https://doi.org/10.1016/J.PALAEO.2008.03.037

Tyson, R., Haines, S., & Hodges, K. E. (2010). Modelling the Canada lynx and snowshoe hare population cycle: The role of specialist predators. *Theoretical Ecology*, *3*(2), 97–111. https://doi.org/10.1007/S12080-009-0057-1

U.S. National Park Service (2020). Dall Sheep, https://www.nps.gov/articles/about-dall-sheep.htm

van den Berg, M., Loonen, M. J. J. E., & Çakırlar, C. (2021). Judging a reindeer by its teeth: A user-friendly tooth wear and eruption pattern recording scheme to estimate age-at-death in reindeer (Rangifer tarandus). *International Journal of Osteoarchaeology*, *31*(3), 417. https://doi.org/10.1002/OA.2961

van der Merwe, N. J., & Medina, E. (1991). The canopy effect, carbon isotope ratios and foodwebs in amazonia. *Journal of Archaeological Science*, *18*(3), 249–259. https://doi.org/10.1016/0305-4403(91)90064-V

Van Klinken, G. J. (1999). Bone Collagen Quality Indicators for Palaeodietary and Radiocarbon Measurements. *Journal of Archaeological Science*, *26*(6), 687–695. https://doi.org/10.1006/JASC.1998.0385

Van Valkenburgh, B. (2009). Costs of carnivory: Tooth fracture in Pleistocene and recent carnivorans. *Biological Journal of the Linnean Society*, *96*(1), 68–81. https://doi.org/10.1111/J.1095-8312.2008.01108.X

Veselý, L., Balzani, P., Haubrock, P. J., Buřič, M., Glon, M., Ercoli, F., Ruokonen, T. J., Kainz, M. J., Hämäläinen, H., & Kouba, A. (2024). Species-specific trophic discrimination factors can reduce the uncertainty of stable isotope analyses. *Hydrobiologia*, *851*(14), 3471–3487. https://doi.org/10.1007/S10750-024-05513-6/FIGURES/3

Volmer, R., Hertler, C., & van der Geer, A. (2016). Niche overlap and competition potential among tigers (Panthera tigris), sabertoothed cats (Homotherium ultimum, Hemimachairodus zwierzyckii) and Merriam's Dog (Megacyon merriami) in the Pleistocene of Java. *Palaeogeography, Palaeoclimatology, Palaeoecology*, *441*, 901–911. https://doi.org/10.1016/J.PALAEO.2015.10.039

Wacker, L., Christl, M., & Synal, H. A. (2010). Bats: A new tool for AMS data reduction. *Nuclear Instruments and Methods in Physics Research Section B: Beam Interactions with Materials and Atoms*, *268*(7–8), 976–979. https://doi.org/10.1016/J.NIMB.2009.10.078

Wang, Y., & Cerling, T. E. (1994). A model of fossil tooth and bone diagenesis: implications for paleodiet reconstruction from stable isotopes. *Palaeogeography, Palaeoclimatology, Palaeoecology*, *107*(3–4), 281–289. https://doi.org/10.1016/0031-0182(94)90100-7

Warsen, S. A., Frair, J. L., & Teece, M. A. (2014). Isotopic investigation of niche partitioning among native carnivores and the non-native coyote (Canis latrans). *Isotopes in Environmental and Health Studies*, *50*(3), 414–424. https://doi.org/10.1080/10256016.2014.897946

Wassmann, P., Duarte, C. M., Agustí, S., & Sejr, M. K. (2011). Footprints of climate change in the Arctic marine ecosystem. *Global Change Biology*, *17*(2), 1235–1249. https://doi.org/10.1111/J.1365-2486.2010.02311.X

Wathen, C. A., Isaksson, S., & Lidén, K. (2022). On the road again—a review of pretreatment methods for the decontamination of skeletal materials for strontium isotopic and concentration analysis. *Archaeological and Anthropological Sciences 2022 14:3*, *14*(3), 1–16. https://doi.org/10.1007/S12520-022-01517-2

Weber, M., Weber, K., Winkler, D. E., & Tütken, T. (2025). Calcium and strontium isotopes in extant diapsid reptiles reflect dietary tendencies-a reference frame for diet reconstructions in the fossil record. *Proceedings. Biological Sciences*, *292*(2038). https://doi.org/10.1098/RSPB.2024.2002

Weiskopf, S. R., Rubenstein, M. A., Crozier, L. G., Gaichas, S., Griffis, R., Halofsky, J. E., Hyde, K. J. W., Morelli, T. L., Morisette, J. T., Muñoz, R. C., Pershing, A. J., Peterson, D. L., Poudel, R., Staudinger, M. D., Sutton-Grier, A. E., Thompson, L., Vose, J., Weltzin, J. F., & Whyte, K. P. (2020). Climate change effects on biodiversity, ecosystems, ecosystem services, and natural resource management in the United States. *Science of The Total Environment*, *733*, 137782. https://doi.org/10.1016/J.SCITOTENV.2020.137782

Wiens, J. A., Stralberg, D., Jongsomjit, D., Howell, C. A., & Snyder, M. A. (2009). Niches, models, and climate change: Assessing the assumptions and uncertainties. *Proceedings of the National Academy of Sciences of the United States of America*, *106*(SUPPL. 2), 19729–19736. https://doi.org/10.1073/PNAS.0901639106/SUPPL_FILE/0901639106SI.PDF

Wildlife Management Advisory Council (North Slope). (2021). *Yukon North Slope Wildlife Conservation and Management Plan – Companion Report*.

Wolff, J. O. (1978). Food Habits of Snowshoe Hares in Interior Alaska. *The Journal of Wildlife Management*, *42*(1), 148. https://doi.org/10.2307/3800702

Wooller, M. J., Bataille, C., Druckenmiller, P., Erickson, G. M., Groves, P., Haubenstock, N., Howe, T., Irrgeher, J., Mann, D., Moon, K., Potter, B. A., Prohaska, T., Rasic, J., Reuther, J., Shapiro, B., Spaleta, K. J., & Willis, A. D. (2021). Lifetime mobility of an Arctic woolly mammoth. *Science*, *373*(6556), 806–808. https://doi.org/10.1126/SCIENCE.ABG1134/SUPPL_FILE/SCIENCE.ABG1134_SM.PDF

Wooller, M. J., Zazula, G. D., Edwards, M., Froese1, D. G., Boone, R. D., Parker, C., & Bennett, B. (2007). *Stable Carbon Isotope Compositions of Eastern Beringian Grasses and Sedges: Investigating Their Potential as Paleoenvironmental Indicators*. https://doi.org/10.1657/1523-0430(2007)39

Yang, H., Zhang, D., Winkler, J. A., Huang, Q., Zhang, Y., Wu, P., Liu, J., Ouyang, Z., Xu, W., Chen, X., Wu, D., Zhang, J., & Songer, M. (2024). Field experiment reveals complex warming impacts on giant pandas' bamboo diet. *Biological Conservation*, *294*, 110635. https://doi.org/10.1016/J.BIOCON.2024.110635

Yeakel, J. D., Guimarães, P. R., Bocherens, H., & Koch, P. L. (2013). The impact of climate change on the structure of Pleistocene food webs across the mammoth steppe. *Proceedings of the Royal Society B: Biological Sciences*, *280*(1762). https://doi.org/10.1098/RSPB.2013.0239

Yukon Department of Environment, Caribou Program, & Fish and Wildlife Branch. (2024). *Yukon caribou herd ranges map 2024 | Yukon.ca*. https://yukon.ca/en/yukon-caribou-herd-ranges-map-2024

Yukon Wildlife. (2024a). *Muskox*. https://yukon.ca/en/outdoor-recreation-and-wildlife/yukon-wildlife/muskox

Yukon Wildlife. (2024b). *Snowshoe Hare*. https://yukon.ca/en/outdoor-recreation-and-wildlife/yukon-wildlife/snowshoe-hare

Yukon Wildlife. (2024c). *Arctic Ground Squirrel*. https://yukon.ca/en/outdoor-recreation-and-wildlife/yukon-wildlife/arctic-ground-squirrel

Yukon Wildlife. (2025a). *Wood Bison*. https://yukon.ca/en/outdoor-recreation-and-wildlife/yukon-wildlife/wood-bison

Yukon Wildlife. (2025b). *Woodland Caribou*. https://yukon.ca/en/outdoor-recreation-and-wildlife/yukon-wildlife/woodland-caribou

Yukon Wildlife. (2025c). *Moose*. https://yukon.ca/en/outdoor-recreation-and-wildlife/yukon-wildlife/moose

Zazula, G. D., Froese, D. G., Elias, S. A., Kuzmina, S., La Farge, C., Reyes, A. V., Sanborn, P. T., Schweger, C. E., Scott Smith, C. A., & Mathewes, R. W. (2006a). Vegetation buried under Dawson tephra (25,300 14C years BP) and locally diverse late Pleistocene paleoenvironments of Goldbottom Creek, Yukon, Canada. *Palaeogeography, Palaeoclimatology, Palaeoecology*, *242*(3–4), 253–286. https://doi.org/10.1016/J.PALAEO.2006.06.005

Zazula, G. D., Telka, A. M., Harington, C. R., Schweger, C. E., & Mathewes, R. W. (2006b). New spruce (Picea spp.) macrofossils from Yukon Territory: Implications for late Pleistocene refugia in Eastern Beringia. *Arctic*, *59*(4), 391–400. https://doi.org/10.14430/arctic288

Zimov, S. A., Chuprynin, V. I., Oreshko, A. P., Chapin, F. S., Reynolds, J. F., & Chapin, M. C. (1995). Steppe-tundra transition: A herbivore-driven biome shift at the end of the Pleistocene. *American Naturalist*, *146*(4), 765–794. https://doi.org/10.1086/285824

Zimov, S. A., Zimov, N. S., Tikhonov, A. N., & Chapin, I. S. (2012). Mammoth steppe: a high-productivity phenomenon. *Quaternary Science Reviews*, *57*, 26–45. https://doi.org/10.1016/J.QUASCIREV.2012.10.005

Appendix A: Supplementary Figures

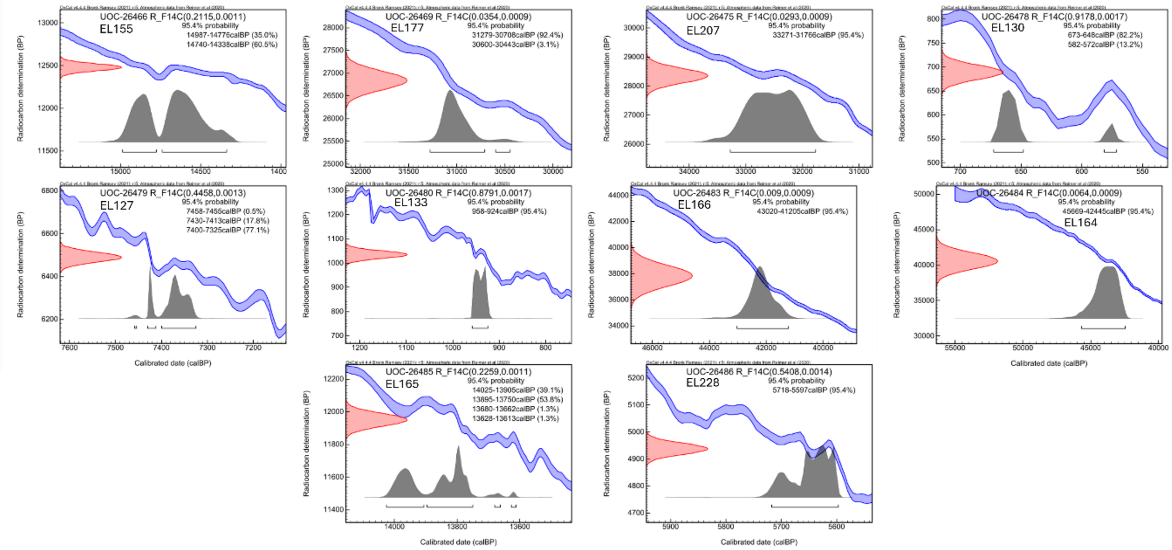

Figure 1. Radiocarbon calibration plots of samples that underwent radiocarbon dating in this thesis using OxCal v4.4 (Bronk Ramsey, 2009) depicting an age range (BP) with associated probability (95.4%).

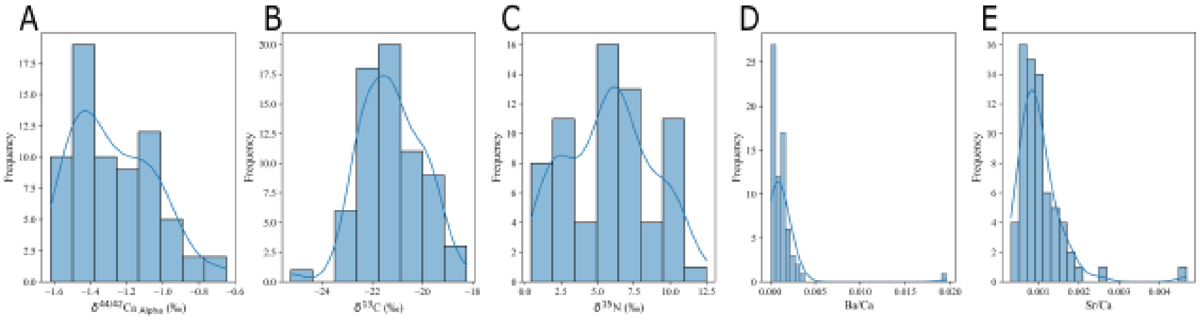

Figure 2. Histograms illustrating the distribution of: A) δ^{13}C (‰); B) δ^{15}N (‰); C) $\delta^{44/42}$Ca$_{\text{alpha}}$ (‰); D) Sr/Ca; and E) Ba/Ca to assess normality.

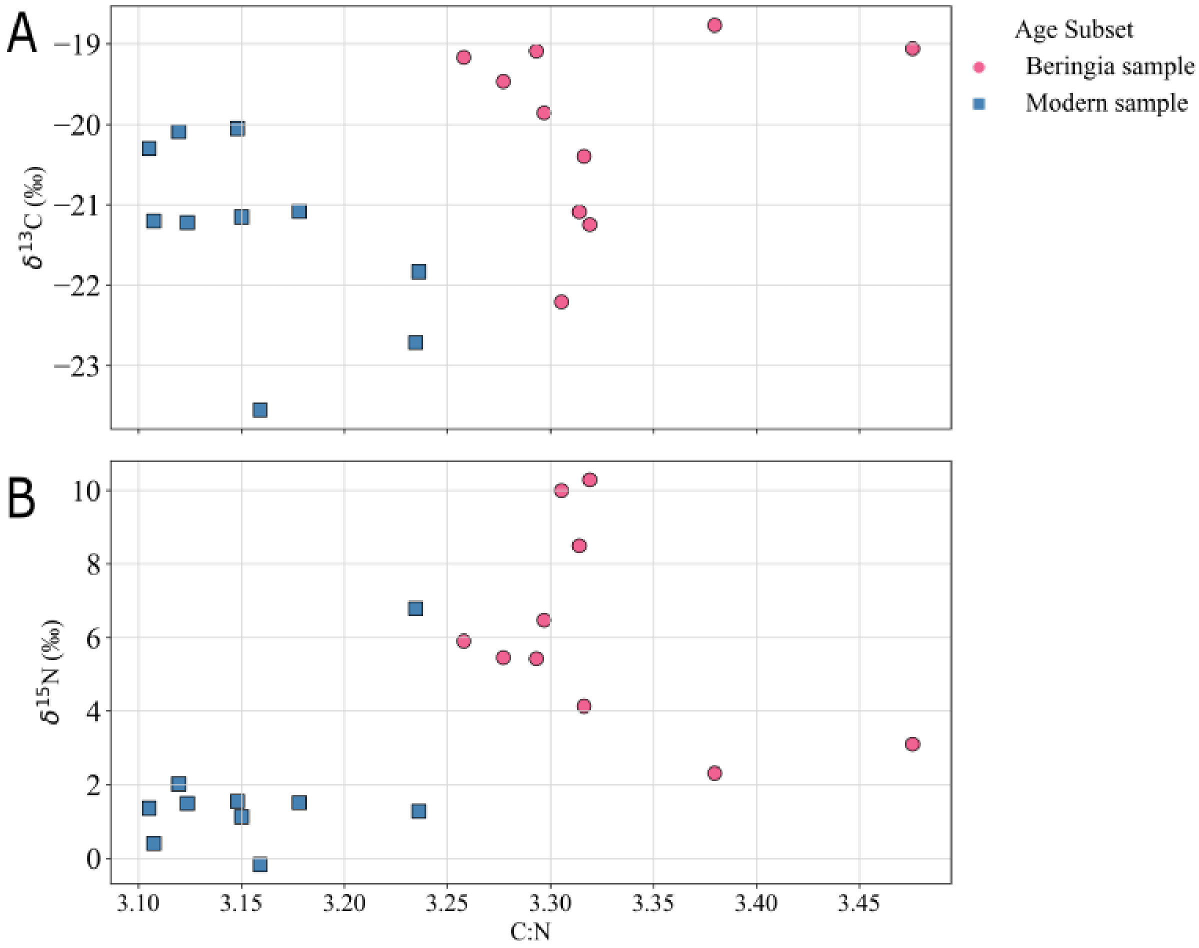

Figure 3. Plot of A) δ¹³C (‰); and B) δ¹⁵N (‰) versus atomic C:N ratio of modern (blue squares) and Beringian fossil (pink circles) samples. All samples fall within the accepted C:N range (2.9-3.6), indicating well preserved collagen.

Appendix B: Supplementary Tables

Table 1. Percent contributions and standard deviation of prey species sources to the diets of modern gray wolves [<11 ka BP], post-LGM gray wolf [11-19 ka BP], LGM gray wolf [19-26 ka BP], and D) Pre-LGM gray wolves [>26ka BP], from traditional proxy ($\delta^{13}C$ [‰] and $\delta^{15}N$ [‰]) BSIMMs including compiled published prey source data* from uninformative and informed mixing models. Priors used in the informed mixing models listed and calculated based on comparison of the average mass of each prey species to the target prey mass of a wolf pack.

**Note: References for published herbivore carbon and nitrogen stable isotope values from listed in Appendix D Table 4.*

Age subset	Prey species	Mean dietary contribution (%); uninformed model	Standard deviation (%); uninformed model	Prior; informed model	Mean dietary contribution (%); informed model	Standard deviation (%); informed model
Modern gray wolves	Bison	8.9	7.6	0.387	3.8	5.3
	Caribou	4.7	4.4	2.224	10.5	6.5
	Dall Sheep	7.9	7.9	1.006	8.6	8.7
	Arctic ground squirrel	17.6	15.2	0.730	12.4	13.4
	Snowshoe hare	52.2	20.5	0.732	56.9	19.4
	Moose	8.8	8.5	0.921	7.8	7.8
Post-LGM gray wolves	Arctic ground squirrel	22	16	0.718	20.7	16.5
	Dall Sheep	16.1	13.8	0.991	18.6	15.4
	Snowshoe hare	21.9	14.6	0.720	22.7	16.7
	Caribou	14.8	10.9	2.190	28.3	13.1
	Bison	25	17.1	0.381	9.8	12.6
LGM gray wolves	Bison	32.8	21.3	0.249	5	11.5
	Woolly mammoth	24.3	18.7	0.021	0.4	3
	Horse	14.7	14.2	2.657	77.8	20.1
	Caribou	10.7	9.9	1.428	10	8.5
	Dall sheep	17.5	17.1	0.646	6.8	12
Pre-LGM gray wolves	Bison	8.2	7.8	0.177	1.3	3.1
	Horse	23	19.5	1.891	44.8	10.7
	Woolly mammoth	12.7	10.2	0.015	0	0
	Muskox	20.6	14.8	2.441	30.9	16.4
	Caribou	14.1	12.9	1.017	16.1	11.8
	Dall sheep	21.3	18.8	0.460	6.9	10.7

Table 2. Percent contributions and standard deviation of prey species sources to the diets of modern gray wolves [<11 ka BP], post-LGM gray wolf [11-19 ka BP], LGM gray wolf [19-26 ka BP], and D) Pre-LGM gray wolves [>26ka BP], from traditional proxy ($\delta^{13}C$ [‰] and $\delta^{15}N$ [‰]) BSIMMs from uninformative and informed mixing models. Priors used in the informed mixing models listed and calculated based on comparison of the average mass of each prey species to the target prey mass of a wolf pack.

Age subset	**Prey species**	**Mean dietary contribution (%); uninformed model**	**Standard deviation (%); uninformed model**	**Prior; informed model**	**Mean dietary contribution (%); informed model**	**Standard deviation (%); informed model**
Modern gray wolves	Caribou	5.8	5.7	1.981	12.1	8.2
	Dall sheep	6.3	5.9	0.896	5.3	5.4
	Arctic ground squirrel	17.9	15.8	0.650	13.1	14.7
	Snowshoe hare	60.9	19.6	0.652	62.2	19.2
	Moose	9.1	8.3	0.821	7.3	7.8
Pre-LGM gray wolves	Bison	6.1	7.3	0.177	1	2.3
	Horse	58.5	22.8	1.891	69.4	13.4
	Woolly mammoth	6.8	7.9	0.015	0.1	0.7
	Muskox	17.2	13.7	2.441	22.9	11.9
	Caribou	5.8	6.8	1.017	4.6	5
	Dall sheep	5.5	6.9	0.460	2.1	3.1

Table 3. Percent contributions and standard deviation of prey species sources to the diets of modern gray wolves [<11 ka BP], post-LGM gray wolf [11-19 ka BP], LGM gray wolf [19-26 ka BP], and D) Pre-LGM gray wolves [>26ka BP], from traditional and novel proxies ($\delta^{13}C$ [‰], $\delta^{15}N$ [‰], and $\delta^{44/42}Ca_{Alpha}$ [‰]) BSIMMs from uninformative and informed mixing models. Priors used in the informed mixing models listed and calculated based on comparison of the average mass of each prey species to the target prey mass of a wolf pack.

Age subset	**Prey species**	**Mean dietary contribution (%); uninformed model**	**Standard deviation (%); uninformed model**	**Prior; informed model**	**Mean dietary contribution (%); informed model**	**Standard deviation (%); informed model**
Modern gray wolves	Caribou	3.7	3.2	1.981	6.7	4.1
	Dall sheep	4	3.7	0.896	3.5	3.7
	Arctic ground squirrel	26.5	21.4	0.650	26.6	25.6
	Snowshoe hare	59.8	22.6	0.652	58.2	26.9
	Moose	6.1	5.4	0.821	5	4.8
Pre-LGM gray wolves	Bison	3.4	3.3	0.177	0.7	1.5
	Horse	82.8	7.5	1.891	83.5	8.1
	Woolly mammoth	3.1	2.9	0.015	0	0.1
	Muskox	4.8	5.1	2.441	11.7	7.6
	Caribou	2.5	2.3	1.017	2.4	2.3
	Dall sheep	3.4	3.5	0.460	1.6	2.4

Appendix C: Data Availability Tables

Table 1. Specimen metadata compiling including sample ID, CMN specimen ID, 14C ID, species, sample type, Age subset, Feeding behaviour, Gut physiology, region, latitude and longitude, Enamel substrate, Bone substrate, and carbon, nitrogen and radiocarbon reference.

Sample ID	Specimen ID	14C ID	Species	Sample type	Age subset	Feeding behaviour	Gut physiology	Region	Latitude	Longitude	Enamel substrate	Bone substrate	δ13C,δ15N, 14C Reference
EL110	CMNMA 36094	N/A	Rangifer tarandus	Modern sample	Modern	Mixed	Polygastric	Old Crow	67.6	-139.8	m3	N/A	Landry et al. (2021)
EL112	CMNMA 36095	N/A	Rangifer tarandus	Modern sample	Modern	Mixed	Polygastric	Old Crow	67.6	-139.8	m3	N/A	Landry et al. (2021)
EL115	CMNMA 33487	N/A	Rangifer tarandus	Modern sample	Modern	Mixed	Polygastric	Old Crow	67.6	-139.8	m3	N/A	Landry et al. (2021)
EL118	CMNMA 31747	N/A	Rangifer tarandus	Modern sample	Modern	Mixed	Polygastric	Old Crow	61.1	-128.5	m3	N/A	Landry et al. (2021)
EL122	CMNMA 36278	N/A	Rangifer tarandus	Modern sample	Modern	Mixed	Polygastric	Old Crow	60.1	-133.4	M3	N/A	Landry et al. (2021)
EL125	CMNFV 33764	UOC-26473	Rangifer tarandus	Beringia sample	Pre-LGM	Mixed	Polygastric	Dawson	64.1	-139.4	m3	Jaw bone	this study
EL127L	CMNFV 51488	UOC-26470	Rangifer tarandus	Beringia sample	Modern	Mixed	Polygastric	Old Crow	68.4	-141.4	m3	Jaw bone	this study
EL130	CMNFV 51492	UOC-26469	Rangifer tarandus	Beringia sample	Modern	Mixed	Polygastric	Old Crow	68.4	-141.4	m3	Jaw bone	this study
EL133L	CMNFV 51480	UOC-26471	Rangifer tarandus	Beringia sample	Modern	Mixed	Polygastric	Old Crow	68.4	-141.4	m3	Jaw bone	this study
EL136	CMNMA 31759	N/A	Canis lupus	Modern sample	Modern	Carnivore	Monogastric	Dawson	63.4	-139.5	m1	N/A	Landry et al. (2021)
EL137	CMNMA 33453	N/A	Canis lupus	Modern sample	Modern	Carnivore	Monogastric	Dawson	62.6	-140.0	m1	N/A	Landry et al. (2021)
EL138	CMNMA 33455	N/A	Canis lupus	Modern sample	Modern	Carnivore	Monogastric	Dawson	62.6	-140.0	m1	N/A	Landry et al. (2021)
EL139	CMNMA 31760	N/A	Canis lupus	Modern sample	Modern	Carnivore	Monogastric	Dawson	63.4	-139.5	m1	N/A	Landry et al. (2021)
EL140	CMNMA 33456	N/A	Canis lupus	Modern sample	Modern	Carnivore	Monogastric	Dawson	63.7	-135.4	m1	N/A	Landry et al. (2021)
EL141	CMNMA 36162	N/A	Canis lupus	Modern sample	Modern	Carnivore	Monogastric	Old Crow	67.3	137.8	m1	N/A	Landry et al. (2021)
EL142	CMNMA 33454	N/A	Canis lupus	Modern sample	Modern	Carnivore	Monogastric	Dawson	62.6	-140.0	m1	N/A	Landry et al. (2021)
EL143	CMNMA 30923	N/A	Canis lupus	Modern sample	Modern	Carnivore	Monogastric	Dawson	63.7	-135.4	m1	N/A	Landry et al. (2021)
EL144	CMNMA 30924	N/A	Canis lupus	Modern sample	Modern	Carnivore	Monogastric	Dawson	63.7	-135.4	m1	N/A	Landry et al. (2021)

Sample ID	Specimen ID	14C ID	Species	Sample type	Age subset	Feeding behaviour	Gut physiology	Region	Latitude	Longitude	Enamel substrate	Bone substrate	δ13C,δ15N, 14C Reference
EL145	CMNMA 30925	N/A	Canis lupus	Modern sample	Modern	Carnivore	Monogastric	Dawson	63.7	-135.4	m1	N/A	Landry et al. (2021)
EL146	CMNFV 48450	N/A	Canis lupus	Beringia sample	Pre-LGM	Carnivore	Monogastric	Old Crow	68.4	-141.4	M1	N/A	Landry et al. (2021)
EL147	CMNFV 48020	N/A	Canis lupus	Beringia sample	Pre-LGM	Carnivore	Monogastric	Old Crow	68.4	-141.4	m1	N/A	Landry et al. (2021)
EL148	CMNFV 29050	UOC-26474	Rangifer tarandus	Beringia sample	Pre-LGM	Mixed	Polygastric	Dawson	64.1	-139.4	M3	Jaw bone	this study
EL149	CMNMA 31751	N/A	Canis lupus	Modern sample	Modern	Carnivore	Monogastric	Dawson	63.4	-139.5	m1	N/A	Landry et al. (2021)
EL150	CMNMA 34691	N/A	Canis lupus	Modern sample	Modern	Carnivore	Monogastric	Y.T.-B.C.	60.0	-133.9	m1	N/A	Landry et al. (2021)
EL151	CMNMA 33457	N/A	Canis lupus	Modern sample	Modern	Carnivore	Monogastric	Dawson	62.6	-140.0	m1	N/A	Landry et al. (2021)
EL152	CMNMA 14106	N/A	Canis lupus	Modern sample	Modern	Carnivore	Monogastric	Dawson	63.3	-138.3	m1	N/A	Landry et al. (2021)
EL153	CMNMA 18133	N/A	Canis lupus	Modern sample	Modern	Carnivore	Monogastric	Ross River	62.0	-132.4	m1	N/A	Landry et al. (2021)
EL154	CMNFV 13524	UOC-26464	Bison priscus, bison crassicornis	Beringia sample	Pre-LGM	Grazer	Polygastric	Dawson	63.7	-138.5	m3	Jaw bone	this study
EL155	CMNFV 16523	UOC-26466	Bison sp.	Beringia sample	Post-LGM	Grazer	Polygastric	Old Crow	68.4	-141.4	m3	Jaw bone	this study
EL156	CMNFV 15241	UOC-26468	Bison sp.	Beringia sample	Pre-LGM	Grazer	Polygastric	Old Crow	68.4	-141.4	m3	Jaw bone	this study
EL157	CMNFV 35552	UOC-26467	Bison sp.	Beringia sample	Pre-LGM	Grazer	Polygastric	Dawson	64.0	-139.2	m3	Jaw bone	this study
EL158	CMNFV 34651	UOC-26465	Bison sp.	Beringia sample	Pre-LGM	Grazer	Polygastric	Dawson	63.7	-138.5	m3	Jaw bone	this study
EL159	CMNFV 48454	N/A	Canis lupus	Beringia sample	Pre-LGM	Carnivore	Monogastric	Old Crow	68.4	-141.4	p4	N/A	Landry et al. (2021)
EL160	CMNFV 48432	N/A	Canis lupus	Beringia sample	Pre-LGM	Carnivore	Monogastric	Old Crow	68.4	-141.4	m1	N/A	Landry et al. (2021)
EL161	CMNFV 28866	N/A	Canis lupus	Beringia sample	Pre-LGM	Carnivore	Monogastric	Old Crow	68.4	-141.4	m1	N/A	Landry et al. (2021)
EL162	CMNFV 25954	N/A	Canis lupus	Beringia sample	Pre-LGM	Carnivore	Monogastric	Dawson	64.0	-139.2	m1	N/A	Landry et al. (2021)
EL163	CMNFV 48614	N/A	Canis lupus	Beringia sample	Pre-LGM	Carnivore	Monogastric	Old Crow	68.4	-141.4	m1	N/A	Landry et al. (2021)
EL164	CMNFV 18716	UOC-26476	Canis lupus	Beringia sample	Pre-LGM	Carnivore	Monogastric	Old Crow	68.4	-141.4	p4	Jaw bone	this study

Sample ID	Specimen ID	14C ID	Species	Sample type	Age subset	Feeding behaviour	Gut physiology	Region	Latitude	Longitude	Enamel substrate	Bone substrate	δ13C,δ15N, 14C Reference
EL165	CMNFV 27197	UOC-26477	Canis lupus	Beringia sample	Post-LGM	Carnivore	Monogastric	Old Crow	68.4	-141.4	p4	Jaw bone	this study
EL166	CMNFV 24902	UOC-26475	Canis lupus	Beringia sample	Pre-LGM	Carnivore	Monogastric	Old Crow	68.4	-141.4	p4	Jaw bone	this study
EL176	CMNFV 22509	UOC-26467	Ovibos sp.	Beringia sample	Pre-LGM	Grazer	Polygastric	Old Crow	68.4	-141.4	m3	Jaw bone	this study
EL177	CMNFV 35265	UOC-26464	Ovis dalli	Beringia sample	Pre-LGM	Grazer	Polygastric	Dawson	64.0	-139.2	m3	Jaw bone	this study
EL178	CMNFV 33762	UOC-26466	Ovis dalli	Beringia sample	Pre-LGM	Grazer	Polygastric	Dawson	64.0	-139.2	m3	Jaw bone	this study
EL179	CMNFV 17703	UOC-26468	Ovis dalli	Beringia sample	Pre-LGM	Grazer	Polygastric	Dawson	65.6	-138.3	m3	Jaw bone	this study
EL180	CMNMA 29419	N/A	Lepus americanus	Modern sample	Modern	Grazer	Monogastric	Dawson	64.5	-138.2	Bone, vertabrae	Vertabrae	this study
EL183	CMNMA 33702	N/A	Lepus americanus	Modern sample	Modern	Grazer	Monogastric	Old Crow	67.8	-139.7	Bone, vertabrae	Vertabrae	this study
EL185	CMNMA33732	N/A	Urocitellus parryii	Modern sample	Modern	Mixed	Monogastric	Old Crow	67.8	-139.8	Bone, femer	Femer	this study
EL187	CMNMA33746	N/A	Urocitellus parryii	Modern sample	Modern	Mixed	Monogastric	Whitehorse	64.6	-138.3	Bone, femer	Femer	this study
EL190	CMNMA29841	N/A	Ovis dalli	Modern sample	Modern	Grazer	Polygastric	Dawson	64.6	-138.2	m3	Jaw bone	this study
EL191	CMNMA30626	N/A	Ovis dalli	Modern sample	Modern	Grazer	Polygastric	Y.T.-B.C.	67.6	-136.4	m3	Jaw bone	this study
EL192	CMNMA 26303	N/A	Alces alces	Modern sample	Modern	Browser	Polygastric	NWT	67.6	-135.3	m3	Jaw bone	this study
EL195	CMNMA 29838	N/A	Alces alces	Modern sample	Modern	Browser	Polygastric	Dawson	64.6	-138.4	m3	Jaw bone	this study
EL196	CMNMA 29839	N/A	Alces alces	Modern sample	Modern	Browser	Polygastric	Dawson	64.8	-138.3	m3	Jaw bone	this study
EL200	CMNMA 29837	N/A	Alces alces	Modern sample	Modern	Browser	Polygastric	Dawson	64.6	-138.4	m3	Jaw bone	this study
EL201	CMNMA 30623	N/A	Alces alces	Modern sample	Modern	Browser	Polygastric	Ivvaik National Park (North Y.T.)	68.8	-140.2	m3	Jaw bone	this study
EL202	CMNFV 34743	UOC-26465	Mammuthus primigenius	Beringia sample	Pre-LGM	Grazer	Monogastric	Dawson	64.1	-139.4	M3	Dentin, M3	this study
EL205	CMNFV 57180	UOC-26484	Mammuthus primigenius	Beringia sample	Pre-LGM	Grazer	Monogastric	Old Crow	68.4	-141.4	M3	Dentin, M3	this study
EL207	CMNFV 49389	UOC-26485	Mammuthus primigenius	Beringia sample	Pre-LGM	Grazer	Monogastric	Old Crow	68.4	-141.4	M3	Dentin, M3	this study

Sample ID	**Specimen ID**	**14C ID**	**Species**	**Sample type**	**Age subset**	**Feeding behaviour**	**Gut physiology**	**Region**	**Latitude**	**Longitude**	**Enamel substrate**	**Bone substrate**	**δ13C,δ15N, 14C Reference**
EL208	CMNFV 34742	UOC-26483	Mammuthus primigenius	Beringia sample	Pre-LGM	Grazer	Monogastric	Dawson	64.1	-139.4	M3	Dentin, M3	this study
EL210	CMNFV 43088	UOC-26472	Mammuthus primigenius	Beringia sample	Pre-LGM	Grazer	Monogastric	Old Crow	68.4	-141.4	M3	Dentin, M3	this study
EL220	CMNFV 35964	N/A	Canis lupus	Beringia sample	Pre-LGM	Carnivore	Monogastric	Dawson	64.0	-139.2	m1	N/A	Landry et al. (2021)
EL223	CMNFV 43051	N/A	Canis lupus	Beringia sample	Pre-LGM	Carnivore	Monogastric	Old Crow	68.4	-141.4	P4	N/A	Landry et al. (2021)
EL224	CMNFV 9929	N/A	Canis lupus	Beringia sample	LGM	Carnivore	Monogastric	Dawson	64.0	-139.2	P4	N/A	Landry et al. (2021)
EL226	CMNFV 24939	N/A	Canis lupus	Beringia sample	Pre-LGM	Carnivore	Monogastric	Old Crow	68.4	-141.4	M1	N/A	Landry et al. (2021)
EL228	CMNFV18597	UOC-26486	Lepus americanus	Beringia sample	Modern	Grazer	Monogastric	Old Crow	68.4	-141.4	Bone	Bone	this study
EL229	CMNFV 44469	N/A	Equus sp.	Beringia sample	Pre-LGM	Grazer	Monogastric	Dawson	64.1	-139.4	P4	N/A	Landry et al. (in prep)
EL230	CMNFV 7748	N/A	Equus sp.	Beringia sample	LGM	Grazer	Monogastric	Dawson	64.1	-139.4	P4	N/A	Landry et al. (in prep)
EL231	CMNFV 46520	N/A	Equus sp.	Beringia sample	LGM	Grazer	Monogastric	Dawson	64.1	-139.4	P4	N/A	Landry et al. (in prep)
EL232	CMNFV 23670	N/A	Equus sp.	Beringia sample	Pre-LGM	Grazer	Monogastric	Old Crow	68.4	-141.4	P4	N/A	Landry et al. (in prep)
EL233	CMNFV 20139	N/A	Equus sp.	Beringia sample	Pre-LGM	Grazer	Monogastric	Old Crow	68.4	-141.4	P4	N/A	Landry et al. (in prep)
EL234	CMNFV 31317	UOC-26487	Urocitellus parryii	Beringia sample	Pre-LGM	Mixed	Monogastric	Old Crow	68.4	-141.4	Bone	Bone	this study

Table 2. Radiocarbon, stable isotope and elemental data compiling including sample ID, CMN specimen ID, 14C ID, C:N, 14C age (radiocarbon age [BP]), 14C age uncertainty (radiocarbon age uncertainty [BP]), Cal (Calibrated radiocarbon age [BP]), Median cal [Median calibrated radiocarbon age [BP]), δ^{13}C (‰)*, δ^{15}N (‰), $\delta^{44/42}\mathrm{Ca}_{\mathrm{Alpha}}$ (‰), Analytical precision for calcium isotopes (2SE $\delta^{44/42}\mathrm{Ca}_{\mathrm{Alpha}}$ [‰]), Sr/Ca, Ba/Ca, and Ca/P.

*Note: δ^{13}C values have undergone atmospheric CO_2 correction following the protocols in Long et al., 2005

Sample ID	**Specimen ID**	**C:N**	**14C age (BP)**	**14C age uncertainty (BP)**	**Cal (BP)**	**Median cal (BP)**	**δ13C (‰)***	**δ15N (‰)**	**δ44/42Ca Alpha (‰)**	**2SE δ44/42Ca Alpha**	**Sr/Ca**	**Ba/Ca**	**Ca/P**
EL110	CMNMA 36094	N/A	N/A	N/A	N/A	N/A	-21.8	2.3	-1.282	0.049	6.78E-04	1.38E-03	1.620
EL112	CMNMA 36095	N/A	N/A	N/A	N/A	N/A	-20.2	2.8	-1.303	0.035	6.22E-04	1.15E-03	1.649
EL115	CMNMA 33487	N/A	N/A	N/A	N/A	N/A	-21.0	4.3	-1.371	0.050	4.78E-04	4.15E-04	1.661
EL118	CMNMA 31747	N/A	N/A	N/A	N/A	N/A	-20.1	4.3	-1.388	0.087	1.12E-03	1.05E-03	1.642
EL122	CMNMA 36278	N/A	N/A	N/A	N/A	N/A	-19.9	2.9	-1.255	0.064	1.31E-03	1.44E-03	1.613
EL125	CMNFV 33764	3.33	>42400	N/A	N/A	N/A	-18.4	2.2	-1.462	0.128	8.96E-04	7.13E-04	1.417
EL127L	CMNFV 51488	3.33	6490	25	7458-7325	7391.5	-17.8	2.04	-1.406	0.072	6.52E-04	1.88E-03	1.466
EL130	CMNFV 51492	3.37	690	20	673-572	622.5	-19.1	2.47	-1.390	0.058	6.45E-04	1.34E-03	1.429
EL133L	CMNFV 51480	3.38	1040	20	958-924	941	-18.9	2.31	-1.446	0.063	9.62E-04	2.21E-03	1.661
EL136	CMNMA 31759	N/A	N/A	N/A	N/A	N/A	-22.1	6.5	-1.461	0.071	7.41E-04	2.11E-04	1.686
EL137	CMNMA 33453	N/A	N/A	N/A	N/A	N/A	-22.6	5.8	-1.360	0.093	6.23E-04	2.08E-04	1.641

Sample ID	Specimen ID	C:N	14C age (BP)	14C age uncertainty (BP)	Cal (BP)	Median cal (BP)	δ13C (‰)*	δ15N (‰)	δ44/42Ca Alpha (‰)	2SE δ44/42Ca Alpha	Sr/Ca	Ba/Ca	Ca/P
EL138	CMNMA 33455	N/A	N/A	N/A	N/A	N/A	-22.6	5.6	-1.451	0.079	6.03E-04	1.57E-04	1.609
EL139	CMNMA 31760	N/A	N/A	N/A	N/A	N/A	-21.1	6.4	-1.526	0.075	8.37E-04	1.81E-04	1.588
EL140	CMNMA 33456	N/A	N/A	N/A	N/A	N/A	-22.5	5.7	-1.576	0.045	5.45E-04	1.57E-04	1.629
EL141	CMNMA 36162	N/A	N/A	N/A	N/A	N/A	-19.6	7.5	-1.579	0.024	4.43E-04	2.12E-04	1.627
EL142	CMNMA 33454	N/A	N/A	N/A	N/A	N/A	-22.3	5.7	-1.490	0.055	5.60E-04	1.48E-04	1.689
EL143	CMNMA 30923	N/A	N/A	N/A	N/A	N/A	-22.3	7.2	-1.489	0.059	8.96E-04	3.38E-04	1.669
EL144	CMNMA 30924	N/A	N/A	N/A	N/A	N/A	-19.1	7.7	-1.416	0.093	8.62E-04	3.10E-04	1.644
EL145	CMNMA 30925	N/A	N/A	N/A	N/A	N/A	-21.0	6.4	-1.337	0.045	8.01E-04	1.99E-04	1.622
EL146	CMNFV 48450	N/A	see Landry et al. (2021)	see Landry et al. (2021)	see Landry et al. (2021)	39190	-19.0	10.3	-1.464	0.074	7.06E-04	1.40E-03	1.302
EL147	CMNFV 48020	N/A	see Landry et al. (2021)	see Landry et al. (2021)	see Landry et al. (2021)	39190	N/A	N/A	-1.473	0.059	8.02E-04	2.46E-03	1.277
EL148	CMNFV 29050	3.48	>42400	N/A	N/A	N/A	-19.2	3.1	-1.383	0.039	1.06E-03	1.54E-03	1.592
EL149	CMNMA 31751	N/A	N/A	N/A	N/A	N/A	-25.3	5.8	-1.565	0.067	9.99E-04	4.79E-04	1.637

Sample ID	**Specimen ID**	**C:N**	**14C age (BP)**	**14C age uncertainty (BP)**	**Cal (BP)**	**Median cal (BP)**	**δ13C (‰)***	**δ15N (‰)**	**δ44/42Ca Alpha (‰)**	**2SE δ44/42Ca Alpha**	**Sr/Ca**	**Ba/Ca**	**Ca/P**
EL150	CMNMA 34691	N/A	N/A	N/A	N/A	N/A	-22.2	6.6	-1.446	0.043	1.11E-03	1.95E-04	1.652
EL151	CMNMA 33457	N/A	N/A	N/A	N/A	N/A	-22.6	5.5	-1.485	0.053	6.53E-04	1.36E-04	1.657
EL152	CMNMA 14106	N/A	N/A	N/A	N/A	N/A	-20.2	8.1	-1.608	0.050	6.51E-04	1.94E-04	1.613
EL153	CMNMA 18133	N/A	N/A	N/A	N/A	N/A	-22.4	7	-1.533		4.63E-04	2.97E-04	1.644
EL154	CMNFV 13524	3.26	>42400	N/A	N/A	N/A	-19.3	5.9	-1.000	0.088	1.09E-03	8.75E-04	1.655
EL155	CMNFV 16523	3.30	12500	45	14987-14338	14662.5	-20.6	2.52	-1.101	0.107	8.30E-04	2.43E-03	1.408
EL156	CMNFV 15241	3.31	>42400	N/A	N/A	N/A	-20.4	5.27	-1.114	0.059	7.32E-04	2.60E-03	2.348
EL157	CMNFV 35552	3.31	>42400	N/A	N/A	N/A	-20.2	4.23	-1.139	0.061	6.82E-04	1.25E-03	1.520
EL158	CMNFV 34651	3.28	>42400	N/A	N/A	N/A	-19.6	5.45	-1.132	0.031	9.42E-04	1.36E-03	1.504
EL159	CMNFV 48454	N/A	see Landry et al. (2021)	see Landry et al. (2021)	see Landry et al. (2021)	44500	-21.1	5.8	-1.619	0.044	8.83E-04	2.21E-03	1.325
EL160	CMNFV 48432	N/A	see Landry et al. (2021)	see Landry et al. (2021)	see Landry et al. (2021)	39190	-22.4	9.8	-1.286	0.047	9.68E-04	1.27E-03	1.509

Sample ID	Specimen ID	C:N	14C age (BP)	14C age uncertainty (BP)	Cal (BP)	Median cal (BP)	δ13C (‰)*	δ15N (‰)	δ44/42Ca Alpha (‰)	2SE δ44/42Ca Alpha	Sr/Ca	Ba/Ca	Ca/P
EL161	CMNFV 28866	N/A	see Landry et al. (2021)	see Landry et al. (2021)	see Landry et al. (2021)	44500	-21.6	9.9	-1.513	0.038	7.82E-04	1.48E-03	1.445
EL162	CMNFV 25954	N/A	>49 900	N/A	N/A	N/A	-20.6	9.7	-1.281	0.097	1.82E-03	8.88E-04	1.337
EL163	CMNFV 48614	N/A	see Landry et al. (2021)	see Landry et al. (2021)	see Landry et al. (2021)	39190	-21.8	7.4	-1.543	0.089	1.11E-03	1.43E-03	1.376
EL164	CMNFV 18716	3.35	40600	1200	45669-42445	44057	-20.6	10.97	-1.486	0.072	7.81E-04	8.48E-04	1.499
EL165	CMNFV 27197	3.30	12000	40	14025-13613	13819	-19.9	6.47	-1.381	0.080	7.13E-04	6.70E-04	1.469
EL166	CMNFV 24902	3.43	37900	820	43020-41205	42112.5	-20.6	10.42	-1.404	0.076	9.75E-04	1.12E-03	1.384
EL176	CMNFV 22509	3.32	>42400		N/A	N/A	-20.5	4.13	-1.405	0.048	7.23E-04	1.35E-03	1.512
EL177	CMNFV 35265	3.29	26900	210	31279-30443	30861	-19.2	5.42	-1.151	0.079	1.48E-03	1.60E-03	1.334
EL178	CMNFV 33762	3.29	>42400	N/A	N/A	N/A	-19.0	6.87	-0.977	0.068	1.67E-03	2.00E-03	1.634
EL179	CMNFV 17703	3.36	>42400	N/A	N/A	N/A	-20.1	3.43	-1.029	0.080	1.99E-03	1.42E-03	1.347
EL180	CMNMA 29419	N/A	N/A	N/A	N/A	N/A	N/A	N/A	-1.113	0.085	2.50E-03	1.87E-03	1.630
EL183	CMNMA 33702	3.16	N/A	N/A	N/A	N/A	-23.6	-0.17	-1.046	0.050	1.03E-03	1.18E-03	1.814

Sample ID	Specimen ID	C:N	14C age (BP)	14C age uncertainty (BP)	Cal (BP)	Median cal (BP)	δ13C (‰)*	δ15N (‰)	δ44/42Ca Alpha (‰)	2SE δ44/42Ca Alpha	Sr/Ca	Ba/Ca	Ca/P
EL185	CMNMA 33732	3.23	N/A	N/A	N/A	N/A	-22.8	6.79	-0.856	0.048	5.78E-04	1.77E-04	1.728
EL187	CMNMA 33746	3.24	N/A	N/A	N/A	N/A	-21.9	1.28	-0.913	0.095	9.44E-04	2.47E-04	1.683
EL190	CMNMA 29841	3.15	N/A	N/A	N/A	N/A	-20.1	1.55	-1.209	0.036	1.11E-03	8.72E-04	1.688
EL191	CMNMA 30626	3.12	N/A	N/A	N/A	N/A	-20.2	2.02	-1.537	0.017	1.11E-03	1.71E-03	1.667
EL192	CMNMA 26303	3.12	N/A	N/A	N/A	N/A	-21.4	1.49	-1.189	0.094	1.21E-03	5.60E-04	1.724
EL195	CMNMA 29838	3.11	N/A	N/A	N/A	N/A	-21.3	0.41	-1.148	0.062	7.13E-04	1.62E-04	1.642
EL196	CMNMA 29839	3.11	N/A	N/A	N/A	N/A	-20.4	1.36	-1.069	0.006	3.21E-04	3.05E-04	1.626
EL200	CMNMA 29837	3.18	N/A	N/A	N/A	N/A	-21.2	1.51	-1.215	0.061	9.50E-04	4.57E-04	1.637
EL201	CMNMA 30623	3.15	N/A	N/A	N/A	N/A	-21.2	1.13	-1.061	0.058	5.57E-04	5.74E-05	1.685
EL202	CMNFV 34743	3.31	>42400	N/A	N/A	N/A	-21.2	8.49	-1.078	0.096	8.89E-04	3.07E-04	1.342
EL205	CMNFV 57180	3.36	>42400	N/A	N/A	N/A	-21.1	9.99	-1.014	0.082	1.17E-03	6.60E-04	1.279
EL207	CMNFV 49389	3.32	28400	260	33271-31766	32518.5	-21.4	10.28	-1.083	0.073	8.83E-04	3.07E-04	1.409

Sample ID	Specimen ID	C:N	14C age (BP)	14C age uncertainty (BP)	Cal (BP)	Median cal (BP)	δ13C (‰)*	δ15N (‰)	δ44/42Ca Alpha (‰)	2SE δ44/42Ca Alpha	Sr/Ca	Ba/Ca	Ca/P
EL208	CMNFV 34742	3.31	>42400	N/A	N/A	N/A	-20.9	8.08	-1.287	0.076	1.69E-03	1.61E-03	1.214
EL210	CMNFV 43088	3.31	>42400	N/A	N/A	N/A	-22.3	9.99	-1.208	0.092	1.53E-03	2.94E-03	1.493
EL220	CMNFV 35964	N/A	>49 900	N/A	N/A	N/A	-21.2	9.5	-1.240	0.106	9.45E-04	1.25E-03	1.997
EL223	CMNFV 43051	N/A	see Landry et al. (2021)	see Landry et al. (2021)	see Landry et al. (2021)	45400	-21.8	9.4	-1.271	0.101	1.32E-03	2.86E-03	1.631
EL224	CMNFV 9929	N/A	see Landry et al. (2021)	see Landry et al. (2021)	see Landry et al. (2021)	20910	-21.7	12.5	-1.025	0.040	1.74E-03	5.29E-04	1.506
EL226	CMNFV 24939	N/A	see Landry et al. (2021)	see Landry et al. (2021)	see Landry et al. (2021)	39190	-20.3	6.7	-1.371	0.090	9.95E-04	1.35E-03	1.481
EL228	CMNFV 18597	3.41	4940	25	5718-5597	5657.5	-23.0	1.77	-0.969	0.094	4.67E-03	1.96E-02	1.571
EL229	CMNFV 44469	N/A	28800	see Landry et al. (in prep)	32976	32976	-20.2	5.1	-0.862	0.063	1.45E-03	6.35E-04	1.484
EL230	CMNFV 7748	N/A	18228	see Landry et al. (in prep)	22188	22188	-21.0	6	-0.648	0.057	1.43E-03	1.02E-04	1.385
EL231	CMNFV 46520	N/A	20201	see Landry et al. (in prep)	24288	24288	-21.4	6.5	-0.701	0.067	1.18E-03	1.01E-03	1.441

Sample ID	Specimen ID	C:N	14C age (BP)	14C age uncertainty (BP)	Cal (BP)	Median cal (BP)	δ13C (‰)*	δ15N (‰)	δ44/42Ca Alpha (‰)	2SE δ44/42Ca Alpha	Sr/Ca	Ba/Ca	Ca/P
EL232	CMNFV 23670	N/A	37904	see Landry et al. (in prep)	42170	42170	-21.7	6.7	-0.929	0.027	1.55E-03	3.44E-03	1.399
EL233	CMNFV 20139	N/A	40425	see Landry et al. (in prep)	43792	43792	-21.1	5.5	-1.033	0.126	9.97E-04	1.11E-03	1.696
EL234	CMNFV 31317	3.41	>42400	1400	N/A	N/A	-21.2	2.5	-0.957	0.023	4.76E-03	2.63E-02	1.070

Table 3. REE data compiling including sample ID, CMN specimen ID, REE NASC normalized concentrations*, La/Sm, LA/Yb, and Europium concentration (ppm).

Sample ID	Specimen ID	Sample type	Region	La*	Ce*	Pr*	Nd*	Sm*	Eu*	Gd*	Tb*	Dy*	Ho*	Er*	Tm*	Yb*	Lu*	La/Sm	La/Yb	Eu (ppm)
EL110	CMNMA 36094	Modern sample	Old Crow	5.77E-03	3.42E-03	6.74E-03	3.67E-03	2.11E-02	6.58E-02	4.03E-03	6.27E-03	4.05E-03	4.71E-03	3.20E-03	5.80E-03	3.81E-03	1.99E-02	2.73E-01	1.51E+00	8.16E-02
EL112	CMNMA 36095	Modern sample	Old Crow	2.19E-03	9.74E-04	1.29E-03	1.74E-03	1.92E-02	5.46E-02	2.23E-03	3.04E-03	8.67E-04	1.06E-03	2.29E-03	2.47E-03	0.00E+00	1.12E-02	1.14E-01	N/A	6.77E-02
EL115	CMNMA 33487	Modern sample	Old Crow	1.99E-03	7.72E-04	1.86E-03	1.34E-03	1.01E-02	2.51E-02	1.46E-03	2.09E-03	1.36E-03	2.87E-03	1.13E-03	1.67E-03	7.37E-04	8.23E-03	1.97E-01	2.70E+00	3.12E-02

Sample ID	Specimen ID	Sample type	Region	La*	Ce*	Pr*	Nd*	Sm*	Eu*	Gd*	Tb*	Dy*	Ho*	Er*	Tm*	Yb*	Lu*	La/Sm	La/Yb	Eu (ppm)
EL118	CMNMA 31747	Modern sample	Old Crow	1.70E-03	7.82E-04	7.90E-04	2.35E-03	2.34E-02	7.67E-02	2.66E-03	2.37E-03	5.07E-04	1.35E-03	1.12E-03	1.95E-03	1.10E-03	5.44E-03	7.26E-02	1.55E+00	9.51E-02
EL122	CMNMA 36278	Modern sample	Old Crow	7.31E-04	3.05E-04	8.27E-04	1.96E-03	3.11E-02	9.35E-02	9.32E-04	2.19E-03	1.63E-04	2.45E-03	8.08E-04	2.90E-03	0.00E+00	5.26E-03	2.35E-02	N/A	1.16E-01
EL125	CMNFV 33764	Beringia sample	Dawson	2.06E-02	9.47E-03	2.11E-02	9.20E-03	2.25E-02	3.18E-02	3.16E-02	3.02E-02	2.22E-02	2.68E-02	1.76E-02	1.54E-02	1.62E-02	1.78E-02	9.17E-01	1.27E+00	3.95E-02
EL127L	CMNFV 51488	Beringia sample	Old Crow	9.04E-02	4.70E-02	1.05E-01	4.50E-02	1.20E-01	1.44E-01	1.70E-01	1.67E-01	1.07E-01	1.41E-01	9.24E-02	8.51E-02	7.09E-02	6.90E-02	7.55E-01	1.28E+00	1.79E-01
EL130	CMNFV 51492	Beringia sample	Old Crow	9.58E-02	6.18E-02	1.19E-01	6.60E-02	1.74E-01	2.11E-01	2.48E-01	2.25E-01	1.62E-01	1.86E-01	1.32E-01	1.18E-01	1.05E-01	1.09E-01	5.52E-01	9.16E-01	2.62E-01
EL133L	CMNFV 51480	Beringia sample	Old Crow	8.12E-02	4.21E-02	9.36E-02	4.20E-02	1.02E-01	1.33E-01	1.61E-01	1.48E-01	9.80E-02	1.29E-01	8.13E-02	7.42E-02	8.02E-02	6.99E-02	7.94E-01	1.01E+00	1.65E-01
EL136	CMNMA 31759	Modern sample	Dawson	9.56E-04	3.87E-04	5.11E-04	5.46E-04	5.21E-03	0.00E+00	3.31E-03	1.29E-02	6.55E-04	1.30E-03	1.35E-03	8.74E-04	2.48E-03	5.28E-03	1.84E-01	3.86E-01	0.00E+00
EL137	CMNMA 33453	Modern sample	Dawson	9.72E-04	3.04E-04	1.84E-03	5.61E-04	5.53E-03	1.34E-02	1.39E-03	6.45E-03	1.46E-03	4.95E-03	8.06E-04	1.07E-02	3.52E-04	5.24E-03	1.76E-01	2.76E+00	1.66E-02
EL138	CMNMA 33455	Modern sample	Dawson	7.54E-04	4.85E-04	4.95E-04	4.53E-04	4.15E-03	1.19E-02	2.72E-03	4.63E-03	4.76E-04	4.02E-03	5.24E-04	6.21E-03	6.86E-04	0.00E+00	1.82E-01	1.10E+00	1.47E-02
EL139	CMNMA 31760	Modern sample	Dawson	6.64E-04	5.13E-04	8.25E-04	7.75E-04	5.23E-03	2.20E-02	4.65E-04	3.23E-03	0.00E+00	1.68E-03	2.69E-04	1.45E-03	0.00E+00	0.00E+00	1.27E-01	N/A	2.72E-02

Sample ID	**Specimen ID**	**Sample type**	**Region**	**La***	**Ce***	**Pr***	**Nd***	**Sm***	**Eu***	**Gd***	**Tb***	**Dy***	**Ho***	**Er***	**Tm***	**Yb***	**Lu***	**La/Sm**	**La/Yb**	**Eu (ppm)**
EL140	CMNMA 33456	Modern sample	Dawson	1.47E-03	7.96E-04	1.61E-03	7.44E-04	4.99E-03	1.09E-02	1.96E-03	3.74E-03	7.62E-04	2.57E-03	2.52E-04	2.85E-03	6.60E-04	0.00E+00	2.95E-01	2.23E+00	1.35E-02
EL141	CMNMA 36162	Modern sample	Old Crow	5.36E-04	2.02E-04	3.08E-04	4.32E-04	4.72E-03	1.34E-02	4.51E-04	2.30E-03	0.00E+00	8.88E-04	2.61E-04	2.39E-03	0.00E+00	2.54E-03	1.14E-01	N/A	1.66E-02
EL142	CMNMA 33454	Modern sample	Dawson	3.13E-03	1.06E-03	1.81E-03	1.03E-03	4.69E-03	1.29E-02	1.14E-03	2.61E-03	9.60E-04	2.18E-03	2.64E-04	2.85E-04	3.46E-04	2.58E-03	6.68E-01	9.04E+00	1.61E-02
EL143	CMNMA 30923	Modern sample	Dawson	1.07E-04	4.67E-05	1.23E-04	4.89E-04	6.22E-03	2.20E-02	0.00E+00	3.69E-04	4.74E-04	7.41E-05	0.00E+00	4.22E-04	0.00E+00	0.00E+00	1.73E-02	N/A	2.73E-02
EL144	CMNMA 30924	Modern sample	Dawson	6.39E-04	2.16E-04	7.94E-04	5.22E-04	5.82E-03	2.18E-02	6.72E-04	1.19E-03	3.13E-04	1.10E-03	0.00E+00	1.39E-04	0.00E+00	7.58E-03	1.10E-01	N/A	2.71E-02
EL145	CMNMA 30925	Modern sample	Dawson	6.36E-04	2.61E-04	4.26E-04	3.53E-04	5.65E-03	1.42E-02	1.12E-03	4.55E-04	0.00E+00	2.93E-04	5.16E-04	0.00E+00	0.00E+00	2.52E-03	1.13E-01	N/A	1.75E-02
EL146	CMNFV 48450	Beringia sample	Old Crow	1.07E-01	6.62E-02	1.30E-01	7.82E-02	1.97E-01	2.38E-01	2.95E-01	2.58E-01	2.01E-01	2.29E-01	1.66E-01	1.51E-01	1.31E-01	1.31E-01	5.43E-01	8.16E-01	2.95E-01
EL147	CMNFV 48020	Beringia sample	Old Crow	1.20E-01	6.95E-02	1.41E-01	7.57E-02	1.82E-01	2.33E-01	2.54E-01	2.08E-01	1.44E-01	1.63E-01	1.09E-01	1.07E-01	8.54E-02	9.28E-02	6.57E-01	1.40E+00	2.89E-01
EL148	CMNFV 29050	Beringia sample	Dawson	2.69E-02	1.43E-02	2.54E-02	1.19E-02	3.03E-02	5.66E-02	3.97E-02	2.75E-02	2.03E-02	2.38E-02	1.75E-02	1.51E-02	1.45E-02	1.68E-02	8.88E-01	1.86E+00	7.02E-02
EL149	CMNMA 31751	Modern sample	Dawson	2.83E-02	1.64E-02	2.92E-02	1.62E-02	4.96E-02	7.06E-02	5.53E-02	5.22E-02	4.16E-02	4.73E-02	4.29E-02	3.62E-02	2.14E-02	1.87E-01	5.72E-01	1.32E+00	8.75E-02

Sample ID	**Specimen ID**	**Sample type**	**Region**	**La***	**Ce***	**Pr***	**Nd***	**Sm***	**Eu***	**Gd***	**Tb***	**Dy***	**Ho***	**Er***	**Tm***	**Yb***	**Lu***	**La/Sm**	**La/Yb**	**Eu (ppm)**
EL150	CMNMA 34691	Modern sample	Y.T.-B.C.	6.81E-03	2.98E-03	1.20E-02	2.68E-03	1.12E-02	2.20E-02	2.02E-02	1.46E-02	1.51E-02	9.57E-03	2.31E-02	1.59E-02	2.02E-02	1.04E-01	6.06E-01	3.38E-01	2.73E-02
EL151	CMNMA 33457	Modern sample	Dawson	8.81E-04	2.96E-04	1.48E-03	7.53E-04	3.44E-03	1.15E-02	1.81E-03	4.52E-03	1.58E-03	3.56E-03	2.61E-04	4.22E-03	1.03E-03	1.27E-02	2.56E-01	8.58E-01	1.43E-02
EL152	CMNMA 14106	Modern sample	Dawson	6.99E-03	4.49E-03	6.42E-03	4.21E-03	1.18E-02	2.07E-02	1.09E-02	1.02E-02	5.03E-03	9.36E-03	5.54E-03	9.08E-03	6.92E-03	3.68E-02	5.95E-01	1.01E+00	2.56E-02
EL153	CMNMA 18133	Modern sample	Ross River	1.18E-02	8.52E-03	1.58E-02	1.11E-02	3.01E-02	5.15E-02	2.98E-02	3.44E-02	2.26E-02	3.03E-02	1.83E-02	2.34E-02	2.79E-02	1.71E-01	3.93E-01	4.23E-01	6.39E-02
EL154	CMNFV 13524	Beringia sample	Dawson	5.88E-02	2.96E-02	5.56E-02	2.73E-02	6.32E-02	7.26E-02	1.01E-01	7.46E-02	6.11E-02	8.05E-02	6.11E-02	5.86E-02	6.71E-02	6.60E-02	9.29E-01	8.76E-01	9.00E-02
EL155	CMNFV 16523	Beringia sample	Old Crow	1.62E-02	9.20E-03	1.88E-02	9.51E-03	2.62E-02	3.20E-02	3.29E-02	2.64E-02	1.94E-02	2.17E-02	1.26E-02	1.46E-02	1.30E-02	2.48E-02	6.19E-01	1.24E+00	3.97E-02
EL156	CMNFV 15241	Beringia sample	Old Crow	1.93E-01	1.21E-01	2.54E-01	1.30E-01	3.40E-01	3.76E-01	4.70E-01	4.23E-01	3.03E-01	3.56E-01	2.38E-01	2.13E-01	1.98E-01	1.87E-01	5.68E-01	9.72E-01	4.66E-01
EL157	CMNFV 35552	Beringia sample	Dawson	1.30E-01	5.38E-02	1.16E-01	4.61E-02	1.01E-01	9.38E-02	1.43E-01	1.04E-01	6.96E-02	7.95E-02	5.72E-02	4.56E-02	4.78E-02	4.08E-02	1.29E+00	2.72E+00	1.16E-01
EL158	CMNFV 34651	Beringia sample	Dawson	2.35E-02	9.79E-03	2.25E-02	8.92E-03	2.00E-02	2.54E-02	2.98E-02	2.37E-02	1.70E-02	2.16E-02	1.67E-02	2.26E-02	2.13E-02	2.80E-02	1.17E+00	1.10E+00	3.15E-02
EL159	CMNFV 48454	Beringia sample	Old Crow	5.04E-02	2.82E-02	6.14E-02	3.13E-02	7.66E-02	1.18E-01	1.05E-01	8.88E-02	6.19E-02	7.59E-02	4.89E-02	4.70E-02	4.19E-02	3.29E-02	6.58E-01	1.20E+00	1.46E-01

Sample ID	**Specimen ID**	**Sample type**	**Region**	**La***	**Ce***	**Pr***	**Nd***	**Sm***	**Eu***	**Gd***	**Tb***	**Dy***	**Ho***	**Er***	**Tm***	**Yb***	**Lu***	**La/Sm**	**La/Yb**	**Eu (ppm)**
EL160	CMNFV48432	Beringia sample	Old Crow	1.06E-01	5.40E-02	1.17E-01	5.46E-02	1.32E-01	1.58E-01	1.96E-01	1.69E-01	1.13E-01	1.43E-01	9.27E-02	8.85E-02	7.79E-02	7.46E-02	8.06E-01	1.36E+00	1.96E-01
EL161	CMNFV28866	Beringia sample	Old Crow	5.68E-02	3.15E-02	6.73E-02	3.40E-02	8.67E-02	1.04E-01	1.12E-01	1.05E-01	6.88E-02	9.46E-02	6.10E-02	5.79E-02	4.92E-02	5.53E-02	6.55E-01	1.15E+00	1.28E-01
EL162	CMNFV25954	Beringia sample	Dawson	7.79E-02	4.11E-02	8.05E-02	3.62E-02	8.58E-02	1.03E-01	1.20E-01	1.07E-01	7.38E-02	9.97E-02	6.28E-02	5.67E-02	6.36E-02	5.34E-02	9.08E-01	1.22E+00	1.28E-01
EL163	CMNFV48614	Beringia sample	Old Crow	3.76E-02	1.84E-02	4.02E-02	1.82E-02	5.19E-02	7.79E-02	6.94E-02	6.18E-02	4.01E-02	5.57E-02	3.64E-02	2.94E-02	2.61E-02	2.65E-02	7.24E-01	1.44E+00	9.66E-02
EL164	CMNFV18716	Beringia sample	Old Crow	1.35E-01	7.20E-02	1.58E-01	7.46E-02	1.85E-01	1.93E-01	2.59E-01	2.27E-01	1.43E-01	1.79E-01	1.05E-01	1.04E-01	9.46E-02	7.92E-02	7.29E-01	1.42E+00	2.40E-01
EL165	CMNFV27197	Beringia sample	Old Crow	4.15E-03	2.06E-03	4.46E-03	2.13E-03	7.28E-03	1.96E-02	7.05E-03	5.47E-03	3.74E-03	6.56E-03	4.25E-03	4.40E-03	3.11E-03	4.22E-03	5.70E-01	1.33E+00	2.43E-02
EL166	CMNFV24902	Beringia sample	Old Crow	1.10E-01	6.25E-02	1.40E-01	6.86E-02	1.67E-01	1.91E-01	2.37E-01	2.25E-01	1.48E-01	1.90E-01	1.21E-01	9.79E-02	9.88E-02	8.39E-02	6.54E-01	1.11E+00	2.37E-01
EL176	CMNFV22509	Beringia sample	Old Crow	1.02E-01	5.02E-02	1.11E-01	4.91E-02	1.22E-01	1.44E-01	1.75E-01	1.46E-01	9.70E-02	1.25E-01	8.25E-02	6.59E-02	6.92E-02	6.67E-02	8.35E-01	1.47E+00	1.78E-01
EL177	CMNFV35265	Beringia sample	Dawson	2.24E-02	9.57E-03	2.04E-02	9.74E-03	2.57E-02	4.42E-02	2.36E-02	2.03E-02	1.26E-02	1.89E-02	1.07E-02	1.22E-02	6.94E-03	6.96E-03	8.73E-01	3.23E+00	5.48E-02
EL178	CMNFV33762	Beringia sample	Dawson	1.11E-01	5.12E-02	1.13E-01	4.94E-02	9.54E-02	1.03E-01	1.44E-01	1.21E-01	8.35E-02	1.08E-01	7.63E-02	7.23E-02	7.76E-02	6.91E-02	1.16E+00	1.43E+00	1.28E-01

Sample ID	**Specimen ID**	**Sample type**	**Region**	**La***	**Ce***	**Pr***	**Nd***	**Sm***	**Eu***	**Gd***	**Tb***	**Dy***	**Ho***	**Er***	**Tm***	**Yb***	**Lu***	**La/Sm**	**La/Yb**	**Eu (ppm)**
EL179	CMNFV17703	Beringia sample	Dawson	3.12E-02	8.54E-03	2.62E-02	1.17E-02	2.74E-02	4.69E-02	2.79E-02	4.59E-02	2.07E-02	4.40E-02	1.66E-02	3.01E-02	1.87E-02	3.21E-02	1.14E+00	1.67E+00	5.81E-02
EL180	CMNMA29419	Modern sample	Dawson	1.68E-03	5.81E-04	1.45E-03	1.72E-03	2.61E-02	8.10E-02	1.87E-03	1.40E-03	7.65E-04	1.02E-03	7.22E-04	2.72E-03	0.00E+00	5.28E-03	6.42E-02	N/A	1.00E-01
EL183	CMNMA33702	Modern sample	Old Crow	3.36E-03	1.79E-03	3.95E-03	2.55E-03	1.57E-02	4.11E-02	4.31E-03	2.95E-03	1.61E-03	1.67E-03	2.31E-03	1.92E-03	2.79E-03	1.39E-02	2.14E-01	1.20E+00	5.10E-02
EL185	CMNMA33732	Modern sample	Old Crow	1.61E-04	7.41E-05	1.68E-04	2.69E-04	2.67E-03	1.13E-02	4.61E-04	4.39E-04	4.30E-04	1.51E-04	3.55E-04	4.78E-04	4.65E-04	1.73E-03	6.01E-02	3.45E-01	1.40E-02
EL187	CMNMA33746	Modern sample	Whitehorse	2.23E-04	2.70E-04	3.41E-04	2.35E-04	3.48E-03	1.31E-02	0.00E+00	3.19E-04	4.38E-04	2.05E-04	0.00E+00	3.90E-04	0.00E+00	0.00E+00	6.41E-02	N/A	1.63E-02
EL190	CMNMA29841	Modern sample	Dawson	4.01E-04	1.22E-04	2.42E-04	1.57E-03	2.13E-02	6.61E-02	4.44E-04	2.72E-04	0.00E+00	5.09E-04	0.00E+00	4.14E-04	0.00E+00	0.00E+00	1.88E-02	N/A	8.19E-02
EL191	CMNMA30626	Modern sample	Y.T.-B.C.	1.82E-03	9.47E-04	1.43E-03	2.05E-03	3.56E-02	9.52E-02	2.84E-03	2.32E-03	1.07E-03	1.93E-03	1.01E-03	1.22E-03	1.65E-03	1.72E-02	5.13E-02	1.11E+00	1.18E-01
EL192	CMNMA26303	Modern sample	NWT	4.24E-05	6.15E-05	4.87E-04	6.50E-04	1.13E-02	3.99E-02	4.46E-04	4.28E-03	1.56E-04	2.93E-03	1.03E-03	1.00E-02	0.00E+00	2.51E-03	3.77E-03	N/A	4.94E-02
EL195	CMNMA29838	Modern sample	Dawson	9.29E-04	5.21E-04	9.70E-04	1.09E-03	6.71E-03	1.96E-02	8.89E-04	1.13E-02	1.55E-03	8.02E-03	7.71E-04	1.80E-02	2.35E-03	0.00E+00	1.39E-01	3.95E-01	2.43E-02
EL196	CMNMA29839	Modern sample	Dawson	7.54E-04	2.28E-04	7.21E-04	6.60E-04	6.65E-03	1.93E-02	1.10E-03	1.35E-03	4.62E-04	2.02E-03	0.00E+00	5.35E-03	0.00E+00	7.45E-03	1.13E-01	N/A	2.39E-02

Sample ID	Specimen ID	Sample type	Region	La*	Ce*	Pr*	Nd*	Sm*	Eu*	Gd*	Tb*	Dy*	Ho*	Er*	Tm*	Yb*	Lu*	La/Sm	La/Yb	Eu (ppm)
EL200	CMNMA 29837	Modern sample	Dawson	2.49E-04	6.02E-05	0.00E+00	5.82E-04	8.47E-03	2.83E-02	1.09E-03	6.24E-04	6.11E-04	7.17E-04	5.05E-04	1.77E-03	3.31E-04	2.46E-03	2.94E-02	7.54E-01	3.51E-02
EL201	CMNMA 30623	Modern sample	Ivvaik National Park (North Y.T.)	0.00E+00	0.00E+00	0.00E+00	0.00E+00	0.00E+00	6.29E-01	0.00E+00	2.94E-01	0.00E+00	2.36E-01	0.00E+00	4.48E-01	0.00E+00	0.00E+00		N/A	7.80E-01
EL202	CMNFV 34743	Beringia sample	Dawson	1.76E-02	7.80E-03	1.68E-02	7.63E-03	1.50E-02	1.96E-02	2.34E-02	2.36E-02	1.06E-02	1.96E-02	1.18E-02	1.11E-02	9.59E-03	1.14E-02	1.17E+00	1.83E+00	2.43E-02
EL205	CMNFV 57180	Beringia sample	Old Crow	8.01E-03	4.25E-03	9.37E-03	4.92E-03	1.11E-02	1.60E-02	1.55E-02	1.71E-02	7.06E-03	1.36E-02	6.53E-03	8.54E-03	6.75E-03	7.81E-03	7.24E-01	1.19E+00	1.98E-02
EL207	CMNFV 49389	Beringia sample	Old Crow	1.06E-03	4.69E-04	1.16E-03	3.65E-04	2.36E-03	3.67E-03	2.56E-03	5.21E-03	1.25E-03	2.41E-03	1.14E-03	3.00E-03	8.75E-04	1.77E-03	4.49E-01	1.21E+00	4.56E-03
EL208	CMNFV 34742	Beringia sample	Dawson	1.03E-02	4.63E-03	1.07E-02	5.34E-03	1.06E-02	1.20E-02	1.54E-02	1.66E-02	9.04E-03	1.25E-02	8.80E-03	8.63E-03	5.98E-03	6.90E-03	9.78E-01	1.73E+00	1.49E-02
EL210	CMNFV 43088	Beringia sample	Old Crow	8.03E-02	4.44E-02	9.66E-02	4.81E-02	1.13E-01	1.37E-01	1.70E-01	1.52E-01	1.02E-01	1.32E-01	8.73E-02	7.76E-02	6.38E-02	7.21E-02	7.09E-01	1.26E+00	1.70E-01
EL220	CMNFV 35964	Beringia sample	Dawson	9.49E-02	3.74E-02	9.09E-02	3.40E-02	7.34E-02	7.79E-02	1.02E-01	8.87E-02	5.81E-02	7.71E-02	5.52E-02	4.24E-02	4.19E-02	3.58E-02	1.29E+00	2.26E+00	9.65E-02

Sample ID	**Specimen ID**	**Sample type**	**Region**	**La***	**Ce***	**Pr***	**Nd***	**Sm***	**Eu***	**Gd***	**Tb***	**Dy***	**Ho***	**Er***	**Tm***	**Yb***	**Lu***	**La/Sm**	**La/Yb**	**Eu (ppm)**
EL223	CMNFV43051	Beringia sample	Old Crow	1.91E-01	9.41E-02	2.04E-01	9.12E-02	2.18E-01	2.42E-01	2.96E-01	2.56E-01	1.65E-01	1.94E-01	1.28E-01	1.08E-01	9.93E-02	9.02E-02	8.78E-01	1.93E+00	3.00E-01
EL224	CMNFV9929	Beringia sample	Dawson	4.00E-02	1.54E-02	3.74E-02	1.75E-02	3.66E-02	4.60E-02	4.96E-02	4.64E-02	3.12E-02	3.92E-02	2.46E-02	2.09E-02	2.00E-02	2.17E-02	1.09E+00	1.99E+00	5.70E-02
EL226	CMNFV24939	Beringia sample	Old Crow	4.09E-01	1.91E-01	4.22E-01	1.95E-01	4.29E-01	4.93E-01	6.63E-01	5.72E-01	3.79E-01	5.00E-01	3.18E-01	2.68E-01	2.52E-01	2.26E-01	9.54E-01	1.63E+00	6.11E-01
EL228	CMNFV18597	Beringia sample	Old Crow	3.19E-01	1.57E-01	3.52E-01	1.70E-01	4.69E-01	6.64E-01	6.69E-01	6.60E-01	4.35E-01	6.07E-01	3.88E-01	3.68E-01	3.37E-01	3.14E-01	6.80E-01	9.47E-01	8.24E-01
EL229	CMNFV44469	Beringia sample	Dawson	6.00E-03	2.57E-03	5.95E-03	2.67E-03	5.22E-03	7.24E-03	5.85E-03	6.70E-03	4.14E-03	4.60E-03	3.22E-03	5.13E-03	3.85E-03	4.90E-03	1.15E+00	1.56E+00	8.98E-03
EL230	CMNFV7748	Beringia sample	Dawson	1.84E-03	9.77E-04	1.95E-03	7.46E-04	2.03E-03	1.95E-03	1.42E-03	4.08E-03	1.11E-03	2.76E-03	7.77E-04	2.04E-03	2.30E-03	1.26E-03	9.08E-01	8.00E-01	2.42E-03
EL231	CMNFV46520	Beringia sample	Dawson	3.51E-02	1.56E-02	3.50E-02	1.38E-02	3.08E-02	3.72E-02	4.36E-02	3.22E-02	2.22E-02	2.95E-02	1.68E-02	1.75E-02	1.65E-02	1.90E-02	1.14E+00	2.13E+00	4.61E-02
EL232	CMNFV23670	Beringia sample	Old Crow	9.86E-02	4.76E-02	9.98E-02	4.87E-02	1.16E-01	1.36E-01	1.83E-01	1.51E-01	9.67E-02	1.31E-01	9.07E-02	7.73E-02	7.95E-02	7.41E-02	8.52E-01	1.24E+00	1.69E-01
EL233	CMNFV20139	Beringia sample	Old Crow	8.84E-02	4.05E-02	8.21E-02	4.03E-02	8.04E-02	1.04E-01	1.60E-01	1.18E-01	8.21E-02	1.10E-01	7.47E-02	6.09E-02	5.65E-02	6.11E-02	1.10E+00	1.57E+00	1.28E-01
EL234	CMNFV31317	Beringia sample	Old Crow	1.25E+00	6.02E-01	1.30E+00	5.93E-01	1.29E+00	1.50E+00	1.97E+00	1.65E+00	1.09E+00	1.48E+00	9.34E-01	8.00E-01	7.50E-01	7.49E-01	9.65E-01	1.67E+00	1.86E+00

Table 4. Compiled prey source database including specimen ID, Radiocarbon ID, Species, Age subset, Feeding behaviour, Gut physiology, Region, latitude and longitude, Substrate, 14C age (radiocarbon age [BP]), 14C age uncertainty (radiocarbon age uncertainty [BP]), Cal (Calibrated radiocarbon age [BP]), Median cal [Median calibrated radiocarbon age [BP]), $\delta^{13}C$ (‰)*, $\delta^{15}N$ (‰), carbon and nitrogen isotopes reference, and radiocarbon reference.

Refernces:

Debruyne, Regis, Genevieve Chu, Christine E. King, Kirsti Bos, Melanie Kuch, Carsten Schwarz, and others, ‘Out of America: Ancient DNA Evidence for a New World Origin of Late Quaternary Woolly Mammoths’, Current Biology, 18.17 (2008), 1320–26 <https://doi.org/10.1016/j.cub.2008.07.061>

Fox-Dobbs, Kena, Jennifer A. Leonard, and Paul L. Koch, ‘Pleistocene Megafauna from Eastern Beringia: Paleoecological and Paleoenvironmental Interpretations of Stable Carbon and Nitrogen Isotope and Radiocarbon Records’, Palaeogeography, Palaeoclimatology, Palaeoecology, 261.1–2 (2008), 30–46 <https://doi.org/10.1016/j.palaeo.2007.12.011>

Halffman, Carrin M., Ben A. Potter, Holly J. McKinney, Takumi Tsutaya, Bruce P. Finney, Brian M. Kemp, and others, ‘Ancient Beringian Paleodiets Revealed through Multiproxy Stable Isotope Analyses’, Science Advances, 6.36 (2020), eabc1968 <https://doi.org/10.1126/sciadv.abc1968>

Kelly, A, 'Survival of the flexible? Niche breadth and persistence for bison and Equus sps of Beringia'. Thesis. University of Cincinnati, (2022)

Leonard, Jennifer A., Carles Vilà, Kena Fox-Dobbs, Paul L. Koch, Robert K. Wayne, and Blaire Van Valkenburgh, ‘Megafaunal Extinctions and the Disappearance of a Specialized Wolf Ecomorph’, Current Biology, 17.13 (2007), 1146–50 <https://doi.org/10.1016/j.cub.2007.05.072>

Metcalfe, Jessica Z, 'Late Pleistocene climate and proboscidean paleoecology in North America: Insights from stable isotope compositions of skeletal remains' , Electronic Thesis and Dissertation Repository. 194, (2011)

Rabanus-Wallace, M. Timothy, Matthew J. Wooller, Grant D. Zazula, Elen Shute, A. Hope Jahren, Pavel Kosintsev, and others, ‘Megafaunal Isotopes Reveal Role of Increased Moisture on Rangeland during Late Pleistocene Extinctions’, Nature Ecology & Evolution, 1.5 (2017), 0125 <https://doi.org/10.1038/s41559-017-0125>

Raghavan, Maanasa, Gonçalo Espregueira Themudo, Colin I. Smith, Grant Zazula, and Paula F. Campos, ‘Musk Ox (Ovibos Moschatus) of the Mammoth Steppe: Tracing Palaeodietary and Palaeoenvironmental Changes over the Last 50,000 Years Using Carbon and Nitrogen Isotopic Analysis’, Quaternary Science Reviews, 102 (2014), 192–201 <https://doi.org/10.1016/j.quascirev.2014.08.001>

Schwartz-Narbonne, R., F.J. Longstaffe, K.J. Kardynal, P. Druckenmiller, K.A. Hobson, C.N. Jass, and others, ‘Reframing the Mammoth Steppe: Insights from Analysis of Isotopic Niches’, Quaternary Science Reviews, 215 (2019), 1–21 <https://doi.org/10.1016/j.quascirev.2019.04.025>

Schwartz-Narbonne, Rachel, Fred J. Longstaffe, Jessica Z. Metcalfe, and Grant Zazula, ‘Solving the Woolly Mammoth Conundrum: Amino Acid 15N-Enrichment Suggests a Distinct Forage or Habitat’, Scientific Reports, 5.1 (2015), 9791 <https://doi.org/10.1038/srep09791>

Szpak, Paul, Darren R. Gröcke, Regis Debruyne, Ross D.E. MacPhee, R. Dale Guthrie, Duane Froese, and others, ‘Regional Differences in Bone Collagen δ13C and δ15N of Pleistocene Mammoths: Implications for Paleoecology of the Mammoth Steppe’, Palaeogeography, Palaeoclimatology, Palaeoecology, 286.1–2 (2010), 88–96 https://doi.org/10.1016/j.palaeo.2009.12.009

**Note: $\delta^{13}C$ values have undergone atmospheric CO_2 correction following the protocols in Long et al., 2005*

Specimen ID	**Radiocarbon ID**	**Species**	**Age subset**	**Feeding behaviour**	**Gut physiology**	**Region**	**Latitude**	**Longitude**	**Substrate**	**14C age (BP)**	**14C age uncertainty (BP)**	**Cal (BP)**	**Median cal (BP)**	**δ13C (‰)***	**δ15N (‰)**	**δ13C, δ15N Reference**	**14C age Reference**
YG 421.117	UCIAMS-33039	Bison sp.	LGM	Grazer	Polygastric (Ruminant)	Yukon Canada	63.83	-138.9	Mandible	17670.00	40	21382	21382	-20.1	7.2	Kelly (2022)	Kelly (2022)
F:AM 60044	CAMS119970	Equus sp.	LGM	Grazer	Monogastric	Alaska USA	64.1078895	-141.8993638	Bone	18630.00	100	21927-22591	22259	-21.5	3.5	Leonard et al. (2007)	Leonard et al. (2007)
F:AM 60023	CAMS120058	Equus sp.	LGM	Grazer	Monogastric	Alaska USA	64.1078895	-141.8993638	Bone	19000.00	100	22567-23167	22867	-22.1	2.5	Leonard et al. (2007)	Leonard et al. (2007)
F:AM 60027	CAMS120059	Equus sp.	LGM	Grazer	Monogastric	Alaska USA	64.1078895	-141.8993638	Bone	19590.00	110	23031-23731	23381	-21.4	3.6	Leonard et al. (2007)	Leonard et al. (2007)
F:AM 142420	CAMS119973	Equus sp.	LGM	Grazer	Monogastric	Alaska USA	64.1078895	-141.8993638	Bone	19870.00	110	23485-24120	23802.5	-21.8	5	Leonard et al. (2007)	Leonard et al. (2007)
F:AM 142430	CAMS119983	Equus sp.	LGM	Grazer	Monogastric	Alaska USA	64.1078895	-141.8993638	Bone	19950.00	110	23553-24206	23879.5	-22.0	3.2	Leonard et al. (2007)	Leonard et al. (2007)
F:AM 60020	CAMS120062	Equus sp.	LGM	Grazer	Monogastric	Alaska USA	64.1078895	-141.8993638	Bone	19950.00	120	23550-24210	23880	-21.9	4	Leonard et al. (2007)	Leonard et al. (2007)
F:AM 142427	CAMS119980	Equus sp.	LGM	Grazer	Monogastric	Alaska USA	64.1078895	-141.8993638	Bone	19960.00	110	23562-24216	23889	-21.7	4.7	Leonard et al. (2007)	Leonard et al. (2007)
F:AM 142426	CAMS119979	Equus sp.	LGM	Grazer	Monogastric	Alaska USA	64.1078895	-141.8993638	Bone	20300.00	120	23944-24544	24244	-21.8	5.1	Leonard et al. (2007)	Leonard et al. (2007)

Specimen ID	Radiocarbon ID	Species	Age subset	Feeding behaviour	Gut physiology	Region	Latitude	Longitude	Substrate	14C age (BP)	14C age uncertainty (BP)	Cal (BP)	Median cal (BP)	δ13C (‰)*	δ15N (‰)	δ13C, δ15N Reference	14C age Reference
F:AM 142425	CAMS119978	Equus sp.	LGM	Grazer	Monogastric	Alaska USA	64.1078895	-141.8993638	Bone	20440.00	120	24063-24698	24380.5	-21.4	4.2	Leonard et al. (2007)	Leonard et al. (2007)
F:AM 142419	CAMS119971	Equus sp.	LGM	Grazer	Monogastric	Alaska USA	64.1078895	-141.8993638	Bone	20520.00	120	24167-24779	24473	-21.7	4.5	Leonard et al. (2007)	Leonard et al. (2007)
F:AM 142428	CAMS119981	Equus sp.	LGM	Grazer	Monogastric	Alaska USA	64.1078895	-141.8993638	Bone	21280.00	130	25089-25770	25429.5	-21.6	3.7	Leonard et al. (2007)	Leonard et al. (2007)
F:AM 60026	CAMS120060	Equus sp.	LGM	Grazer	Monogastric	Alaska USA	64.1078895	-141.8993638	Bone	21310.00	140	25111-25800	25455.5	-21.9	4	Leonard et al. (2007)	Leonard et al. (2007)
YG546.1806	UCIAMS 241534	Equus sp.	LGM	Grazer	Monogastric	Yukon Canada	63.82	-139.06	mandible	17500.00	60	21121	21121	-21.2	6.9	Kelly (2022)	Kelly (2022)
YG268.8	CAMS 186979	Equus sp.	LGM	Grazer	Monogastric	Yukon Canada	63.82	-139.03	mandible	17930.00	90	21815	21815	-21.6	7.42	Kelly (2022)	Kelly (2022)
YG 236.235	AA-103835	Equus sp.	LGM	Grazer	Monogastric	Yukon Canada	64.05172864	-139.4248928	Bone	18370.00	260	21615-22388	22001.5	-21.3	9.9	Schwartz-Narbonne et al. (2015)	Schwartz-Narbonne et al. (2015)
YG355.117	CAMS 186981	Equus sp.	LGM	Grazer	Monogastric	Yukon	63.83	-138.91	mandible	21070.00	120	25429	25429	-20.7	6.23	Kelly (2022)	Kelly (2022)

Specimen ID	**Radiocarbon ID**	**Species**	**Age subset**	**Feeding behaviour**	**Gut physiology**	**Region**	**Latitude**	**Longitude**	**Substrate**	**14C age (BP)**	**14C age uncertainty (BP)**	**Cal (BP)**	**Median cal (BP)**	**δ13C (‰)***	**δ15N (‰)**	**δ13C, δ15N Reference**	**14C age Reference**
						Canada											
YG2.1	CAMS 186978	Equus sp.	LGM	Grazer	Monogastric	Yukon Canada	63.97	-139.05	mandible	21080.00	120	25437	25437	-21.1	5.95	Kelly (2022)	Kelly (2022)
AM 8052	AA-14935	Mammuthus sp.	LGM	Grazer	Monogastric	Alaska USA	65.18	-147.5	Dentin/Root dentin/Cementum	18379.00	124	21690-22347	22018.5	-21.6	7	Szpak et al. (2010)	Debruyne et al. (2008)
YG 6.51 YG 6.49	Beta-70099	Mammuthus sp.	LGM	Grazer	Monogastric	Yukon Canada	63.69914577	-138.6098038	Bone	17950.00	120	21233-22002	21617.5	-21.3	10.5	Mecalfe (2011)	Reported in Metcalfe et al. (2016)
F:AM 143760	Unknown	Ovis dalli	LGM	Grazer	Polygastric (Ruminant)	Alaska USA	64.1078895	-141.8993638	Skull and horncone	21660.00	380	25278-26616	25947	-20.1	7.6	Schwartz-Narbonne et al. (2019)	Schwartz-Narbonne et al. (2019)
YG 312.1	AA-103830	Ovis dalli	LGM	Grazer	Polygastric (Ruminant)	Yukon Canada	64.05172864	-139.4248928	metatarsal	18120.00	240	21394-22237	21815.5	-19.6	7.5	Schwartz-Narbonne et al. (2019)	Schwartz-Narbonne et al. (2019)

Specimen ID	Radiocarbon ID	Species	Age subset	Feeding behaviour	Gut physiology	Region	Latitude	Longitude	Substrate	14C age (BP)	14C age uncertainty (BP)	Cal (BP)	Median cal (BP)	δ13C (‰)*	δ15N (‰)	δ13C, δ15N Reference	14C age Reference
F:AM 142441	AA-48686	Rangifer tarandus	LGM	Mixed	Polygastric (Ruminant)	Alaska USA	64.1078895	-141.8993638	Bone	17300.00	222	20390-21129	20759.5	-20.7	5.4	Leonard et al. (2007)	Leonard et al. (2007)
F:AM 142438	AA-48680	Rangifer tarandus	LGM	Mixed	Polygastric (Ruminant)	Alaska USA	64.1078895	-141.8993638	Bone	21000.00	361	24605-25692	25148.5	-20.7	3.6	Leonard et al. (2007)	Leonard et al. (2007)
G171745	Unknown	Bison sp.	Modern	Grazer	Polygastric (Ruminant)	Alaska USA	63.356	-145.775	rib	7630.00	30	8379-8512	8445.5	-22.3	5.2	Halffman et al. (2020)	Halffman et al. (2020)
G-171742	Unknown	Bison sp.	Modern	Grazer	Polygastric (Ruminant)	Alaska USA	63.356	-145.775	Long bone	8634.00	27	9562-9662	9612	-21.5	5	Halffman et al. (2020)	Halffman et al. (2020)
G-171741	Unknown	Bison sp.	Modern	Grazer	Polygastric (Ruminant)	Alaska USA	63.356	-145.775	mandible	8634.00	27	9562-9662	9612	-21.7	5.2	Halffman et al. (2020)	Halffman et al. (2020)
G-158405	Unknown	Bison sp.	Modern	Grazer	Polygastric (Ruminant)	Alaska USA	63.965	-145.026	metatarsal	8880.00	20	9910-10160	10035	-22.3	2.4	Halffman et al. (2020)	Halffman et al. (2020)
G-166796	Unknown	Bison sp.	Modern	Grazer	Polygastric (Ruminant)	Alaska USA	63.965	-145.026	humerus	8880.00	20	9910-10160	10035	-22.1	3.5	Halffman et al. (2020)	Halffman et al. (2020)

Specimen ID	Radiocarbon ID	Species	Age subset	Feeding behaviour	Gut physiology	Region	Latitude	Longitude	Substrate	14C age (BP)	14C age uncertainty (BP)	Cal (BP)	Median cal (BP)	δ13C (‰)*	δ15N (‰)	δ13C, δ15N Reference	14C age Reference
G-166797	Unknown	Bison sp.	Modern	Grazer	Polygastric (Ruminant)	Alaska USA	63.965	-145.026	innominate	8880.00	20	9910-10160	10035	-22.4	5.7	Halffman et al. (2020)	Halffman et al. (2020)
G-158484	Unknown	Bison sp.	Modern	Grazer	Polygastric (Ruminant)	Alaska USA	63.965	-145.026	metacarpal	8880.00	20	9910-10160	10035	-22.0	6.2	Halffman et al. (2020)	Halffman et al. (2020)
G-158483	Unknown	Bison sp.	Modern	Grazer	Polygastric (Ruminant)	Alaska USA	63.965	-145.026	metatarsal	9400.00	60	10430-11040	10735	-22.0	5.5	Halffman et al. (2020)	Halffman et al. (2020)
G-158406	Unknown	Bison sp.	Modern	Grazer	Polygastric (Ruminant)	Alaska USA	63.965	-145.026	metatarsal	9506.00	38	10659-11072	10865.5	-23.1	2.6	Halffman et al. (2020)	Halffman et al. (2020)
G-166790	Unknown	Ovis dalli	Modern	Grazer	Polygastric (Ruminant)	Alaska USA	63.807	-148.939	tibia	622.00	31	551-659	605	-20.9	1.5	Halffman et al. (2020)	Halffman et al. (2020)
G-158463	Unknown	Ovis dalli	Modern	Grazer	Polygastric (Ruminant)	Alaska USA	63.807	-148.939	ulna	622.00	31	551-659	605	-20.7	1.5	Halffman et al. (2020)	Halffman et al. (2020)
G-158464	Unknown	Ovis dalli	Modern	Grazer	Polygastric (Ruminant)	Alaska USA	63.807	-148.939	patella	622.00	31	551-659	605	-20.9	1.9	Halffman et al. (2020)	Halffman et al. (2020)

Specimen ID	**Radiocarbon ID**	**Species**	**Age subset**	**Feeding behaviour**	**Gut physiology**	**Region**	**Latitude**	**Longitude**	**Substrate**	**14C age (BP)**	**14C age uncertainty (BP)**	**Cal (BP)**	**Median cal (BP)**	**δ13C (‰)***	**δ15N (‰)**	**δ13C, δ15N Reference**	**14C age Reference**
G-158387	Unknown	Ovis dalli	Modern	Grazer	Polygastric (Ruminant)	Alaska USA	63.807	-148.939	astragalus	622.00	31	551-659	605	-22.2	2.6	Halffman et al. (2020)	Halffman et al. (2020)
G-158389	Unknown	Ovis dalli	Modern	Grazer	Polygastric (Ruminant)	Alaska USA	63.807	-148.939	metapodial	622.00	31	551-659	605	-22.3	3.7	Halffman et al. (2020)	Halffman et al. (2020)
G-167351	Unknown	Rangifer tarandus	Modern	Mixed	Polygastric (Ruminant)	Alaska USA	60.988	-141.937	phalanx	622.00	31	154-505	329.5	-20.4	5.3	Halffman et al. (2020)	Halffman et al. (2020)
G-158379	Unknown	Rangifer tarandus	Modern	Mixed	Polygastric (Ruminant)	Alaska USA	63.807	-148.939	metatarsal	320.00	63	154-505	329.5	-18.7	2	Halffman et al. (2020)	Halffman et al. (2020)
G-158380	Unknown	Rangifer tarandus	Modern	Mixed	Polygastric (Ruminant)	Alaska USA	63.807	-148.939	metacarpal	320.00	63	154-505	329.5	-19.3	2.4	Halffman et al. (2020)	Halffman et al. (2020)
G-158378	Unknown	Rangifer tarandus	Modern	Mixed	Polygastric (Ruminant)	Alaska USA	63.807	-148.939	radius	320.00	63	154-505	329.5	-19.1	2.4	Halffman et al. (2020)	Halffman et al. (2020)
G-158456	Unknown	Rangifer tarandus	Modern	Mixed	Polygastric (Ruminant)	Alaska USA	63.807	-148.939	metacarpal	320.00	63	154-505	329.5	-19.1	2.4	Halffman et al. (2020)	Halffman et al. (2020)

Specimen ID	Radiocarbon ID	Species	Age subset	Feeding behaviour	Gut physiology	Region	Latitude	Longitude	Substrate	14C age (BP)	14C age uncertainty (BP)	Cal (BP)	Median cal (BP)	δ13C (‰)*	δ15N (‰)	δ13C, δ15N Reference	14C age Reference
G-158455	Unknown	Rangifer tarandus	Modern	Mixed	Polygastric (Ruminant)	Alaska USA	63.807	-148.939	tarsal	320.00	63	154-505	329.5	-19.5	2.8	Halffman et al. (2020)	Halffman et al. (2020)
G-158454	Unknown	Rangifer tarandus	Modern	Mixed	Polygastric (Ruminant)	Alaska USA	63.807	-148.939	metatarsal	320.00	63	154-505	329.5	-19.0	2.9	Halffman et al. (2020)	Halffman et al. (2020)
G-158377	Unknown	Rangifer tarandus	Modern	Mixed	Polygastric (Ruminant)	Alaska USA	60.988	-141.937	metatarsal	622.00	31	551-659	605	-18.6	3.3	Halffman et al. (2020)	Halffman et al. (2020)
G-171748	Unknown	Rangifer tarandus	Modern	Mixed	Polygastric (Ruminant)	Alaska USA	63.356	-145.775	radius	5980.00	30	6737-6894	6815.5	-18.0	2	Halffman et al. (2020)	Halffman et al. (2020)
YG 630.5	UCIAMS-33023	Bison sp.	Post-LGM	Grazer	Polygastric (Ruminant)	Yukon Canada	63.71	-138.68	mandible	11960.00	30	13785	13785	-20.3	2.2	Kelly (2022)	Kelly (2022)
YG 403.179	UCIAMS-33036	Bison sp.	Post-LGM	Grazer	Polygastric (Ruminant)	Yukon Canada	63.69	-138.61	mandible	11990.00	30	13823	13823	-20.3	2.3	Kelly (2022)	Kelly (2022)
G-167352	Unknown	Lepus americanus	Post-LGM	Grazer	Monogastric	Alaska USA	64.955	-150.52	calcaneus	9990.00	30	11280-11610	11445	-22.9	2.6	Halffman et al. (2020)	Halffman et al. (2020)

Specimen ID	**Radiocarbon ID**	**Species**	**Age subset**	**Feeding behaviour**	**Gut physiology**	**Region**	**Latitude**	**Longitude**	**Substrate**	**14C age (BP)**	**14C age uncertainty (BP)**	**Cal (BP)**	**Median cal (BP)**	**δ13C (‰)***	**δ15N (‰)**	**δ13C, δ15N Reference**	**14C age Reference**
G-158470	Unknown	Lepus americanus	Post-LGM	Grazer	Monogastric	Alaska USA	64.243	-146.0436	innominate	10270.00	20	11850-12120	11985	-22.5	0	Halffman et al. (2020)	Halffman et al. (2020)
G-158430	Unknown	Lepus americanus	Post-LGM	Grazer	Monogastric	Alaska USA	64.243	-146.0436	scapula	10270.00	20	11850-12120	11985	-22.5	0.1	Halffman et al. (2020)	Halffman et al. (2020)
G-158506	Unknown	Lepus americanus	Post-LGM	Grazer	Monogastric	Alaska USA	64.243	-146.0436	scapula	10270.00	20	11850-12120	11985	-22.9	1.2	Halffman et al. (2020)	Halffman et al. (2020)
G-158431	Unknown	Lepus americanus	Post-LGM	Grazer	Monogastric	Alaska USA	64.243	-146.0436	vertebra	10270.00	20	11850-12120	11985	-22.9	1.3	Halffman et al. (2020)	Halffman et al. (2020)
G-158462	Unknown	Ovis dalli	Post-LGM	Grazer	Polygastric (Ruminant)	Alaska USA	63.538	-148.735	phalanx	9866.00	55	11217-11314	11265.5	-20.4	1.2	Halffman et al. (2020)	Halffman et al. (2020)
G-158452	Unknown	Rangifer tarandus	Post-LGM	Mixed	Polygastric (Ruminant)	Alaska USA	63.538	-148.735	metacarpal	9866.00	55	11217-11314	11265.5	-19.0	0.9	Halffman et al. (2020)	Halffman et al. (2020)
G-158376	Unknown	Rangifer tarandus	Post-LGM	Mixed	Polygastric (Ruminant)	Alaska USA	63.538	-148.735	phalanx	9866.00	55	11217-11314	11265.5	-18.8	1	Halffman et al. (2020)	Halffman et al. (2020)

Specimen ID	**Radiocarbon ID**	**Species**	**Age subset**	**Feeding behaviour**	**Gut physiology**	**Region**	**Latitude**	**Longitude**	**Substrate**	**14C age (BP)**	**14C age uncertainty (BP)**	**Cal (BP)**	**Median cal (BP)**	**δ13C (‰)***	**δ15N (‰)**	**δ13C, δ15N Reference**	**14C age Reference**
G-147962	Unknown	Urocitellus parryii	Post-LGM	Mixed	Monogastric	Alaska USA	64.955	-150.52	femur	9990.00	30	11280-11610	11445	-21.4	1.8	Halffman et al. (2020)	Halffman et al. (2020)
G-162878	Unknown	Urocitellus parryii	Post-LGM	Mixed	Monogastric	Alaska USA	64.243	-146.0436	femur	10270.00	20	11850-12120	11985	-23.4	1.1	Halffman et al. (2020)	Halffman et al. (2020)
G-158398	Unknown	Urocitellus parryii	Post-LGM	Mixed	Monogastric	Alaska USA	64.243	-146.0436	femur	10270.00	20	11850-12120	11985	-20.2	1.3	Halffman et al. (2020)	Halffman et al. (2020)
G-162879	Unknown	Urocitellus parryii	Post-LGM	Mixed	Monogastric	Alaska USA	64.243	-146.0436	femur	10270.00	20	11850-12120	11985	-23.2	1.6	Halffman et al. (2020)	Halffman et al. (2020)
G-158397	Unknown	Urocitellus parryii	Post-LGM	Mixed	Monogastric	Alaska USA	64.243	-146.0436	femur	10270.00	20	11850-12120	11985	-21.7	2	Halffman et al. (2020)	Halffman et al. (2020)
G-158473	Unknown	Urocitellus parryii	Post-LGM	Mixed	Monogastric	Alaska USA	64.243	-146.0436	ulna	11080.00	20	12790-13110	12950	-22.6	0.5	Halffman et al. (2020)	Halffman et al. (2020)
G-158474	Unknown	Urocitellus parryii	Post-LGM	Mixed	Monogastric	Alaska USA	64.243	-146.0436	humerus	11080.00	20	12790-13110	12950	-22.1	1.5	Halffman et al. (2020)	Halffman et al. (2020)

Specimen ID	Radiocarbon ID	Species	Age subset	Feeding behaviour	Gut physiology	Region	Latitude	Longitude	Substrate	14C age (BP)	14C age uncertainty (BP)	Cal (BP)	Median cal (BP)	δ13C (‰)*	δ15N (‰)	δ13C, δ15N Reference	14C age Reference
YT03/211 A3266	OxA20865	Bison sp.	Pre-LGM	Grazer	Polygastric (Ruminant)	Yukon Canada	63.75239608	-139.1241407	Unknown	36610.00	340	41079.76891	41079.76891	-19.3	5.455	Rabanus-Wallace et al. (2017)	Rabanus-Wallace et al. (2017)
YG 587.593	UCIAMS-209142	Bison sp.	Pre-LGM	Grazer	Polygastric (Ruminant)	Yukon Canada	63.82	-139.06	mandible	22520.00	140	26837	26837	-20.7	4.5	Kelly (2022)	Kelly (2022)
YG 543.160	UCIAMS-202189	Bison sp.	Pre-LGM	Grazer	Polygastric (Ruminant)	Yukon Canada	63.98	-139.02	mandible	24790.00	170	28827	28827	-20.4	5.5	Kelly (2022)	Kelly (2022)
YG 573.124	UCIAMS-202203	Bison sp.	Pre-LGM	Grazer	Polygastric (Ruminant)	Yukon Canada	63.51	-138.92	mandible	25910.00	200	30147	30147	-20.3	5.4	Kelly (2022)	Kelly (2022)
YG 587.1846	UCIAMS-202208	Bison sp.	Pre-LGM	Grazer	Polygastric (Ruminant)	Yukon Canada	63.82	-139.06	mandible	26360.00	210	30646	30646	-20.4	4.9	Kelly (2022)	Kelly (2022)
YG 406.793	UCIAMS-202211	Bison sp.	Pre-LGM	Grazer	Polygastric (Ruminant)	Yukon Canada	63.82	-139.04	maxilla	26600.00	210	30833	30833	-20.3	4.7	Kelly (2022)	Kelly (2022)
YG 300.51	UCIAMS-209150	Bison sp.	Pre-LGM	Grazer	Polygastric (Ruminant)	Yukon Canada	63.99	-139.23	maxilla	26710.00	210	30900	30900	-20.8	4.6	Kelly (2022)	Kelly (2022)

Specimen ID	Radiocarbon ID	Species	Age subset	Feeding behaviour	Gut physiology	Region	Latitude	Longitude	Substrate	14C age (BP)	14C age uncertainty (BP)	Cal (BP)	Median cal (BP)	δ13C (‰)*	δ15N (‰)	δ13C, δ15N Reference	14C age Reference
YG 110.95	UCIAMS-202206	Bison sp.	Pre-LGM	Grazer	Polygastric (Ruminant)	Yukon Canada	63.91	-139.33	mandible	27950.00	260	31759	31759	-20.6	3.6	Kelly (2022)	Kelly (2022)
YG 110.41	UCIAMS-202215	Bison sp.	Pre-LGM	Grazer	Polygastric (Ruminant)	Yukon Canada	63.91	-139.33	mandible	28500.00	270	32462	32462	-19.4	4.6	Kelly (2022)	Kelly (2022)
YG 610.128	UCIAMS-202209	Bison sp.	Pre-LGM	Grazer	Polygastric (Ruminant)	Yukon Canada	63.84	-139.1	mandible	28770.00	280	32879	32879	-20.4	5	Kelly (2022)	Kelly (2022)
YG 110.96	UCIAMS-209163	Bison sp.	Pre-LGM	Grazer	Polygastric (Ruminant)	Yukon Canada	63.91	-139.33	mandible	28830.00	280	32965	32965	-20.3	4.2	Kelly (2022)	Kelly (2022)
YG 610.64	UCIAMS-202191	Bison sp.	Pre-LGM	Grazer	Polygastric (Ruminant)	Yukon Canada	63.84	-139.1	mandible	28970.00	280	33140	33140	-20.0	4.8	Kelly (2022)	Kelly (2022)
YG 302.144	UCIAMS-202213	Bison sp.	Pre-LGM	Grazer	Polygastric (Ruminant)	Yukon Canada	63.92	-139.35	mandible	29690.00	310	33832	33832	-20.5	5.3	Kelly (2022)	Kelly (2022)
YG 302.222	UCIAMS-33035	Bison sp.	Pre-LGM	Grazer	Polygastric (Ruminant)	Yukon Canada	63.92	-139.35	mandible	30360.00	90	34355	34355	-20.3	4.3	Kelly (2022)	Kelly (2022)

Specimen ID	Radiocarbon ID	Species	Age subset	Feeding behaviour	Gut physiology	Region	Latitude	Longitude	Substrate	14C age (BP)	14C age uncertainty (BP)	Cal (BP)	Median cal (BP)	δ13C (‰)*	δ15N (‰)	δ13C, δ15N Reference	14C age Reference
YG 190.15	UCIAMS-202210	Bison sp.	Pre-LGM	Grazer	Polygastric (Ruminant)	Yukon Canada	63.72	-138.69	maxilla	30370.00	340	34368	34368	-20.6	4.7	Kelly (2022)	Kelly (2022)
YG 161.7	UCIAMS-202227	Bison sp.	Pre-LGM	Grazer	Polygastric (Ruminant)	Yukon Canada	63.97	-139.16	mandible	30460.00	340	34435	34435	-20.6	5.4	Kelly (2022)	Kelly (2022)
YG 550.24	UCIAMS-209149	Bison sp.	Pre-LGM	Grazer	Polygastric (Ruminant)	Yukon Canada	63.96	-138.95	mandible	30800.00	370	34730	34730	-20.6	4.6	Kelly (2022)	Kelly (2022)
YG 302.159	UCIAMS-202213	Bison sp.	Pre-LGM	Grazer	Polygastric (Ruminant)	Yukon Canada	63.92	-139.35	mandible	31010.00	360	34932	34932	-20.2	4.5	Kelly (2022)	Kelly (2022)
YG 453.11	UCIAMS-209141	Bison sp.	Pre-LGM	Grazer	Polygastric (Ruminant)	Yukon Canada	64.03	-140.7	mandible	31090.00	370	35010	35010	-20.4	4.6	Kelly (2022)	Kelly (2022)
YG 267.18	UCIAMS-209161	Bison sp.	Pre-LGM	Grazer	Polygastric (Ruminant)	Yukon Canada	63.72	-138.69	mandible	31130.00	370	35048	35048	-20.3	4.6	Kelly (2022)	Kelly (2022)
YG 543.201	UCIAMS-33021	Bison sp.	Pre-LGM	Grazer	Polygastric (Ruminant)	Yukon Canada	63.98	-139.02	mandible	32440.00	100	36319	36319	-20.0	4.2	Kelly (2022)	Kelly (2022)

Specimen ID	Radiocarbon ID	Species	Age subset	Feeding behaviour	Gut physiology	Region	Latitude	Longitude	Substrate	14C age (BP)	14C age uncertainty (BP)	Cal (BP)	Median cal (BP)	δ13C (‰)*	δ15N (‰)	δ13C, δ15N Reference	14C age Reference
YG 587.406	UCIAMS-33040	Bison sp.	Pre-LGM	Grazer	Polygastric (Ruminant)	Yukon Canada	63.82	-139.06	mandible	32510.00	110	36385	36385	-20.7	4.4	Kelly (2022)	Kelly (2022)
YG 543.257	UCIAMS-33032	Bison sp.	Pre-LGM	Grazer	Polygastric (Ruminant)	Yukon Canada	63.98	-139.02	mandible	32730.00	110	36616	36616	-19.8	4.4	Kelly (2022)	Kelly (2022)
YG 377.58	UCIAMS-202218	Bison sp.	Pre-LGM	Grazer	Polygastric (Ruminant)	Yukon Canada	63.92	-138.91	mandible	32640.00	440	36696	36696	-20.5	4.8	Kelly (2022)	Kelly (2022)
YG 453.6	UCIAMS-209139	Bison sp.	Pre-LGM	Grazer	Polygastric (Ruminant)	Yukon Canada	64.03	-140.7	mandible	32650.00	440	36710	36710	-20.3	4.3	Kelly (2022)	Kelly (2022)
YG 302.221	UCIAMS-209153	Bison sp.	Pre-LGM	Grazer	Polygastric (Ruminant)	Yukon Canada	63.92	-139.35	mandible	32960.00	470	37133	37133	-19.9	4.7	Kelly (2022)	Kelly (2022)
YG 404.656	UCIAMS-209156	Bison sp.	Pre-LGM	Grazer	Polygastric (Ruminant)	Yukon Canada	64.02	-139.16	mandible	32970.00	460	37143	37143	-20.1	4.3	Kelly (2022)	Kelly (2022)
YG 159.12	UCIAMS-202192	Bison sp.	Pre-LGM	Grazer	Polygastric (Ruminant)	Yukon Canada	63.82	-139.04	mandible	33020.00	460	37203	37203	-20.4	5.1	Kelly (2022)	Kelly (2022)

Specimen ID	Radiocarbon ID	Species	Age subset	Feeding behaviour	Gut physiology	Region	Latitude	Longitude	Substrate	14C age (BP)	14C age uncertainty (BP)	Cal (BP)	Median cal (BP)	δ13C (‰)*	δ15N (‰)	δ13C, δ15N Reference	14C age Reference
YG 550.25	UCIAMS-209162	Bison sp.	Pre-LGM	Grazer	Polygastric (Ruminant)	Yukon Canada	63.96	-138.95	mandible	33070.00	470	37262	37262	-20.4	4.5	Kelly (2022)	Kelly (2022)
YG 406.848	UCIAMS-202202	Bison sp.	Pre-LGM	Grazer	Polygastric (Ruminant)	Yukon Canada	63.82	-139.04	mandible	33600.00	500	37860	37860	-20.2	4.7	Kelly (2022)	Kelly (2022)
YG 391.67	UCIAMS-202217	Bison sp.	Pre-LGM	Grazer	Polygastric (Ruminant)	Yukon Canada	63.82	-139.04	mandible	33870.00	520	38214	38214	-20.1	4.9	Kelly (2022)	Kelly (2022)
YG 578.38	UCIAMS-209145	Bison sp.	Pre-LGM	Grazer	Polygastric (Ruminant)	Yukon Canada	63.71	-138.64	mandible	33990.00	520	38388	38388	-20.1	3.6	Kelly (2022)	Kelly (2022)
YG 377.40	UCIAMS-209160	Bison sp.	Pre-LGM	Grazer	Polygastric (Ruminant)	Yukon Canada	63.92	-138.91	mandible	34180.00	540	38640	38640	-20.5	3.9	Kelly (2022)	Kelly (2022)
YG 587.411	UCIAMS-202190	Bison sp.	Pre-LGM	Grazer	Polygastric (Ruminant)	Yukon Canada	63.82	-139.06	mandible	34420.00	550	38934	38934	-20.5	5.4	Kelly (2022)	Kelly (2022)
YG 587.1166	UCIAMS-202193	Bison sp.	Pre-LGM	Grazer	Polygastric (Ruminant)	Yukon Canada	63.82	-139.06	mandible	34470.00	550	38991	38991	-20.4	5.4	Kelly (2022)	Kelly (2022)

Specimen ID	Radiocarbon ID	Species	Age subset	Feeding behaviour	Gut physiology	Region	Latitude	Longitude	Substrate	14C age (BP)	14C age uncertainty (BP)	Cal (BP)	Median cal (BP)	δ13C (‰)*	δ15N (‰)	δ13C, δ15N Reference	14C age Reference
YG 587.1618	UCIAMS-202194	Bison sp.	Pre-LGM	Grazer	Polygastric (Ruminant)	Yukon Canada	63.82	-139.06	mandible	34930.00	590	39472	39472	-20.5	4.9	Kelly (2022)	Kelly (2022)
YG 384.11	UCIAMS-202221	Bison sp.	Pre-LGM	Grazer	Polygastric (Ruminant)	Yukon Canada	63.96	-138.95	mandible	35460.00	630	40037	40037	-20.5	4.9	Kelly (2022)	Kelly (2022)
YG 406.633	UCIAMS-202199	Bison sp.	Pre-LGM	Grazer	Polygastric (Ruminant)	Yukon Canada	63.82	-139.04	mandible	35480.00	630	40058	40058	-20.3	5	Kelly (2022)	Kelly (2022)
YG 190.13	UCIAMS-202204	Bison sp.	Pre-LGM	Grazer	Polygastric (Ruminant)	Yukon Canada	63.72	-138.69	mandible	35630.00	650	40213	40213	-20.3	5.3	Kelly (2022)	Kelly (2022)
YG 512.80	UCIAMS-202198	Bison sp.	Pre-LGM	Grazer	Polygastric (Ruminant)	Yukon Canada	63.71	-138.64	mandible	36800.00	740	41276	41276	-20.0	4.6	Kelly (2022)	Kelly (2022)
YG 587.1617	UCIAMS-33024	Bison sp.	Pre-LGM	Grazer	Polygastric (Ruminant)	Yukon Canada	63.82	-139.06	mandible	38020.00	160	42244	42244	-20.8	3.8	Kelly (2022)	Kelly (2022)
YG 578.39	UCIAMS-202195	Bison sp.	Pre-LGM	Grazer	Polygastric (Ruminant)	Yukon Canada	63.71	-138.64	mandible	38580.00	930	42622	42622	-20.6	5.2	Kelly (2022)	Kelly (2022)

Specimen ID	Radiocarbon ID	Species	Age subset	Feeding behaviour	Gut physiology	Region	Latitude	Longitude	Substrate	14C age (BP)	14C age uncertainty (BP)	Cal (BP)	Median cal (BP)	δ13C (‰)*	δ15N (‰)	δ13C, δ15N Reference	14C age Reference
YG 578.52	UCIAMS-209144	Bison sp.	Pre-LGM	Grazer	Polygastric (Ruminant)	Yukon Canada	63.71	-138.64	mandible	38610.00	940	42645	42645	-19.7	3.9	Kelly (2022)	Kelly (2022)
YG 303.1090	UCIAMS-202228	Bison sp.	Pre-LGM	Grazer	Polygastric (Ruminant)	Yukon Canada	63.9	-139.3	mandible	38830.00	950	42813	42813	-20.1	5	Kelly (2022)	Kelly (2022)
YG 578.34	UCIAMS-33027	Bison sp.	Pre-LGM	Grazer	Polygastric (Ruminant)	Yukon Canada	63.71	-138.64	mandible	39560.00	180	43220	43220	-20.4	4.3	Kelly (2022)	Kelly (2022)
YG 578.41	UCIAMS-209146	Bison sp.	Pre-LGM	Grazer	Polygastric (Ruminant)	Yukon Canada	63.71	-138.64	mandible	39700.00	1100	43502	43502	-20.2	4.6	Kelly (2022)	Kelly (2022)
YG 406.432	UCIAMS-209143	Bison sp.	Pre-LGM	Grazer	Polygastric (Ruminant)	Yukon Canada	63.82	-139.04	mandible	40200.00	1100	43874	43874	-20.2	4.1	Kelly (2022)	Kelly (2022)
"YG 587.1042																	
"	UCIAMS-202186	Bison sp.	Pre-LGM	Grazer	Polygastric (Ruminant)	Yukon Canada	63.82	-139.06	mandible	41400.00	1300	44856	44856	-20.5	5.1	Kelly (2022)	Kelly (2022)

Specimen ID	**Radiocarbon ID**	**Species**	**Age subset**	**Feeding behaviour**	**Gut physiology**	**Region**	**Latitude**	**Longitude**	**Substrate**	**14C age (BP)**	**14C age uncertainty (BP)**	**Cal (BP)**	**Median cal (BP)**	**δ13C (‰)***	**δ15N (‰)**	**δ13C, δ15N Reference**	**14C age Reference**
YG 512.79	UCIAMS-202226	Bison sp.	Pre-LGM	Grazer	Polygastric (Ruminant)	Yukon Canada	63.71	-138.64	mandible	41600.00	1300	45032	45032	-20.5	5.7	Kelly (2022)	Kelly (2022)
YG 612.76	UCIAMS-33041	Bison sp.	Pre-LGM	Grazer	Polygastric (Ruminant)	Yukon Canada	63.93	-139.33	mandible	41880.00	250	45250	45250	-20.0	3.7	Kelly (2022)	Kelly (2022)
YG 377.113	UCIAMS-202223	Bison sp.	Pre-LGM	Grazer	Polygastric (Ruminant)	Yukon Canada	63.92	-138.91	mandible	43400.00	1700	46761	46761	-20.4	5.5	Kelly (2022)	Kelly (2022)
YG 579.105	UCIAMS-202205	Bison sp.	Pre-LGM	Grazer	Polygastric (Ruminant)	Yukon Canada	63.82	-139.04	mandible	43900.00	1800	47161	47161	-20.4	5.5	Kelly (2022)	Kelly (2022)
YG 578.20	UCIAMS-202214	Bison sp.	Pre-LGM	Grazer	Polygastric (Ruminant)	Yukon Canada	63.71	-138.64	mandible	44500.00	1900	47561	47561	-20.1	4.9	Kelly (2022)	Kelly (2022)
YG 587.410	UCIAMS-202212	Bison sp.	Pre-LGM	Grazer	Polygastric (Ruminant)	Yukon Canada	63.82	-139.06	mandible	45580.00	2200	48011	48011	-20.5	5.3	Kelly (2022)	Kelly (2022)
YG 512.77	UCIAMS-209148	Bison sp.	Pre-LGM	Grazer	Polygastric (Ruminant)	Yukon Canada	63.71	-138.64	mandible	45600.00	2200	48020	48020	-20.1	4.5	Kelly (2022)	Kelly (2022)

Specimen ID	**Radiocarbon ID**	**Species**	**Age subset**	**Feeding behaviour**	**Gut physiology**	**Region**	**Latitude**	**Longitude**	**Substrate**	**14C age (BP)**	**14C age uncertainty (BP)**	**Cal (BP)**	**Median cal (BP)**	**δ13C (‰)***	**δ15N (‰)**	**δ13C, δ15N Reference**	**14C age Reference**
YG 613.95	UCIAMS-33020	Bison sp.	Pre-LGM	Grazer	Polygastric (Ruminant)	Yukon Canada	63.71	-138.64	mandible	45620.00	320	49091	49091	-19.9	3.8	Kelly (2022)	Kelly (2022)
YG 587.1616	UCIAMS-33029	Bison sp.	Pre-LGM	Grazer	Polygastric (Ruminant)	Yukon Canada	63.82	-139.06	mandible	46120.00	330	49530	49530	-20.9	5.4	Kelly (2022)	Kelly (2022)
YG 578.27	UCIAMS-33026	Bison sp.	Pre-LGM	Grazer	Polygastric (Ruminant)	Yukon Canada	63.71	-138.64	maxilla	46360.00	370	49640	49640	-20.0	3.9	Kelly (2022)	Kelly (2022)
YG 578.128	UCIAMS-33033	Bison sp.	Pre-LGM	Grazer	Polygastric (Ruminant)	Yukon Canada	63.71	-138.64	mandible	46400.00	370	49658	49658	-20.0	2.5	Kelly (2022)	Kelly (2022)
YG 406.595	UCIAMS-33025	Bison sp.	Pre-LGM	Grazer	Polygastric (Ruminant)	Yukon Canada	63.82	-139.04	mandible	46380.00	350	49663	49663	-20.0	3.6	Kelly (2022)	Kelly (2022)
YG 546.302	UCIAMS-33037	Bison sp.	Pre-LGM	Grazer	Polygastric (Ruminant)	Yukon Canada	63.82	-139.06	mandible	48880.00	470	Infinite	50000.00	-21.0	3.8	Kelly (2022)	Kelly (2022)
F:AM 142435	CAMS119989	Equus sp.	Pre-LGM	Grazer	Monogastric	Alaska USA	64.1078895	-141.8993638	Bone	21840.00	140	25737-26627	26182	-22.5	3.8	Leonard et al. (2007)	Leonard et al. (2007)

Specimen ID	Radiocarbon ID	Species	Age subset	Feeding behaviour	Gut physiology	Region	Latitude	Longitude	Substrate	14C age (BP)	14C age uncertainty (BP)	Cal (BP)	Median cal (BP)	δ13C (‰)*	δ15N (‰)	δ13C, δ15N Reference	14C age Reference
F:AM 142434	CAMS119988	Equus sp.	Pre-LGM	Grazer	Monogastric	Alaska USA	64.1078895	-141.8993638	Bone	22610.00	150	26927-27729	27328	-21.6	3.8	Leonard et al. (2007)	Leonard et al. (2007)
F:AM 60003	CAMS120077	Equus sp.	Pre-LGM	Grazer	Monogastric	Alaska USA	64.1078895	-141.8993638	Bone	24260.00	200	28587-29466	29026.5	-21.9	1.4	Leonard et al. (2007)	Leonard et al. (2007)
F:AM 142431	CAMS119985	Equus sp.	Pre-LGM	Grazer	Monogastric	Alaska USA	64.1078895	-141.8993638	Bone	25710.00	230	30384-31173	30778.5	-21.7	3.9	Leonard et al. (2007)	Leonard et al. (2007)
F:AM 142433	CAMS119987	Equus sp.	Pre-LGM	Grazer	Monogastric	Alaska USA	64.1078895	-141.8993638	Bone	25960.00	240	30573-31316	30944.5	-21.3	2.9	Leonard et al. (2007)	Leonard et al. (2007)
F:AM 60033	CAMS120069	Equus sp.	Pre-LGM	Grazer	Monogastric	Alaska USA	64.1078895	-141.8993638	Bone	39910.00	1330	42781-44872	43826.5	-21.5	2.6	Leonard et al. (2007)	Leonard et al. (2007)
F:AM 60017	CAMS119972	Equus sp.	Pre-LGM	Grazer	Monogastric	Alaska USA	64.1078895	-141.8993638	Bone	41000.00	1500	43302-46072	44687	-22.2	3.6	Leonard et al. (2007)	Leonard et al. (2007)
F:AM 60221	CAMS120067	Equus sp.	Pre-LGM	Grazer	Monogastric	Alaska USA	64.1078895	-141.8993638	Bone	43700.00	2000	45111-49771	47441	-22.3	0.7	Leonard et al. (2007)	Leonard et al. (2007)
YG573.72	UCIAMS 241531	Equus sp.	Pre-LGM	Grazer	Monogastric	Yukon Canada	63.51	-138.93	mandible	22410.00	110	26734	26734	-21.5	5.7	Kelly (2022)	Kelly (2022)
YG573.74	CAMS 186982	Equus sp.	Pre-LGM	Grazer	Monogastric	Yukon Canada	63.51	-138.93	mandible	22470.00	140	26777	26777	-21.5	5.23	Kelly (2022)	Kelly (2022)

Specimen ID	Radiocarbon ID	Species	Age subset	Feeding behaviour	Gut physiology	Region	Latitude	Longitude	Substrate	14C age (BP)	14C age uncertainty (BP)	Cal (BP)	Median cal (BP)	δ13C (‰)*	δ15N (‰)	δ13C, δ15N Reference	14C age Reference
YG417.38	UCIAMS 241569	Equus sp.	Pre-LGM	Grazer	Monogastric	Yukon Canada	63.62	-138.82	mandible	22990.00	130	27289	27289	-21.2	6.3	Kelly (2022)	Kelly (2022)
YG610.1636	CAMS 186984	Equus sp.	Pre-LGM	Grazer	Monogastric	Yukon Canada	63.84	-139.1	mandible	23020.00	150	27319	27319	-21.5	6.38	Kelly (2022)	Kelly (2022)
YG573.37	UCIAMS 241562	Equus sp.	Pre-LGM	Grazer	Monogastric	Yukon Canada	63.51	-138.93	mandible	23160.00	120	27435	27435	-21.3	6.68	Kelly (2022)	Kelly (2022)
YG102.1	CAMS 186977	Equus sp.	Pre-LGM	Grazer	Monogastric	Yukon Canada	63.07	-139.31	mandible	23930.00	170	28093	28093	-21.0	5.53	Kelly (2022)	Kelly (2022)
YG466.2	UCIAMS 241536	Equus sp.	Pre-LGM	Grazer	Monogastric	Yukon Canada	63.78	-138.92	mandible	25100.00	160	29410	29410	-21.0	6	Kelly (2022)	Kelly (2022)
YG302.82	CAMS 186980	Equus sp.	Pre-LGM	Grazer	Monogastric	Yukon Canada	63.92	-139.35	mandible	25190.00	200	29500	29500	-21.3	8.04	Kelly (2022)	Kelly (2022)
YG417.31	UCIAMS 241551	Equus sp.	Pre-LGM	Grazer	Monogastric	Yukon Canada	63.62	-138.82	mandible	25410.00	160	29669	29669	-21.4	4.99	Kelly (2022)	Kelly (2022)

Specimen ID	**Radiocarbon ID**	**Species**	**Age subset**	**Feeding behaviour**	**Gut physiology**	**Region**	**Latitude**	**Longitude**	**Substrate**	**14C age (BP)**	**14C age uncertainty (BP)**	**Cal (BP)**	**Median cal (BP)**	**δ13C (‰)***	**δ15N (‰)**	**δ13C, δ15N Reference**	**14C age Reference**
YG109.4	UCIAMS 241558	Equus sp.	Pre-LGM	Grazer	Monogastric	Yukon Canada	63.82	-139.04	mandible	25490.00	170	29751	29751	-21.0	6.23	Kelly (2022)	Kelly (2022)
YG109.3	UCIAMS 241564	Equus sp.	Pre-LGM	Grazer	Monogastric	Yukon Canada	63.82	-139.04	mandible	25580.00	170	29871	29871	-21.0	6.27	Kelly (2022)	Kelly (2022)
YG404.197	UCIAMS 241524	Equus sp.	Pre-LGM	Grazer	Monogastric	Yukon Canada	64.02	-139.16	mandible	25690.00	170	29989	29989	-21.3	5.34	Kelly (2022)	Kelly (2022)
YG417.74	UCIAMS 241557	Equus sp.	Pre-LGM	Grazer	Monogastric	Yukon Canada	63.62	-138.82	mandible	26080.00	180	30333	30333	-21.3	5.33	Kelly (2022)	Kelly (2022)
YG610.488	CAMS 186985	Equus sp.	Pre-LGM	Grazer	Monogastric	Yukon Canada	63.84	-139.1	mandible	26070.00	220	30348	30348	-21.3	5.85	Kelly (2022)	Kelly (2022)
YG610.1875	UCIAMS 241530	Equus sp.	Pre-LGM	Grazer	Monogastric	Yukon Canada	63.84	-139.1	mandible	26280.00	180	30554	30554	-21.0	4.82	Kelly (2022)	Kelly (2022)
YG404.587	UCIAMS 241571	Equus sp.	Pre-LGM	Grazer	Monogastric	Yukon Canada	64.02	-139.16	mandible	27230.00	200	31276	31276	-21.0	4.43	Kelly (2022)	Kelly (2022)

Specimen ID	**Radiocarbon ID**	**Species**	**Age subset**	**Feeding behaviour**	**Gut physiology**	**Region**	**Latitude**	**Longitude**	**Substrate**	**14C age (BP)**	**14C age uncertainty (BP)**	**Cal (BP)**	**Median cal (BP)**	**δ13C (‰)***	**δ15N (‰)**	**δ13C, δ15N Reference**	**14C age Reference**
YG489.277	UCIAMS 241560	Equus sp.	Pre-LGM	Grazer	Monogastric	Yukon Canada	63.82	-139.03	mandible	27620.00	210	31530	31530	-21.0	4.09	Kelly (2022)	Kelly (2022)
YG650.320	UCIAMS 252668	Equus sp.	Pre-LGM	Grazer	Monogastric	Yukon Canada	63.84	-139.1	mandible	27810.00	220	31726	31726	-20.9	5.6	Kelly (2022)	Kelly (2022)
YG587.287	UCIAMS 241546	Equus sp.	Pre-LGM	Grazer	Monogastric	Yukon Canada	63.82	-139.06	mandible	27850.00	220	31773	31773	-21.0	3.28	Kelly (2022)	Kelly (2022)
YG 178.9	AA-103890	Equus sp.	Pre-LGM	Grazer	Monogastric	Yukon Canada	64.05172864	-139.4248928	Bone	27189.00	420	31560-32226	31893	-21.4	7	Schwartz-Narbonne et al. (2015)	Schwartz-Narbonne et al. (2015)
YG648.314	UCIAMS 252669	Equus sp.	Pre-LGM	Grazer	Monogastric	Yukon Canada	64	-139.11	mandible	28000.00	220	31967	31967	-21.0	5	Kelly (2022)	Kelly (2022)
YG404.7	UCIAMS 241527	Equus sp.	Pre-LGM	Grazer	Monogastric	Yukon Canada	64.02	-139.16	mandible	28440.00	230	32588	32588	-21.2	3.6	Kelly (2022)	Kelly (2022)
YG650.768	UCIAMS 241561	Equus sp.	Pre-LGM	Grazer	Monogastric	Yukon Canada	63.84	-139.1	mandible	28470.00	240	32624	32624	-21.6	5.4	Kelly (2022)	Kelly (2022)

Specimen ID	**Radiocarbon ID**	**Species**	**Age subset**	**Feeding behaviour**	**Gut physiology**	**Region**	**Latitude**	**Longitude**	**Substrate**	**14C age (BP)**	**14C age uncertainty (BP)**	**Cal (BP)**	**Median cal (BP)**	**δ13C (‰)***	**δ15N (‰)**	**δ13C, δ15N Reference**	**14C age Reference**
YG394.28	UCIAMS 241528	Equus sp.	Pre-LGM	Grazer	Monogastric	Yukon Canada	63.99	-139.23	mandible	28480.00	240	32636	32636	-21.4	3.8	Kelly (2022)	Kelly (2022)
YG648.316	UCIAMS 241563	Equus sp.	Pre-LGM	Grazer	Monogastric	Yukon Canada	64	-139.11	mandible	28510.00	240	32675	32675	-21.1	4.67	Kelly (2022)	Kelly (2022)
YG650.588	UCIAMS 241543	Equus sp.	Pre-LGM	Grazer	Monogastric	Yukon Canada	63.84	-139.1	mandible	28660.00	240	32942	32942	-21.6	5.23	Kelly (2022)	Kelly (2022)
YG415.57	UCIAMS 241565	Equus sp.	Pre-LGM	Grazer	Monogastric	Yukon Canada	63.92	-139.35	mandible	28660.00	240	32942	32942	-21.0	3.95	Kelly (2022)	Kelly (2022)
YG610.1128	CAMS 186983	Equus sp.	Pre-LGM	Grazer	Monogastric	Yukon Canada	63.84	-139.1	mandible	28750.00	300	33088	33088	-21.0	5.1	Kelly (2022)	Kelly (2022)
YG150.105	UCIAMS 241553	Equus sp.	Pre-LGM	Grazer	Monogastric	Yukon Canada	63.07	-139.31	mandible	28890.00	250	33343	33343	-21.2	5.86	Kelly (2022)	Kelly (2022)
YG546.558	UCIAMS 241646	Equus sp.	Pre-LGM	Grazer	Monogastric	Yukon Canada	63.82	-139.06	mandible	29170.00	260	33700	33700	-21.2	3.79	Kelly (2022)	Kelly (2022)

Specimen ID	Radiocarbon ID	Species	Age subset	Feeding behaviour	Gut physiology	Region	Latitude	Longitude	Substrate	14C age (BP)	14C age uncertainty (BP)	Cal (BP)	Median cal (BP)	δ13C (‰)*	δ15N (‰)	δ13C, δ15N Reference	14C age Reference
YG404.704	UCIAMS 241644	Equus sp.	Pre-LGM	Grazer	Monogastric	Yukon Canada	64.02	-139.16	mandible	29990.00	290	34459	34459	-21.1	3.99	Kelly (2022)	Kelly (2022)
YG587.1735	UCIAMS 241541	Equus sp.	Pre-LGM	Grazer	Monogastric	Yukon Canada	63.82	-139.06	mandible	32280.00	380	36641	36641	-21.1	3.1	Kelly (2022)	Kelly (2022)
YG546.1730	UCIAMS 241529	Equus sp.	Pre-LGM	Grazer	Monogastric	Yukon Canada	63.82	-139.06	mandible	32390.00	380	36752	36752	-21.2	2.18	Kelly (2022)	Kelly (2022)
YG650.769	UCIAMS 241555	Equus sp.	Pre-LGM	Grazer	Monogastric	Yukon Canada	63.84	-139.1	mandible	32830.00	400	37344	37344	-21.2	3.84	Kelly (2022)	Kelly (2022)
YG610.1445	UCIAMS 241542	Equus sp.	Pre-LGM	Grazer	Monogastric	Yukon Canada	63.84	-139.1	mandible	32940.00	410	37521	37521	-21.1	3.78	Kelly (2022)	Kelly (2022)
YG578.40	UCIAMS 241538	Equus sp.	Pre-LGM	Grazer	Monogastric	Yukon Canada	63.71	-138.64	mandible	33040.00	410	37690	37690	-21.2	2.36	Kelly (2022)	Kelly (2022)
YG587.1128	UCIAMS 241535	Equus sp.	Pre-LGM	Grazer	Monogastric	Yukon Canada	63.82	-139.06	mandible	34040.00	470	39017	39017	-21.3	3.02	Kelly (2022)	Kelly (2022)

Specimen ID	Radiocarbon ID	Species	Age subset	Feeding behaviour	Gut physiology	Region	Latitude	Longitude	Substrate	14C age (BP)	14C age uncertainty (BP)	Cal (BP)	Median cal (BP)	δ13C (‰)*	δ15N (‰)	δ13C, δ15N Reference	14C age Reference
YG 126.26	AA-103821	Equus sp.	Pre-LGM	Grazer	Monogastric	Yukon Canada	64.05172864	-139.4248928	Bone	35800.00	2100	37748-42084	39916	-21.4	4.9	Schwartz-Narbonne et al. (2019)	Schwartz-Narbonne et al. (2019)
YG110.43	UCIAMS 241645	Equus sp.	Pre-LGM	Grazer	Monogastric	Yukon Canada	63.91	-139.33	mandible	35560.00	560	40645	40645	-20.9	2.08	Kelly (2022)	Kelly (2022)
YG402.291	UCIAMS 241566	Equus sp.	Pre-LGM	Grazer	Monogastric	Yukon Canada	63.82	-139.04	mandible	35610.00	570	40688	40688	-20.8	4.39	Kelly (2022)	Kelly (2022)
YG488.268	UCIAMS 241544	Equus sp.	Pre-LGM	Grazer	Monogastric	Yukon Canada	63.82	-139.04	mandible	36540.00	640	41441	41441	-21.0	3.39	Kelly (2022)	Kelly (2022)
YG406.439	UCIAMS 241570	Equus sp.	Pre-LGM	Grazer	Monogastric	Yukon Canada	63.82	-139.04	mandible	41200.00	1100	44097	44097	-21.4	5.04	Kelly (2022)	Kelly (2022)
YG615.125	CAMS 186986	Equus sp.	Pre-LGM	Grazer	Monogastric	Yukon Canada	63.92	-139.35	mandible	41700.00	1500	44551	44551	-21.0	6.13	Kelly (2022)	Kelly (2022)
YG650.321	UCIAMS 241567	Equus sp.	Pre-LGM	Grazer	Monogastric	Yukon Canada	63.84	-139.1	mandible	42300.00	1300	45005	45005	-20.8	3.1	Kelly (2022)	Kelly (2022)

Specimen ID	Radiocarbon ID	Species	Age subset	Feeding behaviour	Gut physiology	Region	Latitude	Longitude	Substrate	14C age (BP)	14C age uncertainty (BP)	Cal (BP)	Median cal (BP)	δ13C (‰)*	δ15N (‰)	δ13C, δ15N Reference	14C age Reference
YG103.5	UCIAMS 241537	Equus sp.	Pre-LGM	Grazer	Monogastric	Yukon Canada	63.91	-139.33	mandible	43000.00	1400	45605	45605	-21.0	1.92	Kelly (2022)	Kelly (2022)
YG587.252	UCIAMS 241545	Equus sp.	Pre-LGM	Grazer	Monogastric	Yukon Canada	63.82	-139.06	mandible	44500.00	1700	47024	47024	-21.2	3.15	Kelly (2022)	Kelly (2022)
YG215.26	UCIAMS 241568	Equus sp.	Pre-LGM	Grazer	Monogastric	Yukon Canada	63.82	-139.04	mandible	45200.00	1900	47812	47812	-21.6	4.02	Kelly (2022)	Kelly (2022)
AM 2446	AA-14855	Mammuthus sp.	Pre-LGM	Grazer	Monogastric	Alaska USA	65	-148	Dentin/Root dentin/Cementum	26022.00	640	30303-31474	30888.5	-21.4	6.4	Szpak et al. (2010)	Debruyne et al. (2008)
YG 130.2	UCIAMS-39891	Mammuthus sp.	Pre-LGM	Grazer	Monogastric	Alaska USA	63.75	-139.1	Bone	36690.00	810	41113-42193	41653	-21.1	6.6	Szpak et al. (2010)	Debruyne et al. (2008)
AM 523	AA-14904	Mammuthus sp.	Pre-LGM	Grazer	Monogastric	Alaska USA	65.18	-147.5	Dentin/Root dentin/Cementum	43239.00	2219	44661-49567	47114	-21.4	4.4	Szpak et al. (2010)	Debruyne et al. (2008)
YG 5.46	UCIAMS-414877	Mammuthus sp.	Pre-LGM	Grazer	Monogastric	Yukon Canada	63.9	-139.1	Bone	22430.00	140	26606-27590	27098	-21.6	9.4	Szpak et al. (2010)	Debruyne et al. (2008)

Specimen ID	Radiocarbon ID	Species	Age subset	Feeding behaviour	Gut physiology	Region	Latitude	Longitude	Substrate	14C age (BP)	14C age uncertainty (BP)	Cal (BP)	Median cal (BP)	δ13C (‰)*	δ15N (‰)	δ13C, δ15N Reference	14C age Reference
YG 5.46	UCIAMS-414877	Mammuthus sp.	Pre-LGM	Grazer	Monogastric	Yukon Canada	63.971	-138.988	Bone	22430.00	140	26606-27590	27098	-21.9	8.7	Mecalfe (2011)	Debruyne et al. (2008)
YG 2.4	AA-85000	Mammuthus sp.	Pre-LGM	Grazer	Monogastric	Yukon Canada	63.991	-139.043	Bone	27380.00	730	31409-32763	32086	-21.1	7	Mecalfe (2011)	Mecalfe (2011)
YG 2.7	UCIAMS-41488	Mammuthus sp.	Pre-LGM	Grazer	Monogastric	Yukon Canada	63.991	-139.043	Bone	27540.00	270	31885-32460	32172.5	-21.2	6.5	Mecalfe (2011)	Debruyne et al. (2008)
YG 3.256	UCIAMS-39115	Mammuthus sp.	Pre-LGM	Grazer	Monogastric	Yukon Canada	63.9	-138.25	Bone	28960.00	310	33020-33852	33436	-21.2	6.8	Szpak et al. (2010)	Debruyne et al. (2008)
YG 3.133	UCIAMS-39112	Mammuthus sp.	Pre-LGM	Grazer	Monogastric	Yukon Canada	63.9	-138.25	Bone	29030.00	310	33093-33896	33494.5	-21.1	7.2	Szpak et al. (2010)	Debruyne et al. (2008)
YG 3.136	UCIAMS-39114	Mammuthus sp.	Pre-LGM	Grazer	Monogastric	Yukon Canada	63.9	-138.25	Bone	29170.00	320	33211-33984	33597.5	-21.5	7.1	Szpak et al. (2010)	Debruyne et al. (2008)
NMC 42135	AA-17538	Mammuthus sp.	Pre-LGM	Grazer	Monogastric	Yukon Canada	64.85	-147.65	Dentin/Root dentin/Cementum	30000.00	1000	33291-35261	34276	-21.3	7.8	Szpak et al. (2010)	Debruyne et al. (2008)

Specimen ID	**Radiocarbon ID**	**Species**	**Age subset**	**Feeding behaviour**	**Gut physiology**	**Region**	**Latitude**	**Longitude**	**Substrate**	**14C age (BP)**	**14C age uncertainty (BP)**	**Cal (BP)**	**Median cal (BP)**	**δ13C (‰)***	**δ15N (‰)**	**δ13C, δ15N Reference**	**14C age Reference**
YG 52.36	UCIAMS-39890	Mammuthus sp.	Pre-LGM	Grazer	Monogastric	Yukon Canada	63.74	-139.33	Bone	30630.00	870	34126-35762	34944	-21.5	6.4	Szpak et al. (2010)	Debruyne et al. (2008)
YG 133.18	UCIAMS-38675	Mammuthus sp.	Pre-LGM	Grazer	Monogastric	Yukon Canada	63.73	-138.6	Bone	32140.00	370	35777-37296	36536.5	-21.3	8.1	Szpak et al. (2010)	Debruyne et al. (2008)
YG 5.130	UCIAMS-39889	Mammuthus sp.	Pre-LGM	Grazer	Monogastric	Yukon Canada	63.9	-139.1	Bone	32470.00	480	36117-37862	36989.5	-21.2	6.9	Szpak et al. (2010)	Debruyne et al. (2008)
YG 133.21	UCIAMS-41489	Mammuthus sp.	Pre-LGM	Grazer	Monogastric	Yukon Canada	63.73	-138.6	Bone	34180.00	590	38503-40517	39510	-21.3	6.8	Mecalfe (2011)	Debruyne et al. (2008)
YG 2.14	AA-84986	Mammuthus sp.	Pre-LGM	Grazer	Monogastric	Yukon Canada	63.991	-139.043	Cementum	35500.00	2000	37551-41794	39672.5	-21.1	7.4	Mecalfe (2011)	Mecalfe (2011)
NMC 42292	AA-17553	Mammuthus sp.	Pre-LGM	Grazer	Monogastric	Yukon Canada	64.08	-138.4	Cementum/Dentin/Root dentin	37920.00	2700	39267-44297	41782	-21.2	7.9	Szpak et al. (2010)	Debruyne et al. (2008)
YG 137.3	UCIAMS-39892	Mammuthus sp.	Pre-LGM	Grazer	Monogastric	Yukon Canada	63.73	-138.6	Bone	39800.00	1200	42777-44670	43723.5	-21.1	7.3	Szpak et al. (2010)	Debruyne et al. (2008)

Specimen ID	**Radiocarbon ID**	**Species**	**Age subset**	**Feeding behaviour**	**Gut physiology**	**Region**	**Latitude**	**Longitude**	**Substrate**	**14C age (BP)**	**14C age uncertainty (BP)**	**Cal (BP)**	**Median cal (BP)**	**δ13C (‰)***	**δ15N (‰)**	**δ13C, δ15N Reference**	**14C age Reference**
YG 29.248	UCIAMS-41493	Mammuthus sp.	Pre-LGM	Grazer	Monogastric	Yukon Canada	63.971	-138.988	Bone	43500.00	1900	45000-49489	47244.5	-21.7	7	Mecalfe (2011)	Debruyne et al. (2008)
YG 3.19	UCIAMS-39887	Mammuthus sp.	Pre-LGM	Grazer	Monogastric	Yukon Canada	63.9	-138.25	Bone	44700.00	200	45806-51176	48491	-21.2	5.7	Szpak et al. (2010)	Debruyne et al. (2008)
F:AM 142458	CAMS120072	Ovibos sp.	Pre-LGM	Grazer	Polygastric (Ruminant)	Alaska USA	64.85653271	-147.5028344	Unknown	41200.00	1500	43428-46298	44863	-20.5	0.1	Fox-Dobbs et al. (2008)	Fox-Dobbs et al. (2008)
YG 157.24	AAR-12023	Ovibos sp.	Pre-LGM	Grazer	Polygastric (Ruminant)	Yukon Canada	64.05172864	-139.4248928	Bone	38350.00	900	42089-43678	42883.5	-20.3	6.8	Raghaven et al. (2014)	Raghaven et al. (2014)